The Pathways and Mechanisms of Skin Electroporation.

by

Tani Chen

M. S. in Chemical Engineering Practice
Massachusetts Institute of Technology, 1995

B. S. in Chemical Engineering
University of Illinois at Urbana-Champaign, 1993

Submitted to the Department of Chemical Engineering
in Partial Fulfillment of the Requirements for the Degree of

Doctor of Science in Chemical Engineering

at the

Massachusetts Institute of Technology

February 1999

Signature of Author.....
Department of Chemical Engineering
December 18, 1998

Certified by.....
Robert Langer
Germeshausen Professor of Chemical and Biomedical Engineering
Thesis Supervisor

Certified by.....
James C. Weaver
Senior Research Scientist, Harvard–MIT Division of Health Sciences and Technology
Thesis Supervisor

Accepted by.....
Robert E. Cohen
St. Laurent Professor of Chemical Engineering
Chair, Committee for Graduate Students

Abstract.

Transdermal drug delivery is the delivery of drugs across the skin without using needles. Since most drugs diffuse slowly across unperturbed skin, many techniques have been investigated to increase molecular transport. One technique is skin electroporation, where short (~1 ms), high-voltage pulses (~100 V_{skin}) are applied to the skin. Previous studies have shown dramatic increases in transport. However, an understanding of how transport occurs was needed, which was the goal of this thesis.

Human cadaver skin and snake skin were used to determine transport pathways across the skin. Snake skin was used as a model of human skin that lacked hair follicles or sweat ducts. By applying high-voltage pulsing to human and snake skin, it was shown that transport occurs through "localized transport regions" (LTRs), which were small, randomly distributed regions forming away from hair follicles and sweat glands. The LTRs appeared in both human and snake skin, along with comparable molecular transport, indicating the importance of these regions during transport.

Molecular transport during skin electroporation occurs very rapidly, usually within the first few pulses (s to min). The voltage that forms across the skin cannot be predicted from the applied voltage alone, and changes with repeated pulsing. A flow-through system was constructed that allowed the simultaneous real-time measurement of the transdermal voltage, the molecular flux, and the inter-pulse impedance.

The transdermal voltage was found to initially decrease rapidly during pulsing, then continue decreasing more slowly with additional pulsing. The impedance at 100 Hz decreased with repeated pulsing, but increased somewhat between pulses, indicating recovery of the skin. The molecular fluxes of four charged fluorescent molecules (sulforhodamine, lucifer yellow, cascade blue, and calcein) were also studied. These molecules were chosen since they had similar molecular weights, hydrophilicities, and electronic charges. However, with repeated pulsing, the flux of sulforhodamine increased steadily, lucifer yellow and cascade blue achieved steady state, and calcein initially increased rapidly, then later decreased.

Skin electroporation is a dynamic process, where the transdermal voltage and molecular flux vary rapidly with repeated pulsing. To achieve control of skin electroporation, these parameters should be carefully monitored in real time.

Thesis Supervisor: Robert Langer
Title: Germeshausen Professor of Chemical and Biomedical Engineering

Thesis Supervisor: James C. Weaver
Title: Senior Research Scientist, Harvard–MIT Division of Health Sciences and Technology

To

Mom and Dad

— and —

To

Hongming

The investigator should have a robust faith — and yet not believe.

— Claude Bernard
French Physiologist
(1813-1878)

When we try to pick out anything by itself, we find it hitched to everything else in the universe.

— John Muir
American Naturalist
(1838-1914)

If we knew what it was we were doing, it would not be called research, would it?

— Albert Einstein
Swiss-American Physicist
(1879-1955)

Sometimes a scream is better than a thesis.

— Ralph Waldo Emerson
American Essayist
(1803-1882)

Acknowledgments.

I would like to thank the following people who have helped me in my work — some have helped me with comments and suggestions, or equipment and supplies, or simply by being there to make my life, uh, interesting — but all of them are greatly appreciated. Without their support, this thesis and this Sc. D. would have never made it out of the pipeline intact.

Mom and Dad, of course, for always being there for me. They don't always understand life in academe (and I'm not sure I do either), but they still have always supported me no matter what I've gotten myself into. Thanks, guys.

Jim Weaver, for his insight and dedication. And his thoroughness in reading and evaluating everything from papers to experiments.

The members of Weaver labs. Elizabeth Gift for, among many other things, building the see-through, high-voltage, Tani-proof (very important!) relay switch for the impedance meter (Section V.4.1 for those of you keeping track). Over 10 000 pulses and no problems! And that see-through box added that certain flair to the experimental equipment.... And Tim Vaughan, for those innumerable conversations about everything from national politics, to chess, to juggling, to bicycling, to English grammar, to various puzzles (such as why "flossy" = "unroof"*), to high-energy particle physics. (Jim, If you're reading this, the previous statement is false, we *only* talked about skin electroporation!)

The first round of skin electroporation people: Mark Prausnitz, for starting me on this journey to discover skin electroporation (Mark, I'm sure you'll enjoy thumbing through the Appendices to see how things have changed since your days in the skin electroporation lab); Uwe "This is garbage!" Pliquett, who can build or fix anything from a pile of junk (that talent *never* ceases to amaze me!); Vanu Bose; Tom Zewert (DNA and reducing agents); and of course, Rita Vanbever (who's now Professor Vanbever — hey, that rhymes!), for her attention, enthusiasm, and stabilization towards this work (and may you not get so wrapped up in your professorship duties that you forget to smell the flowers).

Yuri Chizmadzhev, for those interesting discussions ("you're killers of skin!"), and Steve Burns, for technical help on the latest cutting-edge macrofabrication techniques (yes, macrofabrication. Like cutting through quarter-inch sheet metal or half-inch sheets of plexiglas...).

The second round of skin electroporation dudes (the "MIT Center for Microconduit Studies"): Gowrishankar (who needs more than one name to identify oneself, anyway?), Jason Handwerker (hardworker? Now there's a good name to have), and Ljubomir ("Lou") Ilic. I hope this thesis provides and provokes much thought. It's the sum (or at least as much of it as I can remember) of all of my skin electroporation experiences and knowledge (especially the Appendices).

Bob Langer and his support and enthusiasm. He once called my work "unbelievably thorough." I hope this thesis lives up to expectations.

The first round of skin gurus: Mark Johnson (chemical enhancers), Samir Mitragotri (ultrasound), and Mark Prausnitz (electroporation, of course). I'm sure they must have had some very interesting discussions in their day about which transdermal drug delivery technique was "truly" better....

The second round of skin folks. May this thesis provide thought, discussion, and entertainment: Betty Yu (who's discovered the joys and agonies of baby-sitting computers — I hope mixing skin with computers goes better for you than it did for me), Joanne Farrell (don't you just love dealing with monstrosities!), Yosi Kost, and Hua Tang (I hope your journey through the land of skin research goes more smoothly. May you get through grad school and MIT with your enthusiasm intact!).

My various officemates in E25-143A. What a great office that is — it's the only one of the Langer offices down in that Athena cluster with a window view! Karen Fu, Joachim ("Joe") Siedel, Shane Williams (with that wonderful British sense of humour), Justin Hanes, Maria Tobio, and, of course, Hongming Chen (more on her later).

---

*This thesis was typed using the Dvorak keyboard, a keyboard invented by August Dvorak and William Dealey (patented in 1936), designed to be a logical and efficient keyboard, as opposed to the standard "Qwerty" keyboard. The Qwerty keyboard was designed earlier by Christopher Sholes to be as hopelessly inefficient as possible, to keep fast typists from jamming mechanical typewriters. The finger sequence for typing "flossy" on a standard "Qwerty" keyboard is the exact same sequence for typing "unroof" on a Dvorak keyboard. Furthermore, this pair of words is the longest such possible pair in the English language.

Sachiko Hirosue, for the many assorted conversations in E25-325 (especially when I was nearly sleeping on my feet and probably babbling things that barely made any sense at all), concerning science, life, radio, and especially music. And her tape collection of house and Latin music kept me going in the wee hours of the morning.

John Santini, who's the only other person in the lab who could seriously compete with me for using the spectrofluorimeter at 3 in the morning (hey, he's the other founding member of the Langer Labs' "up-all-night-doing-experiments-sleep-is-for-wimps" club!). It's pretty exciting, trying to hold a meaningful scientific conversation with another person at 4 in the morning when neither one of us has had any sleep whatsoever in the past 36 hours....

The many, many, many other assorted members of Langer labs, in no particular order (and this really is just a small fraction of the lab): Prasad Shastri, Julie Rahman, Rebecca Carrier, Guillermo Ameer, Jinming Gao, David Edwards, David Putnam, Magdalene Badtke, Michael Pishko, Ivan Martin, Ruben Millan, Keith Gooch, Eric Grovender, Jeff Hrkach, Erin Lavik, Jennifer Elisseeff, Ana Jaklenec, Burkhard Kriwet, Giovanni Caponetti, Tommy Thomas, Amy Richards, Lon Cook, Amir Nashat, Laura Niklason, Eric Crumpler, Dan Pack, Bobby Padera, Maria Papadaki, Christine Perez de la Cruz, and many others.

Maria José Alonso, for putting how to do research over the actual research itself. It's good to push the students to think on their own — isn't that why we call them advisors and not slave drivers?

The secretarial staff, for their help in many administrivia matters — Pam Brown and Connie Beal from the Langer Labs, and Jo Anne Sorrento, Terry Parekh, and Lisa Court from the Biomedical Engineering Center of HST.

Bill Deen and Al Grodzinsky, the members of my thesis committee, for their support and encouragement for this project.

J. H. Rytting, for his generous and timely gift of shed black rat snake skin. The snake skin gift came at a critical junction in the life of this thesis, when the particle experiments, the peptide experiments, and the experimentalist had, shall we say, run out of steam. It wasn't just a gift of snake skin, it was a gift of renewed energy. The other really nice thing about using shed snake skin is that you get to go to conferences and mouth off about no animals being harmed during your experiments (not many other people who work in biomedical engineering can say that!). I don't enjoy sacrificing animals on the alter of science, but I do believe there are those times when it may become necessary to do so. However, it is much nicer to avoid altogether (with proper justification) having to kill anything at all.

NDRI (the National Disease Research Interchange) and OTVSC (the Ohio Valley Tissue and Ski Center... oops, I mean the Ohio Valley Tissue and Skin Center!), for supplying cadaver skin (and NDRI also included those wonderful free administration headaches!) over the past couple of years.

Carl Rosow, my pharmacology professor, for bending the rules (a little) for me after I got seriously hosed in pharm class.

Noah Lotan, Bob Langer and the 10.491 class. Oh, the joys of trying to TA seniors who've come down with full-blown cases of senoritis!

Doug Lauffenburger (my former professor from Illinois), and Greg Stephanopolous, both from 10.544. Thanks for putting up with me when my mind was on other things besides TA'ing class (like job hunting and writing this thesis...).

Janet Fischer, for helping me get the 10.544 TA, and in fact get through life in chemical engineering graduate school, and Elaine Aufiero, for her motherly advice during the month of hell.

Eileen Segall, my UROP, for her help in the lab. Dealing with weird smelling chemicals and even weirder-looking pieces of jury-rigged laboratory equipment is not easy, but her boundless enthusiasm was always infectious.

Christine Schmidt (now Professor Christine Schmidt), the graduate student I worked for when I was an undergraduate at Illinois (who worked for Doug, and *both* of them followed me here to MIT!), for her encouragement and support during my graduate studies. And for listening (both in person and through e-mail) to all of those times when I was having trouble in graduate school. Her optimism was always invariably helpful.

WMBR and its endless (and I mean *endless*) energy and insanity — dealing with the insanity at the radio station is a refreshing change from the insanity of the lab. Let me explain that one. In research, you can do experiments until you're blue in the face (and sometimes I did...) without really knowing the outcomes of those experiments (especially when it's buried under 3 MB of data that needs some serious heavy-duty number crunching!). In radio, on the other hand, when you screw up, you know it immediately — and so does the rest of Boston! There are many, many folks at the station, and they all see things from unique points of view. Even though these people come from all walks of life (and believe me, I mean *all*), they work together to make WMBR the success that it is. I think there's a lesson in there somewhere....

The *Rhythm of Taipei*, for getting me started in this radio business, especially Andrew Chen, for sharing with me the joys (and adrenaline rushes) of engineering radio live: simultaneously getting CD's cued and played in the correct order, watching the output levels, signing the logs, and trying to keep track of up to 15 DJ's running amuck around the station; and Jessica Hu, for giving me that crash course in the history of Taiwanese pop music.

The *Rhythm of Taipei* spin-offs: Henry Hwu (who?) and the *Midnight Snacks of Taiwan* (he had the good sense to go to graduate school in chemical engineering... or is that bad sense?); and Aileen Tang and *Sinopop* ("It's not music, it's extreme music!" — at least I think that's the translation from Chinese), for all of her support and enthusiasm over the years, as the times have changed. And, of course, *Dreams of a New Age* and all of its listeners, who can put up with my prattle and sleepy new age (and etc.) music for 2 hours every Monday night.... And to all those musicians I have had the privilege of listening to — my best wishes to your musical endeavors.

The *Virgin Radio*, uh, the *Is This On?* crew (great name, huh? Thought it up myself!): Andrew Nevins, Peter Choyce, Jordan Gruveski, and Joan "Hathaway" Pumphert. Trying to keep things professional (or at least under control!) with all of those brand new, fresh-out-of-the-wrapper DJ's. And listening to everything from commercial rock, to classical, to types of music I'm not even sure have names....

The WMBR Program Board: Juana Sandoval, Fred Bouchard, Julia Goldrosen, Larry McGovern, Linda Pinkow, and Andrew Nevins.

The Monday night crowd at WMBR: Laura Wilson from *Bats in the Belfry*, for her enthusiasm for new age music (as well as every other type of music); Shawn Mamros and his financial wranglings (I've always been impressed at the fastidiousness of his record keeping); Sue Schardt with *In the Margin of the Other* (always such great introductions from her!); Gene Fiero from *Generoso's Bovine Ska Reality* (he's from Tuesday nights, actually — ska cows rule!); and Adam Weintraub & Jeff Chow from the *Groove Canal* (thanks for the 4 hour new age music marathon show!).

The Monday lunch bunch and their S. O.'s: Sherry Gu and Bryan, Lei Zhang and Jonathan, Jane Chang and Ming, Jianfeng Lou and Wei, and Gene Lin and TinhVan. And of course, Hongming. Always great to have something to look forward to at the start of the week, when you're otherwise not sure if you should go to all the trouble of removing your blanket and getting out of bed.

Gene Lin and TinhVan Diep, for all of their support and willingness to listen, especially in the important areas of life, love, marriage, and the best way of invading York (6 points!) with the Welsh when the Romano-British have just fortified it with their calvary and King Arthur. Does writing a thesis count as a Wonder of the World? It's got about 300 shields, uh, pages....

And that miserable little overpacked, overworked cart, stuffed with tons of equipment and yards and yards of tape and hope. Yes, I'm even sticking in a tag in my acknowledgments about my pitiful, mistreated, Tani-proofed equipment (there's even a photo of it in Figure V.1). Well... given the multitudes of hours, jury-rigged repairs, curses, and abuses I heaped on that poor thing, I thought it deserved a little mentioning. Besides, it was my ticket to this Sc. D. thesis. I was actually sad to see it go from E25-325 to be permanently taken out of commission and cannibalized for parts.

And finally to Hongming Chen. Her enthusiasm, support, and love have been limitless and unwavering, even during all of those many bad times. From the time she laughed at all of my ridiculous jokes in Building 20 that Wednesday night, my heart has belonged to her.

Table of Contents.

List of Figures.

List of Tables.

1. Introduction to Skin Electroporation.

Transdermal drug delivery offers many advantages compared to other methods of drug delivery. Transdermal drug delivery can be defined as the transport of drugs across the skin without the use of needles (direct injection). One obvious advantage is that needles and the associated pain are avoided. This is especially important for drugs that have to be repeatedly administered. Avoiding the unpleasantness of needles would lead to improved patient compliance of drug regiments.

Another advantage of transdermal drug delivery is its ability to offer prolonged or sustained delivery, potentially over several days to weeks. Some methods, such as oral or pulmonary delivery techniques, require that the drug be given repeatedly (maintenance dosing) to sustain the proper concentration of drug within the body. With sustained delivery, maintenance dosing could be performed automatically, over a long period of time. Drugs with short half-lives in the body, such as peptides or proteins, could also be delivered over long times.

A final advantage is that molecules only have to cross the skin to reach the bloodstream for systemic circulation. Many molecules taken orally are quickly degraded by the low pH's and enzymes found in the gastrointestinal tract. Especially vulnerable are protein or peptide drugs. Molecules transported across the skin would experience much less harsh conditions than those delivered orally.

The most common form of transdermal drug delivery is the drug "patch," where the drug is contained within a reservoir placed next to the skin (typically resembling a "sticker") (Schaefer and Redelmeier, 1996). The drug molecules cross the skin by simple diffusion ("passive delivery"). Generally speaking, passive transdermal drug delivery is limited to small, lipophilic molecules such as scopolamine, nitroglycerine, and nicotine, which readily permeate the skin. The delivery kinetics are slow, typically taking hours to cross the skin.

Since passive delivery can be slow, many techniques have been developed to enhance molecular transport rates. These techniques include chemical enhancers to enhance transport kinetics; ultrasound, which induces cavitation within the skin to decrease its barrier properties; and iontophoresis, which is the application of a small, constant current that causes molecular transport through the hair follicles and sweat ducts.

One other technique that has recently shown promise is the application of a series of very short (typically ~1 ms, although longer pulses have also been tried), high-voltage pulses (~100 V_{skin}) to the skin, which causes the lipids within the stratum corneum to rearrange, in a phenomenon related to electroporation; hence the term, "skin electroporation." Rearrangement of these lipids allows molecular transport across the skin to take place. Strictly speaking, the high-voltage pulses are applied to the skin, which then causes the phenomenon called "skin electroporation" to occur within the lipids of the

stratum corneum. However, in common speech, many people refer to the entire process more simply as "skin electroporation."

In the 1970's, it was found that the application of a series of short, high-voltage electrical pulses to cells or lipid membranes caused "pores" to form within the lipid membranes, through which ions and molecules could be transported through (Chang, *et al.*, 1992; Weaver and Chizmadzhev, 1996 [a]). After pulsing, these pores would spontaneously reseal; thus, the cells or lipid membranes were not permanently damaged. This process was called "electroporation." Many drugs and even DNA were efficiently delivered into cells by this technique.

By the 1980's, workers had begun applying high-voltage pulsing to sheets of tissues, such as frog skin (Powell, *et al.*, 1989). This led to the idea of applying high-voltage pulsing directly to human skin, to enhance transdermal drug delivery. Early experiments in the lab were highly successful, showing significant enhancements in the transport of several model compounds (Prausnitz, *et al.*, 1993 [a]).

Since then, many compounds have been successfully transported across the skin by skin electroporation techniques. However, the mechanism behind this transport was not well understood. To optimize the applied electrical conditions in skin electroporation to maximize drug transport, a better understanding of how and where molecules cross the skin was needed. This was the goal of this research.

2. Background of the Research.*

The goal of transdermal drug delivery is to find a safe, controllable way to deliver large amounts of drug from the outside of the body, to the blood vessels within the skin, without the use of needles or direct mechanical penetration of the skin. Drug reaching the blood vessels can then be delivered systematically. Important issues in transdermal drug delivery research include increasing delivery rates, controlling drug delivery (the ability to start and stop transport), and ensuring patient safety.

2.1. Structure of the Skin.

The skin is the largest organ of the body. It is highly impermeable to prevent loss of water and electrolytes, dry to prevent microorganism growth, and physically tough to protect the underlying tissues (Ackerman, 1978). The skin is negatively charged (Kasting and Bowman, 1990), and has an electrical resistivity of ~100 kΩ cm (Bose, 1994). The skin is subdivided into two main layers: the outer epidermis and the inner dermis (Figure 2.1).

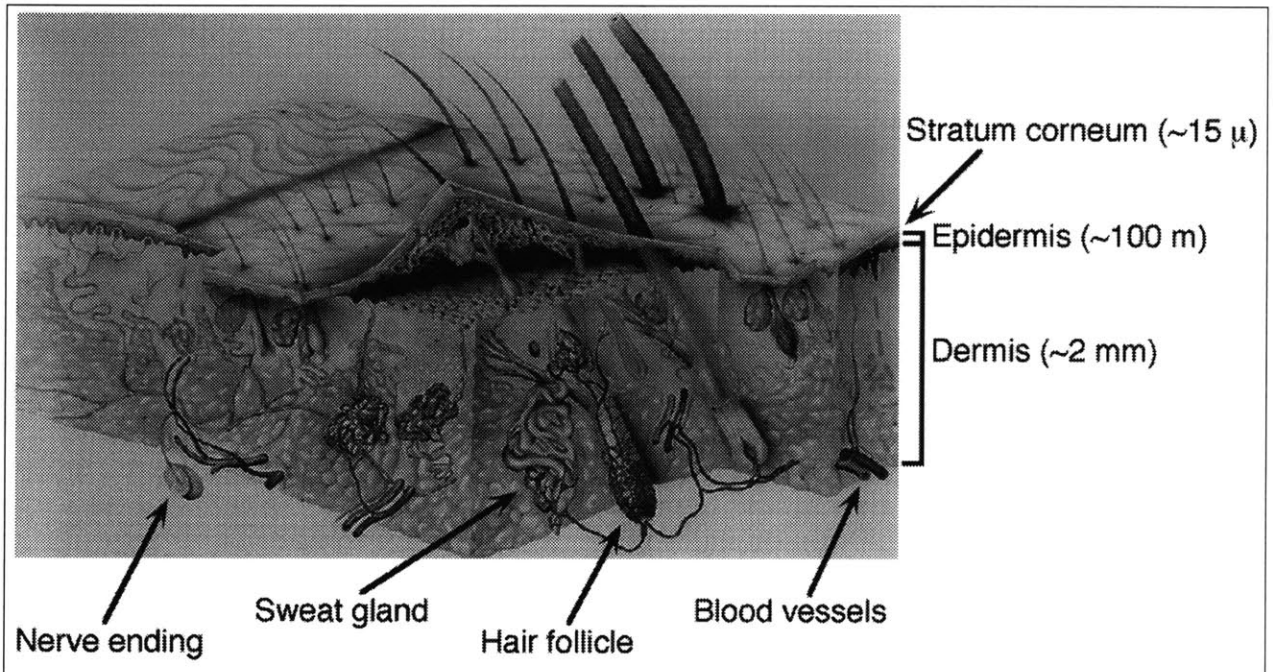

Figure 2.1. Diagram of human skin. The skin is divided into three layers: the stratum corneum, the epidermis, and the dermis. The stratum corneum is the outermost layer of the skin, and the rate-limiting barrier to the entry of molecules into the body. In the dermis are located sweat ducts and hair follicles which extend outward to the surface of the skin, nerve endings, and blood vessels. The drug has to reach the blood vessels in the dermis for systemic circulation of the drug to occur. Figure from Montagna, *et al.* (1992).

*Some of the introductory material in this chapter has also been published in Chen (1998 [a]) and Chen, *et al.* (submitted) [b].

2.1.1. The Epidermis.

The epidermis is the outer layer of the skin, 50 to 100 μ thick (Monteiro-Riviere, 1991; Champion, *et al.*, 1992). The epidermis does not contain nerve endings or blood vessels. The main purpose of the epidermis is to generate a tough layer of dead cells on the surface of the skin, to separate the body from the environment. This top layer is called the stratum corneum, and the dead cells that comprise it are called corneocytes or keratinocytes. The rest of the epidermis is divided into three additional layers: the stratum granulosum, the stratum spinosum, and the stratum basale (at the bottom). These three layers are collectively called the viable epidermis, since the cells in these layers are still alive (Ackerman, 1978).

As the cells of the stratum basale mature into dead corneocytes, they are continuously pushed outward towards the surface of the skin (Figure 2.2), a process that takes ~28 d. Each stage of differentiation is characterized by a layer of the epidermis.

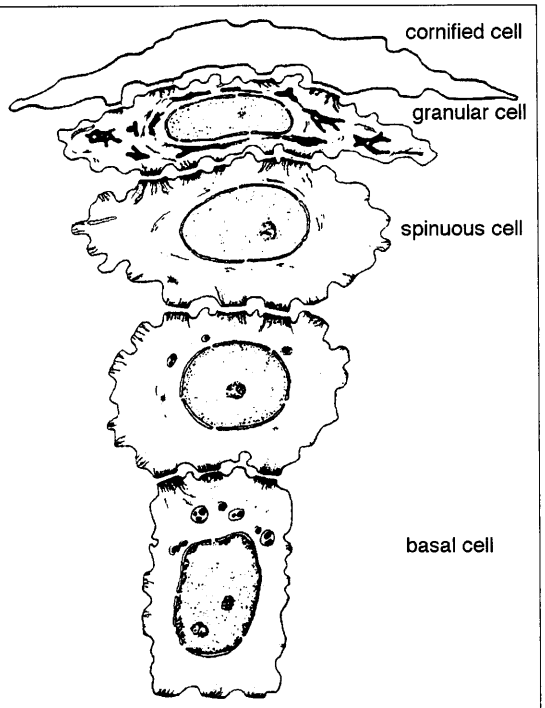

Figure 2.2. Differentiation of epidermal cells to form the stratum corneum. This figure shows representative epidermal cells in the process of forming stratum corneum (cornified cell or corneocyte), the uppermost layer of the skin. The remaining cells are found in various layers of the epidermis: the stratum granulosum (granular cell), the stratum spinosum (spinuous cells), and the stratum basale (basal cell). Figure taken from Ackerman (1978).

The stratum basale consists of stacked columns of corneocytes. As these cells divide, they are pushed upward towards the stratum spinosum, where the cells form interconnecting desmosome junctions and flatten out. At this level, the cells also produce keratin and keratohyalin proteins, giving the cells increased mechanical strength. The cells are then further pushed outwards to the stratum granulosum, where they form course lamellar granules, which are secreted extracellularly to produce intercellular lipids. Most of the organelles, including the nucleus, disappear here (Ackerman, 1978).

Once the corneocytes are fully matured, they die to form the stratum corneum. At this point, the corneocytes are almost completely full of keratin, surrounded by sheets of lipid bilayer membranes. The corneocytes in the stratum corneum are continually sloughed off into the environment and are replaced by the underlying cells (Ackerman, 1978; Wertz and Downing, 1989).

2.1.2. *The Stratum Corneum.*

The stratum corneum remains fairly constant in thickness around the body, around 10 to 20 μ thick, with the exception of the hands and feet, where it is much thicker. It is commonly modeled as a brick wall (Figure 2.3) (Elias, 1983; Elias, 1988). The "bricks" are the flattened, dead corneocytes. The corneocytes are shaped as flattened hexagons, roughly 30 μ in diameter by 0.5 to 0.8 μ thick, and are composed primarily of keratin and keratohyalin proteins (Wertz and Downing, 1989). Typically, there are about 10 to 15 corneocytes stacked vertically across the stratum corneum (Monteiro-Riviere, 1991; Champion, *et al.*, 1992).

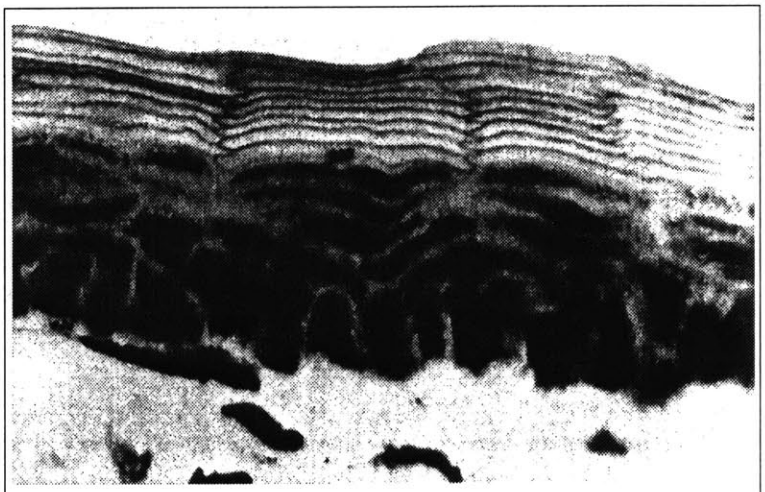

Figure 2.3. Photomicrograph of the stratum corneum. The bricks-and-mortar structure (corneocytes and intercellular lipids, respectively) can clearly be seen here in the uppermost layer of the skin. Photomicrograph from Wertz and Downing (1989).

The corneocytes are encased in sheets of lipid bilayers (the "mortar"). The lipid bilayer sheets are separated by ~50 nm. Typically, there are about 4 to 8 lipid bilayers between each pair of corneocytes. The lipid matrix is primarily composed of ceramides, sphingolipids, cholesterol, fatty acids, and sterols, with very little water present (Lampe, *et al.*, 1983 [a]; Lampe, *et al.*, 1983 [b]; Elias, 1988).

Although it is the thinnest layer of the skin, the stratum corneum is the primary barrier to the entry of molecules or microorganisms across the skin, due to its construction and composition. Most molecules pass through the stratum corneum only with great difficulty, which is why the transdermal drug delivery route has not been more widely used traditionally. Once the molecules have crossed the stratum corneum, diffusion across the epidermis and dermis to the blood vessels occurs rapidly. Thus, most of the attention in transdermal drug delivery research has been focused on transporting molecules and drugs across the stratum corneum.

2.1.3. *The Dermis.*

The dermis is the inner layer of the skin and varies from 1 to 3 mm in thickness. The dermis forms a tough, flexible, elastic covering of the body (Gray and Clemente, 1985), and supplies the epidermis with nutrients, which are transported throughout the epidermis by diffusion. The dermis is composed

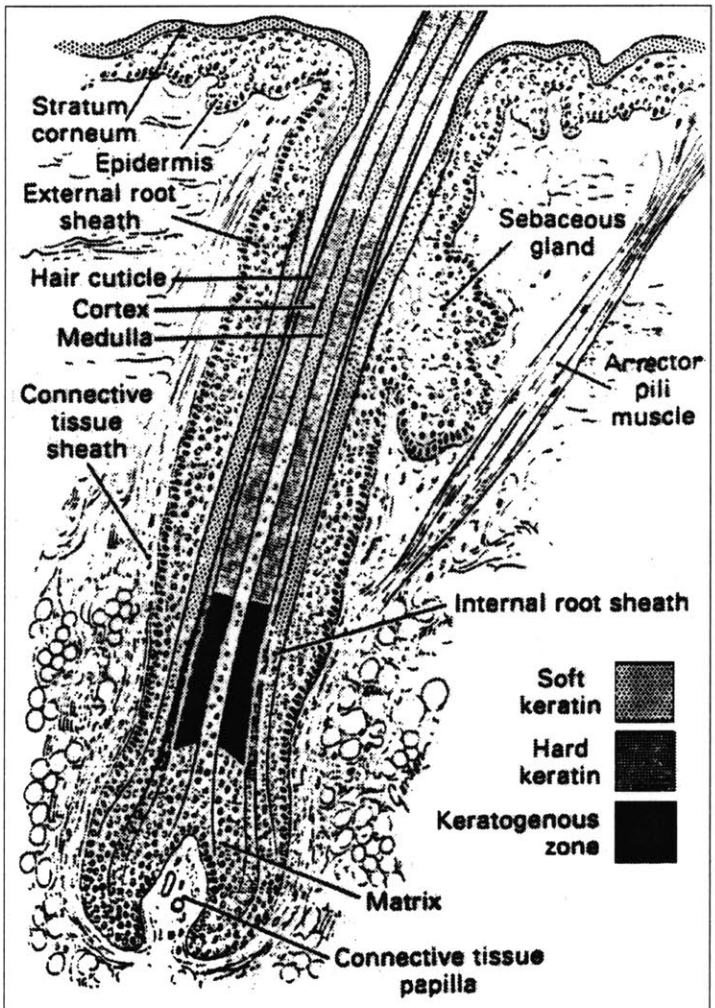

Figure 2.4. Schematic diagram a hair follicle. Note that the hair follicle starts in the dermis and penetrates the epidermis and the stratum corneum to reach the surface of the skin. Based on a figure from Leblond (1951).

mainly of connective tissues and is about 60 to 70% water (Monteiro-Riviere, 1991; Champion, *et al.*, 1992).

The dermis can be subdivided into the papillary dermis and the reticular dermis. The papillary dermis is the outer layer of the dermis and contains an extensive network of capillaries for heat regulation and nourishment of the epidermis, which lacks capillaries (Ackerman, 1978). The reticular dermis is the innermost layer and is composed mainly of connective collagen fibers. The goal of transdermal drug delivery is to get the drug to this layer of the skin, where the blood capillaries are located, to allow the drug to be systematically delivered.

Nerve endings are located in the dermis, including thermoreceptors (for detecting heat and cold), mechanoreceptors (touch and pressure), and noiceptors (itch and pain). They are usually found near the junction between the dermis and the epidermis (Champion, *et al.*, 1992),

Hair follicles start from the dermis and extend outwards to the surface of the skin. Besides the hair bulb, hair shaft, inner root sheath, and outer root sheath, other major components within the dermis are the apocrine sweat gland and the arrector pili muscle (Figure 2.4) (Ackerman, 1978; Champion, *et al.*, 1992).

Sweat glands are located in the dermis and extend outwards to the surface of the skin, completely penetrating the epidermis (Figure 2.5). There are two types of sweat glands: apocrine and eccrine sweat glands. Apocrine sweat glands empty into hair follicles and produce sebaceous fluids continuously at slow rates. Eccrine sweat glands produce sweat to control body temperature. Humans have a much higher density of eccrine sweat ducts than other animals; thus, choosing an animal model can be difficult (see Section 7.1) (Ackerman, 1978; Champion, *et al.*, 1992).

2.2. Transdermal Drug Delivery.

The delivery of drugs or other molecules across the skin offers many advantages over other drug delivery techniques, including the following: (1) no degradation of the drug (especially peptide and protein drugs) by the gastrointestinal tract, especially in the liver; (2) no variation in drug absorption rates due to daily variations in the state of the gastrointestinal system; (3) increased control in the administered dosage, reducing the chances for overdoses, underdoses, or missed doses, and allowing for rapid termination of drug delivery; (4) steady, periodic, long-term, or rate-controlled drug delivery; and (5) increased patient compliance (Bronaugh and Maibach, 1989; Chien, *et al.*, 1989; Hadgraft and Guy, 1989; Champion, *et al.*, 1992; Cullander, 1992; Schaefer and Redelmeier, 1996). Rate-controlled drug delivery is especially important for drugs that are most effective when delivered monthly (estradiol) or daily (insulin) instead of continuously (Hrushesky, 1991).

The most common method of drug delivery is passive diffusion, where the drug is placed next to the skin in a "patch," and allowed to diffuse across. However, this is a very slow technique. The drug can often take hours to cross the skin, and so other techniques have been developed to enhance drug delivery rates. Besides skin electroporation, there include chemical enhancers, ultrasound, or iontophoresis.

Chemical enhancers enhance the diffusion characteristics of the drug across the skin, although the main driving force is still passive diffusion. Ultrasound induces cavitation within the lipids of the stratum corneum, also enhancing diffusion kinetics. Iontophoresis is the application of a small, DC electrical current to the skin, providing an additional driving force for transport.

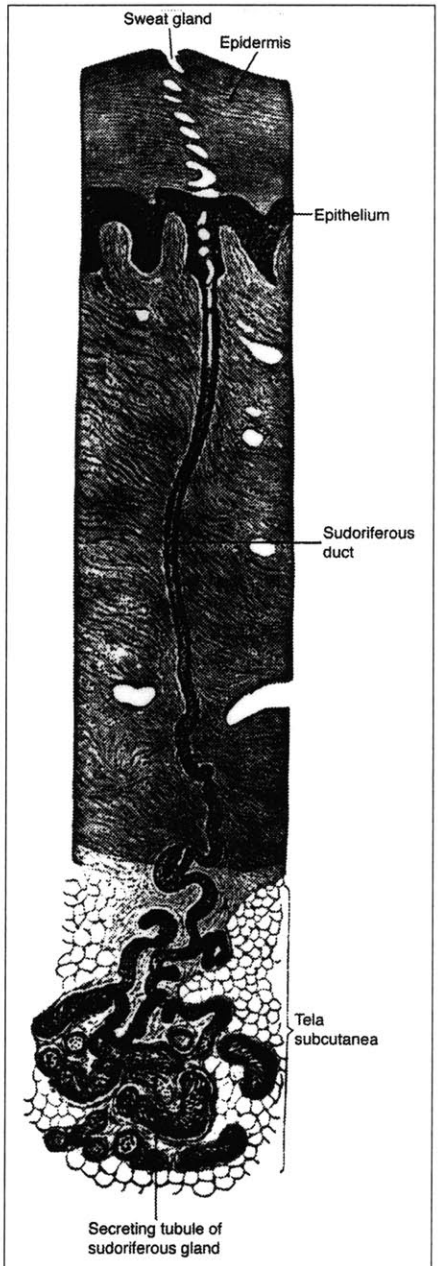

Figure 2.5. Structure of a sweat gland. The sweat gland starts from the dermis and extends to the surface of the skin. From Gray and Clemente (1985).

2.2.1. Passive Delivery.

The most commonly used devices for transdermal drug delivery are passive delivery patches (Guy and Hadgraft, 1989; Hadgraft and Guy, 1989; Langer, 1990; Santus and Baker, 1993). Transport is

governed by the rate of molecular diffusion into and out of the skin, and partitioning of the drug into the skin. Very hydrophilic drugs partition poorly into the skin, due to the lipid bilayers of the stratum corneum; yet very lipophilic drugs which partition easily into the stratum corneum will not partition out again into the bloodstream. The delivery kinetics for passive delivery are usually very slow, typically requiring hours to days for molecular transport across the skin.

Only small, uncharged drugs (typically <400 Da) can be delivered passively, and treatment is only effective when a very small amount of drug is required to have a biological effect (Guy and Hadgraft, 1989). Commercially available drugs delivered passively include clonidine, estradiol, isosorbide dinitrate, nicotine, nitroglycerin, norethisterone, salicylate, scopolamine, and testosterone (Santus and Baker, 1993).

2.2.2. Penetration Enhancers.

Chemical enhancers (or penetration enhancers) are used to decrease the barrier properties of the stratum corneum. Many different classes of enhancers have been identified, including cationic, anionic, and nonionic surfactants (sodium dodecyl sulfate, polyoxamers); fatty acids and alcohols (ethanol, oleic acid, lauric acid, liposomes); anticholinergic agents (benzilonium bromide, oxyphenonium bromide); alkanones (n-heptane); amides (urea, N,N-diethyl-m-toluamide); fatty acid esters (n-butyrate); organic acids (citric acid); polyols (ethylene glycol, glycerol); sulfoxides (dimethylsulfoxide); and terpenes (cyclohexene) (Hadgraft and Guy, 1989; Walters, 1989; Williams and Barry, 1992; Chattaraj and Walker, 1995).

Most of these enhancers interact either with the skin, or with the drug. Interactions with the skin include enhancer partitioning into the stratum corneum, causing disruption of the lipid bilayers (azone, ethanol, lauric acid), binding and disruption of the proteins within the stratum corneum (sodium dodecyl sulfate, dimethyl sulfoxide), or hydration of the lipid bilayers (urea, benzilonium bromide). Drug interactions include modifying the drug into a more permeable state (a prodrug), which would then be metabolized inside the body back to its original form (6-fluorouracil, hydrocortisone) (Hadgraft, 1985); or increasing drug solubilities (ethanol, propylene glycol). In addition, many enhancers may include several mechanisms in their effects. For example, ethanol can simultaneously increase the drug solubility within the donor solution, as well as increasing drug partitioning into the stratum corneum. Thus, it has the paradoxical effect of decreasing the diffusion of certain compounds, such as steroids, across the skin (Johnson, 1996).

Despite a great deal of research (well over 200 compounds have been studied) (Chattaraj and Walker, 1995), there are still no universally applicable mechanistic theories for the chemical enhance-

ment of molecular transport. Most of the work in chemical enhancers has been done largely on a trial-and-error basis (Johnson, 1996).

2.2.3. *Sonophoresis (Ultrasound, Phonophoresis).*

Sonophoresis (also called ultrasound or phonophoresis) is the application of high-frequency (>20 kHz), low intensity (<1 W / cm^2) sound waves to the skin. Most commonly used are "therapeutic" ultrasound ranges (1 to 3 MHz), which have already been established to be safe when applied to humans (Williams, 1983). Enhanced transport occurs primarily due to heating of the skin (Kost, *et al.*, 1989).

However, at "low frequency ultrasound" ranges (20 kHz to 1 MHz), ultrasound is believed to induce cavitation (the formation of gas bubbles) within the lipid bilayers of the stratum corneum. Both stable cavitation (gas bubbles that oscillate at the applied sound frequency) and transient cavitation (bubbles that form and spontaneously implode) occur within the lipid bilayers, causing disruption of the bilayers and allowing molecular transport to take place (Bommannan, *et al.*, 1992 [a]; Bommannan, *et al.*, 1992 [b]; Hsieh, 1994; Mitragotri, *et al.*, 1995 [b]). Several large compounds (insulin, erythropoeitin) have been transported by sonophoresis across the skin at therapeutically useful levels (Mitragotri, *et al.*, 1995 [a]).

2.2.4. *Iontophoresis.*

Iontophoresis can be used to transport drugs or other molecules across the skin. This low-voltage method involves the application of a small, usually constant current to the skin (typically <0.1 to 0.5 mA / cm^2) (Tyle, 1986; Banga and Chien, 1988; Burnette, 1989; Chien and Banga, 1989; Singh and Roberts, 1989; Cullander and Guy, 1992; Amsden and Goosen, 1995; Guy, 1996) to cause molecular transport to occur. Iontophoretic transport occurs primarily through the hair follicles and sweat ducts in the skin (Abramson and Gorin, 1940; Abramson and Engel, 1942; Grimnes, 1984; Burnette and Marrero, 1986; Burnette and Ongpipattanakul, 1988; Cullander and Guy, 1991; Scott, *et al.*, 1993; Chen, *et al.*, 1998 [b]; Chen, *et al.*, in press [b]), although some transport may also be occurring through the corneocytes as well (Potts, *et al.*, 1992; Monteiro-Riviere, *et al.*, 1994).

Iontophoresis has been used successfully in many clinical settings (Abramson, 1941; Schwarz, *et al.*, 1968; Arvidsson, *et al.*, 1984; Sloan and Soltani, 1986; Banga and Chien, 1988; Duvanel, *et al.*, 1988; Chien, *et al.*, 1989; Singh and Roberts, 1989; Meyer, *et al.*, 1990; Ledger, 1992); however, electrical currents greater than 0.5 mA / cm^2 can stimulate nerves within the skin, causing pain or

irritation, and generally limiting its use (Zlotgorski, 1987; Banga and Chien, 1988; Burnette and Ongpipattanakul, 1988; Ledger, 1992). Molecular transport occurs on a scale of a few minutes. Transport occurs primarily by electrical drift, although some transport also occurs by electroosmosis. This phenomenon has been used advantageously in the extraction of glucose (Burnette, 1989).

2.3. High-Voltage Pulsing Causes Electroporation.

Electroporation is believed to be the creation of transient, nanometer-sized pores in lipid bilayer membranes by the application of short, high-voltage pulsing (Neumann, *et al.*, 1989; Chang, *et al.*, 1992). During electroporation, large increases in molecular flux and ion transport occur across the membrane, and changes in membrane structure are thus inferred. Electroporation is a phenomenon found in all lipid bilayer membrane systems (planar lipid bilayer membranes, plasma membranes in cells, and the skin), and is reversible under certain conditions (Weaver, 1993 [b]).

The mechanism for electroporation is not fully understood. The "pore" in electroporation is defined to be some type of aqueous pathway created during the high-voltage pulse. Inferential evidence supports an opening appearing in the lipid membrane during the pulse (Neumann, *et al.*, 1989; Chang and Reese, 1990; Chang, *et al.*, 1992; Orlowski and Mir, 1993; Weaver, 1993 [a]).

2.3.1. Electroporation of Cells and Planar Membranes.

Although electroporation has commonly been used to introduce DNA, RNA, or proteins into cells (Neumann, *et al.*, 1982; Potter, 1988), the mechanism is not fully understood. Typical electroporation waveforms for cells or lipid bilayer membranes may be square or exponentially-decaying, with a transmembrane voltage of ~1 V and a pulse duration of 10 μs to 10 ms (Neumann, *et al.*, 1989; Chang and Reese, 1990; Chang, *et al.*, 1992; Orlowski and Mir, 1993; Weaver, 1993 [b]). During short pulses (0.1 to 10 μs) of less than 1 V, medium pulses (10 to 100 μs) of 0.5 to 1 V, and long pulses (≥1 ms) of 0.2 to 0.5 V, electroporation of cells and membranes is generally reversible (Benz and Zimmermann, 1980; Neumann, *et al.*, 1989).

The mechanism for pore formation in cells or lipid membranes is believed to be as follows. During the high-voltage pulse, hydrophobic or "primary" pores are created in the lipid membrane (Figure 2.6a) and can increase in size up to ~10 nm in diameter (Barnett and Weaver, 1991; Freeman, *et al.*, 1994). After the pulse, the lipid molecules composing the pore rearrange to form hydrophilic or "secondary" pores in ~10 ms, that are ~1 nm in diameter (see Figure 2.6b) (Abidor, *et al.*, 1979; Glaser, *et al.*, 1988). These secondary pores later disappear in >10 s (Glaser, *et al.*, 1988).

2.3.2. *Electroporation of Human Skin.*

Recently, high-voltage pulsing has been applied to biological tissues (Grasso, *et al.*, 1989; Powell, *et al.*, 1989; Okino, *et al.*, 1992; Salford, *et al.*, 1993; Sukharev, *et al.*, 1994), including human skin (Prausnitz, *et al.*, 1993 [a]), to increase the rate of molecular transport for drug delivery applications.

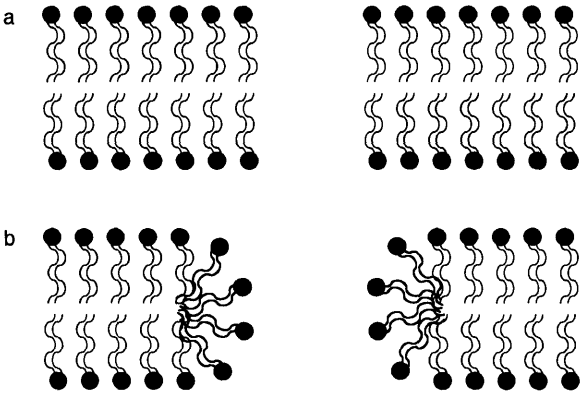

Figure 2.6. Hydrophobic (a) and hydrophilic (b) pores. The hydrophobic pores form during the high-voltage pulse. The lipid molecules then spontaneously rearrange after the pulse to form hydrophilic pores. Based on a drawing from Glaser, *et al.* (1988).

Molecules that have been successfully transported across the skin include charged, fluorescent molecules such as calcein (Prausnitz, *et al.*, 1993 [a]; Prausnitz, *et al.*, 1993 [c]; Prausnitz, *et al.*, 1994; Pliquett, *et al.*, 1995 [b]; Kost, *et al.*, 1996; Pliquett and Weaver, 1996 [a]; Pliquett and Weaver, 1996 [b]; Pliquett, *et al.*, 1996 [b]; Prausnitz, *et al.*, 1996 [b]; Chen, *et al.*, 1998 [b]; Chen, *et al.*, 1998 [c]; Vanbever, *et al.*, submitted), sulforhodamine (Kost, *et al.*, 1996; Pliquett and Weaver, 1996 [a]; Pliquett, *et al.*, 1996 [b]; Chen, *et al.*, 1998 [b]; Chen, *et al.*, 1998 [c]; Vanbever, *et al.*, submitted), lucifer yellow (Prausnitz, *et al.*, 1993 [a]; Chen, *et al.*, 1998 [c]), and cascade blue (Chen, *et al.*, 1998 [c]). Several drugs have also been transported across the skin during high-voltage pulsing, including luteinizing hormone releasing hormone (LHRH) (Bommannan, *et al.*, 1994; Riviere, *et al.*, 1995), metoprolol (Vanbever, *et al.*, 1994; Vanbever and Préat, 1995), fentanyl (Vanbever, *et al.*, 1996 [a]; Vanbever, *et al.*, 1996 [b]; Vanbever, *et al.*, 1998 [a]; Vanbever, *et al.*, 1998 [b]), domperidone (Jadoul and Préat, 1997 [a]), alnitidan (Jadoul, *et al.*, 1998), and cyclosporin A (Wang, *et al.*, 1998). Larger molecules have also been successfully transported across the skin, including heparin (Prausnitz, *et al.*, 1995 [b]; Vanbever, *et al.*, 1997; Weaver, *et al.*, 1997), and several oligonucleotides (Zewert, *et al.*, 1995).

High-voltage pulsing has been directly applied clinically to humans for the treatment of head and neck tumors. Bleomycin, a drug used to treat the tumors, was not delivered across the skin by high-voltage pulsing, but rather was directly injected into the body. High-voltage pulsing was then applied to the head and neck tumors, causing the bleomycin dissolved in the bloodstream to become incorporated into the tumor cells, which in turn caused the tumor cells to die. Significant reductions in tumor size were noted after both high-voltage pulsing and bleomycin were applied to the tumor, compared to controls of high-voltage pulsing only or bleomycin only. Side effects noted during treatment were some muscle twitches during pulsing and slight edema after pulsing (Mir, *et al.*, 1991; Belehradek, *et al.*, 1993).

In skin electroporation, new aqueous pathways are created across the stratum corneum, through which molecular transport takes place. The aqueous pathways that form during high-voltage pulsing across the stratum corneum are hypothesized to be the result of rearrangements of lipids within the lipid bilayers surrounding the corneocytes (Prausnitz, *et al.*, 1993 [a]; Chizmadzhev, *et al.*, 1995; Pliquett and Weaver, 1996 [a]; Chizmadzhev, *et al.*, 1998 [a]).

Typically, the high-voltage pulses applied to the skin are exponentially decaying pulses, ~1 ms long (Prausnitz, *et al.*, 1993 [a]), although longer pulses have been tried (Vanbever, *et al.*, 1998 [b]; Vanbever, *et al.*, submitted). The voltage drop that forms across the stratum corneum is typically ~100 V_{skin}. The voltages across the dermis and epidermis are usually much smaller and negligible, due to the much lower electrical resistivities of the dermis and epidermis, compared to the stratum corneum. Stratum corneum voltages less than ~50 V_{skin} appear to be insufficient to cause significant molecular transport during pulsing (Chen, *et al.*, 1998 [c]; Chizmadzhev, *et al.*, 1998 [a]).

The high-voltage pulses are usually applied at the rate of one pulse every 5 s for 1 h (~720 pulses totally), although this frequency and duration were chosen somewhat arbitrarily (Prausnitz, *et al.*, 1993 [a]); quicker and slower rates of pulsing have also been applied. Molecular transport usually occurs almost immediately, with detectable levels of transport after only about a minute of pulsing (Chen, *et al.*, 1998 [c]). This is significantly much faster than the drug transport rates observed during passive delivery, where drug transport is usually measured in hours, or in iontophoresis, where transport occurs on a time scale of several minutes.

During a high-voltage pulse, aqueous pathways are created in the stratum corneum and the electrical resistivity of the skin drops dramatically, by up to 4 orders of magnitude (Prausnitz, *et al.*, 1993 [a]). Molecular transport takes place across the new pathways created during the pulse (Pliquett, *et al.*, 1996 [b]). After the pulse, the pathways begin to close, and the skin begins to recover its barrier properties.

2.3.3. Combination of Skin Electroporation with Other Methods.

Further enhancements in transdermal drug delivery have also been achieved by combing high-voltage pulsing with other transdermal enhancement techniques. Studies combining high-voltage pulsing with ultrasound (Kost, *et al.*, 1996), iontophoresis (Bommannan, *et al.*, 1994), or novel chemical enhancers (Vanbever, *et al.*, 1997; Weaver, *et al.*, 1997) have all shown synergistic increases in molecular transport. An interesting chemical enhancer for skin electroporation was demonstrated by using long macromolecules, such as dextrans or polylysines, as the chemical enhancer (Weaver, *et al.*, 1997; Vanbever, *et al.*, 1997; Prausnitz, *et al.*, in press). This enhancement was believed to work essentially by a "foot-in-the-door" approach (Weaver, *et al.*, 1997), where the long, thin

macromolecules appear to keep the aqueous pathways in the skin open longer, allowing more molecular transport to take place.

2.3.4. *New Aqueous Pathways through the Stratum Corneum.*

The stratum corneum is typically modeled as ~100 lipid bilayers in series, with the intercellular lipids and the corneocytes arranged in a bricks-and-mortar pattern (Figure 2.3) (Elias, 1983; Elias, 1988; Wertz and Downing, 1989). Sweat ducts and hair follicles penetrate the stratum corneum from the dermis. There are three potential routes across the skin for molecular transport: through only the lipid bilayers (called the "intracellular" or "tortuous" pathway), through the lipids and keratinocytes (called the "intercellular" or "straight-through" pathway), or through sweat ducts and hair follicles (the "shunt" pathways) (Figure 2.7). Electroporation may involve the creation of new aqueous pathways to increase molecular transport through some or all of these routes.

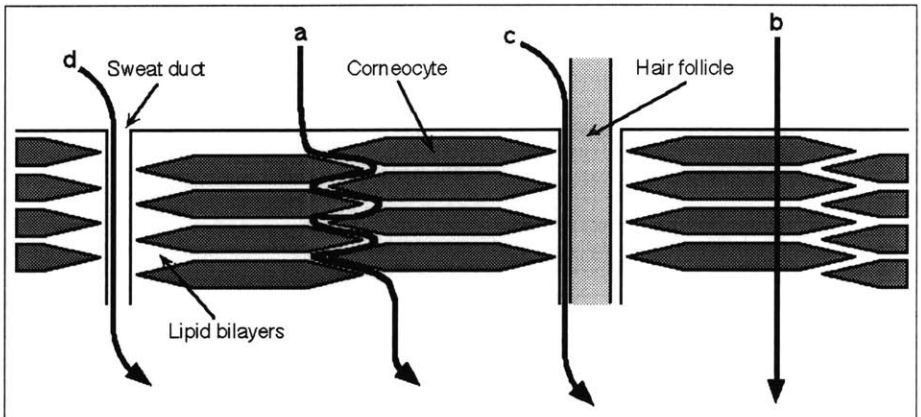

Figure 2.7. Pathways for transport across the stratum corneum. The "tortuous" pathway (a) stays only within the lipids in the stratum corneum. The "straight-through" pathway (b) crosses both lipid bilayers and corneocytes. The "shunt" pathways go through either hair follicles (c) or sweat ducts (d).

One pathway for molecular transport remains in the lipid bilayers and goes around the corneocytes. This pathway is termed the intracellular pathway or the tortuous pathway. Since the lipid bilayers are continuous throughout the stratum corneum, only a few (<10) bilayers have to be penetrated to form a continuous route through the stratum corneum for molecular transport. This is believed to be the main pathway during passive diffusion (Figure 2.7a) (Boddé, *et al.*, 1989; Boddé, *et al.*, 1991; Cullander, 1992; Potts and Guy, 1992).

A transport pathway that crosses both the lipid bilayers and the corneocytes is called the intercellular pathway or the straight-through pathway (Figure 2.7b). This pathway crosses more lipid bilayers, including the corneocyte lipid envelopes (Swartzendruber, *et al.*, 1987), than does the intracellular pathway. This pathway could be part of the skin "reservoir" effect, or the continued high rate of molecular flux out of the skin after high-voltage pulsing (Prausnitz, *et al.*, 1993 [a]) or iontophoresis (Wearley, *et al.*, 1989), as molecules can get trapped within the corneocytes during transport.

A third transport pathway goes through hair follicles (Figure 2.7c), or sweat ducts (Figure 2.7d), called the shunt pathway. The hair follicles and sweat ducts are collectively called the "appendages" of the skin. Only a few lipid bilayers separate the appendages from the dermis. Sweat ducts and hair follicles cover ~0.1% of the skin surface area (Abramson and Gorin, 1940); however, this pathway may still be important for molecular transport (Abramson and Gorin 1940; Grimnes, 1984; Burnette and Marrero, 1986; Burnette and Ongpipattanakul, 1988; Cullander, 1992; Potts and Guy, 1992; Scott, *et al.*, 1992; Scott, *et al.*, 1993).

2.3.5. Formation of Localized Transport Regions (LTRs).

On a larger scale, the aqueous pathways formed during high-voltage pulsing are concentrated in small regions which are distributed randomly throughout the stratum corneum. These regions have been named "LTRs," for "localized transport regions" (Figure 2.8) (Pliquett, *et al.*, 1996 [b]).

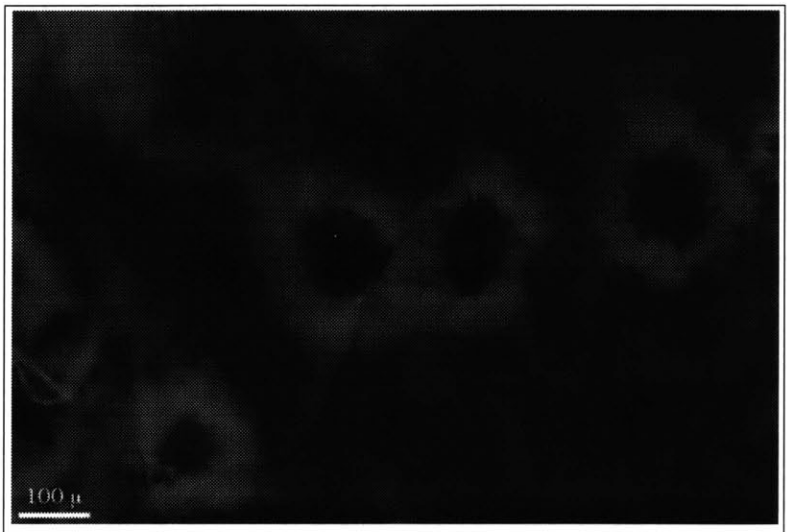

Figure 2.8. LTRs on the surface of the skin. The localized transport regions (LTRs) form randomly on human skin during high-voltage pulsing, seen in this photomicrograph of the surface of the skin as red circles surrounded by green rings. The LTRs are typically ~100 µ in diameter.

The LTRs are typically ~100 µ in diameter. Microscopic analyses of the LTRs have not shown any intrinsic skin structures in these regions, such as sweat ducts or hair follicles. The LTRs form spontaneously and randomly during high-voltage pulsing, but have not been observed during iontophoresis (Chen, *et al.*, 1998 [b]). Experiments have shown that both molecular transport and electrical currents occur primarily through these regions during pulsing (Pliquett, *et al.*, 1996 [b]).

Molecular transport through the LTRs is believed to occur by a combination of electrical drift (ion movement in the electric field during the pulse) and electroosmosis (solvent movement in response to the electric field). Since the LTRs are created spontaneously during pulsing, the number of LTRs does not appear to be limited to pre-existing structures within the skin, a limitation of iontophoretic transdermal methods.

2.3.6. In Vivo *Experiments.*

There have been fewer *in vivo* studies of skin electroporation, and none in humans. In an early study, calcein was successfully transported into the circulating blood of anesthetized hairless rats during high-voltage pulsing, although these studies did not include optimized electrodes or pulsing conditions. Under some pulsing conditions, however, no visible damage to the skin was observed (Prausnitz, *et al.*, 1993 [a]; Prausnitz, *et al.*, 1993 [b]).

In later studies, fentanyl, a potent painkiller, was delivered into hairless rats by high-voltage pulsing. The analgesia caused by fentanyl was measured by the tail-withdraw reaction method in response to a 55 °C water bath, and by head twitching in response to stimulation of the eyes and ears with a small metal rod. Analgesia due to fentanyl transport across the skin occurred very quickly (~5 min) after high-voltage pulsing, but no significant analgesia was observed during transport by iontophoresis or passive diffusion, thus demonstrating both molecular transport and retention of activity during high-voltage pulsing (Vanbever, *et al.*, 1998 [b]).

After high-voltage pulsing had been applied to the hairless rats, the condition of the skin was not significantly different from control specimens, where acceptable iontophoretic currents had been applied instead of pulsing. The condition of the skin was determined by transepidermal water loss measurements (how fast water was lost through the skin), skin coloration techniques (especially redness), and laser Doppler flowmetry (to measure blood flowrates). All of the skin measurements showed comparable skin irritation for both high-voltage pulsing and iontophoresis (Vanbever, *et al.*, 1998 [a]).

In a different set of experiments, LHRH was delivered across an isolated perfused porcine skin flap by either iontophoresis, or iontophoresis plus several high-voltage pulses. After the experiment, the skin was assessed using histological evaluation, and various tests for erythema (redness) and edema (swelling). The addition of several high-voltage pulses to iontophoresis did not result in any more irritation than iontophoresis alone (Riviere, *et al.*, 1995). Thus, as shown in both systems, the application of high-voltage pulsing to the skin does not irritate the skin any more than does iontophoresis, an already accepted technique.

3. Electrical Properties of Phosphate-Buffered Saline (PBS).

In skin electroporation research, many authors have reported the average molecular flux through the skin as a function of the voltage applied to the permeation chamber (Prausnitz, *et al.*, 1993 [a]; Vanbever, *et al.*, 1994; Prausnitz, *et al.*, 1995 [b]; Vanbever and Préat, 1995; Vanbever, *et al.*, 1996 [a]; Vanbever, *et al.*, 1996 [b]; Vanbever, *et al.*, submitted). However, it has been shown that the peak transdermal voltage governs molecular transport, not the applied voltage (Pliquett and Weaver, 1996 [a]). Thus, an accurate measurement of the transdermal voltage is vital in understanding the phenomenon of skin electroporation. Typically, the transdermal voltage is measured by placing two additional "measurement" or "sensing" electrodes on either side of the skin, between the two pulsing electrodes. Directly using the pulsing electrodes for voltage measurements could introduce problems with electrochemistry or electrode polarization.

However, the transdermal voltage cannot be measured simply by placing the two measurement electrodes directly onto the skin itself. If the electrodes were placed flush against the skin, there could be pinching or shearing of the skin, as well as electrochemical reactions with the skin. Thus, there always should be a slight gap between the measurement electrodes and the skin, filled with an electrolytic solution. Typically the electrolytic solution is phosphate-buffered saline (PBS) (Prausnitz, *et al.*, 1993 [a]).

In many experiments, such as the ones described in this thesis, there may be other components between the two measurement electrodes besides PBS and the skin, such as polyacrylamide gel (Appendices IV and V) or polycarbonate membranes (Section 5.3.4). Typically, however, the resistivities of these things are comparable to the resistivity of PBS.

Thus, for accurate measurements of the transdermal voltage during high-voltage pulsing, it is first necessary to get an accurate measurement of the resistance of only PBS within the chamber. Once this is known, the voltage drop across the skin during pulsing can be calculated, using Ohm's Law and subtracting the contribution due to PBS.

3.1. Method of Determining the Resistance of PBS.

Applying Ohm's Law to find the transdermal voltage, U_{skin}, gives the following equation:

$$U_{skin} = U_{inner} - I\,R_{PBS}^{Donor} - I\,R_{PBS}^{Receptor}, \tag{3.1}$$

where U_{inner} is the voltage drop across the inner measurement electrodes during the pulse, I is the current through the skin during the pulse, and R_{PBS}^{Donor} and $R_{PBS}^{Receptor}$ are the resistances of the PBS solutions in the donor and receptor compartments, respectively. The two PBS resistances can be lumped together into one overall resistance, R_{PBS}, giving the following equation:

$$U_{skin} = U_{inner} - I\,R_{PBS}. \tag{3.2}$$

R_{PBS} is a constant that depends on the actual geometry of the apparatus. It can be estimated from the resistivity of saline, ρ_{PBS}, an intrinsic property, by this equation:

$$R_{PBS} = \frac{\rho_{PBS}\,L}{A}, \tag{3.3}$$

where L is the distance between the measurement electrodes and A is the cross-sectional area between them. This equation is exact only for an electric field between two infinite parallel plates (a perfectly homogeneous field) (Sears, *et al.*, 1987); however, it can be used as a reasonable approximation of the resistances in this system. The resistivity of saline is typically given as 0.67 Ω m (from Lide, 1991).

Practically speaking, it is better to directly measure the resistance of PBS in the system rather than estimating it from the resistivity and the geometry of the system. Directly measuring the resistance of PBS accounts for any non-idealities in the system. Setting U_{skin} to 0 in Equation 3.2 and solving for R_{PBS} yields the following:

$$R_{PBS} = \frac{U_{inner}}{I}. \tag{3.4}$$

By separately measuring U_{inner} and I during pulsing, without any skin present ($U_{skin} = 0$), the constant R_{PBS} can thus be directly obtained.

Since R_{PBS} was an extrinsic property that depended on the actual geometry of the system, each time a new experimental apparatus was constructed, the experiments had to be repeated to obtain a new value for R_{PBS}. A check on each value of R_{PBS} was also obtained by solving Equation 3.3 for each new geometry.

3.2. Preparation of PBS.

Phosphate-buffered saline (PBS) was prepared by combining 138 m$\underline{M}$ NaCl (or 16 g NaCl per 2 l water) (Sigma, St. Louis, MO), 8.1 m$\underline{M}$ Na_2HPO_4 (2.30 g) (Mallinckrodt, Paris, KY), 2.7 m$\underline{M}$ KCl (0.40 g) (Mallinckrodt), and 1.1 m$\underline{M}$ KH_2PO_4 (0.40 g) (Mallinckrodt) in de-ionized water (for a total of

150 mM). The solution was adjusted to pH 7.4 by adding HCl (Mallinckrodt) and NaOH (Mallinckrodt) as necessary (Prausnitz, *et al.*, 1993 [a]). The solution was then stirred under vacuum for >30 min to de-gas the solution (see Section 4.1.3).

3.3. PBS Resistance in the Original System (Prausnitz, *et al.* 1993 [a]).

The first experimental system used to study skin electroporation *in vitro* simply consisted of two pulsing electrodes and the skin in a glass permeation chamber, surrounded by PBS solution (Prausnitz, *et al.*, 1993 [a]; also see Appendix II). Since there were no inner measurement electrodes present, the resistance of PBS was determined by using the voltage settings on the high-voltage pulser itself ($U_{applied}$*) and measuring the current during the pulse. Thus, $U_{applied}$ was used in place of U_{inner} in Equation 3.4 (Prausnitz, *et al.*, 1993 [a]):

$$R_{PBS} = \frac{U_{applied}}{I}. \tag{3.5}$$

By applying pulses to the chamber without any skin present, and measuring the resulting current, Prausnitz, *et al.* (1993 [a]) determined R_{PBS} to be 480 Ω.

Based on the original system described in Prausnitz, *et al.*, (1993 [a]), the author of this thesis, using the same equipment, independently measured A to be 0.63 cm^2 and L to be 6.1 cm. With these geometrical values, Equation 3.3 estimated R_{PBS} to be 649 Ω. The large discrepancy between the measured (480 Ω) and calculated (649 Ω) values for R_{PBS} shows the importance of independently determining the transdermal voltage with measurement electrodes during pulsing.

3.4. PBS Resistance in the Original System, using a High-Voltage Probe.

Because of the discrepancy between the measured and the calculated values for R_{PBS}, new measurements of R_{PBS} were taken with a grounded, 1000× high-voltage probe (Tektronix, Wilsonville, OR), connected to an inner pair of measurement electrodes. The voltage drop across the inner electrodes was determined by measuring the voltage at each electrode separately on subsequent pulses,

---

* $U_{applied}$ is used in this thesis to represent the voltage produced by the high-voltage pulser. Although the notation $U_{electrode}$ or U_{elect} is more commonly used in the literature, this notation could become confused with the voltage drop appearing across the inner electrodes (called U_{inner} in this thesis). Thus, $U_{applied}$ is used instead.

and subtracting the two measurements. These measurements of R_{PBS} are shown in Figure 3.1, after a series of pulses were applied to the permeation chamber without any skin present.

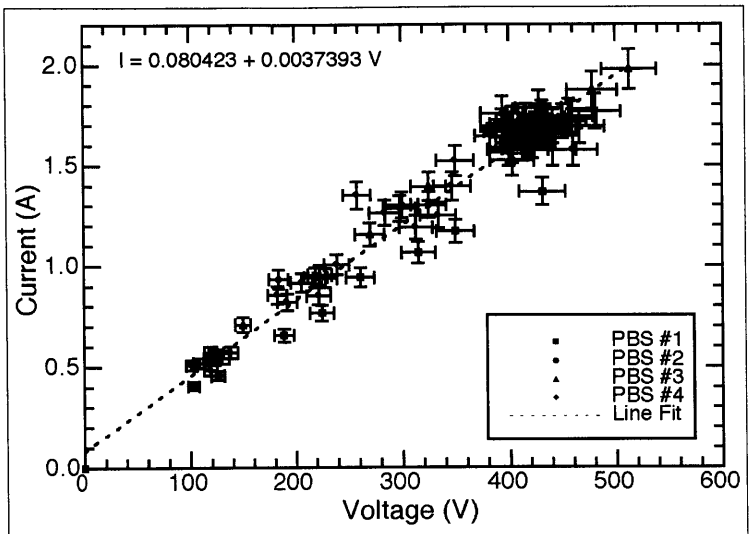

Figure 3.1. Current versus voltage relationship for PBS. Four different PBS solutions in the original permeation chamber are plotted here. Measurements of the voltage-current relationship for each of the four solutions all fall on the same line. Thus, PBS behaves as an ideal Ohmic resistance of 271 Ω.

The peak current during each pulse is plotted against the peak voltage drop across the inner electrodes. For an ideal Ohmic resistance, this plot should yield a straight line through the origin (Sears, *et al.*, 1987). As can be seen in Figure 3.1, these experiments were repeated four times, using new PBS solutions and new electrodes each time. The four PBS solutions fall on the same line, and are indistinguishable. The reciprocal of the slope, or R_{PBS}, is 271 Ω. Thus, not only did PBS behave like an ideal Ohmic resistance, it could be consistently prepared every time.

The distance between the inner measurement electrodes, L, was 3.1 cm and A, the cross-sectional area of the chamber, was found to be 0.64 cm^2. Equation 3.3 would thus estimate R_{PBS} to be 330 Ω, reasonably close to the measured value of R_{PBS} of 271 Ω.

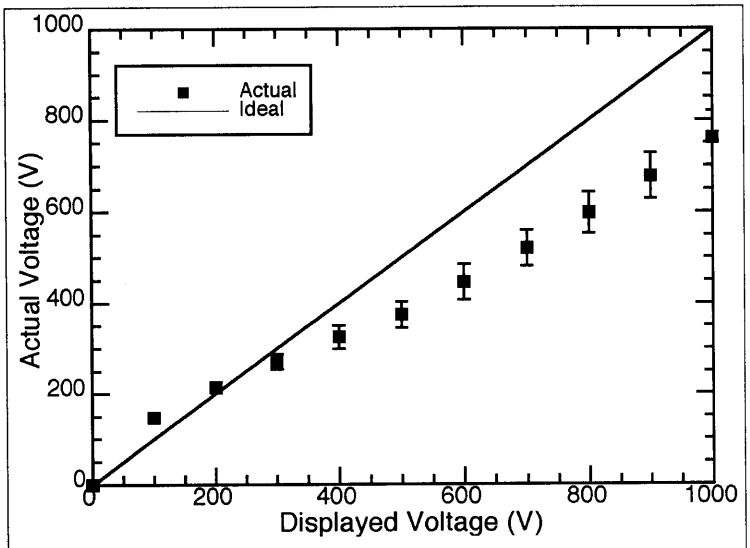

Figure 3.2. Deviation of the actual voltage versus the displayed voltage on a high-voltage pulser. The displayed voltage on the pulser (Electroporation System 600, BTX), and the actual voltage produced by the pulser can be off by as much as 20%. The transdermal voltage should thus be measured independently, and the display on the high-voltage pulser should not be used.

In a different set of experiments, shown in Figure 3.2, the voltage actually produced by one of the high-voltage pulsers (Electroporation System 600, BTX, San Diego CA) was plotted against the voltage the pulser was set to produce. Note that especially at high-voltages, the voltage the pulser shows that it is producing and the voltage actually being produced can be off by more than 20%. Thus, the display on the pulser itself should not be used for the transdermal voltage measurements (see Section 3.3).

3.5. PBS Resistance in the Flow-Protection System (Appendix III).

The flow-protection system described in Appendix III consisted of the two outer pulsing electrodes surrounded by polyacrylamide gel and bathed in a stream of PBS. Between the two inner measurement electrodes were the skin and PBS solution. During experimentation with this equipment, the voltage measurements were switched from the grounded voltage probe to an active differential high-voltage probe (Active Differential Probe B9017RT, Yokogawa, Newman, GA), allowing the voltage drop to be directly measured, instead of determining the difference between two subsequent voltage measurements. Also, a newly redesigned permeation chamber was used, featuring a smaller inner volume. This caused the measurement electrodes to be positioned closer together.

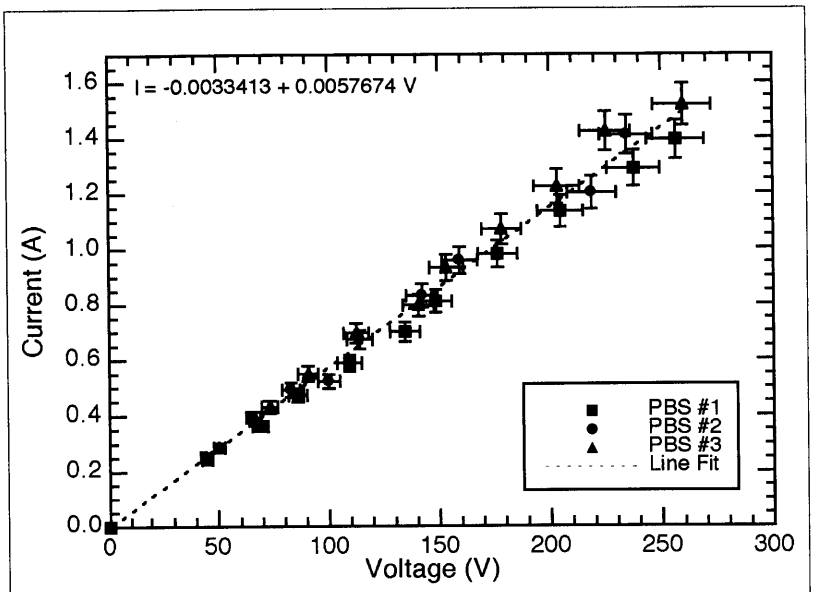

Figure 3.3. Current versus voltage relationship for the flow-protected electrodes, grounded probe. Voltage measurements were taken separately on inner electrodes on either side of the skin during subsequent pulses. The line fit gave a resistance of 173 Ω. Note the overlap of the three PBS solutions, indicating that PBS was made consistently each time.

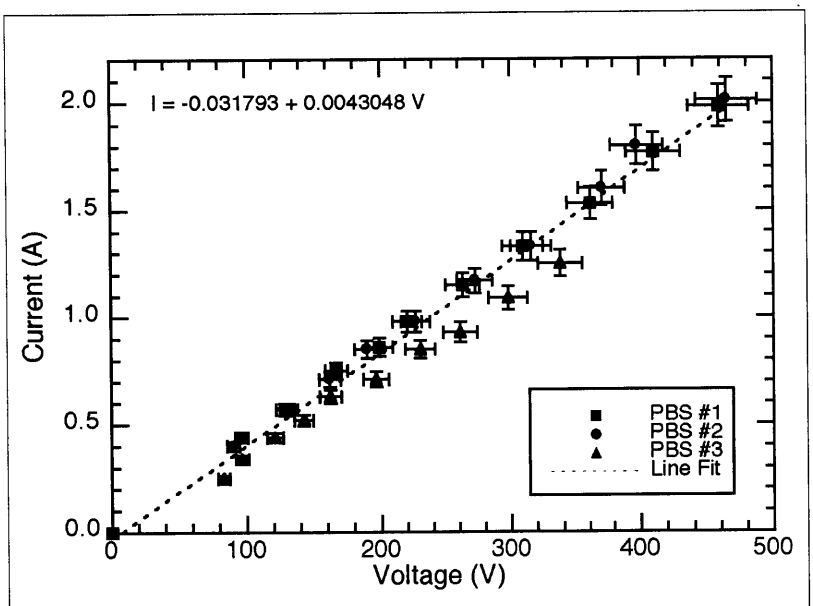

Figure 3.4. Current versus voltage relationship for the flow-protected electrodes, differential probe. The voltage drop across the inner electrodes was measured using a differential high-voltage probe during pulsing. Measurements of the three solutions overlap, indicating that the PBS solutions were made consistently each time. The resistance of PBS was found to be 232 Ω. Compare with Figure 3.3.

Figure 3.3 shows the R_{PBS} measurements using the original grounded high-voltage probe, and Figure 3.4 shows the R_{PBS} measurements using the new differential high-voltage probe, in the new permeation chamber. Each plot shows the results from three different experiments. Each set of experiments used fresh PBS solution and polyacrylamide gel.

The resistance of the PBS solution, as determined by the grounded high-voltage probe, was 173 Ω; however, for the same system, the

differential high-voltage probe found the resistance of PBS to be 232 Ω. The differential high-voltage probe was more accurate, since it directly made single measurements, unlike the grounded high-voltage probe, which used the difference between subsequent measurements in the calculation of R_{PBS}.

The inner volumes of the new permeation chambers were slightly smaller than the original chambers. The cross-sectional area (A) of the inner compartment remained 0.64 cm^2; however, the volume of this compartment was decreased from 3.1 ml to 2.6 ml. The distance between the inner electrodes (L) was shortened from 3.1 cm to 2.4 cm. Equation 3.3 thus estimated R_{PBS} to be 255 Ω.

The estimated value of R_{PBS} (255 Ω) was closer to the measurements made by the differential high-voltage probe (232 Ω), than the grounded probe (173 Ω). Thus, in the remaining skin electroporation experiments, the differential high-voltage probe was used to measure the transdermal voltage.

3.6. PBS Resistance in the Flow-Through System (Appendix IV).

In the flow-through system described in Appendix IV (also see Chen, *et al.*, in press [a]), polyacrylamide gel was used to decrease the volume of the receptor compartment to ~200 µl. The same permeation chambers from the previous section were used here; the decrease in volume was due to additional polyacrylamide gel in the receptor compartment. Tygon and teflon tubing were used to allow PBS solution to flow in and out of the receptor compartment during the experiment. Thus, between the two inner measurement electrodes were the PBS solution, the polyacrylamide gel in the receptor compartment, and two plastic tubes used to allow for PBS flow.

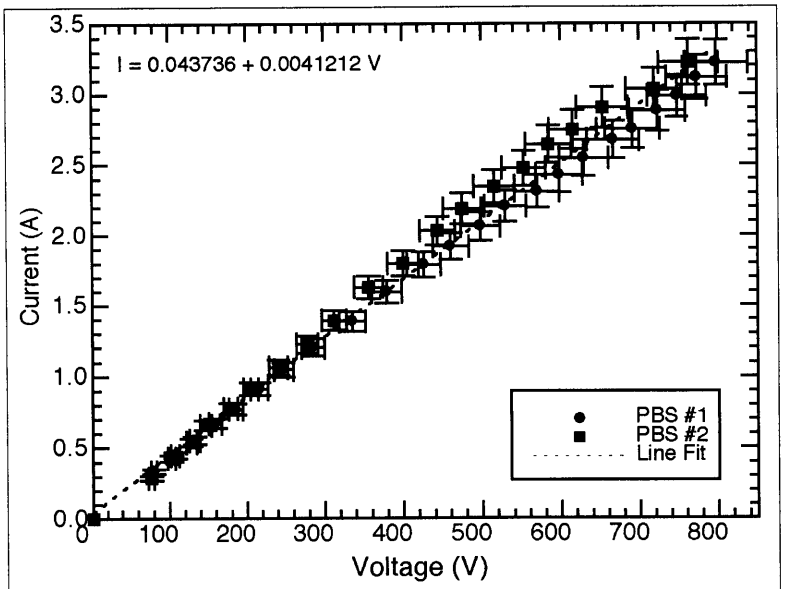

Figure 3.5. Current versus voltage relationship in the flow-through system. Between the inner measurement electrodes were the skin, PBS, polyacrylamide gel, and two plastic tubes. The resistivity of this system was 243 Ω, similar to the value of 232 Ω when no polyacrylamide gel was present.

Despite these modifications, the electrical properties of the system did not change significantly. The resistance of the PBS and the polyacrylamide gel in this new system, after two independent experiments (shown in Figure 3.5), was found to be 243 Ω, similar to the old value of 232 Ω.

The structure of polyacrylamide gel consists of networks of polymer filaments, surrounded by the bathing solution, which in this case was PBS. Thus, the electrical resistivity of polyacrylamide gel

should have been very close to the resistivity of PBS. Experimentally, similar resistivities were found (243 Ω with the gel, versus 232 Ω for only PBS). Assuming that the resistivity of polyacrylamide gel is equal to the resistivity of PBS, then from Equation 3.3, R_{PBS} for this system would be estimated to be 255 Ω. This estimate was very close to what was observed experimentally. Thus, polyacrylamide gel does not contribute to the resistances within the system any more than PBS does.

3.7. PBS Resistance in the Double Flow-Through System (Appendix V).

In the last set of experiments, the donor compartment was fitted with a flow-through system, similar to the one in the receptor compartment. Thus, between the two measurement electrodes were the skin, PBS solution, polyacrylamide gel, and four plastic tubes, to allow the flow of liquid in and out of both the donor and receptor compartments.

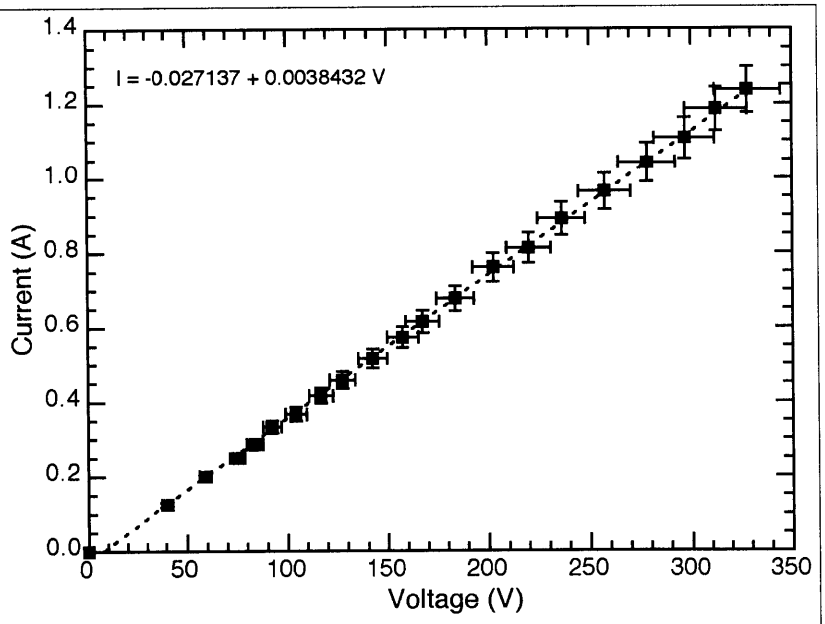

Figure 3.6. Current versus voltage relationship in the double flow-through system. Despite differences in the amount of polyacrylamide gel present, the measured resistance, 260 Ω, was comparable to previous measurements using the same chamber (232 Ω and 243 Ω, from Figures 3.4 and 3.5, respectively).

As previously described, the resistivity of the polyacrylamide gel was found to be comparable to the resistivity of PBS. Thus, since the same glass chamber was used in these experiments, with the same geometry, Equation 3.3 would still estimate 255 Ω for R_{PBS}.

Experimentally, a value of 260 Ω was measured for R_{PBS}, as shown in Figure 3.6. Although only one set of measurements was performed, the value of R_{PBS} that was found was very close to the previously measured values (232 Ω and 243 Ω), as well as the estimated value (255 Ω). Thus, even though nearly all of the chamber was filled with polyacrylamide gel, the resistance of the system was still comparable to only PBS.

3.8. The System is Non-Ohmic at Very High Voltages.

In some experiments, the pulser was set to produce very high voltages ($U_{applied}$ > 1000 V)). This is higher than the highest voltage actually used during any of the skin electroporation experiments described in this thesis ($U_{applied}$ ≤ 1000 V).

In this regime, some unpredictable deviations in the current versus voltage relationship (Ohm's Law) were observed, as shown in Figure 3.7. Since the transdermal voltages in this regime could not be accurately determined, the higher applied voltages were not used.

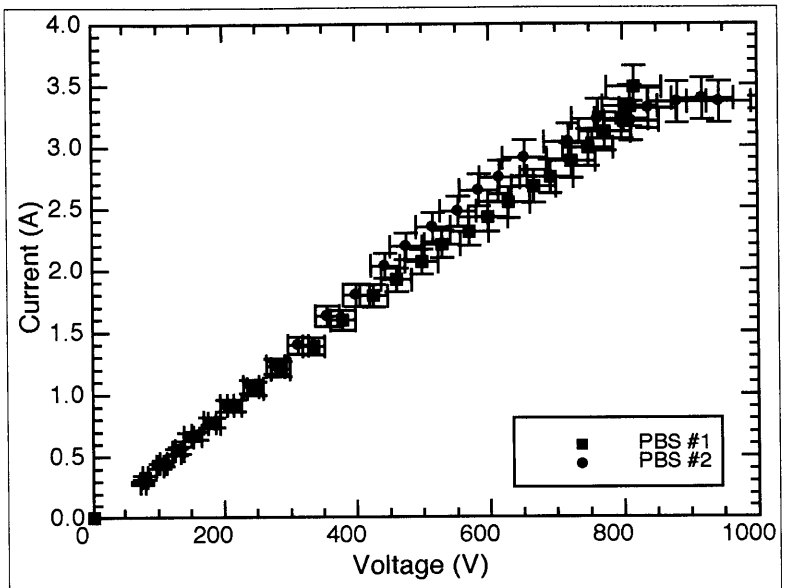

Figure 3.7. Current versus voltage relationship at very high voltages. At large applied voltages ($U_{applied}$ > 1000 V, which corresponds to U_{inner} ~ 1000 V), PBS no longer behaves as an ideal Ohmic resistance.

3.9. R_{PBS} is Constant in the Skin Electroporation Experiments.

In conclusion, PBS was found to behave as an ideal Ohmic resistance at low to moderate applied voltages ($U_{applied}$ < 1000 V). PBS could be made consistently every time. The measured values of PBS resistance agreed with resistance values estimated from the known resistivity of saline (0.67 Ω m) (from Lide, 1991), and the geometry of the system (Equation 3.3).

The polyacrylamide gel used in these experiments, which was composed of polymer filaments surrounded by PBS solution, also had similar resistivities as PBS. Thus, the resistivity of the polyacrylamide gel was assumed to be that of PBS in subsequent calculations.

At very high voltages ($U_{applied}$ > 1000 V), significant deviations from linearity were seen in the current versus voltage relationship. Fortunately, these voltages were much higher than the voltages used in the skin electroporation experiments described in this thesis, and thus the resistance of PBS between the two measurement electrodes was assumed to be constant during the skin electroporation experiments.

4. Physical Properties of the Fluorescent Tracers.

Although many biologically relevant substances have been successfully transported across the skin by skin electroporation, such as luteinizing hormone releasing hormone (LHRH) (Bommannan, *et al.*, 1994; Riviere, *et al.*, 1995), heparin (Prausnitz, *et al.*, 1995 [b]; Vanbever, *et al.*, 1997; Weaver, *et al.*, 1997), oligonucleotides (Zewert, *et al.*, 1995; Regnier, *et al.*, in press [a]), cyclosporin A (Wang, *et al.*, 1998), and several small molecular weight drugs (Vanbever, *et al.*, 1994; Vanbever and Préat, 1995; Vanbever, *et al.*, 1996 [a]; Vanbever, *et al.*, 1996 [b]; Jadoul and Préat, 1997 [a]; Jadoul, *et al.*, 1998; Vanbever, *et al.*, 1998 [b]), surrogate fluorescent tracers are often used instead of biological compounds in molecular transport studies, since the tracers can be selected to have certain desired physical properties.

In particular, the tracers should have small to medium molecular weights, to mimic the sizes of typically important biological compounds. Also, the tracers should be hydrophilic, so that they remain in solution (and within the aqueous pathways created during pulsing), and the tracers should not partition passively through the skin. The tracers should be charged, to facilitate transport during pulsing. Finally, the tracers should give a very strong signal and be quantifiably detectable at concentrations as low as 10^{-8} M, as well as being easy to use and prepare.

During the course of this thesis, four fluorescent compounds were identified that had most or all of these physical properties: calcein, sulforhodamine, lucifer yellow, and cascade blue (Table 4.1). Calcein (Prausnitz, *et al.*, 1993 [a]; Prausnitz, *et al.*, 1993 [c]; Prausnitz, *et al.*, 1994; Pliquett, *et al.*, 1995 [b]; Kost, *et al.*, 1996; Pliquett and Weaver, 1996 [a]; Pliquett, *et al.*, 1996 [b]; Pliquett and Weaver, 1996 [b]; Prausnitz, *et al.*, 1996 [b]; Chen, *et al.*, 1998 [b]; Chen, *et al.*, 1998 [c]; Vanbever, *et al.*, submitted), sulforhodamine (Kost, *et al.*, 1996; Pliquett and Weaver, 1996 [a]; Pliquett, *et al.*, 1996 [b]; Chen, *et al.*, 1998 [b]; Chen, *et al.*, 1998 [c]; Vanbever, *et al.*, submitted), and lucifer yellow (Prausnitz, *et al.*, 1993 [a]; Chen, *et al.*, 1998 [c]) have been used in previous skin electroporation studies. All four compounds have similar molecular weights (ranging from 457 Da for lucifer yellow to 623 Da for calcein), and were all negatively charged, varying from -1 for sulforhodamine to -4 for calcein. All four molecules were considered to be very hydrophilic and brightly fluorescent.

However, since molecular transport during skin electroporation depends not only on the applied

Table 4.1. Physical Properties of the Four Fluorescent Tracers.

Name	MW (Da)	Nominal Charge at pH 7.4	K_{ow}	Excitation Wavelength (nm)	Emission Wavelength (nm)	Source (Catalog Number)
Sulforhodamine	607	-1	~0.057	586	607	Molecular Probes (S-359)
Lucifer Yellow	457	-2	<<1	428	535	Molecular Probes (L-453)
Cascade Blue	596	-3	<<1	399	421	Molecular Probes (C-687)
Calcein	623	-4	<<1	496	517	Molecular Probes (C-481)

electrical conditions, but also on the physical properties of the molecules (Prausnitz, *et al.*, 1993 [a]; Pliquett and Weaver, 1996 [a]; Vanbever, *et al.*, 1997; Chen, *et al.*, 1998 [c]; Vanbever, *et al.*, 1998 [c]), a study of the physical properties of these molecules was also needed. This chapter looks at some of the physical properties of these fluorescent tracers. Calcein was studied the most intensely, due to its extensive use as a tracer, and its unusual transport behavior (Pliquett and Weaver, 1996 [b]; Chen, *et al.*, 1998 [c]; Vanbever, *et al.*, submitted).

4.1 Calcein.

In skin electroporation research, one of the most widely used fluorescent tracers is calcein (Prausnitz, *et al.*, 1993 [a]; Prausnitz, *et al.*, 1993 [c]; Prausnitz, *et al.*, 1994; Pliquett, *et al.*, 1995 [b]; Kost, *et al.*, 1996; Pliquett and Weaver, 1996 [a]; Pliquett and Weaver, 1996 [b]; Pliquett, *et al.*, 1996 [b]; Prausnitz, *et al.*, 1996 [b]; Chen, *et al.*, 1998 [b]; Chen, *et al.*, 1998 [c]; Vanbever, *et al.*, submitted), a low molecular weight (623 Da), highly charged, green fluorescent molecule (496 nm excitation, 517 nm emission) (Haugland, 1992; Prausnitz, *et al.*, 1993 [a]; Pliquett and Weaver, 1996 [a]). Calcein was originally picked as a tracer because of its small molecular weight, high electronic charge (nominally -4 at pH 7.4), high hydrophilicity, and intense fluorescence.

Calcein (or 2',7'-bis[[bis(carboxymethyl)amino]methyl] fluorescein; N,N'-[(3',6'-dihydroxy-3-oxospiro-[isobenzofuran-1(3H),9'-[9H]xanthene]-2',7'-diyl)bis(methylene)]bis[N-(carboxymethyl)glycine; CAS #1461-15-0) (Figure 4.1) is a derivative of fluorescein, and it has traditionally been used to detect trace amounts of calcium ions in solution, hence its name. When calcein chelates a calcium ion, it results in a slight shift in its fluorescence spectra. Concentrations as low as 0.08 ppm (or 4.4 μM) of Ca^{2+} can be detected with calcein solutions (Cheng, *et al.*, 1982).

Commercial sources of calcein typically include up to five different isomers besides the 2,7 form (Figure 4.2), which are very difficult to separate (Cheng, *et al.*,

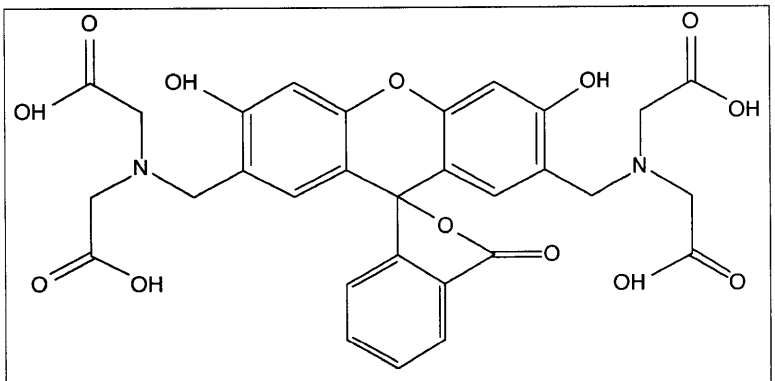

Figure 4.1. The molecular structure of calcein. Calcein is a brightly fluorescent, hydrophilic molecule ($C_{30}H_{26}O_{13}N_2$, 622.54 Da), that is often used in skin electroporation experiments.

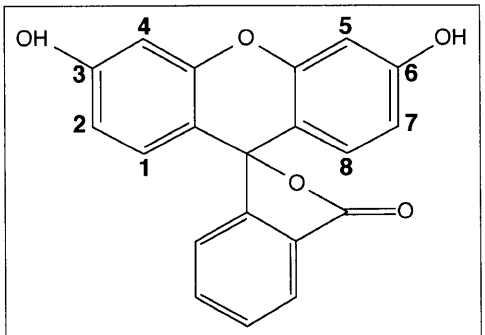

Figure 4.2. The two [bis(carboxymethyl)-amino]methyl groups isomerize to the 2, 4, 5, and 7 positions. Each numbered position is identified in the above figure. There are six different possible isomers of calcein. Only the 2,7 isomer is considered to be the correct form of calcein.

1982; Haugland, 1992). The two [bis(carboxymethyl)amino]methyl groups can isomerize to any two of the 2, 4, 5, and 7 positions on fluorescein, such that only about 50% of the calcein is in the correct 2,7 form. The isomeric mixtures are usually sufficient for Ca^{2+} detection purposes, although high purity calcein (up to 95% pure) can be obtained which has been chromatographically purified (Haugland, 1992; Molecular Probes, personal communication).

When investigators researching skin electroporation began studying the transdermal flux of calcein in real time, they found a puzzling drop in the observed efflux of calcein after repeated pulsing (Pliquett and Weaver, 1996 [a]; Pliquett and Weaver, 1996 [b]; Chen, *et al.*, 1998 [c]; Vanbever, *et al.*, submitted; see also Section 8.2.2). This drop had been seen by different investigators, using different equipment, different pulsing protocols, and even different suppliers of calcein.

The drop in calcein intensity had typically been attributed to the degradation of calcein by either electrochemical by-products, or pH changes due to the pulsing electrodes, instead of a drop in the transdermal flux of calcein across the skin (Pliquett and Gusbeth, in preparation). Another possibility that was proposed was that calcein was chelating calcium ions in the skin as it was transported across, causing its fluorescence to decrease. Further possibilities include quenching of calcein by either light or oxygen, enzymatic degradation by the skin, and the nonspecific binding of calcein to the equipment. However, despite many control experiments, no single cause had been identified. The purpose of the following series of experiments was to determine what the drop in the intensity of calcein was due to.

4.1.1. Calcein Drop Observed in Different Systems.

The drop in calcein efflux with repeated pulsing has been seen in at least three independent systems. The drop was first observed in Pliquett and Weaver (1996 [b]), where pulses were applied from U_{skin} = 65 to 230 V, with a time constant (τ) of 1.1 ms, 1 pulse per minute for 1 h (Figure 4.3). Different electrical conditions were used in Vanbever, *et al.* (submitted), and a much faster drop in calcein fluorescence was observed (in Figure 4.4, 20 pulses were applied, $U_{applied}$ = 300 V, with τ = 100 ms, 1 pulse every 6 min; in Figure 4.5, 20 pulses were applied, $U_{applied}$ = 400 V, τ = 300 ms, 1 pulse every 6 min). In both

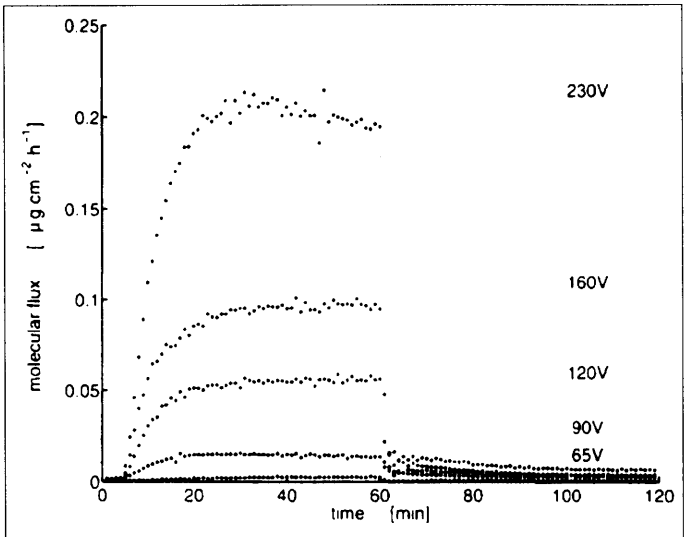

Figure 4.3. The flux of calcein drops with repeated pulsing. The flux at 230 V shows the greatest decrease with repeated pulsing. Pulsing conditions used were U_{skin} = 65 to 230 V, τ = 1.1 ms, 1 pulse every min for 1 h. From Pliquett and Weaver (1996 [b]).

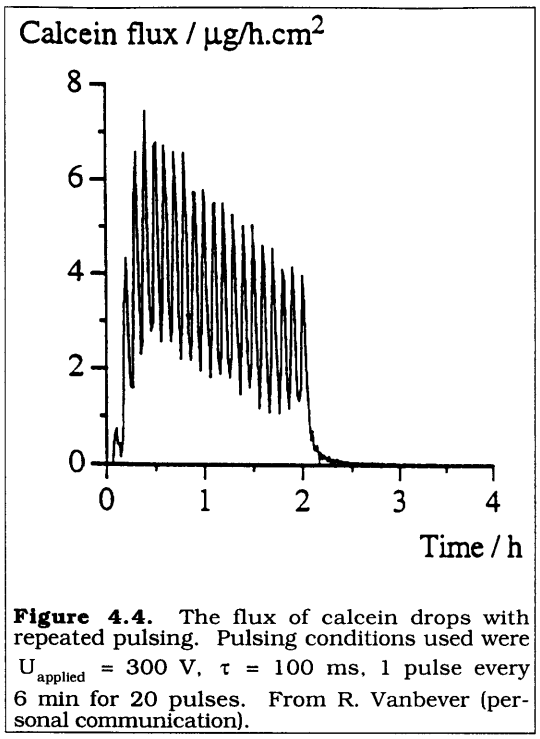

Figure 4.4. The flux of calcein drops with repeated pulsing. Pulsing conditions used were $U_{applied}$ = 300 V, τ = 100 ms, 1 pulse every 6 min for 20 pulses. From R. Vanbever (personal communication).

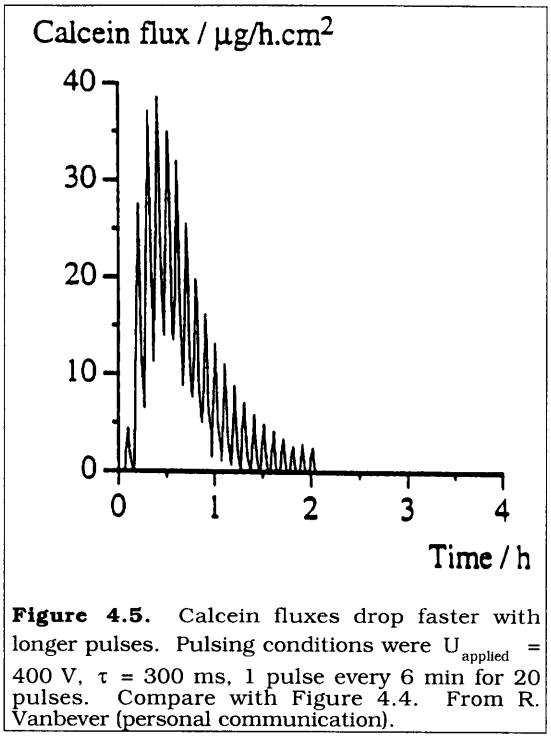

Figure 4.5. Calcein fluxes drop faster with longer pulses. Pulsing conditions were $U_{applied}$ = 400 V, τ = 300 ms, 1 pulse every 6 min for 20 pulses. Compare with Figure 4.4. From R. Vanbever (personal communication).

cases, the fluorescence of calcein began to drop after the first 5 or 6 pulses. Finally, in Chen, *et al.* (1998 [c]) and Section 8.2.2, the drop in calcein fluorescence was observed in both human skin and shed black rat snake skin (Figures 8.4d and 8.8d). The same protocol was used in both cases: $U_{applied}$ = 1000 V, τ = 1 ms, 1 pulse every 5.6 s for 1 h).

These results imply that the drop in calcein fluorescence is real and not simply an artifact of the experimental apparatuses used. At least two different sources of calcein were used (Sigma and Molecular Probes, Eugene, OR), as well as two types of skin (human and snake). The preparation procedures were different for human skin and snake skin (see Section 7.3.1). Despite these variations in electrical protocols, equipment, calcein sources, and types of skin, drops in the fluorescence of calcein were observed in all of these cases.

4.1.2. Calcein has 6 pKa's.

Calcein has 6 pKa values, which indicates that the calcein molecules can be present in solution with charges anywhere from 0 to -6. However, at pH 7.4, most of the calcein is present at charge -4. The pKa's of calcein are shown in Table 4.2 (L represents the calcein molecule). The distribution of calcein at a pH

Table 4.2. Calcein pKa's (Cheng, *et al.*, 1982).

H_6L	$\rightleftharpoons$	H_5L^- + H^+	pK_{a_1}	= 2.1
H_5L^-	$\rightleftharpoons$	H_4L^{2-} + H^+	pK_{a_2}	= 2.9
H_4L^{2-}	$\rightleftharpoons$	H_3L^{3-} + H^+	pK_{a_3}	= 4.2
H_3L^{3-}	$\rightleftharpoons$	H_2L^{4-} + H^+	pK_{a_4}	= 5.5
H_2L^{4-}	$\rightleftharpoons$	HL^{5-} + H^+	pK_{a_5}	= 10.8
HL^{5-}	$\rightleftharpoons$	L^{6-} + H^+	pK_{a_6}	= 11.7

of 7.4, relative to the nominal form (H_2L^{4-}), is shown in Table 4.3.

Table 4.3. Calcein Distribution at pH 7.4, Relative to H_2L^{4-}.

H_6L	5.01×10^{-6}
H_5L^-	3.16×10^{-5}
H_4L^{2-}	6.31×10^{-4}
H_3L^{3-}	1.26×10^{-2}
H_2L^{4-}	1
HL^{5-}	3.98×10^{-4}
L^{6-}	5.01×10^{-5}

Thus, 72.9% of the calcein molecules in PBS solution at pH 7.4 are in the -4 state. The remaining 27.1% of the calcein molecules can be in configurations that vary in charge from 0 to -6. However, calcein retains a negative charge in nearly all of these states. Only 5.01×10^{-4}% of the calcein molecules in solution are not negatively charged (in the H_6L state).

4.1.3. Calcein Not Quenched by Light or Oxygen.

From a stock solution of 10^{-3} M calcein (Molecular Probes) in 150 mM degassed PBS (Section 3.2), a standard curve for calcein in solution was prepared, decreasing by an order of magnitude stepwise, down to a final concentration of 10^{-10} M. Fluorescence measurements were taken immediately after the standard curve was prepared (0 h). This is the solid curve shown in Figure 4.6. Further measurements were taken again after 1, 2, and 3 h. Between measurements, the calcein calibration solutions were allowed to sit on an undisturbed bench in the lab. The solutions were not covered, thus permitting exposure to both light and oxygen in the air. However, after degassing, there was no oxygen in solution.

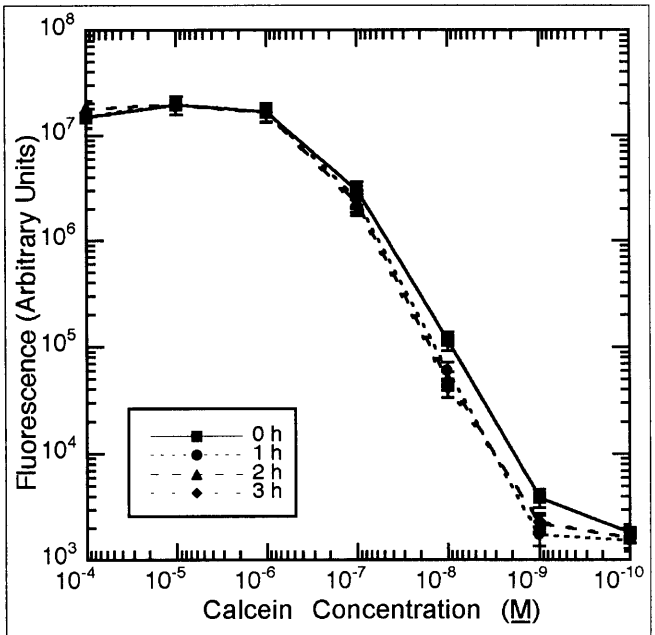

Figure 4.6. Calcein intensities after 3 h of exposure to light and O_2. The fluorescence intensity of calcein in solution drops only slightly after 3 h.

As shown in Figure 4.6, even after 3 h of exposure, there was only a small drop in the fluorescence intensity of calcein. This was most pronounced in the first hour of the 10^{-8} M sample, where the fluorescence decreased from 1.1×10^{-5} (in arbitrary fluorescence units) to 5.9×10^{-4} in the first hour.

However, this drop may not be important, since during a typical skin electroporation experiment, the calcein donor solution is prepared 2 to 3 h before the start of an experiment. The solution is not used immediately, since calcein takes about 30 min to fully dissolve, and a 1 h passive control period

is also needed at the start of the experiment to allow the skin to fully hydrate. After 2 to 3 h of exposure to light and oxygen, the calcein calibration solutions do not continue to decrease as quickly in intensity.

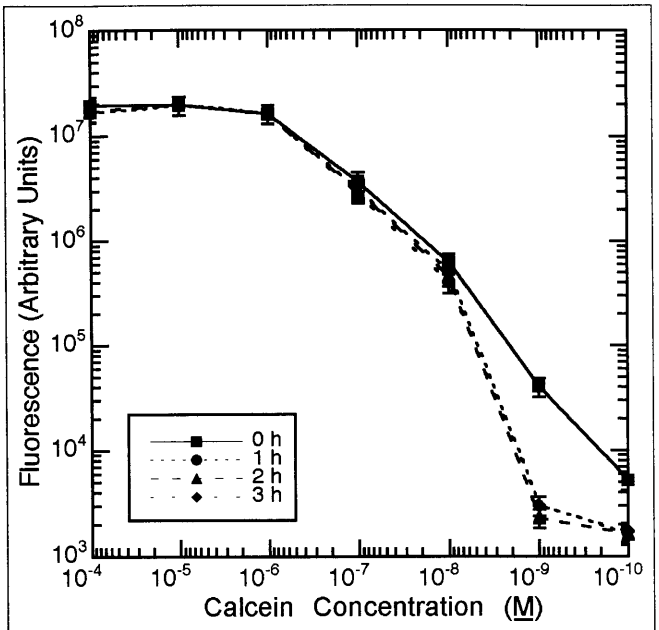

Figure 4.7. Calcein intensities after 3 h of exposure to light, O_2, and human skin. Only a slight drop is seen in the fluorescence, even after 3 h.

4.1.4. *Calcein not Quenched by Exposure to the Skin or the Pulsing Electrodes.*

Besides the standard calibration curve described in the previous section, three other standard curves were prepared, using PBS that had either been exposed to human skin (passively) for 1 h, unprotected electrodes used to apply high-voltage pulsing for 1 h to PBS, or to both the skin and the high-voltage pulsing electrodes (as would be experienced in a typical skin electroporation experiment). The high-voltage pulsing conditions used were $U_{applied}$ = 1000 V, τ = 1 ms, one pulse every 5 s. For all three calibration curves, fluorescence measurements were taken immediately after preparation (0 h, shown as the solid curves in Figures 4.7, 4.8, and 4.9), and 1, 2, and 3 h afterwards. All of the solutions were left on an undisturbed bench in the lab between measurements. The solutions were not covered, thus permitting exposure to both light and oxygen in the air.

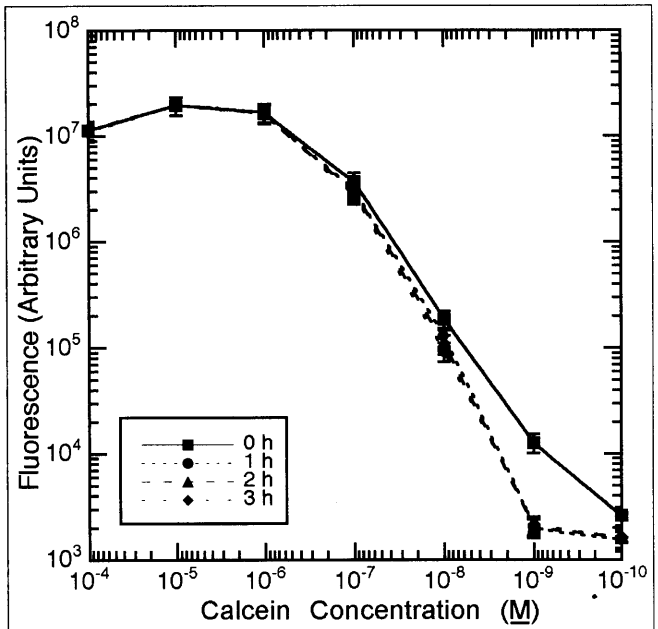

Figure 4.8. Calcein intensities after 3 h of exposure to light, O_2, and the pulsing electrodes. There is a slight drop in the fluorescence of calcein after 3 h.

Figure 4.7 shows the calcein calibration curve using PBS exposed to human skin, Figure 4.8 shows the standard curve using PBS exposed to only the pulsing electrodes, and Figure 4.9 shows the standard curve after exposure to both human skin and the pulsing electrodes. In all three cases, the standard curves after 1 h decreased slightly (especially at the 10^{-9} M concentration), but did not decrease further afterwards.

As in the previous section, this drop is probably unimportant, since the calcein donor solution is typically prepared 2 to 3 h before an experiment. In addition, all three calibration curves are not significantly different from calibration curves prepared with unexposed PBS (Figure 4.6), which would not be the case if the skin or the pulsing electrodes released substances that degrade calcein. Thus, these results indicate that exposure to either human skin, or to electrochemical by-products generated by the pulsing electrodes (or both, as in a typical experiment) do not significantly affect the fluorescence intensity of calcein.

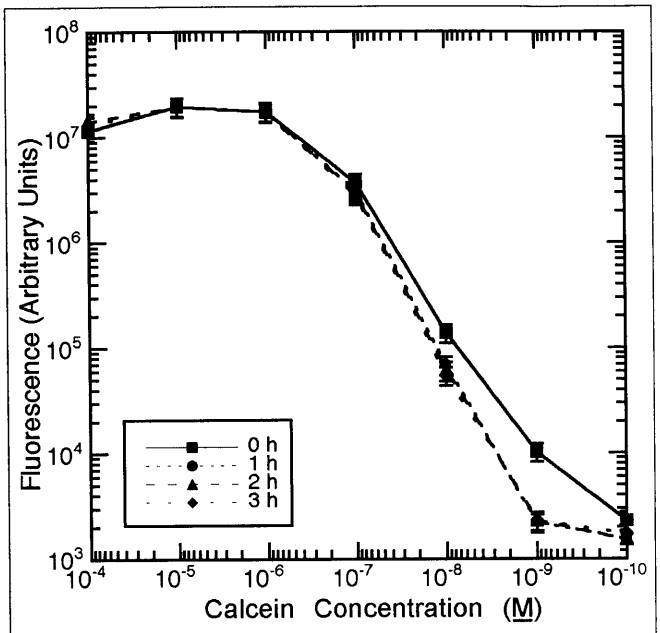

Figure 4.9. Calcein intensities after 3 h of exposure to light, O_2, skin, and the pulsing electrodes. Despite these influences, there is only a slight drop in the fluorescence of calcein, even after 3 h.

4.1.5. Calcein Intensity Constant at Moderate pH's (5 to 9).

Eleven different standard curves for calcein (Molecular Probes) in degassed PBS were prepared, in which the pH of the PBS solution was systematically altered from 3 through 13, through addition of appropriate amounts of either HCl (Mallinckrodt) or NaOH (Mallinckrodt). In some cases this required fairly large amounts of HCl or NaOH, which significantly changed the molarity of the final solution, especially for the strongly acidic or strongly basic solutions. Each PBS solution was prepared at the appropriate pH before the addition of calcein. The concentration of calcein at each pH was varied stepwise by an order of magnitude from 10^{-3} M to 10^{-10} M. Each standard curve was measured for calcein fluorescence immediately after preparation.

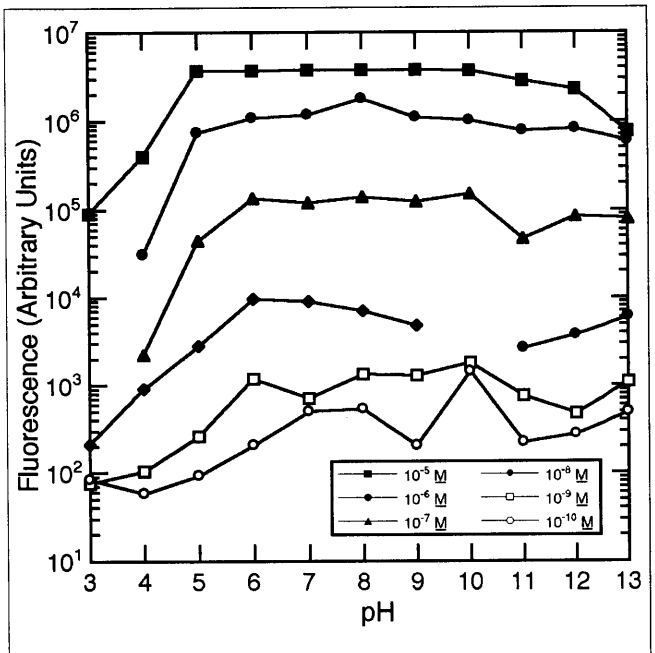

Figure 4.10. The intensity of calcein as a function of the solution pH. At moderate pH's (between 5 and 9), the fluorescence of calcein is essentially constant.

As can be seen in Figure 4.10, the standard curve for calcein did not significantly change for pH's between 5 and 9. However, if the solution was too acidic (pH < 5) or too basic (pH > 9), a

decrease in calcein fluorescence was observed.

These results are in agreement with the literature. In Cheng, *et al.* (1982), the fluorescence intensity of calcein was shown to vary slightly with the pH at moderate pH ranges (from 6 through 9) (see Figure 4.11). And in Pliquett and Gusbeth (in preparation), calcein was shown to be degraded at low pH's (Figure 4.12). The pH that caused calcein degradation in those experiments was not specified; however, further calculations* indicate that a pH of around 4 was reached during the experiment. Thus, small changes in pH during an experiment (±2 pH units) should not have a significant effect on the fluorescence intensity of calcein, but larger changes in pH would. With flow-protected electrodes (see Appendix III), the pH's of the donor and receptor solution should not change significantly during a typical skin electroporation experiment; thus, the effect of pH on calcein fluorescence should not present a problem.

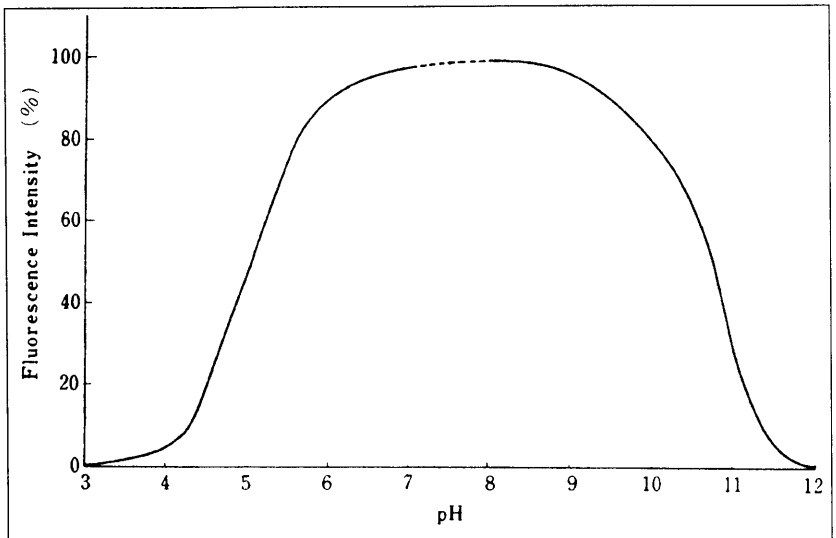

Figure 4.11. The intensity of calcein as a function of the solution pH. At moderate pH's, the fluorescence of calcein stays fairly constant. From Cheng, *et al.* (1982).

4.1.6. Calcein Intensity Unaffected by Ca^{2+} in Solution.

Five standard curves of calcein (Molecular Probes) in degassed PBS were prepared, ranging in concentrations from 10^{-3} M to 10^{-10} M in order-of-magnitude steps. To test the effect of Ca^{2+} concentrations on the fluorescence of calcein, varying concentrations of $CaCl_2$ were added to each standard curve. The concentration of $CaCl_2$ in PBS was systematically changed from 10^{-4} M to 1 M. The 1 M concentration was near the saturation point of $CaCl_2$, so higher concentrations were not possible. In each case, the appropriate amount of $CaCl_2$ was first added to PBS and allowed to fully dissolve, before adding calcein and preparing the standard curves. Each standard curve was measured for calcein fluorescence immediately after preparation.

---

* In the experiments of Pliquett and Gusbeth (in preparation), 500 μA of iontophoretic current was applied to a flow-through chamber for 10 min, with fresh PBS being supplied at the rate of ~1 ml/min. Dividing the current by the flowrate and a Faraday (96 484 C/mol) gives the final concentration of ions produced, 3.11×10^{-4} M. If these ions are assumed to be all hydrogen ions, then the pH of the solution would be 3.51 (ignoring the effects of the PBS buffering). Thus, with PBS buffering, the pH of the solution after 500 μA of iontophoresis can be estimated to be ~4.

The calcein standard curves can be seen in Figure 4.13. At low concentrations of $CaCl_2$, the fluorescence of calcein stayed constant. High concentrations (1 M) of $CaCl_2$ in PBS turned the solution a milky white color, affecting the measurement of the calcein fluorescence intensities. A concentration of 1 M $CaCl_2$ in PBS is probably above the saturation point, and thus a milky white suspension was formed.

The intensity of calcein was not expected to change much with the addition of Ca^{2+} ions in solution. The primary effect of the binding of Ca^{2+} to calcein is a small shift in the fluorescence emission of calcein, rather than a decrease in fluorescence (Cheng, *et al.*, 1982; Haugland, 1992).

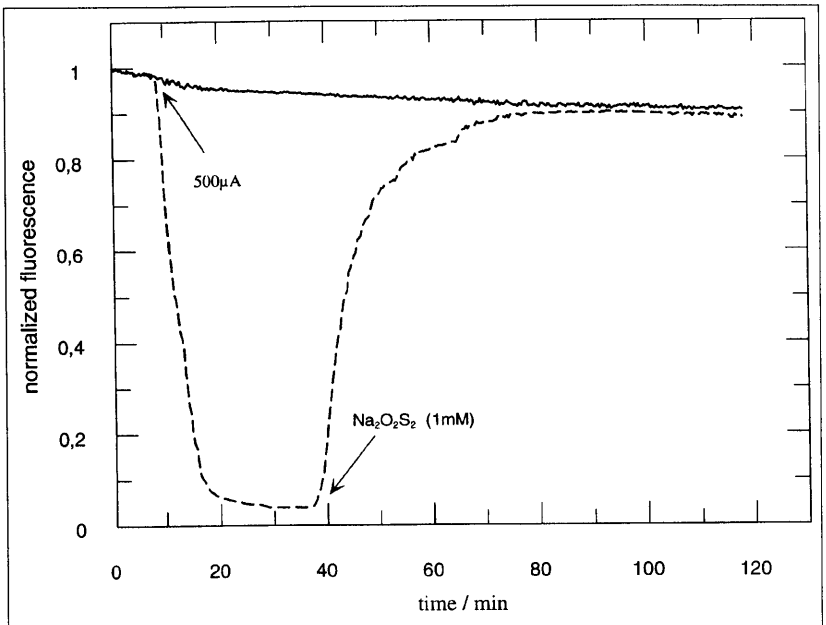

Figure 4.12. Degradation of calcein. The dotted curve shows the degradation of calcein (in arbitrary fluorescence units) as 500 µA of current is applied to a solution of 10^{-7} M calcein in PBS in a flow-through system, causing the pH to drop to roughly 4 (see footnote on previous page). After 40 min, the addition of sodium thiosulfate ($Na_2S_2O_3$ [*sic* in figure]) neutralizes the acidic pH, and calcein recovers its fluorescence. The solid line is a control curve, where no current was applied. A slight decrease (roughly 10%) in the fluorescence of calcein over time was observed during the control. From Pliquett and Gusbeth (in preparation).

4.1.7. Calcein Not Affected by Chemical By-Products.

In a different set of experiments, using a permeation chamber containing cadaver skin, as well as pulsing electrodes protected by polyacrylamide gel and a steady PBS stream (Chen, *et al.*, 1998 [a]; Appendix IV), the polyacrylamide gel surrounding the donor side pulsing electrode was intentionally broken, to allow any chemical by-products produced by the pulsing electrode to contaminate the calcein donor solution. The intensity and shape of the calcein efflux curve

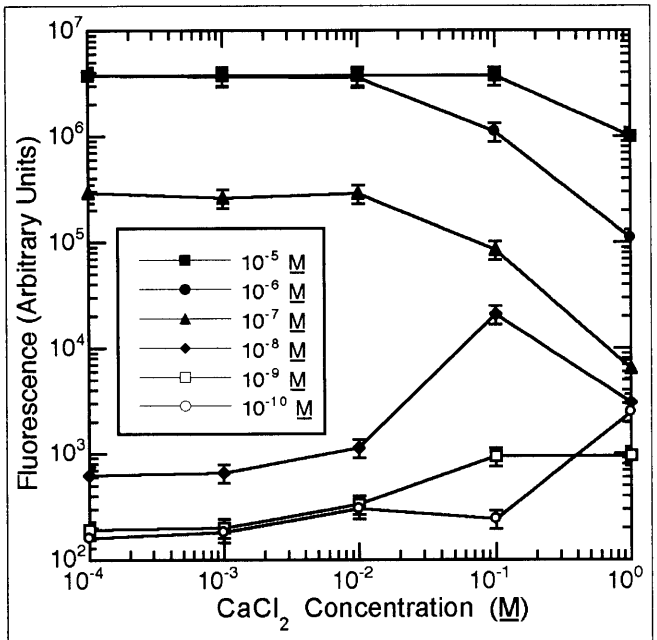

Figure 4.13. Calcein intensities as a function of Ca^{2+} concentration. Except for the saturated $CaCl_2$ solutions which appeared cloudy (1 M $CaCl_2$), the intensity of calcein was not significantly affected by the presence of Ca^{2+} ions.

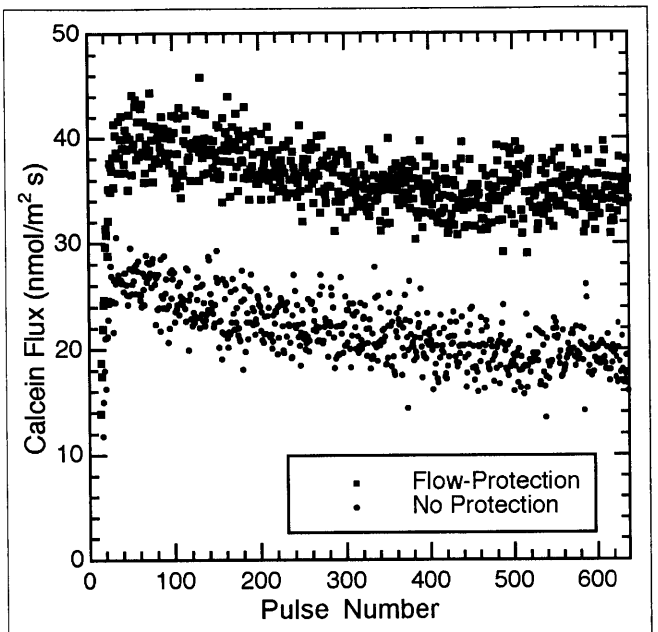

Figure 4.14. Calcein drops with and without the flow-protection system. Error bars removed for clarity. The efflux profile of calcein as it is transported across the skin during electroporation is not affected by the condition of the polyacrylamide gel surrounding the pulsing electrodes. Chemical by-products from the pulsing electrodes do not significantly affect molecular transport. Although the two experiments were performed under the same nominal conditions with the same applied voltages, the differences in flux are due to differences in the transdermal voltage.

through the skin, as measured by the flow-through system, was compared to the usual experiments in which the polyacrylamide gel did not break. High-voltage pulsing ($U_{applied}$ = 1000 V, τ = 1 ms) was applied to the skin, one pulse every 5.6 s for 1 h.

Even at large voltages ($U_{applied}$ = 1000 V), there were no appreciable differences in the efflux profiles of calcein through the skin, between experiments involving flow-protected electrodes, and the experiments without flow-protected electrodes (Figure 4.14). Both sets of experiments had similar efflux profiles and similar drops in calcein fluorescence during the experiment. Thus, it appears that the chemical by-products produced by the donor side pulsing electrode do not significantly affect the fluorescence of calcein.

The receptor side pulsing electrode was not tested, due to the difficulty in breaking only the polyacrylamide gel surrounding the flow-protection electrode, without affecting the receptor flow-through system. However, the receptor side electrode is not only protected by the flow-protection system, but the receptor flow-through system as well. Fresh PBS is continuously pumped through the receptor compartment in both systems, so that any pH changes or chemical by-products would be immediately washed out of the system.

4.1.8. Integrity of the Flow-Protection System.

In another set of experiments, using skin in an *in vitro* system with flow-protected electrodes (Chen, *et al.*, in press [a]; see also Appendix IV), a solution of calcein in PBS (at approximately 1 mM concentration) was intentionally pumped through the electrode flow-protection system, while only fresh, uncontaminated PBS was used in the donor solution and the receptor flow-through system. High-voltage pulsing ($U_{applied}$ = 1000 V, τ = 1 ms) was applied to the skin, one pulse every 5.6 s for 1 h.

As the data in Figure 4.15 indicate, the flow-protection system was able to maintain separation of the PBS in the receptor compartment, and the PBS flowing around the electrodes throughout the entire experiment. Even after 1 h of pulsing, there was no significant transport of calcein into the flow-

through sampling system from the flow-protection system. Thus, the polyacrylamide gel can maintain separation of the two compartments during a typical flow-through experiment.

It was noted that after the end of the first hour, calcein had diffused from the electrode flow-protection system into the polyacrylamide gel. Calcein had penetrated approximately 1.0 cm into the polyacrylamide gel, as determined by visual inspection. Given this rate, it would take several hours (at least 10 to 15 h before calcein could diffuse entirely across the polyacrylamide gel. Since the time for diffusion (~10 h) is much greater than a typical experiment (~2 h), the diffusion of calcein through the polyacrylamide gel could safely be ignored.

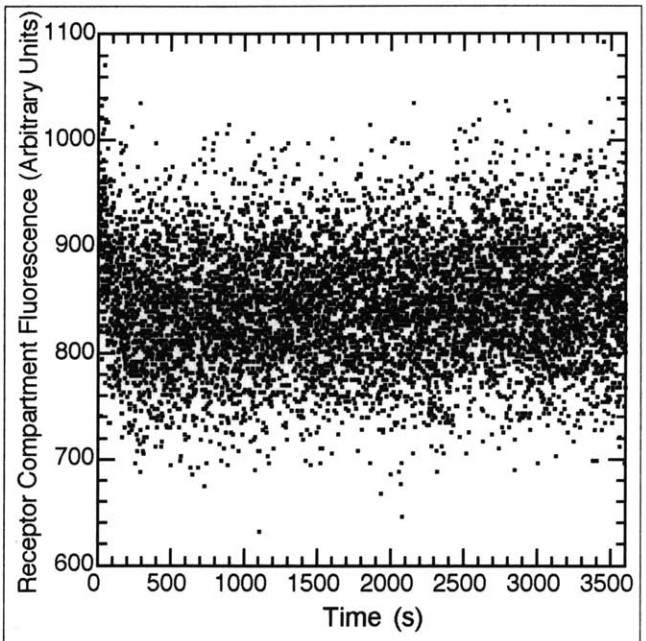

Figure 4.15. Calcein in the flow-protection system does not reach the receptor compartment. Error bars removed for clarity. The flow-through sampling stream does not record any calcein fluorescence during a typical 1 h skin electroporation experiment. The typical fluorescence of only PBS (no calcein) in the flow-through system is ~800 (in arbitrary fluorescence units).

4.1.9. Skin Does Not Release Calcein-Degrading Products.

A piece of human epidermis was grounded in a solution of PBS to produce a thick "slurry," which was then used instead of PBS to produce a standard curve for calcein (stepwise from 10^{-3} M to 10^{-10} M). This standard curve was compared against a normal calcein standard curve prepared using only PBS.

Figure 4.16 indicates that there was no significant degradation of calcein by the PBS mixed with ground skin. Since the "slurry" was a suspension of organic particles, it appeared somewhat cloudy, which caused a slight increase in the fluorescence of the skin-exposed calcein solution at the 10^{-9} M concentration, compared to the PBS control. At higher concentrations of calcein, however, the two curves were indistinguish-

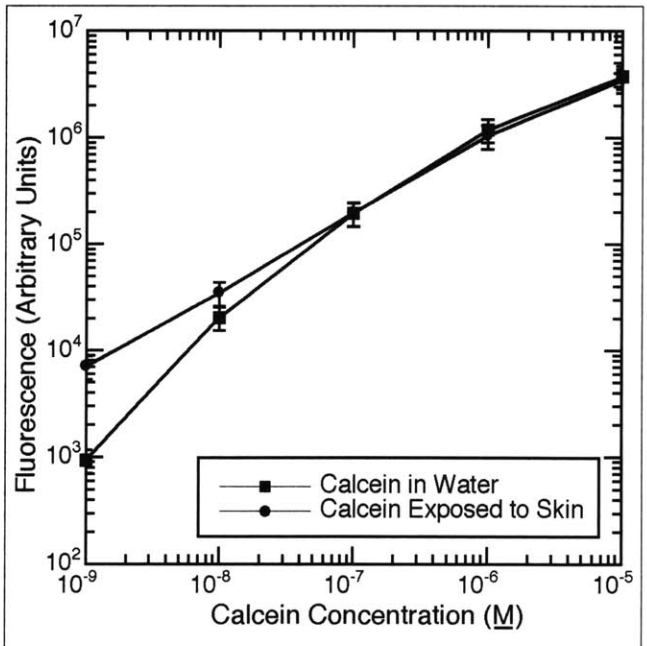

Figure 4.16. Calcein exposed to ground human skin does not decrease in intensity. The fluorescence of calcein was not significantly different from the control solution.

able. Thus, the skin does not appear to be releasing any substances that cause the degradation of calcein.

4.1.10. Iontophoresis of Calcein.

Instead of applying high-voltage pulsing, constant current iontophoresis at 1 mA / cm^2 was applied to human skin for 1 h. As before, the molecular transport across the skin was measured *in vitro* in real time, using a flow-through apparatus (Chen, *et al.*, in press [a]; Appendix IV).

The flux of calcein across the skin during this experiment is shown in Figure 10.2d. The flux of calcein slowly increased until it reached a steady-state plateau, at approximately 45 min (~2700 s). Steady-state transport was maintained until the end of the experiment (~3600 s). While iontophoresis was being applied, no decrease in the fluorescence of calcein was observed.

Although molecular transport during iontophoresis probably uses a different pathway through the skin than does electroporation (Pliquett, *et al.*, 1996 [b]; Chen, *et al.*, 1998 [b]), the skin does not appear to directly cause the degradation of calcein during molecular transport.

4.1.11. Water/Octanol Partition Coefficient of Calcein.

A calcein standard curve was prepared in a mixture of 50 vol% 1-octanol (Sigma) and 50 vol% deionized water. Calcein concentrations were varied stepwise from 10^{-3} M to 10^{-10} M. In each case, after vigorous shaking of the mixture for ~1 min, the solution was allowed to separate into a hydrophobic (1-octanol) and a hydrophilic (water) phase. The ratio of the amount of material in the 1-octanol phase to the amount in the water phase is defined as the octanol-water partition coefficient, K_{ow}, a commonly accepted measure of the hydrophilicity or hydrophobicity of a substance.

The fluorescence from each phase was measured separately and compared to the corresponding standard curve of calcein prepared in either water or 1-octanol. However, calcein appears to be too hydrophilic to be measured by this technique. Calcein does not dissolve in 1-octanol to any measurable extent; thus, a calibration curve could not be constructed. The K_{ow} for calcein was thus found to be $<<1$ (Table 4.1), but a numerical value could not be determined.

Calcein appears to stay within the aqueous pathways that form across the skin during skin electroporation. It does not dissolve well in lipophilic environments, and it is probably not getting bound to the lipid regions of the skin. However, nonspecific binding of calcein to the skin might account for the increase in the fluorescence of calcein on the surface of the skin after pulsing.

4.1.12. *Drop in Calcein Flux is Not an Artifact.*

As can be seen in this extensive series of experiments, calcein does not appear to be degraded by light, oxygen, moderate pH's, or changes in the concentration of Ca^{2+}. The drop in calcein flux during skin electroporation has also not been satisfactorily explained by electrochemical by-products or degradation by the skin. One final explanation may simply be that the drop in flux is real, not an artifact. Drops in molecular transport have also been observed during pulsing in other, unrelated fluorescent molecules (lucifer yellow and cascade blue) during skin electroporation experiments using snake skin instead of human skin (see Section 8.3.1, Figures 8.8b and 8.8c). Thus, the drop in calcein flux during pulsing may be a property of skin electroporation, not a property of the calcein molecule.

4.2. Sulforhodamine.

Sulforhodamine (or sulforhodamine 101; 9-(2,4-disulfophenyl)-2,3,6,7,12,13,16,17-octahydro-1H,5H,11H,15H-xantheno[2,3,4-i,j:5,6,7,i',j']diquinolizin-18-ium; CAS #60311-02-6) (Figure 4.17) has not been used as extensively as calcein in the research of skin electroporation (Kost, *et al.*, 1996; Pliquett and Weaver, 1996 [a]; Pliquett, *et al.*, 1996 [b]; Chen, *et al.*, 1998 [b]; Chen, *et al.*, 1998 [c]; Vanbever, *et al.*, submitted). It is commonly used alongside calcein (Kost, *et al.*, 1996; Pliquett and Weaver, 1996 [a]; Pliquett, *et al.*, 1996 [b]; Chen, *et al.*, 1998 [b]; Vanbever, *et al.*, submitted), since the fluorescence spectra of the two compounds do not significantly interfere with each other (Pliquett and Weaver, 1996 [a]; also see Section 4.2.2). Sulforhodamine fluoresces in the red region (excitation at 586 nm, emission at 607 nm) (Haugland, 1992; Pliquett and Weaver, 1996 [a]). The molecular weight of sulforhodamine is similar to that of calcein (607 Da, compared to 623 Da), and although it is zwitterionic, its total electronic charge is -1 at pH 7.4 (Molecular Probes, personal communication; M. R. Prausnitz, personal communication). Sulforhodamine was originally selected since it was thought to be very hydrophilic; however, later experiments (described in Section 4.2.1) have shown that it is not.

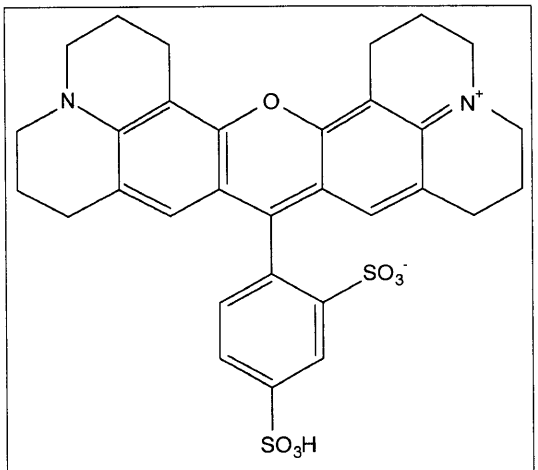

Figure 4.17. The molecular structure of sulforhodamine ($C_{31}H_{30}O_7N_2S_2$, 606.72 Da). Sulforhodamine is often used simultaneously with calcein in skin electroporation experiments. However, it is only weakly hydrophilic.

4.2.1. *Sulforhodamine is Only Weakly Hydrophilic.*

To measure the partition coefficient for sulforhodamine, a standard curve was prepared using a mixture of 50 vol% 1-octanol (Sigma) and 50 vol% de-ionized water. Sulforhodamine concentrations were varied stepwise from 10^{-3} M to 10^{-10} M. In each case, after ~1 min of vigorous shaking, the solution was allowed to separate into a hydrophobic (1-octanol) and a hydrophilic (water) phase. The fluorescence of each phase was measured separately and compared to the corresponding standard curve of sulforhodamine in either water or 1-octanol.

It was found that sulforhodamine dissolved quite readily in 1-octanol and still maintained its intense fluorescence. Its K_{ow} was found to be 0.057 ± 0.28 (in other words, 1 part in 1-octanol to 16 parts in water) (Table 4.1), indicating that sulforhodamine is only weakly hydrophilic.

Thus, sulforhodamine should not have been used as a tracer of the aqueous pathways formed during skin electroporation (Pliquett, *et al.*, 1996 [b]; Kost, *et al.*, 1996; Chen, *et al.*, 1998 [b]; Vanbever, *et al.*, submitted). Sulforhodamine is only weakly hydrophilic, and it can also enter hydrophobic regions of the skin. Since calcein and sulforhodamine have much different K_{ow}'s, this may explain why calcein and sulforhodamine are not observed in the same regions within the LTRs of the skin (see Figure 7.13a). The centers of the LTR's are probably very hydrophobic, explaining the separation of calcein and sulforhodamine within the LTRs.

4.2.2. *Independence of the Fluorescence of Calcein and Sulforhodamine.*

Since calcein and sulforhodamine have often been used simultaneously in skin electroporation research (Kost, *et al.*, 1996; Pliquett and Weaver, 1996 [a]; Chen, *et al.*, 1998 [b]; Vanbever, *et al.*, submitted), it was important to first establish that the fluorescence spectra of both com-

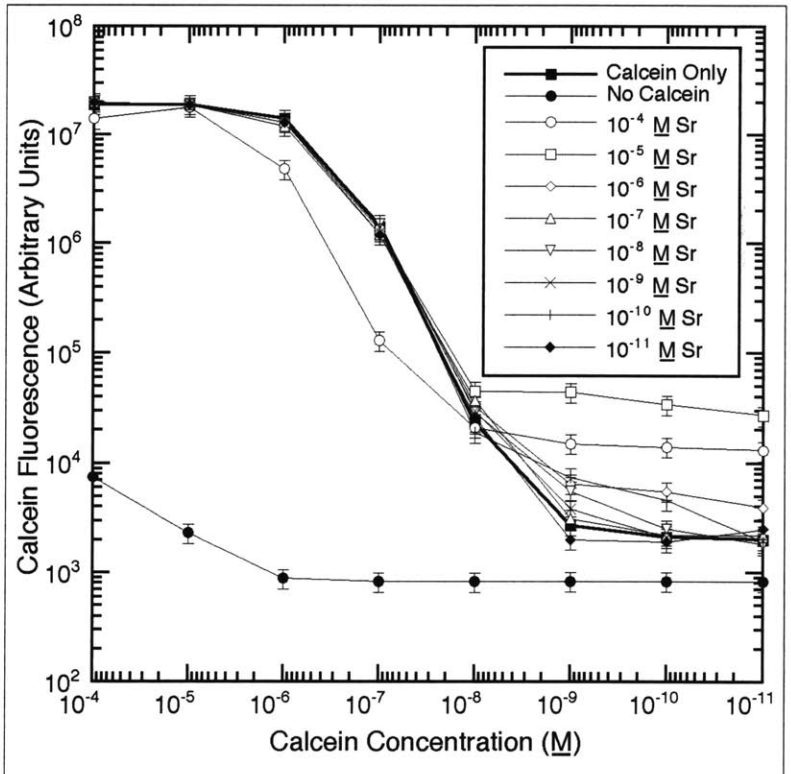

Figure 4.18. Calcein fluorescence intensity is not affected by sulforhodamine ("Sr"). The heavy line indicates the standard curve that would be observed if no sulforhodamine were present. The other curves indicate the calcein standard curve in the presence of varying amounts of sulforhodamine. These curves are not significantly different than the heavy line with sulforhodamine concentrations from 10^{-5} M to 10^{-8} M, indicating the range where calcein and sulforhodamine can be used and quantified simultaneously. Also see Figure 4.19.

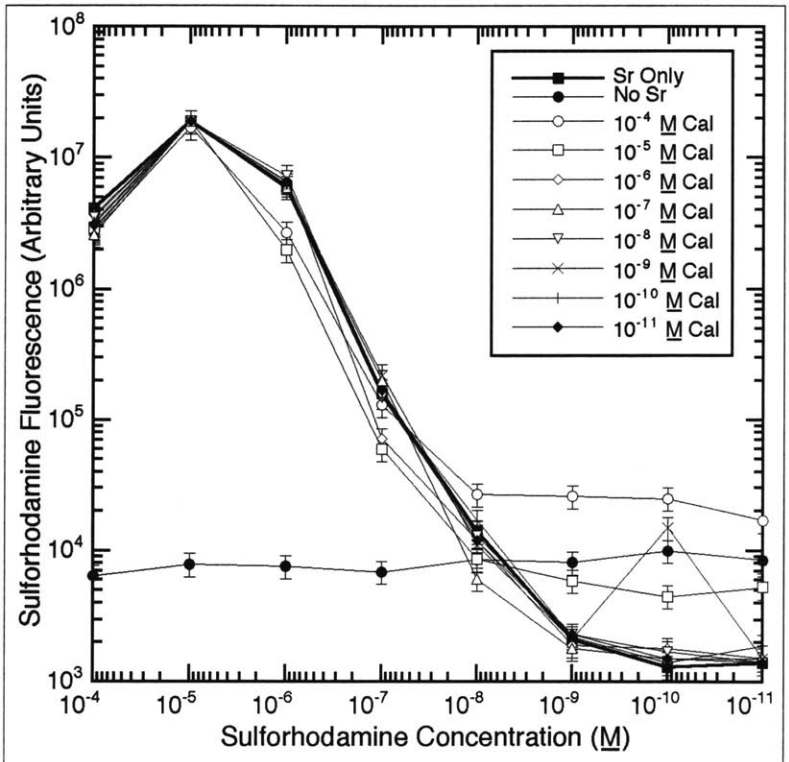

Figure 4.19. Sulforhodamine ("Sr") fluorescence intensity is not affected by calcein ("Cal"). The heavy line shows the standard curve if no calcein were present. The other curves indicate the sulforhodamine standard curve in the presence of varying amounts of calcein. The curves are not distinguishable at calcein concentrations from 10^{-5} M to 10^{-8} M, indicating the range where calcein and sulforhodamine can be used and quantified simultaneously. Also see Figure 4.18.

pounds do not significantly interfere with each other, thus allowing quantitative measurements of both species to be taken simultaneously.

A calibration matrix was prepared with both calcein and sulforhodamine. The concentrations of calcein and sulforhodamine in PBS were each independently varied stepwise from 10^{-3} M to 10^{-10} M, and compared with calibration curves containing only calcein or sulforhodamine.

As Figures 4.18 and 4.19 show, calcein and sulforhodamine do not significantly affect each other's fluorescence. Working ranges from 10^{-5} M to 10^{-8} M were established for both species, where the standard curve is essentially linear. This is the same working range for each molecule by itself (heavy lines in Figures 4.18 and 4.19). Beyond 10^{-8} M, however, there is some interference of fluorescence intensities between the two species, seen as a slightly higher background. Thus, calcein and sulforhodamine can be detected and quantified independently of each other, allowing their simultaneous use in skin electroporation experiments.

4.3. Lucifer Yellow.

Comparatively less has been done with lucifer yellow as a tracer in skin electroporation. Prausnitz, *et al.* (1993) examined the average flux of lucifer yellow through the skin, and found it to be similar to calcein. Real-time measurements of the lucifer yellow flux can be seen in Chen, *et al.*, (1998 [c]) and in Figure 8.4b. In addition, a passive permeation study of lucifer yellow through the stratum corneum was conducted by Mansbridge and Knapp (1993), who

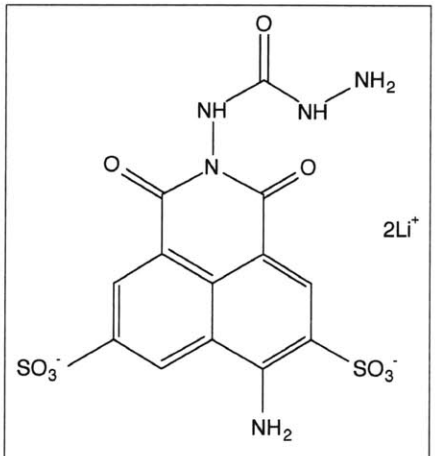

Figure 4.20. The molecular structure of lucifer yellow ($Li_2(C_{13}H_9O_9N_5S_2)$, 457.25 Da.

found that lucifer yellow did not diffuse significantly through the stratum corneum, although it diffused quite readily through the epidermis and dermis, where it stayed in the intercellular regions.

Lucifer yellow (also known as 6-amino-2-[(hydrazinocarbonyl)amino-2,3-dihydro-1,3-dioxo-1H-benz[de]isoquinoline-5,8-disulfonic acid, dilithium salt; CAS #67769-47-5) has a nominal charge of -2 and a molecular weight of 457 Da, somewhat smaller than the other three molecular tracers discussed in this chapter. Its molecular structure can be seen in Figure 4.20. It is excited by ultraviolet light (428 nm) and emits yellow light (555 nm) (Haugland, 1992).

Lucifer yellow was found to be very hydrophilic (K_{ow} << 1), using a procedure similar to the one described in Section 4.1.11, using lucifer yellow instead of calcein. Like calcein, lucifer yellow proved unable to dissolve in 1-octanol; thus, a lucifer yellow calibration curve could not be constructed.

4.4. Cascade Blue.

Cascade blue (or 8-hydroxypyrene-1,3,6-trisulfonic acid, trisodium salt; acetic acid, [(3,6,8-trisulfo-1-pyrenly)oxy]-1-hydrazide, trisodium salt; CAS #137182-38-8) has been studied much less than the other fluorescent tracers. Cascade blue has not been previously used in skin electroporation or transdermal drug delivery research.

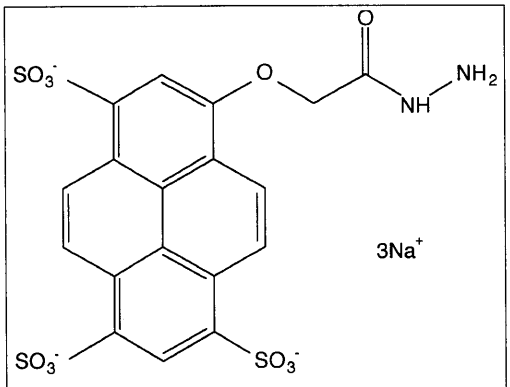

Figure 4.21. The structure of cascade blue. It is a fluorescent molecule that is excited by ultraviolet light and emits blue light. It has a molecular formula of $Na_3(C_{18}H_{11}O_{11}N_2S_3)$ and a molecular weight of 596.45 Da.

Using the procedure of Section 4.1.11, cascade blue was found to be very hydrophilic (K_{ow} << 1). Cascade blue was also unable to dissolve significantly in 1-octanol; thus, a calibration curve for cascade blue could not be constructed.

Cascade blue is excited by 399 nm light (ultraviolet light) and fluoresces at 421 nm (blue light) (Haugland, 1992). It has a molecular weight of 596 Da and a nominal electric charge of -3. The structure of cascade blue can be seen in Figure 4.21. It is highly water-soluble (Haugland, 1992) and has previously been used in the staining of yeast cells (Whitaker, *et al.*, 1991). It is one of the few molecules which fluoresces brightly at wavelengths less than 500 nm (Whitaker, *et al.*, 1991). It can be used in conjunction with lucifer yellow, since the absorption spectra for lucifer yellow and cascade blue do not overlap significantly (Haugland, 1992).

5. Particles are Not Transported across the Skin.*

Numerous studies have shown that applying a series of high-voltage electrical pulses to human skin causes the enhanced transport of various molecules across the skin, which may be useful in transdermal drug delivery. Molecules that have been successfully transported across human skin include fluorescent, low molecular weight tracers such as lucifer yellow (457 Da) (Prausnitz, *et al.*, 1993 [a]; Chen, *et al.*, 1998 [c], cascade blue (596 Da) (Chen, *et al.*, 1998 [c]), sulforhodamine (607 Da) (Kost, *et al.*, 1996; Pliquett and Weaver, 1996 [a]; Pliquett, *et al.*, 1996 [b]; Chen, *et al.*, 1998 [b]; Chen, *et al.*, 1998 [c]; Vanbever, *et al.*, submitted), and calcein (623 Da) (Prausnitz, *et al.*, 1993 [a]; Prausnitz, *et al.*, 1993 [c]; Prausnitz, *et al.*, 1994; Pliquett, *et al.*, 1995 [b]; Kost, *et al.*, 1996; Pliquett and Weaver, 1996 [a]; Pliquett and Weaver, 1996 [b]; Pliquett, *et al.*, 1996 [b]; Prausnitz, *et al.*, 1996 [b]; Chen, *et al.*, 1998 [b]; Chen, *et al.*, 1998 [c]; Vanbever, *et al.*, submitted). Biologically relevant compounds have also been successfully transported across human skin *in vitro*, including luteinizing hormone releasing hormone (LHRH, 1182 Da) (Bommannan, *et al.*, 1994; Riviere, *et al.*, 1995), several oligonucleotides (4.8 to 7.0 kDa) (Zewert, *et al.*, 1995; Regnier, *et al.*, in press [a]) and heparin (5 to 30 kDa) (Prausnitz, *et al.*, 1995 [b]; Vanbever, *et al.*, 1997; Weaver, *et al.*, 1997). Recently, there have been several reports of the transport of particles (10 nm to 45 μ in diameter) (Hofmann, *et al.*, 1995; Prausnitz, *et al.*, 1996 [a]) into (Prausnitz, *et al.*, 1996 [a]) or across human skin (Hofmann, *et al.*, 1995; Zhang, *et al.*, 1997).

It has been hypothesized that the application of high-voltage pulsing to human skin causes molecular transport by electroporation (Prausnitz, *et al.*, 1993 [a]; Chizmadzhev, *et al.*, 1995; Chizmadzhev, *et al.*, 1998 [a]). Moreover, high-voltage pulses have been shown to cause the formation of small, localized transport regions ("LTRs") within the stratum corneum (Zewert, *et al.*, 1995; Pliquett, *et al.*, 1996 [b]; Prausnitz, *et al.*, 1996 [a]; Chen, *et al.*, 1998 [b]; Vanbever, *et al.*, submitted). For short pulses (1 to 10 ms), the LTRs are approximately 100 μ in diameter, and are randomly distributed on the stratum corneum, not associated with the sweat ducts or hair follicles (Pliquett, *et al.*, 1996 [b]). LTRs have also been shown to be sites of charged particle entry into the stratum corneum (Prausnitz, *et al.*, 1996 [a]).

However, only one study (Zhang, *et al.*, 1997) reports the number of particles actually delivered across the skin after high-voltage pulsing. Using microspheres 20 μ in diameter, it was reported that the transport of 1.62×10^5 particles / cm^2 through human skin xenograft on nude mice was achieved after the application of three 120 $V_{applied}$, 10 ms pulses. However, for a better understanding of how

*These results have also been reported in Chen, *et al.* (submitted, [a]).

different size particles might be transported across human skin during various high-voltage pulsing protocols, more accurate, quantitative measurements of the amount of particle transport were needed, which motivated the current investigation.

5.1. Overview.

The detection and quantification of particle transport through the skin during high-voltage pulsing was found to be a surprisingly difficult process. During this investigation, several different detection techniques, particle suppliers, and skin preparations were tested, in an attempt to come up with a viable and reproducible protocol for particle detection. A summary of the protocols tried in this investigation is shown in Table 5.1. The rest of this chapter describes the successes and results of each of these protocols.

Table 5.1. Summary of Particle Experiments.

Detection Technique	Particles	Skin Section	Results
Confocal Microscopy	2.16 μ Sigma	Epidermis	Ambiguous detection
Light Microscopy	All Sigma	Epidermis	LTRs on surface (does not determine transport)
Gel Trapping	2.16 μ Sigma, 2.000 μ Bangs	Epidermis	<5 particles / mm^2
Membrane Trapping	2.16 μ Sigma	Epidermis	No detectable transport
Fluorescence Spectrometry	All Molecular Probes	Epidermis, Stratum Corneum	No detectable transport

5.2. Particle Characteristics.

In these experiments, green fluorescent, carboxylate-modified polystyrene latex particles ("beads") were supplied in the donor compartment. The green fluorescence allowed ready detection of the particles, the carboxylated surface groups gave a large net negative charge to each particle, and polystyrene was not reactive with the skin. Three suppliers of the latex particles were used: Sigma, Bangs Laboratories (Carmel, IN), and Molecular Probes.

5.2.1. *Particles from Sigma.*

The green fluorescent (470 nm excitation, 505 nm emission), carboxylate-modified polystyrene latex particles

Table 5.2. Particles from Sigma (Sigma, personal communication).

Diameter (μ)	Concentration (particles / ml)	Charge (e^-)
2.16	4.7×10^{8}	-2.77×10^{7}
1.01	4.6×10^{9}	-4.58×10^{7}
0.431	6.0×10^{10}	-2.33×10^{6}
0.105	4.1×10^{12}	-1.39×10^{5}
0.035	1.1×10^{14}	-4.05×10^{3}

(Sigma) were shipped as a suspension of 2.5 vol% particles in water. No surfactants were used to prevent possible bead aggregation (Sigma, personal communication). The particles were diluted 9:1 by volume in PBS, to a final suspension concentration of 0.25 vol% particles. Particle diameters, surface charges, and final concentrations are provided in Table 5.2. The 2.16 μ diameter particles were used in the particle trapping experiments; the other sizes were used only for fluorescence microscopy

5.2.2. *Microspheres from Bangs Laboratories.*

Yellow fluorescent (460 nm excitation, 540 nm emission), 2.000 μ diameter, carboxylated dyed microspheres were obtained from Bangs Laboratories. The particle suspension had 10% solids and contained an anionic surfactant to prevent aggregation. To remove the surfactant, 1 ml of microspheres was centrifuged (Eppendorf Centrifuge 5415C, Brinkman Instruments, Westbury, NY) for 2 min, then sonicated (Branson Ultrasonic Cleaner, Shelton, CT) for 2 min. After sonication, the supernatant was decanted off and the microspheres resuspended in 1 ml of PBS. This process was repeated 5 times. In the fifth cycle, the microspheres were sonicated for 10 min instead of 2 min. The final concentration of microspheres was ~10% solids (~2.4×10^{10} beads/ml, ~3.0×10^{7} charge) (Bangs Laboratories, personal communication).

5.2.3. *Particles from Molecular Probes.*

The green fluorescent (490 nm excitation, 515 nm emission) carboxylate-modified polystyrene latex particles produced by Molecular Probes were slightly brighter and more highly charged than the particles from Sigma (physical properties shown in Table 5.3), but sometimes aggregated when left undisturbed for several days. The red fluorescent, carboxylate-modified polystyrene latex particles were similar to the green latex particles.

Table 5.3. Particles from Molecular Probes (Molecular Probes, personal communication).

Diameter (μ)	Fluorescence Color	Concentration (particles / ml)	Charge (e^-)
2.10	Green (490/515)	3.9×10^{9}	-5.75×10^{7}
1.03	Green (490/515)	3.3×10^{10}	-4.68×10^{7}
0.557	Green (490/515)	2.1×10^{11}	-1.13×10^{7}
0.216	Green (490/515)	3.6×10^{12}	-1.29×10^{6}
0.093	Green (490/515)	4.5×10^{13}	-1.73×10^{5}
0.014	Green (490/515)	1.3×10^{16}	-2.65×10^{2}
1.03	Red (580/605)	3.3×10^{10}	-4.68×10^{7}
0.557	Red (580/605)	2.1×10^{11}	-1.13×10^{7}
0.216	Red (580/605)	3.6×10^{12}	-1.29×10^{6}
0.093	Red (580/605)	4.5×10^{13}	-1.73×10^{5}
0.020	Red (580/605)	4.5×10^{15}	-1.26×10^{3}

The most important difference between the two types of particles was their fluorescence wavelengths (580 nm excitation, 605 nm emission for the red fluorescent particles).

The particles were shipped as a suspension of 2 vol% beads in water, without any surfactant (Haugland, 1992; Molecular Probes, personal communication). The diameters of the particles ranged from 14 nm to 2.10 μ. Before use, each particle suspension was diluted 9:1 by volume in PBS to a final suspension concentration of 0.2 vol% solids, then sonicated for 15 to 30 min to prevent aggregation (Branson Ultrasonic Cleaner). These particles were used for the fluorescence spectrometry experiments.

5.3. Detection Procedures.

Many detection schemes were tried in this investigation, with varying degrees of success in the unambiguous detection and quantification of particle transport. Either high-voltage pulsing, iontophoresis, or no electrical treatment (passive control) was applied for 1 h (see Section 5.4). Afterwards, one of the following detection methods was then used to assess particle transport through the skin.

5.3.1. Confocal Microscopy.

Initially, confocal microscopy was used as the particle detection technique. Since confocal microscopy can focus on "optical planes" throughout a given specimen, without interference from underlying or overlying planes, the goal was to unambiguously detect fluorescent particles completely contained within the epidermis, indicating that transport of the particle through the entire stratum corneum had occurred. Others (Hofmann, *et al.*, 1995; Zhang, *et al.*, 1997) had reported particle transport through the stratum corneum; however, in those investigations, the skin was cut open using a knife (U. Pliquett, personal communication)! Obviously, this technique could distribute particles throughout the skin simply by the mechanical grinding action of the knife blade, and thus, an unambiguous detection method was needed.

A Bio-Rad MRC-600 Confocal Axioplan Microscope (Bio-Rad, Hercules, CA) was used to study mounted skin specimens. After pulsing, the skin was stained with Nile Red (Molecular Probes), chosen for its ability to stain the lipid regions in the stratum corneum (Prausnitz, *et al.*, 1996 [a]). When excited, Nile Red emits red light; the latex particles used here were fluorescent green (Section 5.2.1). Thus, the stratum corneum and the particles could be differentiated from each other under confocal microscopy (Prausnitz, *et al.*, 1996 [a]).

Immediately after each experiment, both the donor and receptor compartments were emptied, then the skin was carefully removed and gently placed on a microscope slide (Gold Seal Rite-On, No. 3050, Clay Adams, Becton Dickinson, Franklin Lakes, NJ). Excess liquid was blotted off with a paper towel. Next, a drop of mounting solution was added (see Appendix II.3). A 22×22 No. 1 cover slip (Clay Adams) was placed on top and sealed in place with nail polish (Hard as Nails, Sally Hensen, Del Laboratories, Framingdale, NY) (Prausnitz, *et al.*, 1996 [a]).

5.3.2. *Fluorescence Microscopy.*

In both fluorescence and light microscopy, light is passed through the entire specimen to the observer. Thus, it is not possible to differentiate between the different layers of the skin with this technique, unlike in confocal microscopy.

The goal of this section was not to determine if particle transport through the skin had occurred, but to determine under what conditions LTRs formed on the surface of the skin after pulsing with a particle suspension as the donor. LTRs had previously been observed after pulsing (Zewert, *et al.*, 1995; Pliquett, *et al.*, 1996 [b]; Prausnitz, *et al.*, 1996 [a]; Vanbever, *et al.*, submitted), including with a particle suspension (Prausnitz, *et al.*, 1996 [a]).

A biocular fluorescence microscope (Olympus BH-2, Olympus, Woodbury, NY) allowed simultaneous fluorescence and light illumination of slides, gels, or membranes at 4× and 10× magnifications. The excitation source was a mercury arc lamp (Mercury-100, Chiu, Glen Cove, NY), using a 488 nm wavelength filter. Emitted light was viewed using a 515 nm wavelength filter (O515 filter, Olympus). Pictures were taken using a camera (Olympus OM2, Olympus) mounted on the microscope (Pliquett, *et al.*, 1996 [b]).

After each experiment, the donor and receptor compartments were emptied. The skin was carefully removed and gently placed on a microscope slide (Gold Seal Rite-On, No. 3050, Clay Adams, Becton Dickinson). Excess liquid was blotted off with a paper towel. A drop of mounting solution was added (see Section II.3), and a 22×22 No. 1 cover slip (Clay Adams) was placed on top and sealed in place with nail polish (Hard as Nails, Sally Hensen, Del) (Prausnitz, *et al.*, 1996 [a]).

5.3.3. *Particle Trapping with Gels.*

Due to the difficulties in interpreting the confocal microscopy results (see Section 5.6, below), a new approach was needed to detect and quantify particle transport. The goal of this section was to use a gel to trap particles that have crossed the stratum corneum and the epidermis during pulsing. The

gel had to allow ions and currents to move freely across, yet trap any particles entering into it from the epidermis.

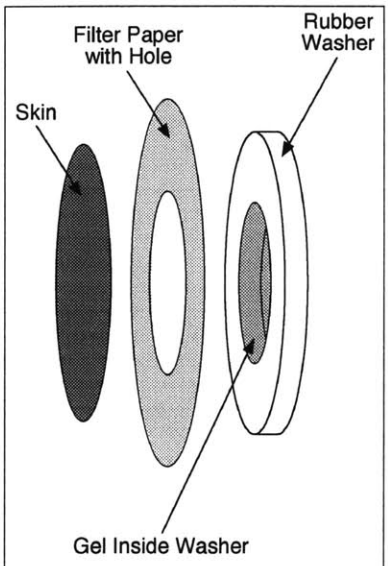

Figure 5.1. Schematic diagram of the gel trapping equipment. Behind the skin was a rubber washer containing either agarose or polyacrylamide gel. Particles that crossed the skin would become embedded in the gel.

Two gels were tested in this investigation: an agarose gel and a polyacrylamide gel. Both had low electrical resistivities (each gel had a resistivity of ~100 Ω m, comparable to PBS), were easy to prepare, and did not allow any particles to diffuse across. The gel was held in place behind the skin by a rubber hose washer (Price Hose Washers No. 010W, Gilmour, Somerset, PA). The inner diameter of the washer was smaller than that of the skin sample to ensure an electrically tight seal (see Figure 5.1).

Agarose solution was first prepared by heating a 2 wt% solution of agarose powder (Gibco BRL, Life Technologies, Gaithersburg, MD) in PBS to 100 °C. Upon cooling to room temperature, agarose solution hardens into a gel.

Polyacrylamide solution was first prepared mixing together 0.75 g of 19:1 acrylamide:bis(N,N'-methylene-bis-acrylamide) powder (Bio-Rad), 43.75 µl of 440 m$\underline{M}$ $(NH_4)_2S_2O_8$ solution (Mallinckrodt), and 3 µl of N,N,N',N'-tetramethylethylenediamine (Bio-Rad) in 5 ml PBS. The polyacrylamide solution needed ~10 min to harden into a gel.

Immediately after preparation, the agarose or polyacrylamide solution was poured into the hose washer and allowed to cool (for agarose) and harden into a gel (~10 to 15 min). Excess gel was carefully scraped away with a razor blade.

A 0.5 inch diameter hole was punched out of a piece of 4.25 cm diameter filter paper (S & S Filter Paper #595, Schleicher and Schuell, Keene, NH). The hole was smaller than the epidermis, so that the epidermis could completely cover the hole.

Before the epidermis was loaded into the permeation chambers, the epidermis was first placed on the filter paper. Both the epidermis and filter paper were then carefully laid on top of the gel. The washer (with the skin, filter paper, and gel) was then loaded into the permeation chambers, with the stratum corneum facing the donor side.

After each experiment, the donor and receptor chambers were emptied, then the washer containing the gel was removed. The washer was set on a microscope slide and examined under a fluorescence microscope (the one described in Section 5.3.2) at 10× magnification. Five locations were chosen at random and the particles in those sections were visually counted and averaged together. Since the diameter of the field-of-view under the microscope was known for this magnification (1.60 mm), by assuming a uniform density of particles on the surface, the number of particles on the surface of the stratum corneum could be estimated.

5.3.4. Particle Trapping by Polycarbonate Membranes.

Since there was still some ambiguity in the results obtained by the gels (see Section 5.8, below), polycarbonate membranes (Poretics, Livermore, CA) were also used to trap particles for quantitative measurement after they had been transported across the skin. A filter hole size of 0.1 μ was chosen since it would not hinder ionic transport or offer any significant electrical resistance, yet it would still be sufficient to trap the 2.16 μ diameter particles.

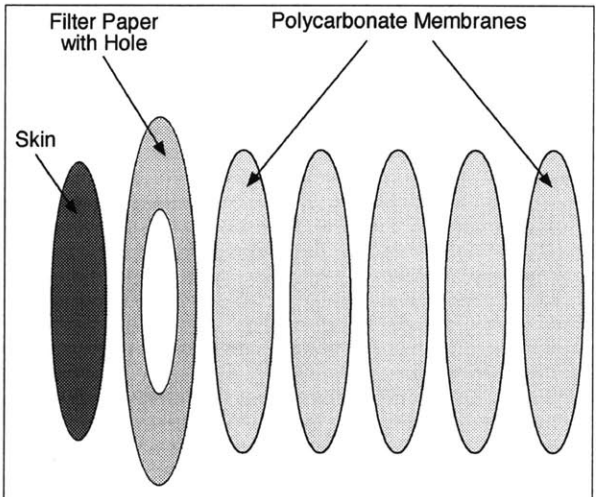

Figure 5.2. Schematic diagram of the membrane trapping equipment. Particles are trapped in a series of polycarbonate membranes. Particles crossing the skin become embedded in the first membrane. The other membranes protect the first one from possible contamination.

The epidermis (including the overlying stratum corneum) was placed on a piece of filter paper with a hole in the middle. This was then placed on five sheets of polycarbonate membrane filters, each with a mesh size of 0.1 μ (see Figure 5.2). The entire assembly (skin, filter paper, and membranes) was loaded into the permetion chambers, with the stratum corneum facing the donor side.

Fluorescent latex particles, with a diameter of 2.16 μ (Sigma), were supplied in the donor compartment (0.25 vol% in PBS). During an experiment, particles transported across the epidermis and the stratum corneum should become lodged in the first membrane. As a conservative precaution, the other four membranes were used to protect the first membrane from contamination.

After each experiment, the donor and receptor compartments were emptied. The first polycarbonate membrane was removed from the chamber, placed on a microscope slide, covered with a cover slip, and sealed in place with nail polish. The other four membranes were discarded.

A biocular fluorescence microscope (described in Section 5.3.2), set at a magnification of 10×, was used to examine the first membrane and count the particles on it. Since the 2.16 μ particles were large enough to be individually seen at a magnification of 10×, they could be individually identified and counted. All of the particles on the polycarbonate membrane were counted several times to ensure an accurate measurement. Typically, however, the total number of brightly fluorescent particles observed on the polycarbonate membrane was <25.

5.3.5. *Detection by Fluorescence Spectroscopy.*

In some experiments, particle transport was measured by spectrofluorimetry, which responds to the total fluorescence within a sample volume and is not an actual particle count. In some of these experiments, only the stratum corneum (no epidermis) was used to ensure that any particles transported across the stratum corneum would not become trapped in the epidermis, allowing the detection of the particles. Any particles transported across the skin should accumulate in the receptor compartment during the experiment. Fluorescent latex particles from Molecular Probes were used in the donor compartment at a concentration of 0.20 vol% in PBS. The diameters of the fluorescent particles ranged from 14 nm to 2.10 μ.

After each experiment, the particle suspension in the receptor compartment was pipetted into a 1.5 ml disposable polystyrene microcuvette (Elkay, Shrewsbury, MA) and vigorously stirred to prevent settling of particles. The microcuvette was then analyzed for fluorescence with a spectrofluorimeter (Fluorolog II F112, Spex, Metuchen, NY). Excitation and emission wavelengths used were 490 nm and 515 nm, respectively.

5.4. Experimental Protocols.

Procedures used to prepare the skin (epidermis or stratum corneum only preparations) are described in Appendix I; the experimental apparatus and detailed techniques used to prepare it are described in Appendix III. Briefly, custom-designed, six port side-by-side permeation chambers, with a skin exposure area of 0.64 cm^2 (circular opening, 0.9 cm in diameter) (Crown Bio Scientific, Somerville, NJ) (Friend, 1992), were fitted with silver wire electrodes in the donor and receptor compartments (Figure III.2), surrounded by a PBS flow-protection system encased in polyacrylamide gel. During an experiment, PBS was pumped around each electrode at a flowrate of ~6 ml/min. This precaution prevented contamination of the donor and receptor compartments by chemical by-products from the electrodes, such as H^+ and OH^- ions.

Applied electrical conditions included passive conditions (no pulsing) for 1 h, and constant current iontophoresis at 1.0 and 10 mA/cm^2 for 1 h, using a custom-built iontophoresis device (U. Pliquett, personal communication). In the high-voltage pulsing experiments, high-voltage, exponentially-decaying pulses were delivered to the permeation chamber by an exponential pulser (Electroporation System 600, BTX), modified to deliver 1 pulse every ~5 s for 1 h (U. Pliquett, personal communication). The time constant (τ) for each pulse was set to ~5 ms, but in some experiments it was systematically changed from 1 to 15 ms. The applied voltage ($U_{applied}$) was set to 1000 V, corresponding to a transdermal voltage (U_{skin}) of ~150 V. However, in other experiments, $U_{applied}$ was also systematically

changed, from 0 to 1500 V, corresponding to a U_{skin} of 0 to ~200 V (Chen, *et al.*, 1998 [c]). Pulses were applied to the skin for 1 h (approximately 720 pulses total). The negative pulsing electrode was placed on the donor side of the chamber, and the positive electrode placed on the receptor side, to provide a favorable driving force for the negatively charged particles.

The current delivered across the skin was determined by measuring the voltage drop across a noninductive 1.2 Ω, 50 W resistor in series with the chamber (Figure III.6), and voltage drops across the skin were measured using grounded high-voltage probes (Tektronics). The electrical resistance between the two measuring electrodes due to the intervening PBS was previously determined by pulsing the chamber without any skin present, as discussed in Section 3.5. Both the current and the voltage drop were recorded every 15 min during pulsing and averaged together to approximately characterize the transdermal voltage.

Initially, prepared cadaver skin (epidermis or stratum corneum) was floated in PBS to remove the wax paper backing.

In the particle trapping experiments, five polycarbonate membranes with a mesh size of 0.1 μ (Poretics), were then placed on the epidermal side of the skin.

In the gel trapping experiments, the epidermis was first placed on the filter paper. Both the epidermis and filter paper were then carefully laid on top of the washer containing the gel. The washer (with the skin, filter paper, and gel) was then loaded into the permeation chamber.

In all cases, the skin was loaded into the permeation chamber with the stratum corneum side facing the donor compartment. The temperature of the chamber was kept constant at 37 °C using a thermostated water bath to continuously flush 37 °C water through the outer jackets of the chamber (see Appendix III).

The condition of each piece of skin was checked by measuring its electrical impedance using a custom-built device that applied a ~1 kHz, ~50 mV bipolar square wave across the skin, and measuring the resulting voltage (U. Pliquett, personal communication). Skin with impedances <50 $k\Omega\,cm^2$ were immediately discarded (Prausnitz, *et al.*, 1993 [a]; Chen, *et al.*, 1998 [b]; M. R. Prausnitz, personal communication).

The donor compartment was filled with a donor particle suspension consisting of a single size of particle in PBS, and the receptor compartment was filled with only PBS. Both compartments were continuously stirred by magnetic stir bars. Prior to the experiment, a 1 h passive control period was used to hydrate the skin (Prausnitz, *et al.*, 1993 [a]) and check for leaks (holes or tears) in the skin. Leaky skin (passive flux above the detection limit) was immediately discarded. After hydrating the skin, either high-voltage pulsing, iontophoresis, or no pulsing (passive control) was applied for 1 h. Each pulsing condition was repeated on 3 to 6 different pieces of skin to ensure reproducibility.

5.5. Cleaning the Equipment.

Although the latex particles were highly charged, due to the large number of carboxylated surface groups ($-COO^-$), they were also found to be very hydrophobic as well, due to their composition (polystyrene). Because of the strong hydrophobicity of the particles, extra care had to be taken to ensure adequate cleaning from the equipment.

A remarkably extensive amount of cleaning and washing was found to be required, to ensure that the permeation chambers were adequately decontaminated of all fluorescent particles between experiments. Between each experiment, the permeation chambers had to be soaked in a >10% bleach solution for >30 min, rinsed in de-ionized water three times, soaked in de-ionized water for >30 min, soaked in chloroform (J. T. Baker, Phillipsburg, NJ) for >30 min, rinsed in de-ionized water three times, washed with detergent (Alconox, Fischer Scientific, Pittsburgh, PA) overnight (~12 h), rinsed in de-ionized water three times, sonicated (Branson Ultrasonic Cleaner) for >30 min, then rinsed again in de-ionized water three more times. The chambers were then carefully checked for contamination by wiping all of the exposed surfaces with tissue paper and carefully examining the tissue paper under a fluorescence microscope; any chamber still found contaminated with fluorescent particles was then subjected to the entire washing protocol again. Other pieces of equipment, such as the pipettes, membranes, and electrodes, were immediately discarded after each experiment to prevent contamination. Without these extremely thorough precautions, it was found that contamination of the equipment by the fluorescent particles between experiments could give completely erroneous results in the amount of particle "transport" observed.

5.6. Confocal Microscopy Results.

It was found that under confocal microscopy, it was nearly impossible to determine the location of a given particle, whether within the stratum corneum, epidermis, or on the surface. There was enough ambiguity in the data that any results and interpretations from these experiments could be open for debate. Reasons for the ambiguity came from the thickness of the optical section (comparable to the thickness of the stratum corneum), the inability of the skin to lay perfectly flat on the microscope slide, and the difficulty in distinguishing the stratum corneum and the epidermis. Given these difficulties, confocal microscopy could not be satisfactorily used to determine whether particles were actually transported through the stratum corneum or not.

5.6.1. Optical Section Thickness Comparable to Stratum Corneum Thickness.

The confocal microscope allowed individual planes (optical sections) within the sample to be studied, without interference from underlying or overlying planes. Although ideally these sections are two-dimensional planes, in reality, there is some thickness to these optical sections. The optical section thickness for the confocal microscope used in these experiments was found to be ~10 μ. Thus, objects separated by <10 μ would all appear to be within the same plane.

The stratum corneum itself is about 10 to 20 μ thick (Elias, 1983). Thus with a 10 μ thick optical section, it would be nearly impossible to accurately determine if a given particle located by confocal microscopy was actually in the epidermis, stratum corneum, or simply on the surface.

5.6.2. Skin Not Flat.

One problem with mounting the skin on a microscope slide is that the skin itself does not lie perfectly flat on the slide. Skin is not a flat tissue, and on a microscopic scale, the skin appears somewhat warped. Thus, in optically sectioning the skin, the same optical plane may image the stratum corneum in one section, but the epidermis in another section. This effect made it very difficult to determine if a particle in a given location was actually in the epidermis or stratum corneum.

5.6.3. Cannot Distinguish the Stratum Corneum from the Epidermis.

Nile Red is a lipid staining compound; however, the intercellular regions of both the stratum corneum and epidermis are rich in lipids. Thus, the cell outlines of both regions will be stained by Nile Red. Usually the stratum corneum and epidermis are differentiated by cell morphologies; however, under confocal microscopy, since the skin does not lie flat on the microscope slide, it is impossible to accurately distinguish between the two regions. Thus, it was not possible to accurately determine if a particle in a given location was within the epidermis or stratum corneum.

5.7. Light Microscopy Results.

In light or fluorescence microscopy, light is passed through the specimen to the observer. Thus, molecular transport through the skin cannot be determined; light or fluorescence microscopy only allows the direct observation of the skin after an experiment.

Others have previously established a connection between fluorescent regions within the skin after pulsing and sites where molecular transport occurs during pulsing with fluorescent molecules (Pliquett, *et al.*, 1996 [b]). Thus, experiments using fluorescence microscopy can still give useful information.

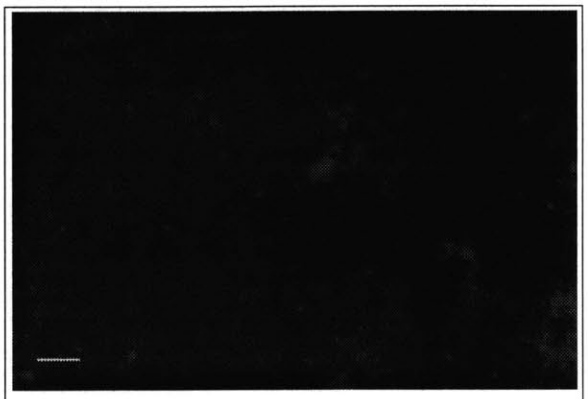

Figure 5.3. Particles on the skin after passive controls. Scale bar = 200 μ. Fluorescent latex particles interact very weakly with the surface of the skin. No significant clustering of particles on the surface of the skin were observed.

5.7.1. No Bead Clustering during Passive Controls.

After passive treatment of the skin (no high-voltage pulsing or iontophoresis) with the 2.16 μ diameter Sigma particles in the donor compartment for 2 h, a sparse, mostly homogenous dispersion of particles was seen on the top surface of the skin under light microscopy (see Figure 5.3). Similar results were obtained with 1.01, 0.431, and 0.035 μ diameter particles. Without an external driving force, the particles interacted only weakly with the stratum corneum and did not cluster together on the surface.

5.7.2. Iontophoresis Causes Clustering of Particles at Hair Follicles.

Application of constant current, 1 mA/cm^2 iontophoresis with the 2.16 μ diameter Sigma particles in the donor compartment for 1 h gave a sparse, mostly homogenous dispersion of particles on the surface of the skin. Moderate clustering of the particles was found at the tips of the hair follicles. Similar results were found with the 1.01 and 0.105 μ diameter particles.

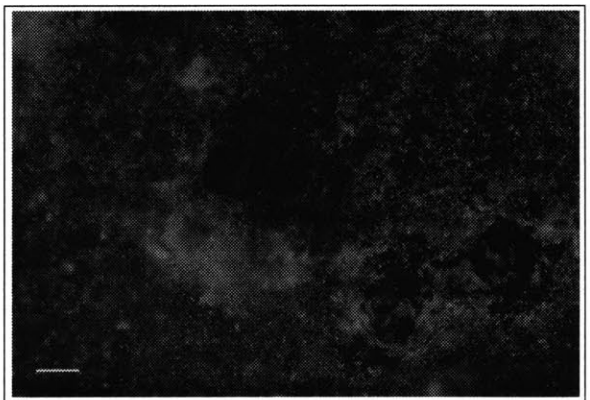

Figure 5.4. Particles on the skin after iontophoresis. Iontophoresis caused the transport of latex particles primarily into the hair follicles (bright spots near center of photomicrograph). Particles were also transported to the skin in areas away from the hair follicles. Compare with Figure 5.3. Scale bar = 200 μ.

Under 10 mA/cm^2 iontophoresis, with 2.16 μ diameter particles in the donor compartment for 1 h, very large concentrations of fluorescent particles were found at the tips of the hair follicles. The rest of the surface of the skin showed very dense, homogenous dispersions of particles (Figure 5.4).

Ion transport across the skin during iontophoresis is believed to occur primarily across sweat ducts and hair follicles (Grimnes, 1984; Burnette and Ongpipattanakul, 1988; Cullander and Guy, 1991; Scott, *et al.*, 1993); however, some current may also cross the stratum corneum itself (Potts, *et al.*,

1992; Monteiro-Riviere, *et al.*, 1994). In the current set of experiments, most of the charged particles appeared to follow the electric field lines and cluster near the hair follicles; however, away from the hair follicles, particles could also be found on the surface of the stratum corneum. This effect seemed more pronounced at higher applied currents. Thus, during iontophoresis, the transport of particles into the skin appears consistent with previous observations of molecular transport through the skin.

5.7.3. Particle Clusters on the Skin after Pulsing were Similar to LTRs.

With the 2.16 μ diameter Sigma particles, fluorescence microscopy after pulsing ($U_{applied}$ = 1000 V, corresponding to U_{skin} ~ 150 V, τ = 5 ms, 1 pulse every 5 s for 1 h) revealed the presence of small, fluorescent clusters of particles on the surface of the stratum corneum (Figure 5.5), ~200 μ in diameter. These clusters were not observed in the passive controls. These clusters were randomly distributed on the surface of the skin, and were not associated with sweat ducts or hair follicles.

The clusters of particles observed on the surface of the skin after pulsing were reminiscent of the "localized transport regions" (LTRs) that were seen on the surface of the skin after applying high-voltage pulsing to the skin (Zewert, *et al.*, 1995; Pliquett, *et al.*, 1996 [b]; Prausnitz, *et al.*, 1996 [a]; Chen, *et al.*, 1998 [b]; Vanbever, *et al.*, submitted). The clustering of particles after high-voltage pulsing has previously been reported by Prausnitz, *et al.* (1996 [a]), who demonstrated the transport of fluorescent latex particles to the surface of the skin by confocal microscopy; however, there was no attempt to measure particle fluxes through the skin.

The clusters of particles present on the surface of the skin are not actually LTRs, since there was no significant transport of any particles through these regions or even through the skin itself (see Sections 5.8 through 5.10, below). However, the appearance of the particle clusters on the surface of the skin was found to be similar to the LTRs. The clusters of particles were randomly distributed, and not associated with sweat ducts or hair follicles (Zewert, *et al.*, 1995; Pliquett, *et al.*, 1996 [b]; Prausnitz, *et al.*, 1996 [a]; Chen, *et al.*, 1998 [b]; Vanbever, *et al.*, submitted).

Given that the particles were highly negatively charged, the same mechanism could be transporting both molecules and particles to the surface of the skin. During high-voltage pulsing, localized ion currents are believed to cross the skin and may be responsible for creating the LTRs for calcein and sulforhodamine (Pliquett, *et al.*, 1996 [b]). Thus, localized ion currents across the surface of the skin, created during high-voltage pulsing, could also be responsible for transporting particles to the surface of the skin and depositing them in clusters. Although there is no significant transport of particles through the stratum corneum during high-voltage pulsing, the appearance and behavior of particle clusters on the surface of the skin is very similar to the appearance and behavior of LTRs.

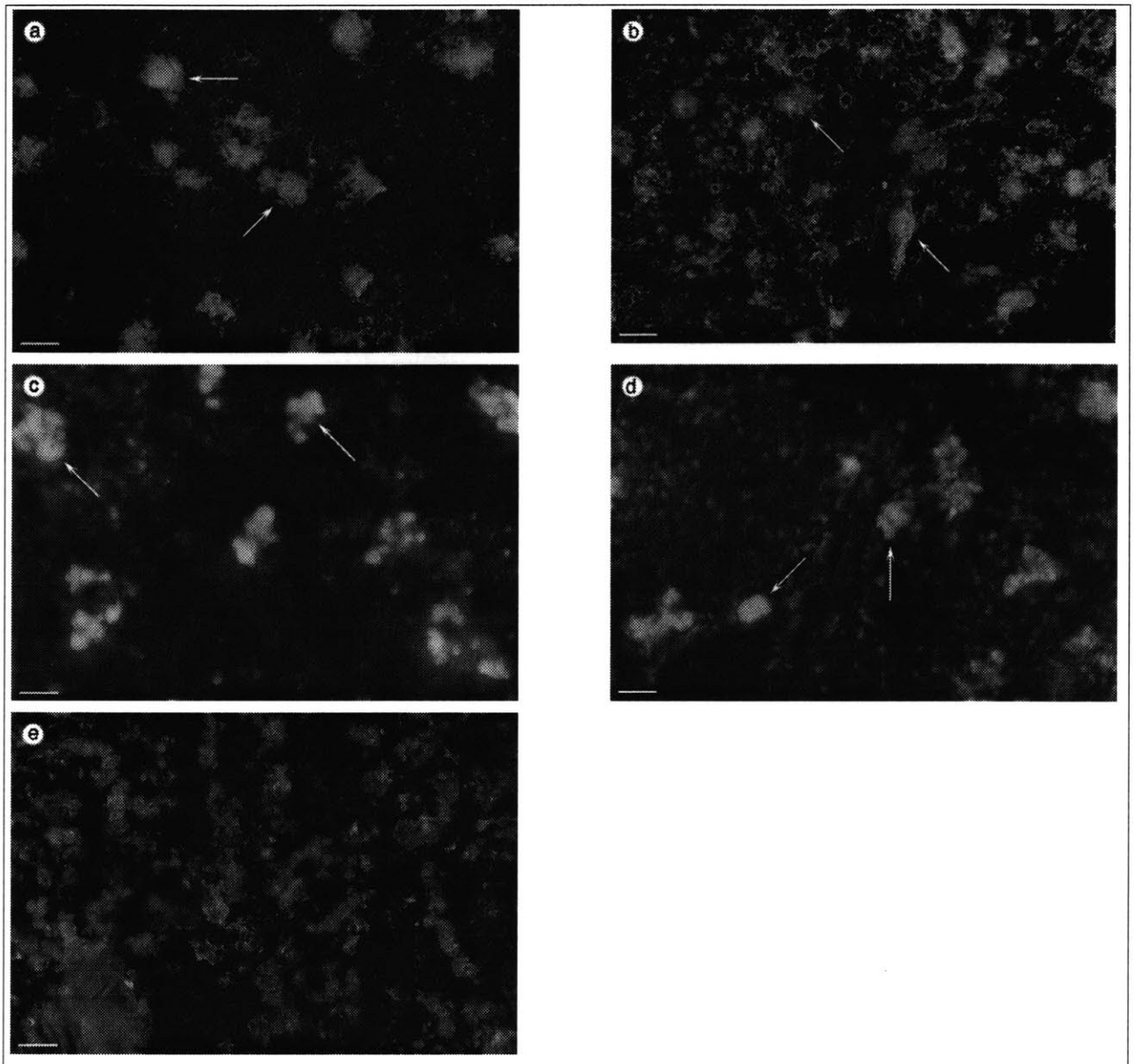

Figure 5.5. Particles on the skin after pulsing as a function of particle size. These photomicrographs of the stratum corneum of human skin were taken under fluorescence microscopy after pulsing. Scale bar = 200 μ. The diameters of the particles present in the donor compartment were as follows: (a) 2.16 μ, (b) 1.01 μ, (c) 431 nm, (d) 105 nm, and (e) 35 nm. For all of the particles except the 35 nm diameter particles (e), prominent clusters of particles were observed on the surface of the skin (some indicated by arrows), randomly distributed, and not associated with sweat ducts or hair follicles. The circular regions in (b) are trapped air bubbles.

5.7.4. Similar Clusters Observed for Different Particle Sizes.

Under the same pulsing conditions ($U_{applied}$ = 1000 V, corresponding to U_{skin} ~ 150 V, τ = 5 ms, 1 pulse every 5 s for 1 h), using fluorescent particles in the donor compartment with diameters ranging from 35 nm to 2.16 μ (particle diameters shown in Table 5.2), resulted in the appearance of small, fluorescent particle clusters on the surface of the stratum corneum (Figures 5.5a through 5.5e). The number of clusters appearing on the skin in each case was approximately the same, ~3 clusters / mm^2

(Figure 5.6a). The diameter of the clusters for each case was also similar, ~200 μ (Figure 5.6b), except with the smallest (35 nm diameter) particles, where no particle clusters were observed.

The size or charge of the particles did not appear to have a major effect on the formation of clusters on the surface of the skin during high-voltage pulsing. The formation of particle clusters appears to depend more on the applied pulsing conditions, rather than the physical properties of the particles.

5.7.5. *Clusters of Particles Found Above ~70 V_{skin}.*

With 2.16 μ diameter particles in the donor compartment, using the same protocol (τ = 5 ms, 1 pulse every 5 s for 1 h), $U_{applied}$ was systematically changed from -1000 V (which corresponds to U_{skin} ~ -100 V) through 0 V (passive control), up to 1500 V (corresponding to U_{skin} ~ 200 V). Fluorescence microscopy of the skin revealed an increase in the surface density of particle clusters observed on the surface of the skin with increasing voltage (see Figures 5.7a through 5.7e, data shown in Figure 5.8a), up to ~8 clusters / mm^2 at $U_{applied}$ = 1500 V; however, after $U_{applied}$ = 500 V (corresponding to U_{skin} ~ 100 V), the diameter of the particle clusters appearing on the surface of the skin stayed fairly constant at ~200 μ (Figure 5.8b).

Very few particle clusters were observed on the skin after pulsing at $U_{applied}$ = 500 V, which corresponds to U_{skin} ~70 V. No particle clusters were observed at voltages less than U_{skin} ~ 70 V,

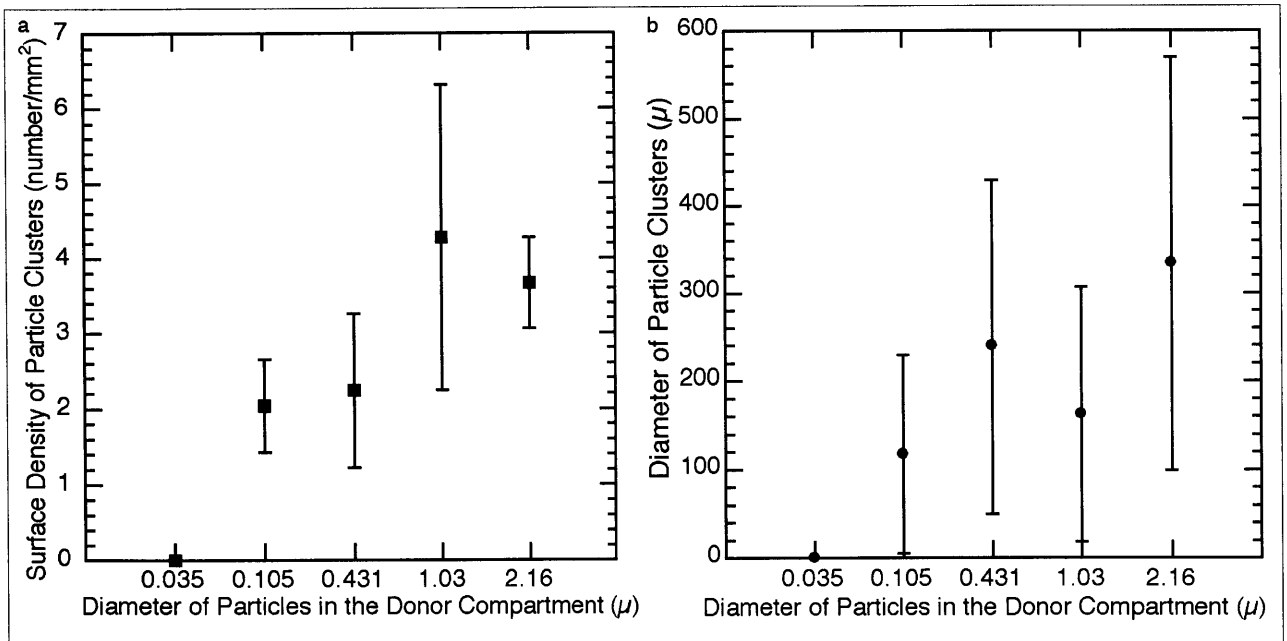

Figure 5.6. Effect of particle size on number density (a) and diameter (b) of particle clusters. (See Figures 5.5a through 5.5e). The diameter of the particles used in the donor compartment varied from 35 nm to 2.16 μ. Except for the smallest (35 nm) particles, both the density and the size of the clusters observed on the stratum corneum after high-voltage pulsing were almost the same, regardless of the size of the particles.

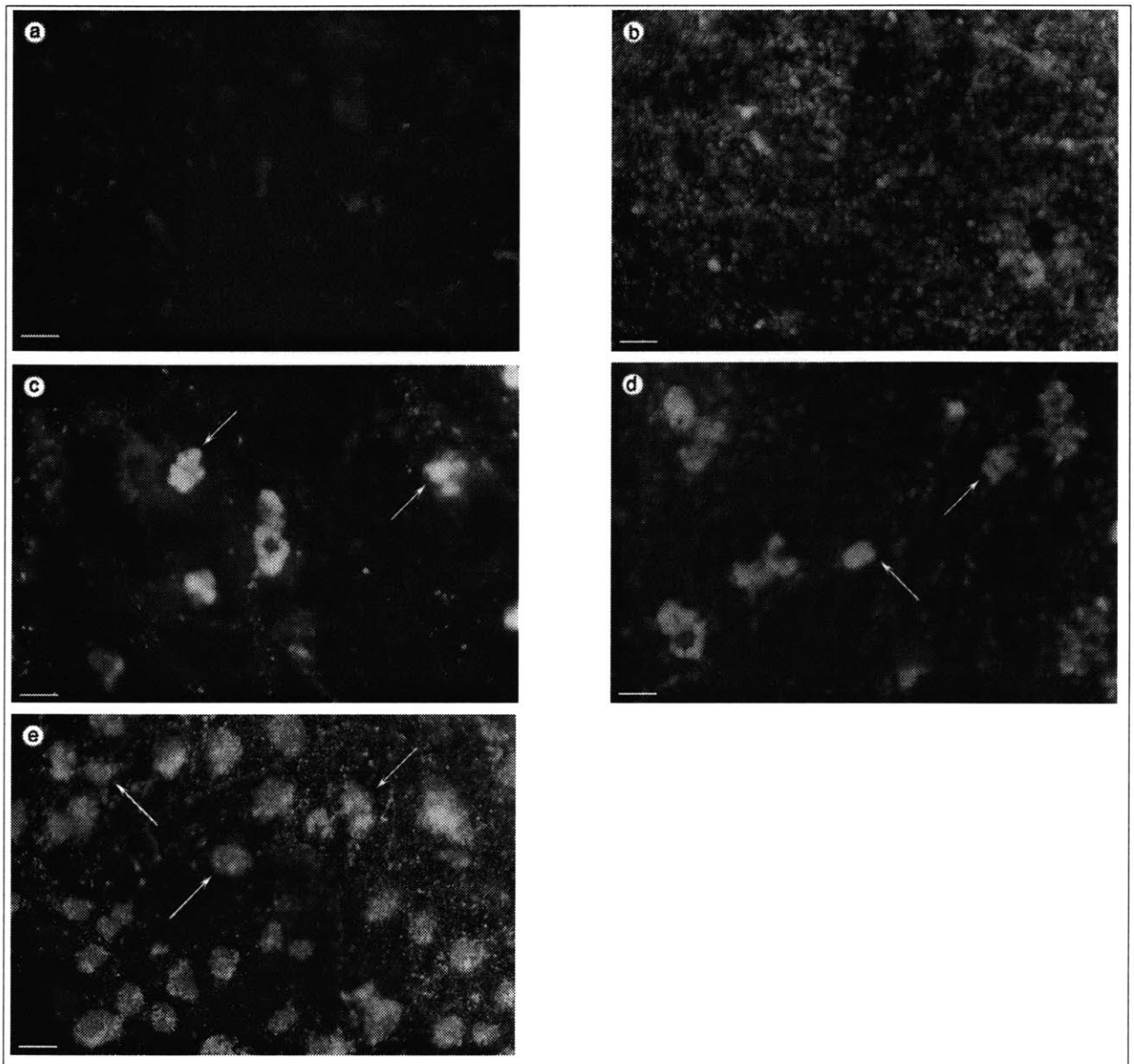

Figure 5.7. Particles on the skin after pulsing as a function of the applied voltage. These photomicrographs of the stratum corneum were taken under fluorescence microscopy, with varying applied voltages (2.16 μ diameter particles, $U_{applied}$ from 0 V to 1500 V, τ = 5 ms, 1 pulse every 5 s for 1 h). Scale bar = 200 μ. Clusters of particles were observed on the surface of the skin at $U_{applied}$ > 250 V, randomly distributed on the surface, and not associated with sweat ducts or hair follicles (some particle clusters indicated by arrows). (a) $U_{applied}$ = 0 V (passive control, no applied pulses. U_{skin} = 0 V). (b) $U_{applied}$ = 250 V (U_{skin} ~ 50 V). (c) $U_{applied}$ = 500 V (U_{skin} ~ 100 V). (d) $U_{applied}$ = 1000 V (U_{skin} ~ 150 V). (e) $U_{applied}$ = 1500 V (U_{skin} ~ 200 V).

including reverse pulsing at U_{skin} ~ -100 V (pulsing with the positive electrode in the donor compartment and the negative electrode in the receptor compartment). This is similar in behavior to the LTRs, which also increase in number density with increasing $U_{applied}$ (and hence U_{skin}), while remaining constant in size (Vanbever, *et al.*, submitted).

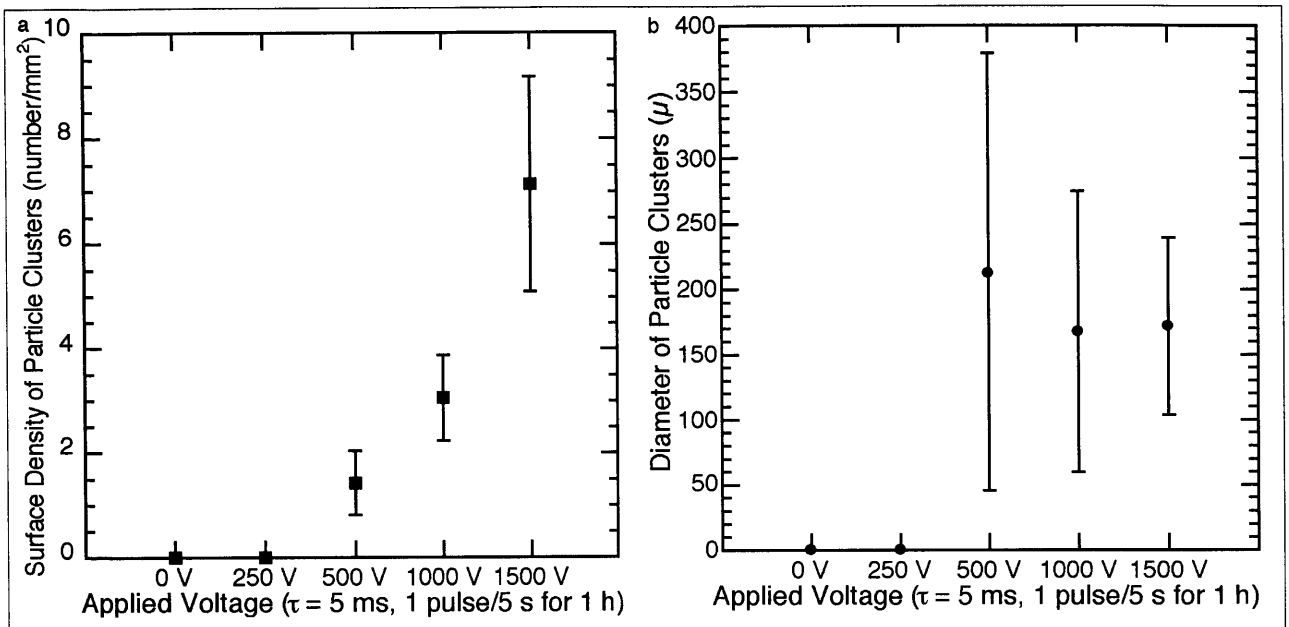

Figure 5.8. Effect of applied voltage on number density (a) and diameter (b) of particle clusters. These data correspond to Figures 5.7a through 5.7e. For $U_{applied}$ > 250 V, the sizes of the clusters of particles remained fairly constant, but the number of clusters observed increased with the voltage.

These results were consistent with the idea that high-voltage pulsing of the skin below U_{skin} ~ 75 V does not cause electroporation of the stratum corneum (Chizmadzhev, *et al.*, 1998 [a]), or increased molecular or ionic transport (see also Section 8.2.4). Since the creation of both particle clusters and LTRs appears similar under various conditions, similar mechanisms are probably responsible for their creation.

5.7.6. Cluster Sizes Increase with Time Constant.

Using the same pulsing protocol ($U_{applied}$ = 1000 V, corresponding to U_{skin} ~ 150 V, with 1 pulse every 5 s for 1 h) with the 2.16 μ diameter particles, systematically altering τ from 1 ms to 15 ms, resulted in changes in both the number and size of the particle clusters observed after 1 h of pulsing (Figures 5.9a through 5.9f). The diameters of the clusters of particles increased from almost undetectable clusters at τ = 1 to 3 ms, up to ~700 μ at τ = 15 ms (Figure 5.10a). Conversely, the number of clusters observed on the surface of the skin decreased, from ~2 clusters / mm^2 at τ = 5 ms, down to ~0.2 clusters / mm^2 at τ = 15 ms (Figure 5.10b).

With the application of high-voltage pulsing with τ = 15 ms, red regions were found in the skin in the centers of the particle cluster areas. These regions appeared red due to the presence of the Nile Red stain, indicating that these areas were filled with lipophilic material.

With increasing τ, there was an increase in the size of the particle clusters (Figure 5.10b), and a decrease in the number density (Figure 5.10a). Similarly, for LTRs, with increasing τ, there was an increase in the size of the LTRs and a decrease in the number density (Vanbever, *et al.*, submitted). The similarity in results between particle transport and molecular transport could indicate that similar mechanisms are involved.

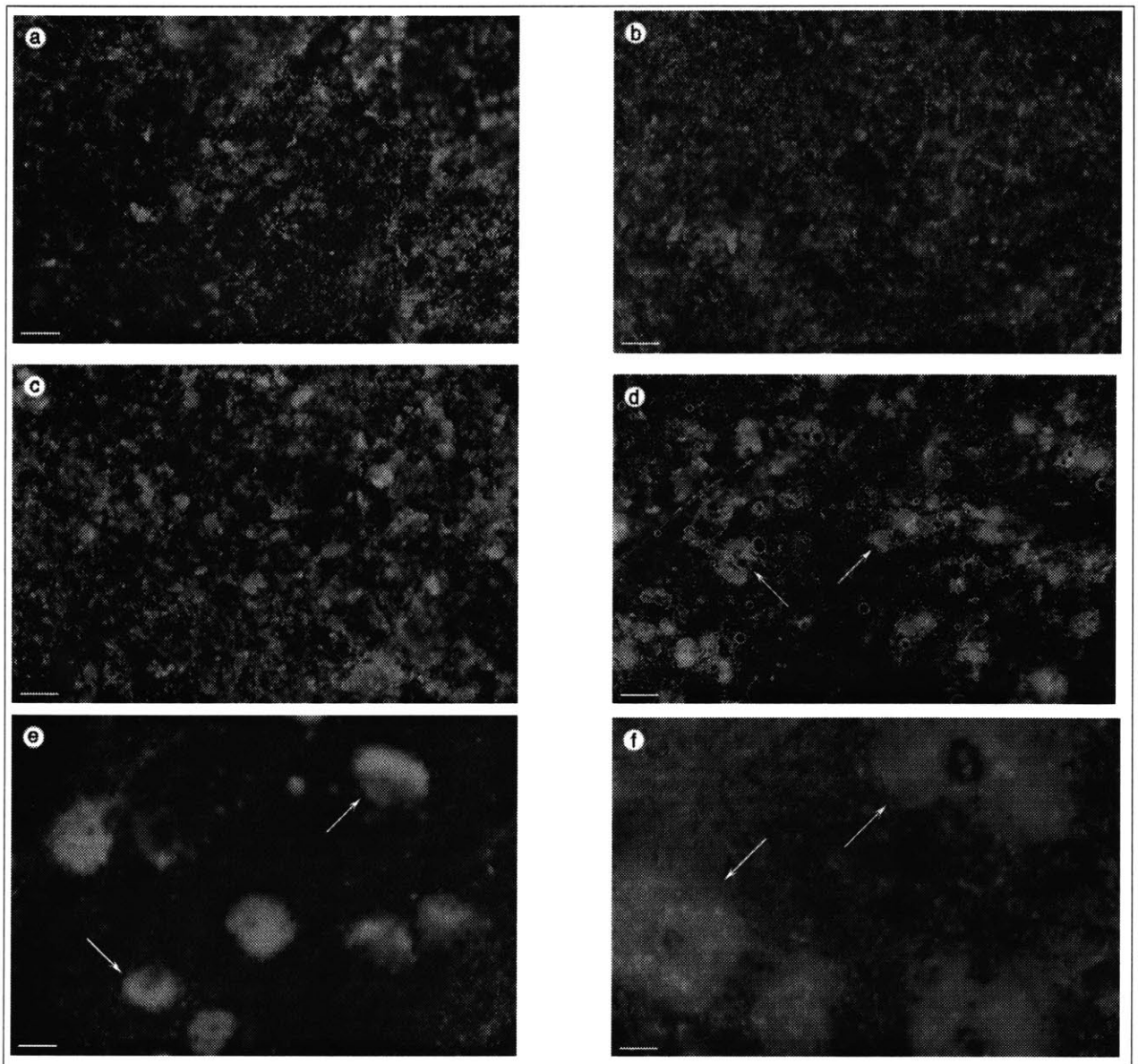

Figure 5.9. Particles on the skin after pulsing as a function of the time constant. These photomicrographs of the stratum corneum were taken under fluorescence microscopy, with τ varying from 1 ms up to 15 ms (2.16 μ diameter particles, $U_{applied}$ = 1000 V, corresponding to U_{skin} ~ 150 V, 1 pulse every 5 s for 1 h). Scale bar = 200 μ. Increasing τ resulted in smaller numbers and larger clusters of particles, randomly distributed on the surface of the skin, not associated with sweat ducts or hair follicles (some clusters indicated by arrows). (a) τ = 1 ms. (b) τ = 2 ms. (c) τ = 3 ms. (d) τ = 5 ms. (e) τ = 10 ms. (f) τ = 15 ms. The circular rings in (d) are trapped air bubbles.

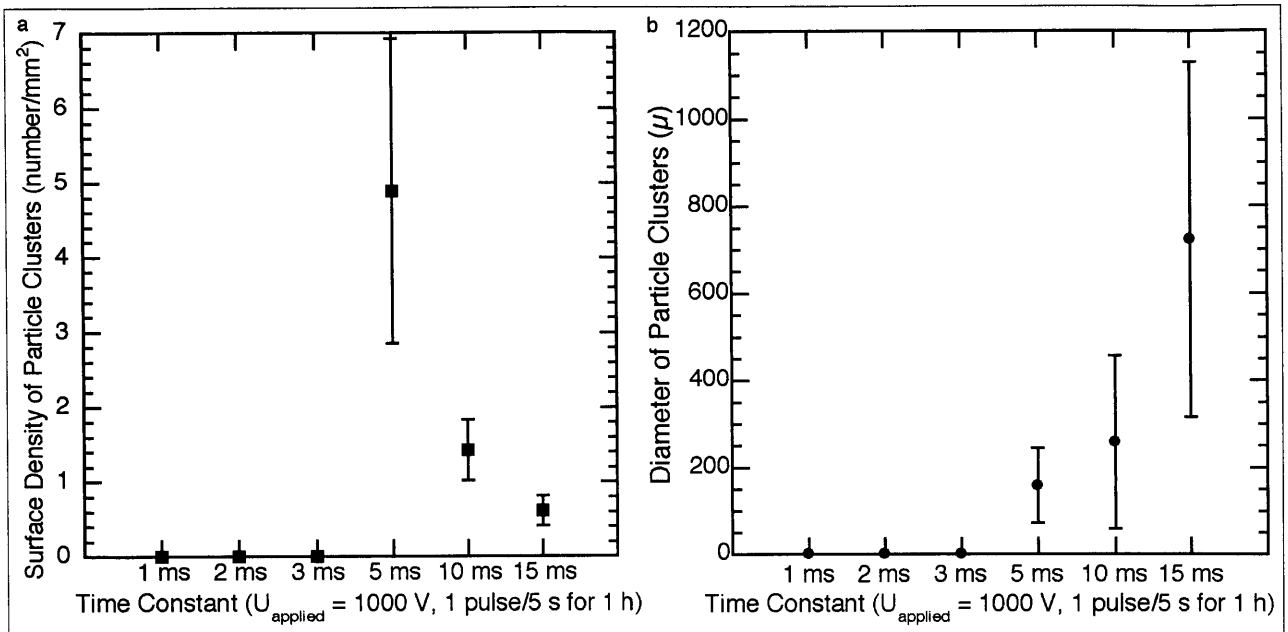

Figure 5.10. Effect of time constant on number density (a) and diameter (b) of particle clusters. These data correspond to the experiments described in Figures 5.9a through 5.9e. The clusters of particles observed on the surface of the skin appeared to increase in size and decrease in number, for increasing τ.

5.8. Particle Counting by Gel Trapping.

During the gel trapping experiments, it was eventually found that the amount of particle transport appeared to be a function of the date of the experiment. In general, more particle transport was observed on later dates rather than on earlier dates. In fact, the date appeared to have a much stronger effect than the actual electrical conditions applied to the skin.

Further investigation into this phenomenon yielded the cause of this relationship: the fluorescent polystyrene particles were very hydrophobic and adhered so strongly to the glass chambers that after several months' worth of experimentation, all of the glass chambers had been severely contaminated by polystyrene particles. Given this contamination, a very stringent washing program was established (previously described in Section 5.5), but even with these precautions, some contamination of particles still remained. Despite the lower level of contamination, it was still impossible to conduct any more gel trapping experiments due to the remaining contamination problems, so only an upper limit of particle transport could be established.

5.8.1. Particles Adhere to Equipment.

Despite much careful washing of equipment as previously described (Section 5.5), it was found that the polystyrene particles adhere to the equipment very strongly and come off only slowly. Some

fluorescent particles were still found to be adhering to the equipment even after one month of stringent washing. Thus, it was not possible to sufficiently clean the equipment between experiments to avoid particle contamination.

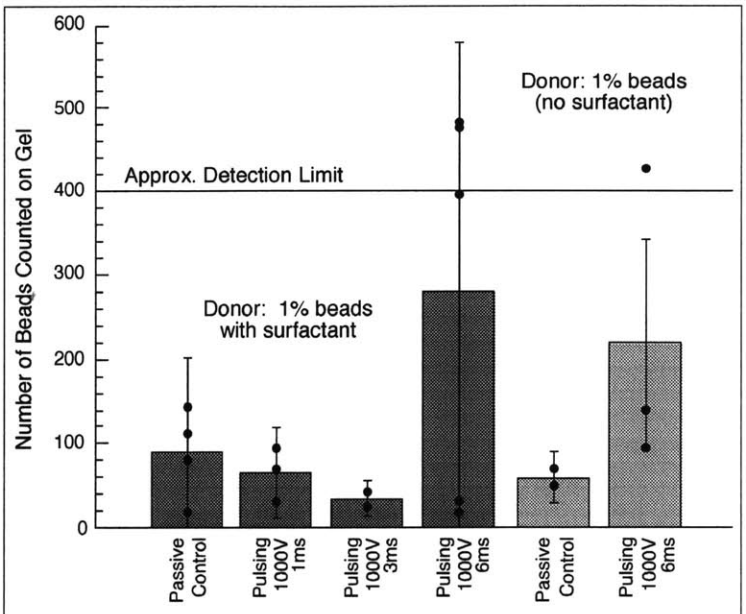

Figure 5.11. Counts of particles trapped by agarose or polyacrylamide gel. Voltages are applied voltages; time constants are given next to the voltages. Points represent individual experiments, columns represent averages of each condition, and error bars represent standard deviations. The number of particles in each case was near the detection limit, ~5 particles / mm^2, corresponding to ~350-400 particles.

5.8.2. *Upper Limit of Transport Established.*

Due to the particle contamination problems, only an upper limit could be established for particle transport. This limit was found to be ~5 particles / mm^2, after the stringent washing protocols previously described in Section 5.5. The same upper limit was found in the passive controls (no pulsing for 2 h), iontophoresis (1 mA / cm^2 for 1 h), and high-voltage pulsing (U_{skin} ~100 V, 1 pulse every 5 s for 1 h, τ = 5 ms) (Figure 5.11).

5.9. Particle Counting by Membrane Trapping.

The total number of 2.16 μ diameter particles found in the polycarbonate membranes after 1 h of pulsing was comparable to the passive controls (Figure 5.12). Smaller particle sizes were more difficult to trap with the polycarbonate membranes and hence were not counted.

Examination of blank slides exposed to just human skin for 1 h (no fluorescent particles) under fluorescence microscopy showed that ran-

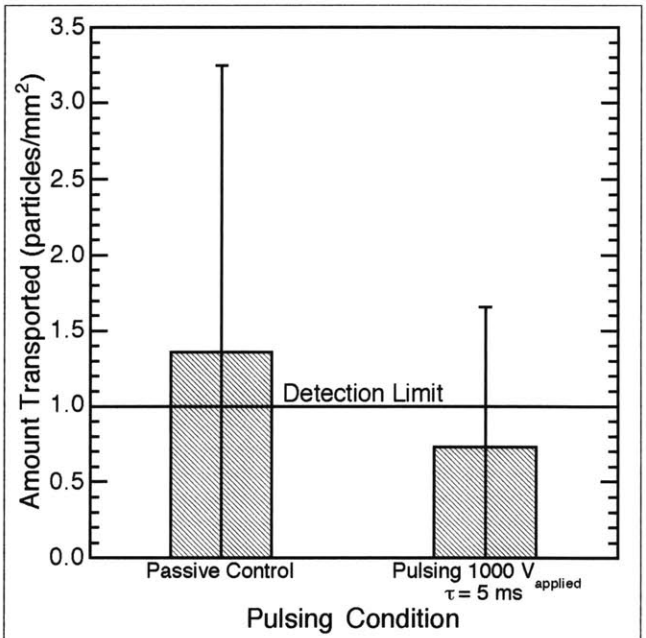

Figure 5.12. Counts of particles trapped by polycarbonate membranes. These counts are only for the 2.16 μ diameter particles, which were easily trapped by the 0.1 μ mesh polycarbonate membrane filters. There was no significant difference between the passive controls and high-voltage pulsing. Measurement values were near the detection limit of the system. Hence, there does not appear to be any transport of particles across the stratum corneum due to high-voltage pulsing

dom bits of dust were sometimes fluorescent, and these bits of dust could sometimes be confused with the particles. Thus, an error of ±1 particle per field-of-view was used (one field-of-view under the microscope was a circle 1.60 mm in diameter). This is the detection limit drawn in Figure 5.12. An error rate of 1 particle per field-of-view corresponds to a total error rate of ±60 particles transported across the skin, much less than the 1.4×10^9 particles provided in the donor compartment.

Thus, with this detection system, <1 particle / mm^2 of transport was observed in both the high-voltage pulsing experiments ($U_{applied}$ = 1000 V, which corresponds to U_{skin} ~ 150 V, τ = 5 ms, 1 pulse every 5 s for 1 h) and in the passive controls (no pulsing), where the lower limit of particle detection, 1 particle / mm^2, was governed by the amount of fluorescent debris present on the surface of the skin.

5.10. Particle Detection by Fluorescence Spectrometry.

Unlike the particle counting experiments, fluorescence spectroscopy techniques were not limited by particles >1 μ in diameter. Thus, in this set of experiments, particles ranging in diameter from 14 nm to 2.10 μ were used, all from Molecular Probes (Table 5.3). In addition, some of the experiments used stratum corneum only preparations instead of epidermis, eliminating the epidermis as a possible barrier to particle transport.

5.10.1. No Increase in Fluorescence After High-Voltage Pulsing or Iontophoresis.

The fluorescence detected in the receptor compartments after passive controls (no pulsing for 2 h), iontophoresis (1 mA / cm^2 for 1 h), and high-voltage pulsing ($U_{applied}$ = 1000 V, corresponding to U_{skin} ~ 150 V, τ = 5 ms, 1 pulse every 5 s for 1 h) did not differ significantly from each other, for experiments involving either the epidermis (with the stratum corneum) or only stratum corneum. See Figures 5.13 (epidermis) and 5.14 (stratum corneum only). In addition, increasing τ from 5 ms to 300 ms did not increase the fluorescence detected in the receptor compartment (data not shown).

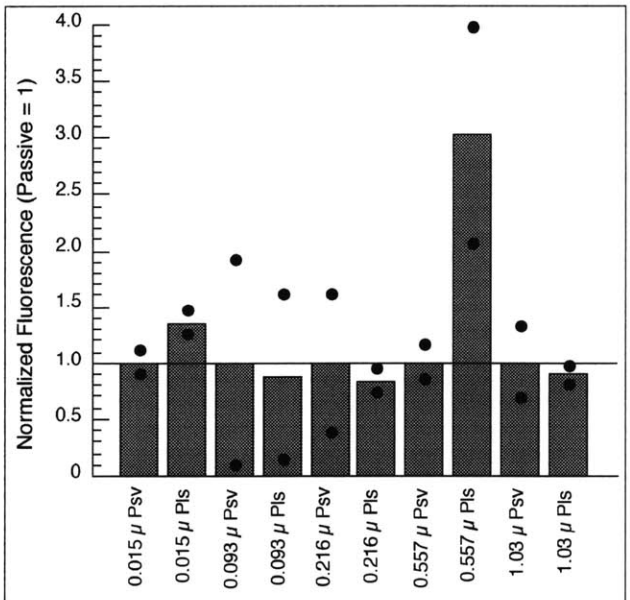

Figure 5.13. Particle detection after transport through the epidermis. The particles were detected in the receptor compartment using fluorescence spectroscopy. The results of high-voltage pulsing conditions ("Pls") are normalized to passive controls ("Psv"). Points represent individual experiments; columns represent averages. No significant enhancement to particle transport was observed.

In Figure 5.14, the striped bars show the receptor compartment fluorescence after 1 h of passive control (no pulsing), and the solid bars show the receptor compartment fluorescence after 1 h of pulsing. For each of the particle sizes used, the calibration curves showed a linear relationship between the concentration of the particles and the observed fluorescence; however, there was a lower limit of fluorescence that could be detected by the spectrofluorimeter. This level has been normalized to 1 in Figure 5.14. In Table 5.4, the minimal number of particles that could be detected with this technique are given.

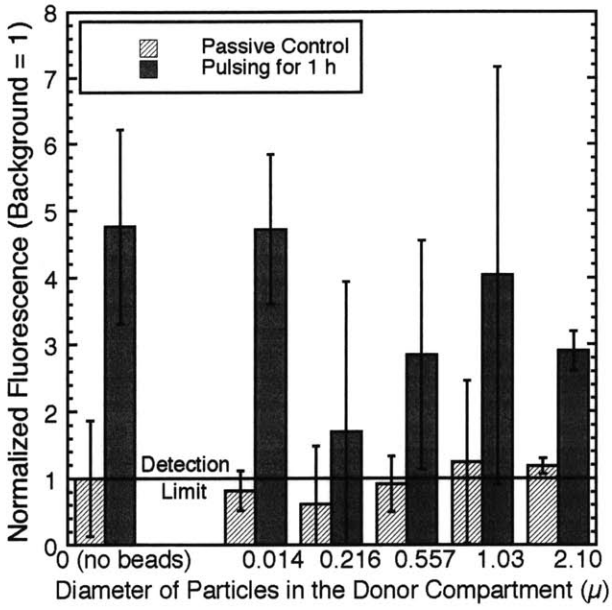

Figure 5.14. Particle detection after transport through the stratum corneum. All of the fluorescence data have been normalized to the detection limit. With both the zero particle control and all of the particle sizes used, applying pulsing caused a roughly 3- to 5-fold enhancement in the fluorescence. This increase is probably not due to particle transport, but instead may be due to the release of fluorescent materials from the skin.

In Figure 5.14, each of the passive controls did not show significantly more fluorescence than the detection limit of the spectrofluorimeter. Thus, under passive controls, no significant particle transport through the skin was detected.

At first glance, it may appear that high-voltage pulsing causes some particle transport across the stratum corneum. However, even if there are no particles in the donor compartment, there is still a roughly 5-fold increase in the fluorescence of the receptor compartment (pair of bars on the far left). This "enhancement" of fluorescence is probably not due to particle transport across the stratum corneum, but instead it could possibly be the release of autofluorescent materials from the stratum corneum.

5.10.2. Upper Limit of 14 nm Established for Pathway Size.

Previous studies have shown that the LTRs on the surface of the skin represent areas of increased ionic and molecular transport during pulsing (Pliquett, *et al.*, 1996 [b]). With the current set of experiments, it was shown that the particles collect on the surface of the skin during pulsing (Figures 5.5a through 5.5e, 5.7a through 5.7e, and 5.9a through 5.9f), yet there is no significant transport of any of the particles across the stratum corneum (Figures 5.11

Table 5.4. Particle Detection Limits.

Diameter (μ)	Detection Limit (particles / mm^2)
2.10	3.0×10^3
1.03	8.7×10^3
0.557	1.8×10^5
0.216	2.6×10^6
0.014	8.5×10^9

through 5.14). Hence, the transient aqueous pathways that are believed to be forming during high-voltage pulsing (Prausnitz, *et al.*, 1993 [a]; Chizmadzhev, *et al.*, 1995; Chizmadzhev, *et al.*, 1998 [a]) appear to be too small to allow the transport of particles. The smallest particles used here had a diameter of 14 nm; thus, if aqueous pathways are forming through the stratum corneum during pulsing, the average diameter of the pathways must be less than 14 nm. This is in agreement with theoretical calculations that have predicted a pathway diameter of ~0.4 nm (Chizmadzhev, *et al.*, 1995), which would allow the passage of ions and molecules across the skin, but not microparticles.

5.11. Conclusions.

Applying a series of short (τ ~ 5 ms), high-voltage pulses to human skin ($U_{applied}$ ~ 1000 V, corresponding to U_{skin} ~ 150 V, 1 pulse every 5 s for 1 h) caused fluorescent, latex particles (14 nm to 2.10 μ in diameter) to form clusters on the surface of the stratum corneum, where the clusters were randomly distributed and not associated with sweat ducts or hair follicles. This was similar in appearance to "localized transport regions" observed with the molecular transport of fluorescent tracers. These clusters of particles were roughly 100 μ in diameter, regardless of the size of the particles used. The clusters increased in number density with the transdermal voltage, and increased in size with the time constant. They appeared to form at transdermal voltages >70 V. Under passive controls (no pulsing), no clusters of particles appeared. Under 1 mA / cm^2 iontophoresis, particles appeared near the hair follicles. Overall, the behavior of the particles on the surface of the skin was very similar to the LTRs observed after molecular transport.

However, no particle transport was ever observed through the stratum corneum, under any of the electrical pulsing protocols, or with any of the detection techniques. Since the smallest particles used were 14 nm in diameter, the size of the aqueous pathways that form across the skin during high-voltage pulsing ("electroporation") must be <14 nm.

Extremely careful analysis, preparation, and cleaning techniques are essential to ensure that false positive results do not occur during experimentation. Based on these results, it was felt that particles could not be transported through the human stratum corneum simply by means of high-voltage pulsing. Additional effects, such as mechanical or pressure forces, may be required to transport particles through the skin, but were not studied here.

6. On the Use and Detection of Peptides to Study Molecular Transport.

In the study of skin electroporation, factors important for molecular transport include both the properties of the applied electrical pulse (transdermal voltage, shape, time constant, pulsing frequency, and the number of pulses) (Prausnitz, *et al.*, 1993 [a]; Vanbever, *et al.*, 1994; Pliquett, *et al.*, 1995 [a]; Vanbever and Préat, 1995; Pliquett and Weaver, 1996 [a]; Prausnitz, *et al.*, 1996 [b]; Vanbever, *et al.*, 1996 [b]), and the physical properties of the molecules being transported (size, charge, and hydrophilicity) (Prausnitz, *et al.*, 1993 [a]; Pliquett and Weaver, 1996 [a]). The original purpose of this study was to determine how the size and charge of a molecule can affect transport across the skin during high-voltage pulsing.

HPLC, or high performance liquid chromatography, is a technique that has been developed to detect and separate molecules at low concentrations. Molecules that have been analyzed using HPLC include biological entities such as peptides, proteins, sugars, and hormones. Molecules are put into solution (the "mobile phase"), which is run through a silica column under high pressures. The molecules are separated by their differences in their interactions with the column packing (the "stationary phase"), which affects how long the molecules will remain in the column (the "retention time"). Interactions with the column packing can be through hydrophilic interactions ("normal phase"), hydrophobic interactions ("reverse phase"), size exclusion, antibody binding, as well as many other types. The most common type of molecular detection is with UV absorbence (190 nm to 400 nm). It has been known to detect proteins at concentrations down to 1 nM (Hancock and Sparrow, 1984; Henschen, *et al.*, 1985).

6.1. Peptides.

A set of molecules with similar properties, varying only one property at a time, was to be studied. Peptides were chosen for this study, since any sequence could be easily synthesized (MIT Biopolymers Laboratory, Cambridge, MA, personal communication), and the size and charge of the peptide could be independently specified, based on the chosen amino acid sequence. However, due to the lack of a defined protocol, this section will briefly describe some of the techniques tried in this project, and their limitations.

Table 6.1. Sources and Molecular Weights of Glu – Leu_n.

Formula	MW (Da)	Source
Glu	147	Sigma
Glu – Leu_2	373	MIT Biopolymers Laboratory
Glu – Leu_4	600	MIT Biopolymers Laboratory

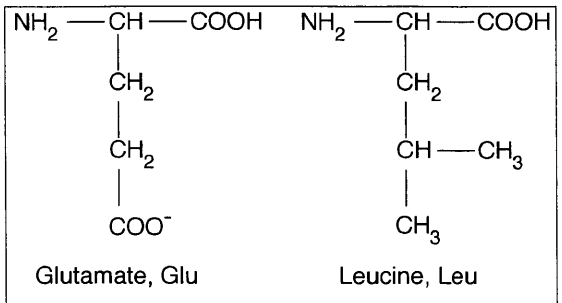

Figure 6.1. Molecular structures of glutamate and leucine. Glutamine is negatively charged, but leucine is neutral at pH ~ 7.

6.1.1. Glu – Leu_n Series.

The first series of peptides examined was Glu – Leu_n, where Glu is the abbreviation for glutamate and Leu is the abbreviation for leucine. The number of leucine residues varied from 0 to 4, as shown in Table 6.1. Figure 6.1 shows that glutamate had a net charge of -1 at a pH of ~7.4, while leucine was uncharged. Amino acids link together to become peptides via an amide bond, where the –COOH group reacts with the $-NH_2$ group to form a –CO – NH – bond, linking the two amino acids, with H_2O as the by-product. Thus, each of these molecules had a charge of -1, while the molecular weights varied from 147 Da to 600 Da.

These peptides were found to be unsatisfactory, due to their very low solubilities in PBS. Although Glu and Glu – Leu_2 were able to dissolve at concentrations of 1 mM, the solubility of Glu – Leu_4 in PBS was found to be about 0.3 mM. Since the leucine residues were very hydrophobic, further additions of leucine onto the peptide chain would decrease the solubility of the peptide chain even further, making this series of peptides unsuitable for study.

6.1.2. Glu – Gln_n Series.

The second series of peptides examined was Glu – Gln_n, where glutamine, or Gln, was chosen to replace leucine. See Table 6.2. Glutamine was an amine and was therefore less hydrophobic than leucine. As shown in Figure 6.2, glutamine had no net charge. Thus, these peptides should have been more hydrophilic than the Glu – Leu_n series.

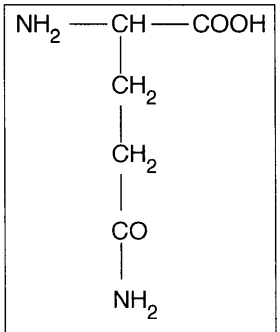

Figure 6.2. Molecular structure of glutamine. Glutamine is a hydrophilic amino acid.

The Glu – Gln_n peptides, all with -1 net charge, were indeed found to be very hydrophilic and dissolved easily in PBS. The MIT Biopolymers Laboratory reported that these peptides were, in fact, too hydrophilic to adhere well to their HPLC C_{18} column (MIT Biopolymers Laboratory, personal communication).

6.2. HPLC Machines.

There were two HPLC machines that were examined in this study. The first machine was a Millennium/Waters 510 system (Milford, MA). The columns tried on this system were the polyaspartic acid column (see Section 6.3.1), and the C_{18} column (Section 6.3.2). The second HPLC machine was a Hewlett-Packard HP 1090 system (Palo Alto, CA). The columns tried on this system were the C_{18} small bore column (Section 6.3.3), and the polyhydroxyethyl aspartamide hydrophilic interaction column (Section 6.3.4). For both machines, the mobile phase consisted of two parts: an aqueous phase (PBS) and an organic phase (HPLC-grade acetonitrile, J. T. Baker), mixed in different ratios.

Table 6.2. Sources and Molecular Weights of Glu – Gln_n.

Formula	MW (Da)	Source
Glu	147	Sigma
Glu – Gln_2	402	MIT Biopolymers Laboratory
Glu – Gln_4	659	MIT Biopolymers Laboratory

6.3. HPLC Columns.

Four different HPLC columns were tested to see if they could adequately separate and resolve the peptide sequences. Many operating conditions were also tried for each column to determine if separation of the peptides could be readily achieved.

6.3.1. Polyaspartic Acid Column.

The first column was a polyaspartic acid weak cation exchange column (4.6 mm inner diameter × 200 mm length, 5 μ silica packing, 300 Å pores) (Nest Group, Southborough, MA). The aqueous phase was varied from 0 to 100% of the mobile phase. Despite the claims of the supplier, this column was not suitable for separating negatively charged peptides, and could only be used to separate positively charged peptides. It was unable to resolve small peptides which differed only on the basis of their size.

6.3.2. C_{18} Column.

The second column was a C_{18} reverse phase column (4.6 mm inner diameter × 200 mm length, 5 μ silica packing, 300 Å pores) (Nest Group). The aqueous phase was varied from 0 to 100% of the mobile phase. This column was borrowed from a co-worker and was about a year old when used.

Although early experiments had shown promise, after several months, it was found that this column was losing its performance characteristics and was no longer able to adequately separate peptides.

6.3.3. C_{18} Small Bore Column.

The third column was a C_{18} reverse phase small bore column (4.6 mm inner diameter × 200 mm length, 5 μ silica packing, 90 Å pores) (Vydac, Hesperia, CA). The smaller pores (90 Å pores instead of 300 Å) allowed the column to separate smaller and more hydrophilic peptides. The aqueous phase was varied from 0 to 100% of the mobile phase. Unfortunately, the $Glu-Gln_n$ peptides were still too hydrophilic to be adequately separated by this column.

6.3.4. Polyhydroxyethyl Aspartamide Column.

The final column used was a polyhydroxyethyl aspartamide hydrophilic interaction chromatography column (4.6 mm inner diameter × 200 mm length, 5 μ silica packing, 200 Å pores) (PolyLC, Columbia, MD). The aqueous phase was 80% of the mobile phase. Both phases were also spiked with 5 m<u>M</u> triethylamine phosphate (made from triethylamine (Aldrich, Milwaukee, WI) in phosphoric acid (Aldrich) and water, then pH adjusted). Due to the hydrophilic stationary phase, this column was able to adequately resolve the $Glu-Gln_n$ peptides into distinct peaks.

6.4. Conclusions.

The $Glu-Gln_n$ peptides developed in this study were found to be separable by HPLC techniques under suitable conditions (polyhydroxyethyl aspartamide column, 215 nm wavelength detection). The peptides could be detected down to a concentration of ~0.1 m<u>M</u>. Unfortunately, with a starting donor concentration of 1 m<u>M</u>, this technique would give a working detection range of only 1 order of magnitude. This would not be suitable for detecting peptide transport through the skin after high-voltage pulsing, which would require a detection range of at least 4 orders of magnitude, down to ~100 n<u>M</u>.

Using a higher starting concentration of peptides would not be reasonable, due to both the change in donor osmolarity and the cost. Both the donor and receptor compartments need to have the same osmolarity, to prevent passive transport due to osmolarity gradients. Also, the receptor compartment is usually filled with 150 m<u>M</u> PBS, mimicking physiological conditions. Thus, the donor concentration of peptide could not be increased above 150 m<u>M</u>. In addition, the cost of the peptide was about

$300/100 mg, or about $3 per experiment. Increasing the donor concentration of peptide to 100 mM would thus cost $300 per experiment, which would not be a reasonable cost for the ~100 experiments that would have eventually been required.

During this study, it was found that the reason peptides cannot be detected at lower concentrations was due to the number of double bonds within the peptide. UV detection measures, in essence, the number of double bonds present within a sample. A typical protein has a molecular weight of ~100 kDa and has many double bonds, even at low concentrations. The small molecular weight peptides used here, on the other hand, were ~100 Da and had only a few double bonds. A greater concentration of the peptide would therefore be necessary for adequate detection. Thus, to measure a peptide at a concentration of ~100 nM, HPLC techniques are not adequate, and a fluorescent or radioactive tag on the peptide would be necessary.

7. Localized Transport Regions are Created during Skin Electroporation.*

Applying a series of high-voltage pulses to human skin has been shown to cause the transport of many types of molecules through the skin in significant amounts. Molecules that have been transported across the skin include charged, fluorescent molecules such as calcein (Prausnitz, *et al.*, 1993 [a]; Prausnitz, *et al.*, 1993 [c]; Prausnitz, *et al.*, 1994; Pliquett, *et al.*, 1995 [b]; Kost, *et al.*, 1996; Pliquett and Weaver, 1996 [a]; Pliquett and Weaver, 1996 [b]; Pliquett, *et al.*, 1996 [b]; Prausnitz, *et al.*, 1996 [b]; Chen, *et al.*, 1998 [b]; Chen, *et al.*, 1998 [c]; Vanbever, *et al.*, submitted), sulforhodamine (Kost, *et al.*, 1996; Pliquett and Weaver, 1996 [a]; Pliquett, *et al.*, 1996 [b]; Chen, *et al.*, 1998 [b]; Chen, *et al.*, 1998 [c]; Vanbever, *et al.*, submitted), and lucifer yellow (Prausnitz, *et al.*, 1993 [a]; Chen, *et al.*, 1998 [c]), and drugs such as luteinizing hormone releasing hormone (LHRH) (Bommannan, *et al.*, 1994; Riviere, *et al.*, 1995), metoprolol (Vanbever, *et al.*, 1994; Vanbever and Préat, 1995), fentanyl (Vanbever, *et al.*, 1996 [a]; Vanbever, *et al.*, 1996 [b]; Vanbever, *et al.*, 1998 [a]; Vanbever, *et al.*, 1998 [b]), domperidone (Jadoul and Préat, 1997), alnitidan (Jadoul, *et al.*, 1998), and cyclosporin A (Wang, *et al.*, 1998). Larger molecules have also been successfully transported across the skin, including heparin (Prausnitz, *et al.*, 1995 [b]; Vanbever, *et al.*, 1997; Weaver, *et al.*, 1997) and several oligonucleotides (Zewert, *et al*, 1995; Regnier, *et al.*, in press [a]).

It has been hypothesized that the mechanism for molecular transport during high-voltage pulsing involves electroporation (Prausnitz, *et al.*, 1993 [a]; Chizmadzhev, *et al.*, 1995; Pliquett and Weaver, 1996 [a]; Chizmadzhev, *et al.*, 1998 [a]). Applying a series of high-voltage pulses to the skin causes small, localized transport regions, or "LTRs," to appear in the stratum corneum (the uppermost layer of the skin), through which molecular transport is concentrated (Zewert, *et al*, 1995; Pliquett, *et al.*, 1996 [b]; Prausnitz, *et al.*, 1996 [a]; Chen, *et al.*, 1998 [b]; Vanbever, *et al.*, submitted). The LTRs are typically ~100 μ in diameter and can be found randomly distributed in the stratum corneum after pulsing. The LTRs are not associated with the sweat ducts or hair follicles (Pliquett, *et al.*, 1996 [b]).

Iontophoresis can also be used to transport drugs or other molecules through the skin. This low-voltage method involves application of a small, often constant current (typically <0.5 mA / cm^2) to the skin (Tyle, 1986; Banga and Chien, 1988; Burnette, 1989; Chien and Banga, 1989; Singh and Roberts, 1989; Cullander and Guy, 1992; Amsden and Goosen, 1995; Guy, 1996). Iontophoretic transport occurs primarily through hair follicles and sweat ducts in the skin (collectively called the "appendages") (Abramson and Gorin, 1940; Abramson and Engel, 1942; Grimnes, 1984; Burnette and Marrero, 1986; Burnette and Ongpipattanakul, 1988; Cullander and Guy, 1991; Scott, *et al.*, 1993; Chen, *et al.*, 1998 [b]; Chen, *et al.*, in press [b]), although some molecular transport may also

*The fluorescence microscopy work has also been reported in Chen, *et al.* (1998 [b]).

be occurring through the stratum corneum itself (Potts, *et al.*, 1992; Monteiro-Riviere, *et al.*, 1994). However, electrical currents greater than 0.5 mA / cm^2 can stimulate nerves within the skin, causing irritation or pain (Banga and Chien, 1988; Burnette and Ongpipattanakul, 1988; Ledger, 1992).

The purpose of this investigation was to determine whether electroporation and iontophoresis are fundamentally different phenomena, a distinction that has previously been raised (Inada, *et al.*, 1994). In these experiments, both phenomena were studied using different animal skins as models for human skin, which have different densities of hair follicles, but were otherwise similar to human skin. Hair follicles are believed to be important for molecular transport during iontophoresis (Abramson and Gorin, 1940; Abramson and Engel, 1942; Grimnes, 1984; Burnette and Marrero, 1986; Burnette and Ongpipattanakul, 1988; Cullander and Guy, 1991; Scott, *et al.*, 1993; Chen, *et al.*, 1998 [b]; Chen, *et al.*, in press [b]), but not during high-voltage pulsing (Pliquett, *et al.*, 1996 [b]; Prausnitz, *et al.*, 1996 [a]). By selecting skin models with different surface densities of hair follicles, the effect of the hair follicles on molecular transport during electroporation and iontophoresis could be studied.

7.1. Animal Models.

Besides human cadaver skin, the model skins chosen for this study were hairless rat skin and shed black rat snake skin (*Elaphe obsoleta*). The hairless rat, despite its name, is covered with very short, fine hair, giving it the appearance of being hairless (Figure 7.1). In fact, it has more hair follicles (typically 75 follicles / cm^2) (Bronaugh, *et al.*, 1982) than human skin (typically 11 follicles / cm^2) (Bronaugh, *et al.*, 1982), and it is somewhat thinner, with a stratum corneum thickness of 10 to 15 μ instead of 15 to 20 μ thick for human stratum corneum (Blair, 1968; Bronaugh, *et al.*, 1982). Hairless rat stratum corneum also has fewer corneocyte layers, 7 to 8 cell layers thick instead of the 15 to 20 cell layers in human skin. Nevertheless, hairless rat skin has often been used as a model for human skin in transdermal drug delivery research (Rougier, *et al.*, 1983; Wester and Maibach, 1985; Bouclier, *et al.*, 1990; Morimoto, *et al.*, 1992; Wester and Maibach, 1993).

In contrast to the hairless rat, the black rat snake (Figure 7.2) is hairless, and its shed skin has been previously used as a model of human skin in passive permeation studies (Itoh, *et al.*, 1990 [a]; Itoh, *et al.*, 1990 [b]; Rigg and Barry, 1990;

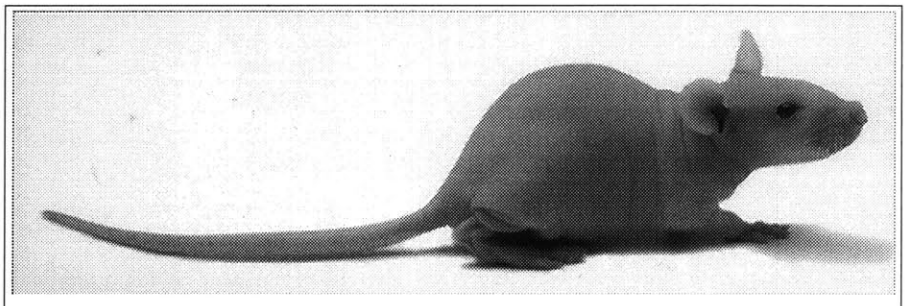

Figure 7.1. A hairless rat. The hairless rat is not really hairless, but is covered with very short, fine hair, giving it only the appearance of being hairless. In fact, the hairless rat has more hair follicles per area than does human skin (Bronaugh, *et al.*, 1982).

Takahashi, *et al.*, 1993). The rate-limiting barrier to the entry of water and other molecules into snake skin is the mesos layer, which is a layer of the skin that is analogous to human stratum corneum (Banerjee and Mittal, 1978; Maderson, *et al.*, 1978; Landmann, 1979; Roberts and Lillywhite, 1980; Landmann, *et al.*, 1981; Lillywhite and Maderson, 1982; Roberts and Lillywhite, 1983; Itoh, *et al.*, 1990 [a]). The mesos layer is ~8 μ thick, with 3 to 5 layers of cornified cells (Banerjee and Mittal, 1978; Landmann, 1979), and it covers the entire snake, including underneath the scales. The scales are only used for mechanical protection, and do not affect molecular transport or water evaporation (Roberts and Lillywhite, 1980; Itoh, *et al.*, 1990 [a]).

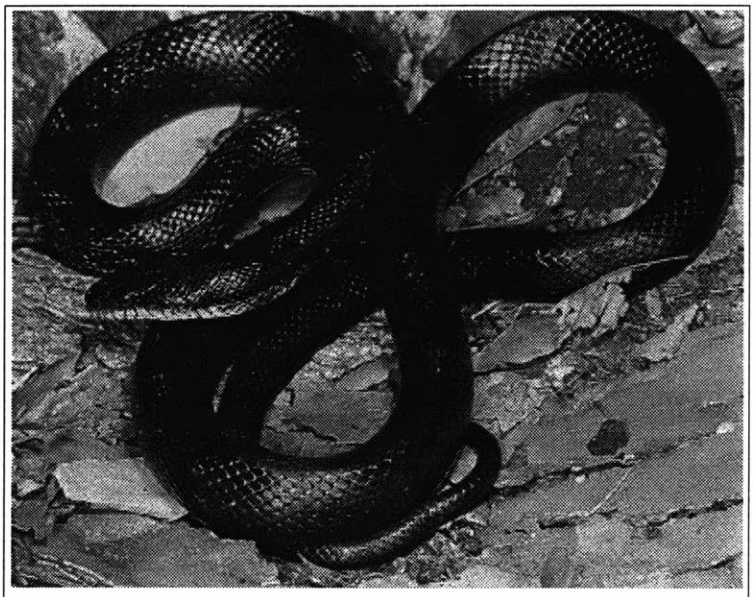

Figure 7.2. A black rat snake. Shed skin from the black rat snake (*Elaphe obsoleta*) can be used as a model of human skin that lacks hair follicles or sweat ducts. Since snake skin that has already been shed off the snake is used, the snake is not harmed in any way.

7.2. Overview.

Either no electrical stimulus (passive control), iontophoresis (1.0 mA / cm^2), or a series of high-voltage pulses (exponential pulses, applied electrode voltage of 1000 V, time constant of 1 ms, corresponding to ~100 V across the skin) was applied to human epidermis, hairless rat epidermis, or shed black rat snake skin for 1 h. The 1.0 mA / cm^2 iontophoresis current value was selected since it represents the maximum limit of what could potentially be applied to humans (weaker currents would not cause as much transport or staining of the stratum corneum). The high-voltage pulsing conditions were similar to other, previous *in vitro* experiments using human skin, and corresponded to approximately 100 V across the skin (Prausnitz, *et al.*, 1993 [a]; Pliquett, *et al.*, 1995 [a]; Pliquett and Weaver, 1996 [a]; Chen, *et al.*, 1998 [c]).

Two fluorescent polar tracer molecules, calcein and sulforhodamine, were used in the donor solution (see Section 4.2.2). Molecular fluxes were measured by spectrofluorimetry, and transport regions were determined by fluorescence microscopy. No measurable transport of calcein or sulforhodamine occurred in the passive controls. During iontophoresis, molecular transport occurred near hair follicles in human and hairless rat epidermis, but no transport was observed in snake skin, which lacked hair

follicles or sweat ducts. During high-voltage pulsing, molecular transport occurred in small, localized transport regions ("LTRs"), distributed randomly around the surface of the skin, in all three types of skin. Another important conclusion that came from this work is that 1 h sampling methods are not suitable for studying electroporation of human skin, which led to the development of the real-time measurement techniques described in Chapter 8 and Appendix IV.

7.3. Materials and Methods.

Either high-voltage pulsing, iontophoresis, or no electrical stimulus (passive control) was applied *in vitro* to human cadaver skin, hairless rat skin, or shed skin from the black rat snake. Custom-designed, six port, side-by-side permeation chambers were used to hold the skin. The donor solution consisted of calcein and sulforhodamine in PBS (see Section 4.2.2). The application electrodes were surrounded by a PBS flow-protection system encased in polyacrylamide gel, to prevent contamination of the donor and receptor compartments by chemical by-products from the electrodes (Appendix III). Furthermore, a different set of electrodes was used to take measurements of the transdermal voltage (see Section 3.5). After the experiment, the molecular flux was determined by spectrofluorimetry, and the regions for molecular transport through the skin were determined by fluorescence microscopy.

7.3.1. Skin Preparation.

Human skin and hairless rat skin were prepared by the heat-stripping method, more fully described in Appendix I. Snake skin did not need to be heat-stripped, since snake skin is somewhat thinner and stronger than human or hairless rat skin.

Briefly, human cadaver skin was stored at -80 °C for up to 6 months (Gummer, 1989). Before use, the epidermis was removed from the dermis and subcutaneous fat. The skin was thawed to room temperature, then submerged for 2 min in de-ionized water at 60 °C. The epidermis (with the overlying stratum corneum) was gently scraped off the dermis, cut into 3/4 inch diameter circles, and stored on wax paper at 4 °C and 95% humidity for up to 10 d (Gummer, 1989).

The preparation techniques for hairless rat skin were similar to those for human skin. Hairless rats (CD strain, Charles River Breeding Laboratories, Cambridge, MA) (Prausnitz, *et al.*, 1993 [a]) were sacrificed by CO_2 asphyxiation. The skin of the rat was removed and submerged in de-ionized water at 60 °C for 2 min. The epidermis (with the stratum corneum) was gently scraped off the dermis, cut into 3/4 inch diameter circles, and stored on wax paper at 4 °C and 95% humidity for up to 10 d.

Shed snake skin from the black rat snake (gift from J. H. Rytting) was collected immediately after shedding and stored at -20 °C. Before use, the snake skin was warmed to room temperature (25 °C). The skin was then placed in de-ionized water for 15 min, cut into 3/4 inch diameter circles, and stored on wax paper at 4 °C and 95% humidity for up to 10 d. Immediately before the experiment, the skin was placed in de-ionized water at 40 °C for 30 min to fully hydrate the skin, before loading into the permeation chamber (Itoh, *et al.*, 1990 [b]; J. H. Rytting, personal communication).

7.3.2. Equipment Preparation.

Phosphate-buffered saline (PBS) was prepared using the methods described in Section 3.2. PBS was used as the receptor solution in the permeation chamber.

The donor solution was composed of high purity calcein (623 Da, -4 charge) (Molecular Probes) and sulforhodamine (607 Da, -1 charge) (Sigma), dissolved in PBS at a concentration of 1 m<u>M</u> each (Pliquett and Weaver, 1996 [a]). The solution was gently stirred for >30 min, (Nutator, Clay Adams, Becton Dickinson) until the calcein and sulforhodamine dissolved.

The permeation chambers are more fully described in Appendix III. Briefly, custom-designed, six port, side-by-side permeation chambers, with a total area of 0.64 cm^2 (circular opening, 0.9 cm in diameter) (Crown Bio Scientific) (Friend, 1992), were fitted with silver wire electrodes in the donor and receptor compartments. Since the application of either high-voltage pulses or constant DC currents caused the electrodes to release chemical by-products (including AgCl, H^+ and OH^- ions), the electrodes were surrounded by a PBS flow-protection system encased in polyacrylamide gel. This precaution prevented electrochemical contamination of the donor and receptor compartments. The flow-protected electrodes were used in all of the experiments (pulsing, iontophoresis, and passive control).

The flow-protected electrodes were constructed by soldering a piece of 0.040 inch diameter silver wire, ~0.5 cm long, to bell wire. The solder and exposed wire were covered by non-conducting silicone rubber (General Electric, Waterford, NY), so that only the silver wire was exposed. A piece of Tygon tubing, 1/32 inch ID, and the electrode were inserted through a truncated 100 µl pipette tip. The top of the pipette was sealed off with epoxy (Devcon, Wood Dale, IL).

Before each experiment, the polyacrylamide gel in the permeation chamber was prepared as follows. A plastic tube was inserted through each half of the permeation chamber and sealed in place with Parafilm (American National Can, Greenwich, CT). Each compartment was turned sideways, and polyacrylamide solution was poured in, completely immersing the plastic tube, leaving empty a compartment volume of 2.1 ml. The polyacrylamide solution was composed of 0.75 g of 19:1 acrylamide:bis(N,N'-methylene-bis-acrylamide) powder (Bio-Rad), 43.75 µl of 440 m<u>M</u> $(NH_4)_2S_2O_8$ solution, and 3 µl of N,N,N',N'-tetramethylethylenediamine (Bio-Rad) in 5 ml of PBS. The poly-

acrylamide solution was allowed to harden (~10 min). After the polyacrylamide gel solidified, the plastic tube and Parafilm were removed from the side, leaving behind an empty channel through the gel. The electrode was then inserted into this channel. During the experiments, PBS was pumped through each channel at a flowrate of ~6 ml/min, using a peristaltic pump (Polystaltic Pump, Buchler Instruments, Kansas City, MO).

7.3.3. Electrical Conditions.

The electrical circuit is more fully described in Section III.4. For both iontophoresis and high-voltage pulsing, the negative electrode was placed on the donor side, and the positive electrode on the receptor side, to provide a favorable driving force for calcein and sulforhodamine, both negatively charged.

Constant current iontophoresis at 1.0 mA/cm^2 (0.64 mA total) was applied for 1 h, using a custom-built, constant current device (Prausnitz, *et al.*, 1993 [a]; U. Pliquett, personal communication).

High-voltage, exponentially decaying pulses were delivered by an exponential pulser (Electroporation System 600, BTX), custom-modified to deliver 1 pulse every 5 s (U. Pliquett, personal communication). The time constant for each pulse was ~1 ms, and the applied voltage was 1000 V, corresponding to a transdermal voltage of approximately 100 V (Pliquett, *et al.*, 1995 [a]; Chen, *et al.*, 1998 [b]; Chen, *et al.*, 1998 [c]). Pulses were applied for 1 h (~720 pulses total).

The current delivered across the skin during high-voltage pulsing was determined by measuring the voltage drop across a noninductive 1.2 Ω, 50 W resistor in series with the permeation chamber. The voltage drop across the resistor was measured by a 10× voltage probe (HP 10071A, Hewlett Packard) connected to a digital oscilloscope (Hewlett Packard 54601, Hewlett Packard), allowing the current to be calculated by Ohm's Law (Prausnitz, *et al.*, 1993 [a]; also see Section 3.5). The voltage drop across the chamber was measured with a grounded, 1000× high-voltage probe (Tektronix), connected to immobilized 0.040 inch diameter, ~0.5 cm long silver wire measuring electrodes placed in each compartment.

The resistance between the two measuring electrodes due to the intervening PBS was previously determined by pulsing the chamber without any skin present to be 171 Ω (Section 3.5). Since the current was measured and recorded during the experiment, Ohm's Law would give the voltage drop between the two measuring electrodes due solely to PBS. The difference between that value, and the value actually measured between the receptor and donor compartments, was the voltage drop across the skin itself. Voltages were recorded every 15 min during pulsing and averaged together to characterize the transdermal voltage.

7.3.4. *Experimental Protocol.*

The skin (human epidermis, hairless rat epidermis, or shed black rat snake skin) was first floated in PBS to remove the wax paper backing, then loaded into the permeation chamber, with the stratum corneum side (human or hairless rat) or the outer surface (black rat snake) facing the donor compartment. Both outer water jackets (donor and receptor compartments) were kept at 37 °C using a thermostated water bath (Neslab, Newington, NH).

The condition of each piece of skin was checked by measuring its electrical resistance with a custom-built device that applied a ~1 kHz, ~50 mV bipolar square wave across the skin, and measured the resulting voltage (U. Pliquett personal communication; Gowrishankar, personal communication). Skin with resistivities <50 $k\Omega\,cm^2$ were not used (Prausnitz, *et al.*, 1993 [a]; Chen, *et al.*, 1998 [b]; M. R. Prausnitz, personal communication).

The donor compartment was filled with the donor solution (calcein and sulforhodamine in PBS), and the receptor compartment filled with only PBS. Both compartments were continuously stirred by magnetic stir bars (Thermix Stirring Hot Plate Model 210T, Fischer Scientific; Spinbar, VWR, West Chester, PA). A 1 h period prior to the experiment was used to fully hydrate the skin (Prausnitz, *et al.*, 1993 [a]) and check for leaks (holes or tears) in the skin. Leaky skin (passive flux above the detection limit, $\sim 10^{-7}$ $\underline{M} / m^2\,s$, or $\sim 10^{-10}$ $mol / m^2\,s$ for this particular experimental apparatus) was not used.

After hydration, either no electrical stimulus (the control, to measure passive molecular fluxes), constant current iontophoresis, or high-voltage pulsing was applied for 1 h. In the iontophoresis experiments, a current of 1.0 mA / cm^2 was applied. In the high-voltage pulsing experiments, exponentially-decaying pulses, with a time constant of 1 ms and an applied voltage of 1000 V, were applied at the rate of one pulse every 5.6 s.

7.3.5. *Fluorescence Measurements.*

After electrical exposure (high-voltage pulsing, iontophoresis, or the passive control), the solution in the receptor compartment was removed and analyzed for fluorescence, to determine if molecular transport through the skin had taken place. The fluorescence was measured with a spectrofluorimeter (Fluorolog II F112, Spex). Excitation and emission wavelengths used were 496 nm and 517 nm, respectively, for calcein, and 586 nm and 607 nm, respectively, for sulforhodamine (Pliquett and Weaver, 1996 [a]). Aliquots were taken after 1 h of passive control, and after 1 h of pulsing. After each aliquot, the receptor compartment was flushed 3× and refilled with fresh PBS. Controls used were PBS only, and a 1:10 dilution calibration series starting from the donor solution. The controls were also measured every hour.

Using the calibration curve, the concentration of tracers within the cuvette could be determined. To convert the concentration to average molecular flux, the concentration was multiplied by the volume of the chamber (measured by completely emptying out the receptor compartment into a graduated cylinder), and divided by the exposed area of the skin (0.64 cm^2) and the time of pulsing (1 h).

7.3.6. Light Microscopy.

The skin was also removed and examined using fluorescence microscopy immediately after experimentation, to determine where the fluorescent molecules were located in the skin. The location of these molecules was interpreted as indicating the regions where molecular transport through the skin had occurred. It has been previously shown that a correlation exists between skin staining and molecular transport (Pliquett and Weaver, 1996 [a]).

The skin was carefully removed and gently placed onto a microscope slide. Excess liquid was gently blotted off with a paper towel. A cover slip was carefully placed on top and sealed in place with clear nail polish (Prausnitz, *et al.*, 1993 [a]; also see Appendix II). This procedure would typically take ~10 min.

A biocular fluorescence microscope (Olympus BH-2, Olympus) was used to study the skin, set at a magnification of 10×. The excitation source was a mercury arc lamp (Mercury-100, Chiu), passing through a 488 nm wavelength filter. Emitted light was then viewed using a 515 nm wavelength filter (O515 filter, Olympus). All of the photomicrographs were taken using a camera (Olympus OM2, Olympus) loaded with 1600 speed Fuji Film (Fuji Photo Film, Tokyo, Japan), mounted on top of the microscope (Pliquett and Weaver, 1996 [a]). The camera was set on automatic exposure (typically, 0.5 to 3.0 s). Microscope fields selected for photography were randomly chosen.

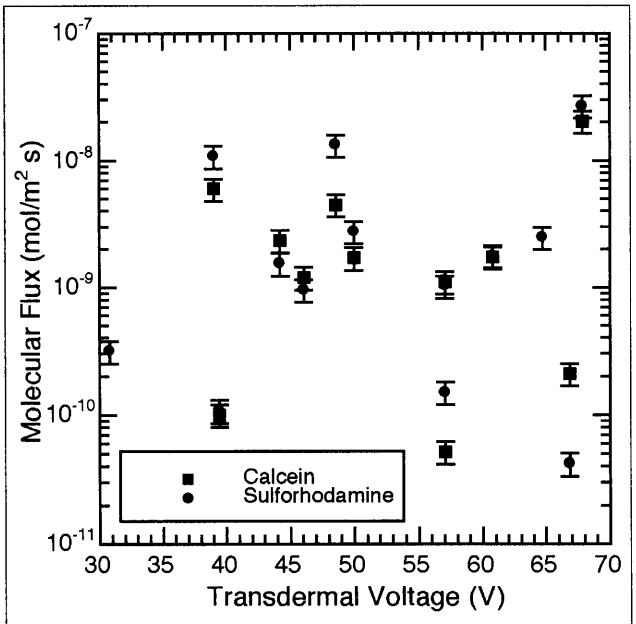

Figure 7.3. Average molecular flux versus the average transdermal voltage. Calcein fluxes are indicated by squares; sulforhodamine fluxes are indicated by circles. Transdermal voltage error bars are not plotted here; see the discussion in Section 7.4. There do not appear to be any identifiable relationships between the molecular fluxes and the transdermal voltage.

7.4. Problems with 1 h Aliquots.

A plot of the molecular flux versus the transdermal voltage is shown in Figure 7.3. No apparent trends were observed for either calcein or sulfo-

rhodamine. Figure 7.4 shows a plot of the LTR number density versus the transdermal voltage. No identifiable trends were observed for the LTR density.

These results came as a surprise, since many authors have described a clear relationship between the molecular flux and the voltage (for example, see Figure 7.7) (Prausnitz, *et al.*, 1993 [a]; Zewert, *et al*, 1995; Vanbever, *et al.*, 1996 [b]). The molecular flux was expected to increase with the transdermal voltage, yet the results presented in Figures 7.3 and 7.4 do not show an obvious relationship.

However, if the same data were plotted with respect to applied voltage, not the transdermal voltage, then increasing trends could easily be seen, as shown in Figure 7.5 for the molecular flux and

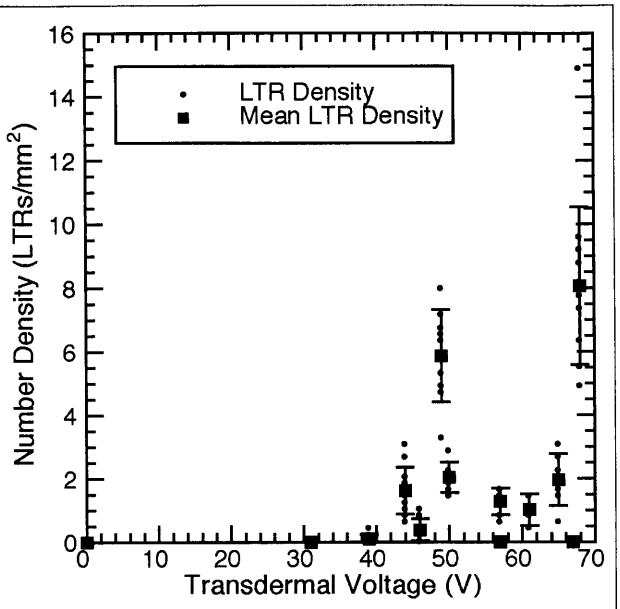

Figure 7.4. Number density of LTRs versus the transdermal voltage. Each individual photomicrograph is shown by an open square; since many photomicrographs were taken during each experiment, the average number density for each experiment is shown as a filled square. Transdermal voltage error bars are not plotted here; see the discussion in Section 7.4. There was no identifiable relationship between the LTR number density and the average transdermal voltage.

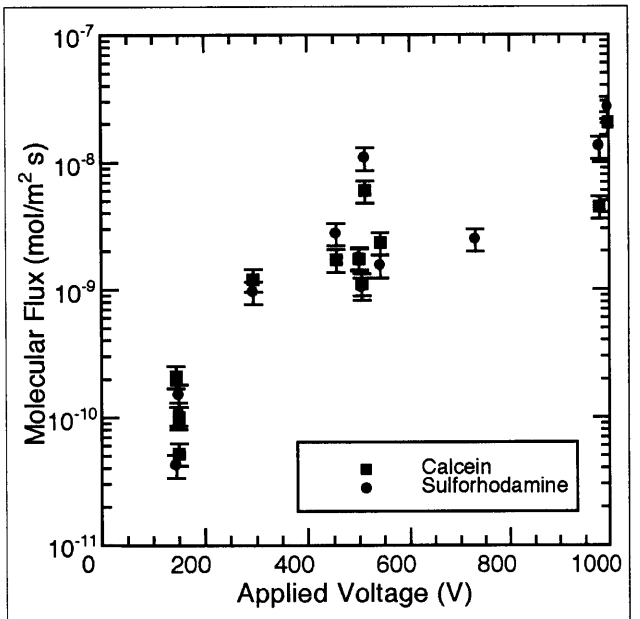

Figure 7.5. Molecular flux versus the applied voltage. There appears to be a relationship between the molecular flux, and the applied (not transdermal) voltage. Both calcein (squares) and sulforhodamine (circles) appear to follow the same trend. Passive fluxes are not shown, but were measured to be below the detection limit of the equipment, $\sim 10^{-10}$ mol / m^2 s.

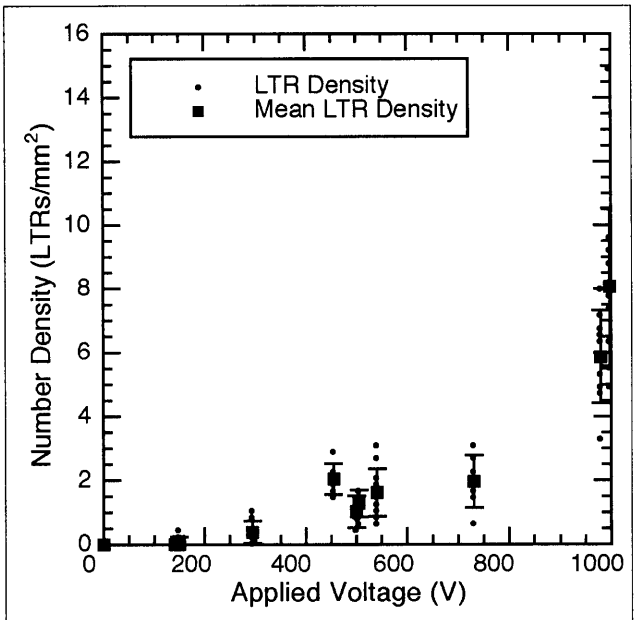

Figure 7.6. Number density of LTRs versus the applied voltage. There appears to be a relationship between the LTR number density after pulsing, and the applied (not transdermal) voltage. Individual photomicrographs are shown as open squares; the average of each set of photomicrographs is shown as a filled square.

Figure 7.6 for the LTR density. This is obviously an incorrect procedure, since it completely ignores the voltage drop contribution due to the PBS solution, yet it produced data that show significant relationships for both the molecular flux and LTR density. In addition, the trends for the molecular flux were similar to the calcein flux results from Prausnitz, *et al.*, (1993 [a]), shown here in Figure 7.7 (10^0 $\mu g / cm^2$ s ~ 10^{-9} mol / m^2 s, for comparison purposes). The investigation into this surprising and somewhat counterintuitive result is discussed in this section.

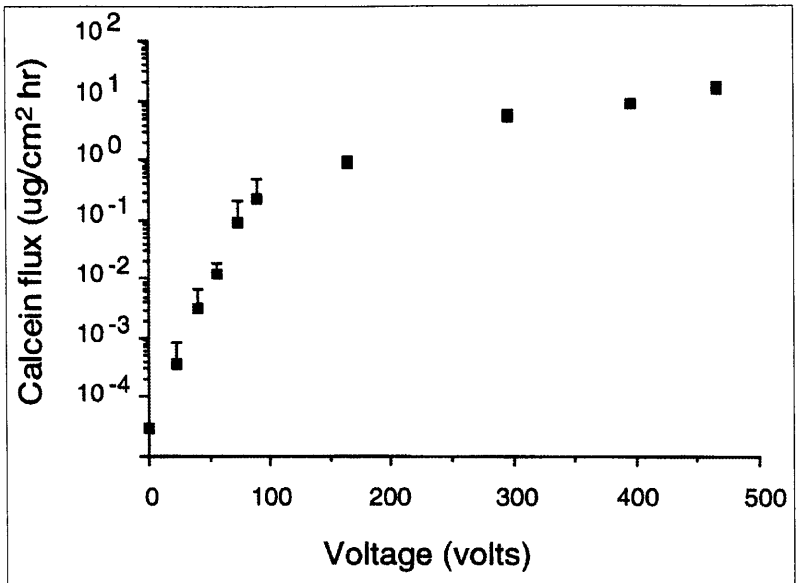

Figure 7.7. Calcein flux appears proportional to the applied voltage. Figure from Prausnitz, *et al.*, (1993 [a]).

7.4.1. Transdermal Voltages Change during the Experiment.

After acquiring the voltage and flux data shown in Figure 7.3, the transdermal voltage measurements were then examined more closely to determine whether there were any systematic measurement errors. The measured transdermal voltages, instead of being averaged together, are plotted with respect to time in Figure 7.8. The measured transdermal voltages exhibited several different behaviors. Some experiments showed approximately constant transdermal voltages (within ±10 V), but most experiments showed a decrease in the transdermal voltage (up to ~60 V), and a few experiments showed an increase in the transdermal voltage (up to ~30 V). Figure 7.9 shows a few representative experiments of these data. Later experiments, using more sensitive equipment, have shown that

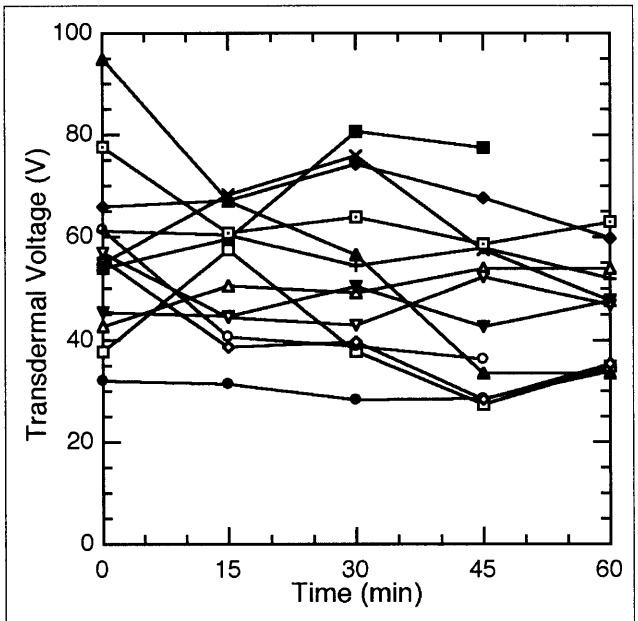

Figure 7.8. Transdermal voltages vary during high-voltage pulsing. Error bars removed for clarity. Despite the large scatter in the data, many of the transdermal voltage measurements are decreasing, indicating a drop in the transdermal voltage over time. This trend was verified in later experiments (see Figures 8.5 and 8.9).

the transdermal voltage consistently decreases with repeated pulsing (see Figures 8.5 and 8.9; a hint of this decrease may be seen in the predominantly downward slanting lines in Figure 7.8); thus, the scatter in the measurements in Figure 7.8 was due to the equipment, not the skin itself.

Simply reporting the average peak transdermal voltage does not adequately describe the experimental conditions. The voltage for each pulse should be reported, especially when it is believed that molecular flux is a strong function of transdermal voltage rather than just the applied voltage. Using averaged values for the transdermal flux could result in systematic measurement errors of up to ±30 V, which could help explain the scatter in the data shown in Figure 7.3.

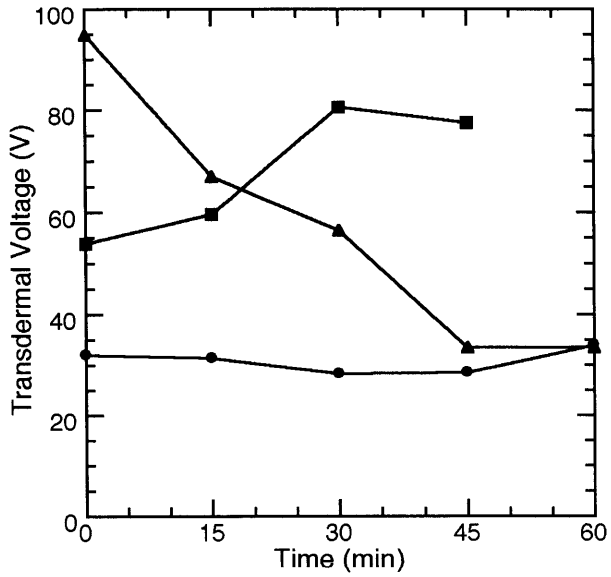

Figure 7.9. Representative transdermal voltage measurements. Error bars removed for clarity. These measurements are taken from Figure 7.8.

7.4.2. Voltage Drops Should be Measured from Donor to Receptor Compartments.

A grounded high-voltage probe was used in the current set of experiments, which measures the voltage drop from the probe to ground. However, others have indicated (Pliquett, *et al.*, 1995 [a]), that there is a significant, variable contribution due to the electrode-electrolyte (PBS) interface. The resistance of the interface can vary, even from pulse to pulse, by up to 30 Ω (U. Pliquett, personal communication). Reasons for these resistance changes include side chemical reactions and gas formation and evolution. Although the flow-protected electrodes prevent chemical contamination from these effects into the donor and receptor solutions, it does not prevent these effects from occurring.

Given a peak current of ~1 A during each pulse, by Ohm's law, a 30 Ω change in resistance would be equivalent to a change of 30 V. Since the transdermal voltage is actually the difference between two sequential measurements, using error propagation, the error in the transdermal voltage could be estimated to be roughly ±40 V ($\sqrt{2}$ 30 V).

Errors of ±40 V could account for the scatter in the data shown in Figure 7.3. Later experiments, using a differential high-voltage probe instead of a grounded probe, have shown very small fluctuations in the voltage measurements, typically ±5 V (see Section 8.1.4). Thus, the use of a grounded high-voltage probe should be avoided.

7.4.3. *No Experimental or Procedural Errors.*

It might be argued that the scatter in Figure 7.3 is due to experimental or procedural errors. This does not seem likely, however. Many controls were performed, including passive controls (skin, but no pulsing), as well as instrument tests (pulsing without any skin, as shown in Figure 3.3). These controls were all highly consistent, with small errors in the voltage measurements. Passive controls did not show significant molecular fluxes (the passive fluxes that were measured were all below the detection limit of the spectrofluorimeter) or LTR formation (as observed from fluorescence microscopy).

Further evidence that the experiments were correctly performed is shown in Figures 7.5 and 7.6. These figures show clear trends between transdermal fluxes and applied voltages; thus, both the fluxes and the voltages were measured correctly during the experiments. In addition, the trends quanitatively match the results of Prausnitz, *et al.* (1993 [a]), shown in Figure 7.7. Errors in the transdermal voltage measurements could be estimated to be ±40 V per measurement, enough to account for the scatter in the data shown in Figure 7.3.

7.4.4. *Comparisons with the Literature.*

The results of this study did not agree with the skin electroporation literature (Prausnitz, *et al.*, 1993 [a]; Prausnitz, *et al.*, 1994; Vanbever, *et al.*, 1994; Pliquett, *et al.*, 1995 [b]; Prausnitz, *et al.*, 1995 [b]; Vanbever and Préat, 1995; Zewert, *et al,* 1995; Pliquett and Weaver, 1996 [a]; Pliquett and Weaver, 1996 [b]; Prausnitz, *et al.*, 1996 [b]; Préat and Vanbever, 1996; Vanbever, *et al.*, 1996 [a]; Vanbever, *et al.*, 1996 [b]; Vanbever, *et al.*, 1996 [c]). The literature has shown clear trends between molecular fluxes and transdermal voltages, even though less accurate equipment and techniques were used in most cases than those used here. This set of experiments seems to be unable to duplicate the trends in the literature. Although a trend between the applied voltage and the resultant molecular flux could be seen (Figures 7.5 and 7.6), this trend does not appear between the transdermal voltage and the molecular flux. The lack of any clear trend for the transdermal voltage is presumably due to the limits and sensitivity of the experimental equipment used, rather than any fundamental problems with what is known about skin electroporation theory.

In the experiments of Prausnitz, *et al.*, (1993 [a]), no measurement electrodes were used, so that the transdermal voltage measurements were based on the applied voltage and were not directly measured. Transdermal voltages were calculated by subtracting the voltage drop due to PBS from the applied voltage. The PBS voltages were calculated from Ohm's Law ($I\ R_{PBS}$), where R_{PBS} was reported to be 480 Ω (see Section 3.3). Also, the values given in the paper are for average molecular fluxes and transdermal voltages over 1 h. However, a clear relationship can still be seen between molecular flux

and transdermal voltage (Figure 7.7). It is not known how such accurate measurements of the transdermal voltage were taken with the equipment described in the paper, since the use of similar techniques in the current study led to wide scatter in the data, as shown in Figure 7.3.

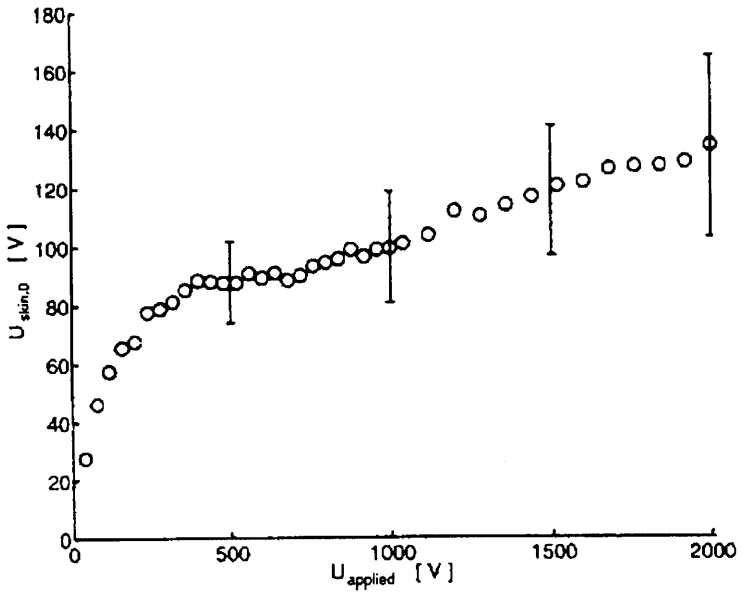

Figure 7.10. The transdermal voltage is not proportional to the applied voltage. The trend shown here from Pliquett, *et al.*, (1995 [a]) indicates that the relationship between the peak applied voltage ($U_{applied}$) and the peak transdermal voltage ($U_{skin,\ 0}$) is not a linear function. Assuming that the transdermal voltage is ~33% of the applied voltage could result in significant errors. Instead, the transdermal voltage during high-voltage pulsing should be measured for each pulse.

Many reports have simply given applied pulsing voltages (Vanbever, *et al.*, 1994; Vanbever and Préat, 1995; Préat and Vanbever, 1996; Vanbever, *et al.*, 1996 [a]; Vanbever, *et al.*, 1996 [b]; Vanbever, *et al.*, 1996 [c]) or estimated the transdermal voltage as being ~33% of the applied voltage (Prausnitz, *et al.*, 1995 [b]; Zewert, *et al*, 1995; Prausnitz, *et al.*, 1996 [b]). However, it has been shown (Pliquett, *et al.*, 1995 [a]) that this is not a reasonable approach, since the transdermal voltage is not linearly proportional to the applied voltage (Figure 7.10).

There are only a few reports in the literature (Pliquett, *et al.*, 1995 [a]; Pliquett, *et al.*, 1995 [b]; Pliquett and Weaver, 1996 [b]) that have directly measured the transdermal voltage, using methods similar to the ones described in the current study. One report has shown that the maximum transdermal voltage obtainable is ~120 V (see Figure 7.10) (Pliquett, *et al.*, 1995 [a]). However, other studies have measured transdermal voltages of over 200 V (Pliquett, *et al.*, 1995 [b]; Pliquett and Weaver, 1996 [b]). This study found maximum transdermal voltages of ~70 V (Figure 7.3), although these numbers are not conclusive, owing to the problems previously discussed. Thus, more work will still be required in this area.

7.4.5. Transdermal Voltages Should be Measured for Each Pulse.

The original purpose of this study was to determine the relationship between the molecular flux and the transdermal voltage, essentially repeating the work of Prausnitz, *et al.*, (1993 [a]) (Figure 7.7). The

purpose of repeating this work was to serve as a control for the experiments described later in this chapter, in the study of the skin electroporation mechanism.

However, the failure to reliably reproduce those earlier results (Figure 7.3), even with the proper controls and measurements (Figures 3.3, 7.5, and 7.6) led to further investigation of the use of the aliquot system for studying the skin electroporation phenomenon. It was discovered that the transdermal voltage can change significantly during a 1 h experiment (Figures 7.8 and 7.9); thus, reporting time-averaged transdermal voltages could introduce measurement errors of up to ±40 V. Instead, the transdermal voltage for each pulse needs to be individually measured and reported. While this approach would require more sophisticated equipment, the results shown in this study indicate that these measurements are necessary.

7.5. Results and Discussion.

For all three types of skin (human epidermis, hairless rat epidermis, and shed black rat snake skin), the passive controls showed insignificant molecular transport, as measured by the fluorescence of the receptor compartment solution (Table 7.1). The fluorescence in all three passive controls was below the detection limit of the spectrofluorimeter, $\sim 10^{-7}$ M / m^2 s, or $\sim 10^{-10}$ mol / m^2 s for this apparatus. Under fluorescence microscopy, no significant staining of the surface of the skin was observed (Figure 7.11a for human epidermis, Figure 7.11b for hairless rat epidermis, and Figure 7.11c for black rat snake skin).

Examination of both the human (Figure 7.12a) and the hairless rat epidermis (Figure 7.12b) preparations after 1 h of 1.0 mA / cm^2 iontophoresis showed brightly stained hair follicles (arrows in both figures). Fluorescence measurements of the receptor compartment solution indicated that significant molecular transport had occurred for both types of skin (Table 7.1).

Table 7.1. Molecular Fluxes of Calcein and Sulforhodamine.

Protocol	Skin	Calcein Flux (mol / m^2 s)	Sulforhodamine Flux (mol / m^2 s)
Passive Control	Human	$<10^{-10}$	$<10^{-10}$
	Hairless Rat	$<10^{-10}$	$<10^{-10}$
	Snake	$<10^{-10}$	$<10^{-10}$
Iontophoresis	Human	$(1.7 \pm 0.7) \times 10^{-8}$	$(3.5 \pm 1.2) \times 10^{-9}$
1.0 mA / cm^2	Hairless Rat	$(8.7 \pm 0.8) \times 10^{-8}$	$(1.5 \pm 0.5) \times 10^{-9}$
for 1 h	Snake	$<10^{-10}$	$<10^{-10}$
High-Voltage Pulsing	Human (57 ± 16 V_{skin})	$(1.1 \pm 0.8) \times 10^{-8}$	$(2.7 \pm 1.3) \times 10^{-9}$
1000 $V_{applied}$	Hairless Rat (72 ± 20 V_{skin})	$(1.9 \pm 0.1) \times 10^{-8}$	$(1.4 \pm 0.8) \times 10^{-8}$
τ = 1 ms	Snake (115 ± 38 V_{skin}	$(1.4 \pm 0.8) \times 10^{-8}$	$(3.6 \pm 1.6) \times 10^{-8}$
1 pulse/5 s for 1 h			

However, examination of the black rat snake skin preparation after the application of iontophoresis (1 h of 1.0 mA/cm^2 current) did not show any significant staining of the skin (Figure 7.12c). Visually, the shed snake skins that had been subjected to iontophoresis treatments were indistinguishable from the passive controls where there was no electrical exposure (compare Figure 7.12c with Figure 7.11c). In addition, no significant fluorescence was detected in the receptor compartment (see Table 7.1), indicating that there was no significant molecular transport across snake skin.

After 1 h of high-voltage pulsing, microscopic examination of the human skin (Figure 7.13a), hairless rat skin (Figures 7.13b and 7.14), and shed black rat snake skin (Figure 7.13c) preparations revealed the presence of LTRs, randomly distributed on the surface (some identified by arrows in the photomicrographs). The LTRs were not correlated with any visible physical structures of the skin, such as sweat ducts or hair follicles, which were also brightly stained in the human and hairless rat skins. Significant molecular fluxes were recorded for all three types of skin, as determined by the fluorescence of the receptor compartment solution after pulsing (Table 7.1). The LTRs were

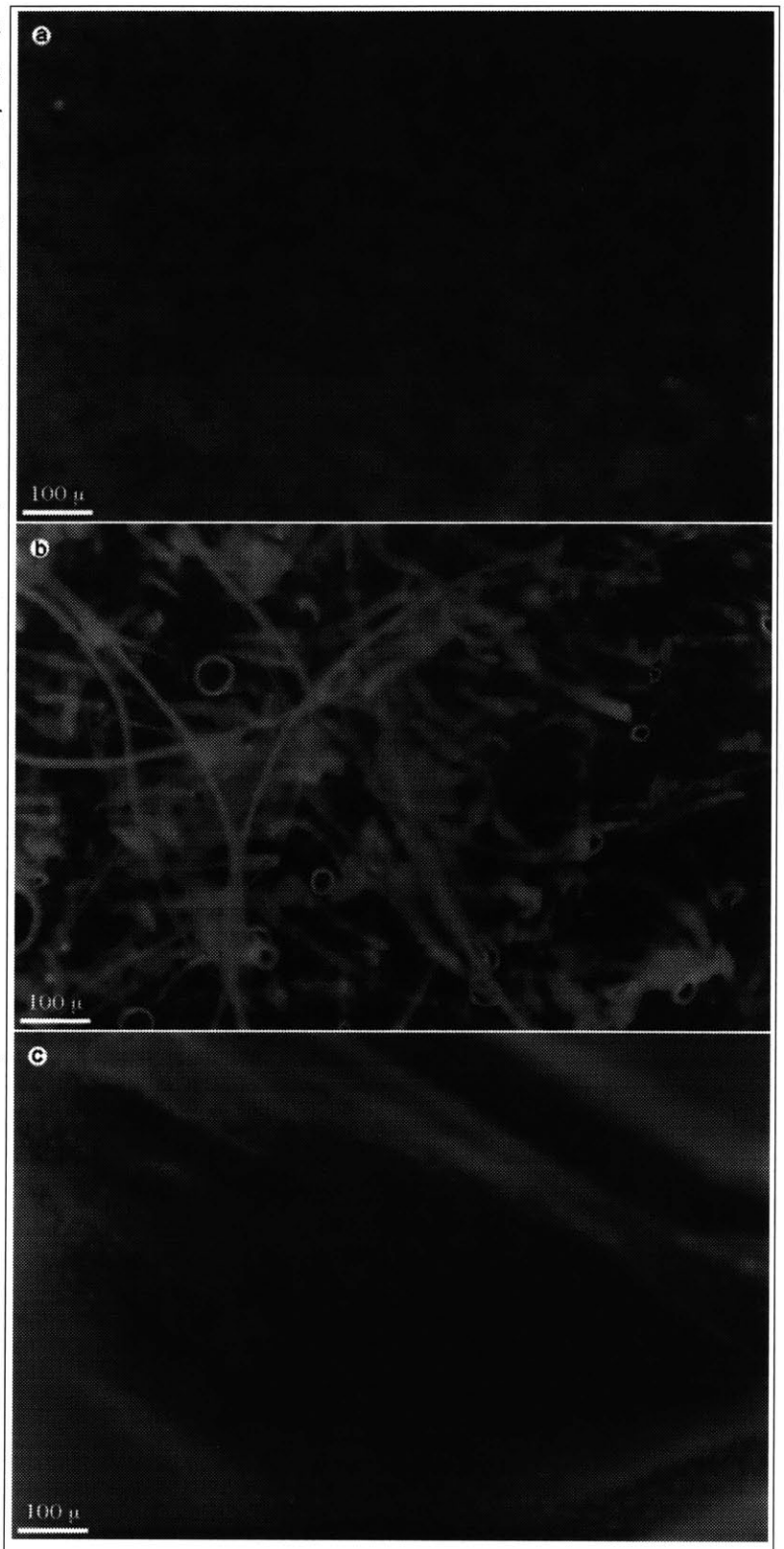

Figure 7.11. No significant staining of the skin during passive controls. With all three skins, no preferential staining was seen. (a) Background absorption into the stratum corneum of human skin. (b) With hairless rat skin, the hair was stained, but the stratum corneum itself cannot be seen. Small circular rings are trapped air bubbles. (c) Background absorption into the mesos layer of snake skin. The red regions are scales.

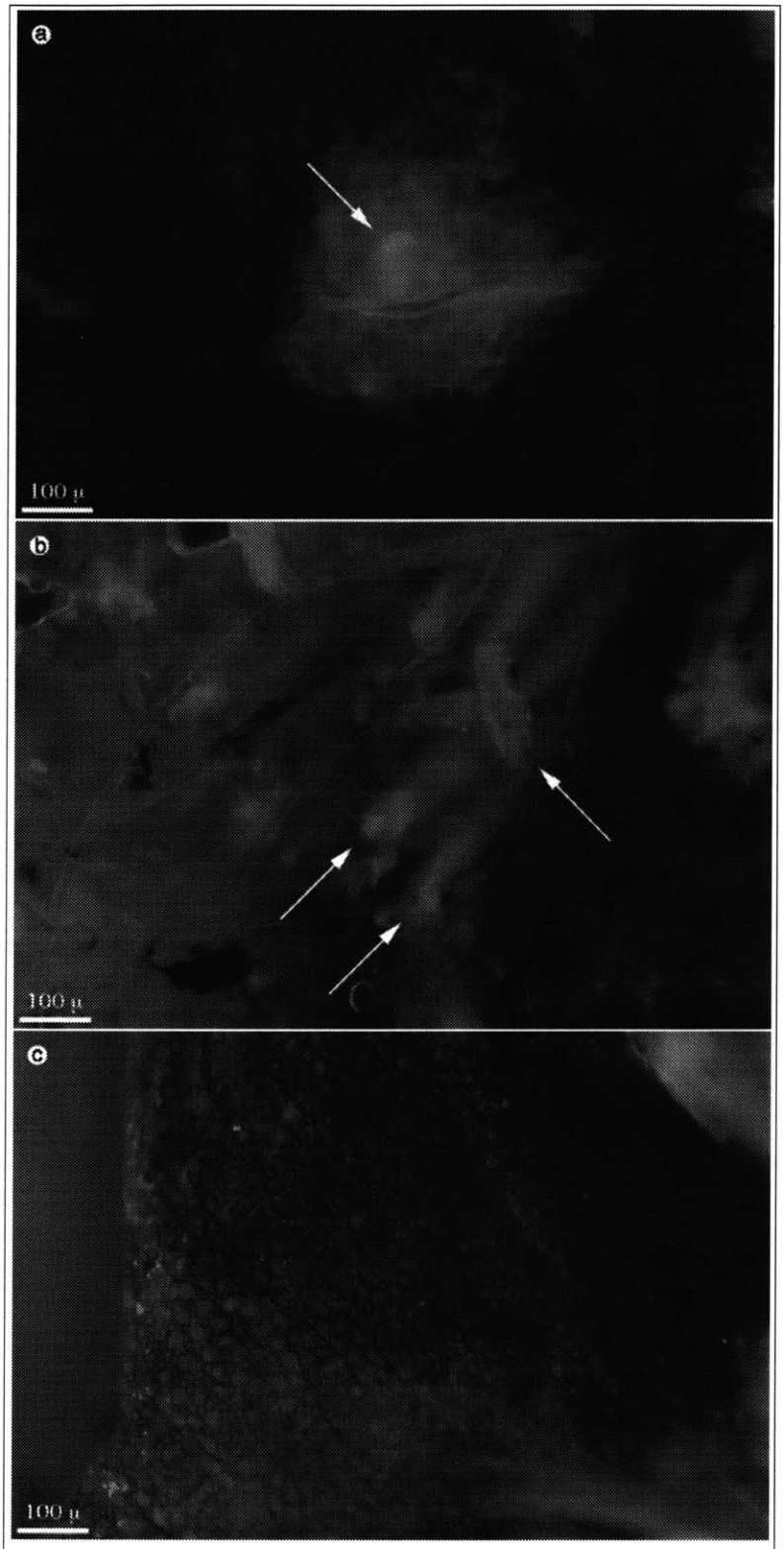

Figure 7.12. Iontophoresis causes molecular transport across the hair follicles. (a) Human skin showed prominent staining near the hair follicles (arrow). Away from the hair follicle, there is only passive background staining. (b) Staining of hair follicles (arrows) was also observed in hairless rat skin. (C) Snake skin after iontophoresis did not show any prominent staining of the mesos layer Compare with Figure 7.11c.

observed after high-voltage pulsing, but were not seen after iontophoresis. It was also noted that the background staining of the skin, not near any of the hair follicles, appeared visually brighter than in the passive controls (however, this cannot be seen in these photomicrographs, due to the automatic exposure of the film).

7.5.1. Poor Quantitative Measurements.

Due to the problems discussed in Section 7.4, the quantitative measurements in Table 7.1 include some rather large errors. It was nearly impossible to report the transdermal voltages and molecular fluxes with a reasonable degree of confidence. Essentially, the table only indicates whether or not molecular transport occurred across the skin, and not a quantitative measurement of the molecular flux.

7.5.2. No Passive Transport.

Since calcein and sulforhodamine do not significantly affect each other's fluorescence (Pliquett and Weaver, 1996 [a]; Pliquett, *et al.*, 1996 [b]; see Section 4.2.2), both tracers were used simultaneously in the donor

compartment. Neither tracer diffused passively across any of the skins, studied, even after 2 h of exposure, as measured by the fluorescence of the receptor compartment solutions (Table 7.1). The fluorescence of the receptor solution was comparable to the fluorescence of PBS only. Under fluorescence microscopy, no significant staining of the surface was observed (Figures 7.11a, 7.11b, and 7.11c).

Thus, calcein and sulforhodamine are useful tracer molecules to employ, since any fluorescence observed during microscopy would be due to molecular transport caused by either constant current iontophoresis or high-voltage pulsing, and not due to background staining or passive diffusion.

7.5.3. *Iontophoresis Causes Transport through Hair Follicles.*

Examination of both the human (Figure 7.12a) and the hairless rat skin (Figure 7.12b) preparations after 1 h of mA/cm^2 iontophoresis revealed brightly stained hair follicles. This was due to the high concentrations of both calcein and sulforhodamine in the hair follicles, indicating that most of the molecular

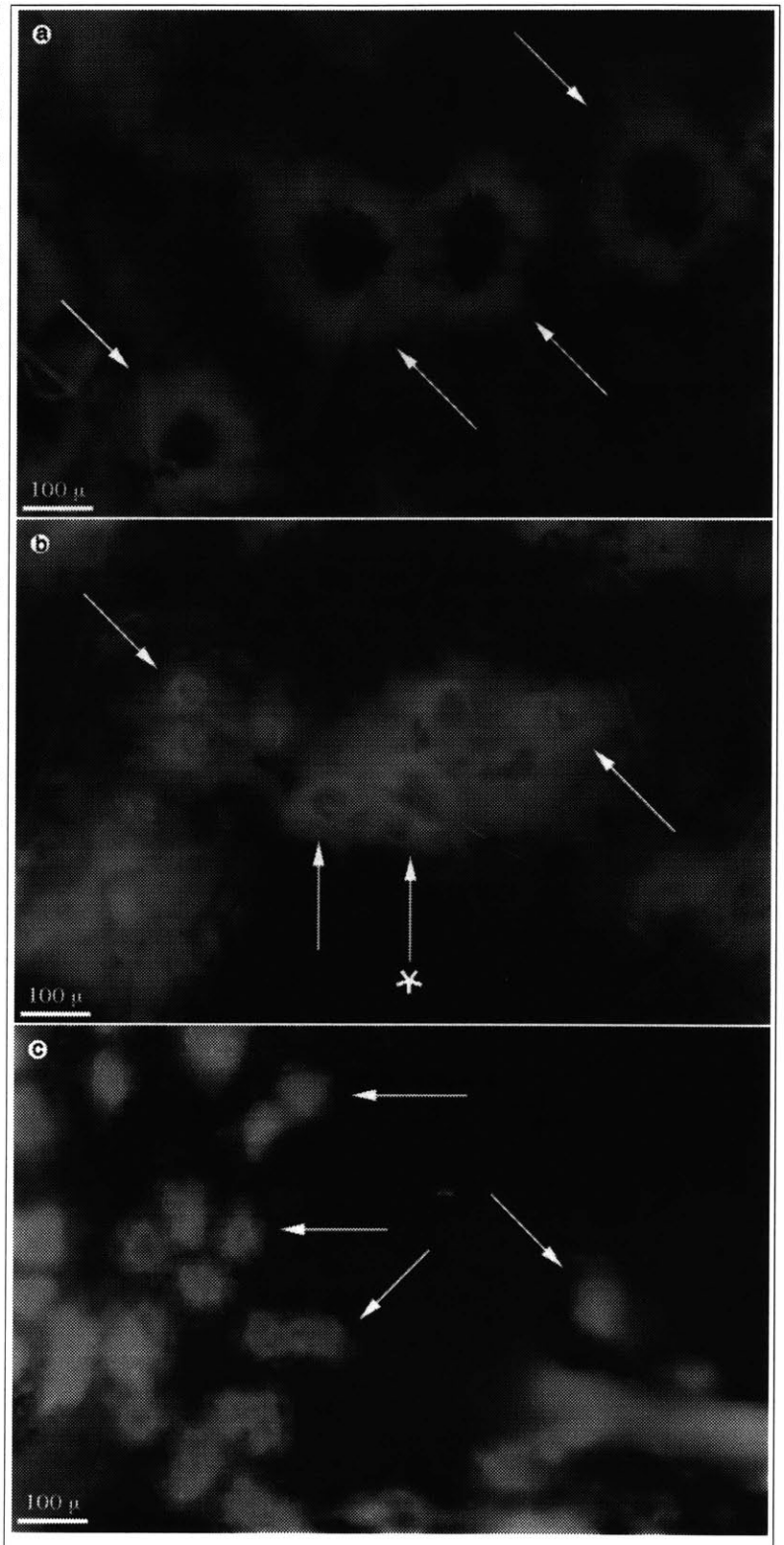

Figure 7.13. Skin electroporation causes molecular transport through LTRs. The LTRs were observed on the surface of each type of skin, randomly distributed; some are identified in the photomicrographs with arrows. The LTRs were not correlated with hair follicles or sweat ducts. Photomicrographs of (a) human skin, (b) hairless rat skin (one hair follicle is identified with a "*"), and (c) shed black rat snake skin.

transport during iontophoresis occurs through the hair follicles. Fluorescence measurements of the receptor solution indicated that significant molecular transport through the skin had occurred (Table 7.1). Also, it was noted that the background staining of the skin, not near any of the hair follicles, was significantly brighter than the passive controls.

Figure 7.14. Hairless rat skin after high-voltage pulsing, showing an array of LTRs. The LTRs where molecular transport occurs appear to be arranged in lines. This photomicrograph is at a lower magnification than Figure 7.13b, to better illustrate the linear arrangement of LTRs.

In contrast, examination of the shed black rat snake skin preparation after iontophoresis (same conditions as before) did not show any staining, as observed by fluorescence microscopy (Figure 7.12c). Visually, shed snake skins that had been subjected to 1 h of mA / cm^2 iontophoresis were indistinguishable from control experiments where no electrical conditions were applied (compare Figure 7.12c with Figure 7.11c). In addition, no fluorescence was detected in the receptor compartment solution (Table 7.1), indicating that there was no significant molecular transport across the skin.

This is direct evidence that molecular transport across the skin during iontophoresis occurs through hair follicles. This was observed as brightly stained hair follicles in both human skin and hairless rat skin, as well as significant amounts of fluorescence in the receptor compartment after the experiment. The black rat snake skin experiments did not show significant molecular transport or any staining of the skin. This is presumably because there are no hair follicles in snake skin to participate in iontophoresis, so no molecular transport could occur.

These observations are in agreement with the literature, where molecular transport during iontophoresis has been shown to occur through hair follicles (Abramson and Gorin, 1940; Abramson and Engel, 1942; Grimnes, 1984; Burnette and Marrero, 1986; Burnette and Ongpipattanakul, 1988; Cullander and Guy, 1991; Scott, *et al.*, 1993; Chen, *et al.*, 1998 [b]; Chen, *et al.*, in press [b]), although some molecular transport may also occur through the corneocytes in the stratum corneum as well (Potts, *et al.*, 1992; Monteiro-Riviere, *et al.*, 1994).

7.5.4. *High-Voltage Pulsing (Electroporation) Causes Transport through LTRs.*

Microscopic examination of the human skin (Figure 7.13a) and black rat snake skin (Figure 7.13c) preparations after 1 h of high-voltage pulsing revealed the presence of LTRs on the skin. The LTRs appeared to be randomly distributed, not correlated with any physical structures of the skin, such as sweat ducts or hair follicles (which were also brightly stained), in agreement with previous findings (Zewert, *et al,* 1995; Pliquett, *et al.*, 1996 [b]). The LTRs in human skin (Figure 7.13a) appeared to be somewhat larger than in shed snake skin (Figure 7.13c); this may be due to species-to-species differences.

The background fluorescence intensity (not near the LTRs or appendages) was also much brighter than in the passive controls. Significant molecular fluxes were also recorded after pulsing, as determined by the fluorescence of the receptor compartment solution (Table 7.1). LTRs were not seen after constant current iontophoresis or in the passive controls.

LTRs and significant molecular transport were both observed in black rat snake skin (Table 7.1 and Figure 7.13c), which lacked hair follicles and sweat ducts. This is in direct contrast to iontophoresis, where no significant molecular transport was observed in snake skin and no LTRs formed (Table 7.1 and Figure 7.12c). Thus, the LTRs form in the corneocytes of the stratum corneum, and are not associated with the appendages in the skin. LTRs have been previously reported in human skin (Zewert, *et al,* 1995; Pliquett, *et al.*, 1996 [b]; Prausnitz, *et al.*, 1996 [a]; Vanbever, *et al.*, submitted), but this is the first time that LTRs were seen in other animal skins as well (Chen, *et al.*, 1998 [b]).

Molecular transport during high-voltage pulsing is believed to occur through the LTRs, which have previously been reported to be the dominant transport pathway through the skin during electroporation (Pliquett, *et al.*, 1996 [b]). However, based on the increase in fluorescence intensities in the background of the skin, observed in the current set of experiments, there may also be a sizable amount of molecular transport through the background regions as well.

7.5.5. *Hairless Rat Skin is a Poor Model of Human Skin for Skin Electroporation.*

Microscopic examination of the hairless rat skin preparation after 1 h of high-voltage pulsing (Figures 7.13b and 7.14) revealed the presence of small, brightly stained regions on the surface of the skin. These regions were reminiscent of LTRs, but were much smaller, being ~25 μ in diameter and comparable to the size of a hairless rat corneocyte, whereas a typical LTR in human skin under these conditions would be ~100 μ in diameter and encompass several corneocytes (Pliquett, *et al.*, 1996 [b]; Vanbever, *et al.*, submitted). These fluorescent regions in hairless rat skin were not correlated with sweat ducts or hair follicles, which were also brightly stained.

However, instead of being distributed randomly on the surface of the skin like the LTRs in human and snake skin, they were observed to be lined up in rows (Figure 7.14). No known physical structures in the surface of rat skin corresponded to this phenomenon. These rows were also observed in experiments using full-thickness (non-heat stripped) hairless rat skin (data and photomicrographs not shown). However, significant amounts of molecular transport were detected across the skin, as determined by measurements of the fluorescence of the receptor compartment solution after pulsing.

Thus, hairless rat skin is not a good model for studying the electroporation of human skin. Besides being significantly more hairy, hairless rat skin does not model LTR formation well. Although hairless rat skin has similar molecular fluxes as human skin during pulsing, it should not be used to model human skin.

7.5.6. Shed Black Rat Snake Skin LTRs Similar to Human Skin.

Shed black rat snake skin seems to be a good model of human skin. The molecular fluxes through both shed black rat snake skin and human skin during electroporation were similar, and LTRs could be found on the surfaces of both types of skin after high-voltage pulsing. Although shed snake skin lacks appendages, this may not be important, since a significant amount of molecular flux is occurring through the LTRs (see Table 7.1). The molecular fluxes through snake skin were comparable to the fluxes through human skin. In addition, shed black rat snake skin is easy to prepare and use, and has previously been used as a model of human skin (Itoh, *et al.*, 1990 [a]; Itoh, *et al.*, 1990 [b]; Rigg and Barry, 1990; Takahashi, *et al.*, 1993).

Snake skin does not have any hair follicles or sweat ducts, and the relatively thick scales do not affect molecular transport, as they provide only mechanical protection (Roberts and Lillywhite, 1980; Itoh, *et al.*, 1990 [a]). Thus, the LTRs that form in snake skin during high-voltage pulsing are interpreted as forming in the corneocytes in the mesos layer, which covers the entire surface, including under the scales (Banerjee and Mittal, 1978; Landmann, 1979). Molecular transport was observed only for high-voltage pulsing, and not during iontophoresis, indicating that the LTRs are involved in molecular transport during pulsing, in agreement with previous studies (Pliquett, *et al.*, 1996 [b]).

Since all three types of skin (human, hairless rat, and shed black rat snake skin)) showed similar results after high-voltage pulsing, LTR formation and molecular transport appear to not be affected by the presence of hair follicles. Thus, the LTRs must be forming in the corneocytes of the stratum corneum (or in the mesos layer, the analog to stratum corneum in snake skin). During high-voltage pulsing, most of the molecular transport across the skin takes place through LTRs that form in the corneocytes, and not through hair follicles or sweat ducts.

7.6. Conclusions.

High-voltage pulsing or constant current iontophoresis was applied to human, hairless rat, and shed black rat snake skin. The three models were chosen since they have differing densities of hair follicles. The goal was to determine where molecular transport across the skin occurs under these conditions, using calcein and sulforhodamine, two fluorescent compounds, to trace the molecular transport pathways.

No molecular transport was seen during the passive controls. Constant current iontophoresis caused molecular transport to occur through the hair follicles in both human and hairless rat skin. Shed black rat snake skin, which does not have any hair follicles, did not show any molecular transport.

Electroporation (high-voltage pulsing) caused molecular transport to occur through localized transport regions (LTRs) that form spontaneously during pulsing, in all three types of skin. The LTRs formed in the corneocytes of the stratum corneum, were randomly distributed, and were not correlated with the appendages. Evidence of this comes from the pulsing of shed black rat snake skin, which showed molecular transport and LTR formation, but lacked appendages. Thus, electroporation and iontophoresis are fundamentally different phenomena.

There are some large uncertainties in the measurements of the molecular flux and transdermal voltage during these experiments, which accounts for the large scatter in the data shown in Figure 7.3. Measurements need to be taken much more frequently than simply once an hour, since skin electroporation is a rapidly changing phenomenon.

8. Molecular Fluxes through Human and Snake Skin in Real Time.*

Many studies have shown that applying a series of short (~1 ms), high-voltage (~100 V_{skin}) electrical pulses to human skin can dramatically increase the rate of transdermal molecular transport, hypothesized to involve electroporation (Prausnitz, *et al.*, 1993 [a]; Chizmadzhev, *et al.*, 1995; Pliquett and Weaver, 1996 [a]; Chizmadzhev, *et al.*, 1998 [a]). This method may provide a useful technique for the transdermal delivery of drugs. Although many experiments have been conducted, using a wide range of molecules (Prausnitz, *et al.*, 1993 [a]; Bommannan, *et al.*, 1994; Vanbever, *et al.*, 1994; Prausnitz, *et al.*, 1995 [b]; Riviere, *et al.*, 1995; Zewert, *et al.*, 1995; Pliquett and Weaver, 1996 [a]; Prausnitz, *et al.*, 1996 [a]; Vanbever, *et al.*, 1996 [b]; Jadoul and Préat, 1997 [a]; Vanbever, *et al.*, 1997; Weaver, *et al.*, 1997; Jadoul, *et al.*, 1998; Wang, *et al.*, 1998; Regnier, *et al.*, in press [a]), electrical conditions (Prausnitz, *et al.*, 1993 [a]; Vanbever, *et al.*, 1994; Pliquett, *et al.*, 1995 [a]; Vanbever and Préat, 1995; Pliquett and Weaver, 1996 [a]; Prausnitz, *et al.*, 1996 [b]; Vanbever, *et al.*, 1996 [a]; Vanbever, *et al.*, 1996 [b]; Gallo, *et al.*, 1997; Vanbever, *et al.*, 1997; Vanbever, *et al.*, submitted), and types of skin (Prausnitz, *et al.*, 1993 [a]; Prausnitz, *et al.*, 1993 [c]; Vanbever, *et al.*, 1994; Riviere, *et al.*, 1995; Gallo, *et al.*, 1997; Chen, *et al.*, 1998 [b]), few studies have been conducted to determine the quantitative relationship between the electrical conditions and molecular transport.

While many authors have described the average transdermal flux across the skin in terms of the peak applied voltage (Prausnitz, *et al.*, 1993 [a]; Vanbever, *et al.*, 1994; Prausnitz, *et al.*, 1995 [b]; Vanbever and Préat, 1995; Vanbever, *et al.*, 1996 [a]; Vanbever, *et al.*, 1996 [b]; Vanbever, *et al.*, submitted), others have shown that it is actually the peak transdermal voltage ($U_{skin,\,0}$) that governs molecular transport (Pliquett and Weaver, 1996 [a]). For a given experimental system, the applied voltage may be correlated with the transdermal voltage, but with widely varying experimental apparatuses in use (Prausnitz, *et al.*, 1993 [a]; Vanbever, *et al.*, 1994; Pliquett, *et al.*, 1995 [b]; Pliquett, *et al.*, 1996 [b]; Gallo, *et al.*, 1997; Chen, *et al.*, 1998 [b]; Chen, *et al.*, 1998 [c]), comparison of the applied voltages is nearly impossible. Hence, it would be more useful to report the average molecular flux versus the average transdermal voltage (Zewert, *et al.*, 1995; Pliquett and Weaver, 1996 [a]; Pliquett and Weaver, 1996 [b]). Theoretical calculations have also predicted a relationship between the molecular flux and the transdermal voltage (Chizmadzhev, *et al.*, 1995; Chizmadzhev, *et al.*, 1998 [a]). In addition, a recent theory has predicted a transition from electroporation of the skin's appendages (the sweat ducts and hair follicles) at $5\ V < U_{skin,\,0} < 30\ V$, to electroporation of the bilayer membranes within the stratum corneum at $U_{skin,\,0} > 30\ V$ (Chizmadzhev, *et al.*, 1998 [a]).

---

*The results with human skin have also been reported in Chen, *et al.* (in press, [c]).

Many studies have used 1 h aliquot measurements of the receptor compartment to study the molecular flux across the skin during pulsing (Prausnitz, *et al.*, 1993 [a]; Bommannan, *et al.*, 1994; Vanbever, *et al.*, 1994; Prausnitz, *et al.*, 1995 [b]; Riviere, *et al.*, 1995; Vanbever and Préat, 1995; Zewert, *et al.*, 1995; Prausnitz, *et al.*, 1996 [b]; Vanbever, *et al.*, 1996 [a]; Vanbever, *et al.*, 1996 [b]; Jadoul and Préat, 1997 [a]; Vanbever, *et al.*, 1997; Weaver, *et al.*, 1997; Vanbever, *et al.*, submitted). However, other studies have used a "flow-through" system, where the contents of the receptor compartment are continuously pumped to a spectrofluorimeter for detection (Friend, 1992; Pliquett, *et al.*, 1995 [b]; Pliquett and Weaver, 1996 [a]; Chen, *et al.*, 1998 [c]; Chen, *et al.*, in press [a]; see also Appendices IV and V). The first use of this method improved the time resolution for molecular transport detection to approximately 1 min (Prausnitz, *et al.*, 1994), and showed that the molecular flux of various fluorescent tracers through the skin can vary considerably with repeated pulsing (Prausnitz, *et al.*, 1994; Pliquett and Weaver, 1996 [a]). These changes in molecular flux were undetectable with 1 h aliquot measurement techniques. Since then, the use of various flow-through systems has been carried out in conjunction with high-voltage pulsing of human skin in several studies (Prausnitz, *et al.*, 1994; Pliquett, *et al.*, 1995 [b]; Kost, *et al.*, 1996; Pliquett and Weaver, 1996 [a]; Pliquett and Weaver, 1996 [b]; Chen, *et al.*, 1998 [c]; Vanbever, *et al.*, submitted).

Shed skin from the black rat snake (*Elaphe obsoleta*) (Figure 7.2) has previously been used as a model of human skin in passive diffusion experiments (Itoh, *et al.*, 1990 [a]; Itoh, *et al.*, 1990 [b]; Rigg and Barry, 1990; Takahashi, *et al.*, 1993). Snake skin models human skin well, due to a layer of the skin called the mesos layer. This layer is analogous to human stratum corneum (Banerjee and Mittal, 1978; Maderson, *et al.*, 1978; Landmann, 1979; Roberts and Lillywhite, 1980; Landmann, *et al.*, 1981; Lillywhite and Maderson, 1982; Roberts and Lillywhite, 1983; Itoh, *et al.*, 1990 [a]), composed of cornified cells and sheets of lipid bilayer membranes. It is ~8 μ thick, with 3 to 5 layers of cornified cells (Banerjee and Mittal, 1978; Landmann, 1979). Snake skin lacks sweat ducts and hair follicles; thus, it is a model of only the stratum corneum of human skin.

To obtain quantitative information during skin electroporation, the simultaneous measurement of the peak transdermal voltages, on a per-pulse basis, and the molecular transport across the skin in real time were sought. The goal of this study was to determine the relationship between the peak transdermal voltage and the resulting molecular flux. In addition to human cadaver skin, shed skin from the black rat snake was used as a control, to determine how the presence of hair follicles and sweat ducts affects molecular transport, on a quantitative basis.

8.1. Materials and Methods.

The flow-through system for measuring the contents of the receptor compartment is more fully discussed in Appendix IV. In these experiments, 1 mM of a fluorescent tracer (either sulforhodamine, lucifer yellow, cascade blue, or calcein; see Chapter 4) was used in the donor compartment. Both human cadaver skin and shed snake skin were used, to determine the importance of hair follicles and sweat ducts in the formation of transport pathways through the skin during high-voltage pulsing. During pulsing, PBS flow-protection was used to protect the donor and receptor compartments from chemical by-products produced by the pulsing electrodes. After the experiment, the skin was removed and examined under fluorescence microscopy. The data stored in real time from the spectrofluorimeter (flux measurements) and the oscilloscope (voltage measurements) were calibrated and processed to give information about the conditions of the experiment.

8.1.1. Skin Preparation.

Human cadaver skin was prepared by the "heat-stripping" method described in Appendix I. Snake skin did not need to be heat-stripped, since it was thinner and stronger than human skin.

Briefly, stored cadaver skin at -80 °C (Gummer, 1989) was thawed to room temperature, then submerged for 2 min in de-ionized water at 60 °C. The epidermis (including the stratum corneum) was gently scraped off of the dermis, cut into 3/4 inch diameter circles, and stored at 4 °C, 95% humidity for up to 10 days (Gummer, 1989). The epidermis was used in all of the experiments described here.

Shed snake skin from the black rat snake was collected immediately after shedding and stored at -20 °C. Before use, the snake skin was allowed to warm to room temperature (25 °C). The skin was then submerged in de-ionized water for 15 min, cut into 3/4 inch diameter circles, and stored on wax paper at 4 °C, 95% humidity for up to 10 days. On the day of the experiment, the skin was placed in de-ionized water at 40 °C for 30 min to rehydrate the skin, before loading into the permeation chambers (Itoh, *et al.*, 1990 [b]; J. H. Rytting, personal communication).

8.1.2. Permeation Chamber with Four-Electrode System.

Phosphate-buffered saline (PBS) was prepared using the methods described in Section 3.2. PBS was used as the receptor solution in the permeation chamber. The donor solution consisted of a fluorescent tracer (one of either sulforhodamine, lucifer yellow, cascade blue, or calcein; see Chapter 4),

dissolved in PBS to a concentration of 1 mM. The solution was gently stirred for >30 min (Nutator, Clay Adams, Becton Dickinson), to allow the tracer time to dissolve.

The flow-through system is more fully described in Appendix IV. Briefly, the permeation chambers were custom-designed, side-by-side permeation chambers, with a skin exposure area of 0.64 cm^2 (circular opening, 0.9 cm in diameter) (Crown Bio Scientific) (Friend, 1992). Each chamber half consisted of an outer water jacket and an inner compartment. Ports extending from the inner compartment allowed direct access to the inner compartment. Each chamber half had one large port near the skin (for the measuring electrodes and the flow-through system) and two small ports away from the skin (for the pulsing electrodes and the electrode flow-protection system). To keep the skin and the donor and receptor solutions constant at 37 °C, water heated by a thermostated water bath (Neslab) was pumped through both outer jackets.

The flow-protected electrodes were constructed by soldering a piece of 0.040 inch diameter silver wire, ~0.5 cm long, to copper bell wire. The solder and exposed wire were covered by nonconducting silicone rubber (General Electric), so that only the silver wire was exposed. A piece of Tygon tubing, 1/32 inch ID, and the electrode were inserted through a truncated 200 µl pipette tip. The top of the pipette was then sealed off with epoxy (Devcon).

The donor compartment measuring electrode was constructed by soldering a piece of 0.040 inch diameter silver wire, ~0.5 cm long, to copper bell wire. The solder and exposed wire were covered by nonconducting silicone rubber, exposing only the silver wire. The wire was inserted through a truncated 1 ml pipette tip and sealed in place with epoxy.

The receptor compartment electrode was constructed by soldering a piece of 0.040 inch diameter silver wire, ~0.5 cm long, to copper bell wire. The solder and exposed wire were covered by nonconducting silicone rubber, so that only the silver wire was exposed. A piece of Teflon tubing, 1/16 inch ID, was used for outflow and a longer piece of Tygon tubing, 1/32 inch ID, was used for inflow. The wire and the two tubes were inserted through a truncated 1 ml pipette tip. A hole was drilled into the side of the 1 ml pipette tip and the Teflon tube was extended through the hole. All of the tubes and wires were sealed in place with epoxy.

The top of a 2 ml centrifuge tube was removed and two holes were drilled the tube: one in the bottom and one in the side. Tygon tubing, 1/32 inch ID, was epoxied to the bottom hole. The Teflon tube from the pipette was extended through the side hole. The centrifuge tube was held in place to the side of the pipette with Parafilm (American National Can).

Before each experiment, plastic tubes were inserted through both compartments and sealed in place with Parafilm. In the receptor compartment, the measuring/flow-through electrode was inserted into the compartment and sealed in place with Parafilm. The tubing within the receptor chamber was wired in place for the gel with stainless steel wire. Both compartments was turned sideways, and polyacrylamide solution was poured in, completely immersing everything, leaving empty a volume of ~2.1 ml

in the donor compartment and ~450 µl in the receptor compartment. The polyacrylamide solution was composed of 0.75 g of 19:1 acrylamide:bis(N,N'-methylene-bis-acrylamide) powder (Bio-Rad), 43.75 µl of 440 mM $(NH_4)_2S_2O_8$ solution, and 3 µl of N,N,N',N'-tetramethylethylenediamine (Bio-Rad) in 5 ml of PBS.

The polyacrylamide solution was allowed to harden (~10 min). After the solution solidified into a gel, the outer plastic tubing and the Parafilm were removed from both compartments, leaving behind an empty channel through the gel. The flow-protected electrodes were then inserted into these channels. During an experiment, PBS was pumped through each outer channel at a flowrate of ~6 ml/min, using two peristaltic pumps (VWR). The stainless steel wire was removed from the receptor compartment, since the tubing in the receptor compartment was immobilized in place by the solidified gel.

8.1.3. Fluorescence Measurements.

Fluorescence measurements were taken with a spectrofluorimeter (Fluorescence Master Series Spectrometer, Photon Technology, Brunswick, NJ). Excitation and emission wavelengths for each fluorescent compound are given in Table 4.1.

The cuvette in the spectrofluorimeter was constructed by drilling two holes into a disposable polystyrene microcuvette (VWR), to allow for inflow and outflow from the cuvette. One hole was drilled approximately 1/4 inch from the bottom of the cuvette for outflow, and the other hole drilled higher in the cuvette (approximately 1/2 inch from the bottom) for inflow. Both holes were connected with Tygon tubing to a peristaltic pump ("Sarah" Cassette Peristaltic Pump, Barnant, Barrington, IL).

The final volume of the cuvette was ~200 µl, and was the minimum amount needed by the spectrofluorimeter for accurate detection and quantification of fluorescent molecules within the cuvette, as determined empirically. Mixing was accomplished by dripping fluid down into the cuvette (the drops entering the cuvette were a sizable fraction of the total volume of the cuvette). The performance of this system was very close to an idealized continuous-stirred tank reactor (Fogler, 1992), and the residence time for the combined chamber-tubing-pump-cuvette system (volume of ~400 µl) was measured to be ~14 s. This was taken to be the time resolution for the flux measurements.

It was found that liquid within the cuvette could not be sucked out by the pump until the level of liquid within the cuvette had completely covered the outlet (which was Tygon tubing, 1/32 inch ID). If the liquid did not completely cover the opening, then air would get sucked into the tubing instead of liquid. This could result in variations in the volume of the liquid within the cuvette. To minimize this problem, a 200 µl pipette tip was affixed to the outlet opening of the cuvette, greatly reducing the diameter of the outlet and minimizing this problem.

A calibration curve was constructed by pumping known concentrations of the donor solution through the flow-through system, starting from the lowest concentrations and going to the highest. The concentrations used were a 1:10 dilution series starting from the donor solution concentration (1 mM).

8.1.4. Electrical Equipment.

High-voltage, exponentially decaying pulses were delivered by a high-voltage pulser (Electroporation System 600, BTX), custom-modified to deliver 1 pulse every ~5 s (U. Pliquett, personal communication). Since the fluorescent tracers were all negatively charged, the negative terminal of the pulser was connected to the pulsing electrode in the donor compartment, and the positive terminal to the receptor compartment, to provide a favorable driving force for the fluorescent tracers.

The time constant on the high-voltage pulser was set at 1 ms. Pulses with peak transdermal voltages between 0 V and ~150 V across the skin were applied for 1 h at the rate of one pulse every 5.56 ± 0.01 s (640 pulses total). This rate was used to facilitate comparison with other experiments in the literature where pulses were given every ~5 s (Prausnitz, *et al.*, 1993 [a]; Prausnitz, *et al.*, 1994; Prausnitz, *et al.*, 1995 [b]; Zewert, *et al.*, 1995; Pliquett and Weaver, 1996 [a]; Pliquett and Weaver, 1996 [b]; Prausnitz, *et al.*, 1996 [b]; Weaver, *et al.*, 1997; Chen, *et al.*, 1998 [b]; Chen, *et al.*, submitted [b]).

Current delivered across the skin during the pulse was determined by measuring the voltage drop across a 1.2 Ω noninductive resistor, connected in series with the permeation chamber. The voltage drop across the resistor was measured by a 10× voltage probe (HP 10071A, Hewlett Packard) connected to a digital oscilloscope (Hewlett Packard 54601, Hewlett Packard). The oscilloscope was connected through an RS-232 interface card (54641A RS-232 Interface Module, Hewlett Packard), attached to the back of the oscilloscope, to a serial port on a 486DX computer (Power Spec 1, manufacturer unknown).

The voltage drop from the receptor to the donor compartment was measured by connecting a differential high-voltage probe (Active Differential Probe B9017RT, Yokogawa) to the immobilized silver wire measuring electrodes in each compartment. This probe was also connected to the same oscilloscope.

The computer was programmed using Turbo C++ (Borland, Scotts Valley, CA), running a program that would count and record both voltage waveforms recorded by the oscilloscope for every pulse. The program is given in Section IV.4.3. The program recorded the waveform data as ASCII characters and did not do any mathematical processing, since between pulses, there was barely sufficient time to download the waveforms from the oscilloscope (at 1200 baud and 1 μs time resolution) and record the data onto the hard drive.

8.1.5. Skin Experimental Protocol.

Prepared, stored skin (human or snake) was floated in PBS for ~1 min to remove the wax paper backing. The skin was loaded into the side-by-side chambers, with the stratum corneum (human) or outer surface (snake) facing the donor compartment. The donor compartment was filled with a donor solution and the flow-through pumps were started. The donor compartment was continuously stirred by a magnetic stir bar (Thermix Stirring Hot Plate Model 210T, Fischer Scientific; Spinbar, VWR).

The condition of the skin was checked by measuring its electrical impedance. A 100 Hz, 0.1 V (peak-to-peak) bipolar sine wave was applied to the skin and the resulting impedance was measured using an LCR meter (Model 5R715 LCR Meter, Stanford Research Systems, Sunnyvale, CA).

The skin was considered bad and was immediately discarded if its electrical resistivity was $<50\ k\Omega\ cm^2$ (or <70 kΩ for this particular apparatus) (Prausnitz, *et al.*, 1993 [a]; M. R. Prausnitz, personal communication). For this apparatus, however, the skin's impedance, not its resistance, was measured. Less current is needed for an accurate measurement of the skin's impedance, and there is no overall net current from the applied bipolar sine wave, and hence no potential iontophoresis. Since the impedance of the skin decreases as the applied frequency increases, a value of $<25\ k\Omega\ cm^2$ of impedance at a frequency of 100 Hz (or <40 kΩ for this apparatus) was used as an indicator of bad skin. Previous experiments have shown that this value compares favorably with the accepted DC resistance of $<50\ k\Omega\ cm^2$ (Gowrishankar, personal communication).

The resistances and impedances of the PBS solution and the polyacrylamide gel were neglected, since their combined resistances were previously measured to be 251 Ω (see Section 3.6), much less than the ~40 kΩ resistances of acceptable skin.

After determining if the skin was acceptable or not, the apparatus was allowed to sit for 1 h to fully hydrate the skin (Prausnitz, *et al.*, 1993 [a]) and check for leaks. Leaky skin (passive flux above the detection limit, $\sim 10^{-8}$ M, or $\sim 10^{-10}\ mol / m^2\ s$ for this particular experimental apparatus), was immediately discarded.

8.1.6. Pulsing Protocol.

High-voltage exponential pulses, with a time constant of 1 ms and transdermal voltages between 0 V and ~150 V across the skin (applied voltages between 0 V and 1000 V) were applied for 1 h at the rate of one pulse every 5.56 s. PBS was pumped through the flow-protection system (across the electrodes) at ~6 ml/min using a peristaltic pump (VWR). PBS was also pumped through the flow-through system (through the receptor compartment and the spectrofluorimeter) at the rate of 0.0322 ml/s (setting "99"

on the "Sarah" pump). Both the spectrofluorimeter computer and the computer recording voltage waveforms were set to record ~1 h of data.

After the experiment, the skin was removed from the chamber for fluorescence microscopy. The data from the two computers (spectrofluorimeter and voltage data) were downloaded to a Sun Sparc 10 (workstation Sun, Palo Alto, CA) for analysis.

8.1.7. Fluorescence Microscopy.

A biocular fluorescence microscope (Olympus BH-2, Olympus) allowed the simultaneous fluorescence and light illumination of the specimen at 4× and 10× magnifications. Pictures were taken using a camera (Olympus OM2, Olympus) mounted on the microscope (Pliquett, *et al.*, 1996 [b]).

Immediately after pulsing, the skin was carefully removed and gently placed onto a microscope slide (Gold Seal Rite-On, No. 3050, Clay Adams, Becton Dickenson). Excess liquid was blotted off with a paper towel. A drop of staining solution was added and a 22×22 No. 1 cover slip (Clay Adams, Becton Dickenson) was placed on top and sealed in place with clear nail polish (Hard as Nails, Sally Hensen, Del) (Prausnitz, *et al.*, 1996 [a]).

Localized transport region (LTR) densities (Pliquett, *et al.*, 1996 [b]) were determined by taking photographs of the skin and visually counting the number of LTRs on each photograph. Since the area of the photograph (at 4× magnification) was known to be 4.91 mm^2, the number density of LTRs on the skin could be determined.

8.1.8. Numerical Analysis.

All of the fluorescence, voltage and calibration data were first downloaded onto a Sun Sparc 10 workstation (Sun). A program written in MatLab 5 (Mathworks, Natick, MA) used these data to determine the molecular flux versus the transdermal voltage for each pulse.

This program can be seen in Section IV.13.4. The program first loaded the voltage and current waveforms and fitted these to an exponential. Since the resistance of the chamber without any skin was 251 Ω, the voltage across the skin could then be calculated by Ohm's Law (see Equation 3.2). The program then loaded the calibration and fluorescence data, and, using deconvolution routines (Pliquett, *et al.*, 1995 [b] see also Section IV.13.2), calculated the molecular flux across the skin. The two data files were synchronized together in time, allowing the program to determine the measured flux for each pulse.

8.2. Human Skin Results.

Rapid changes in both the transdermal voltage and the molecular flux occurred during the repeated pulsing of human skin. These changes occurred very rapidly, on time scales of ~1 to 10 min. Waiting 1 h between measurements could miss many crucial features.

8.2.1. Measurements Yielding Average Values Can Give Significant Errors.

To simulate the 1 h aliquot measurements commonly used in the literature (Prausnitz, *et al.*, 1993 [a]; Bommannan, *et al.*, 1994; Vanbever, *et al.*, 1994; Prausnitz, *et al.*, 1995 [b]; Riviere, *et al.*, 1995; Vanbever and Préat, 1995; Zewert, *et al.*, 1995; Prausnitz, *et al.*, 1996 [b]; Vanbever, *et al.*, 1996 [a]; Vanbever, *et al.*, 1996 [b]; Jadoul and Préat, 1997 [a]; Vanbever, *et al.*, 1997; Weaver, *et al.*, 1997; Vanbever, *et al.*, submitted) with the current data, the transdermal molecular fluxes measured throughout each experiment were averaged over 1 h. Plotting these data versus either the applied voltage (Figure 8.1) or the transdermal voltage (Figure 8.2) resulted in a lot of scatter in the data.

Since it was known that the applied voltage does not correctly predict the transdermal voltage (Pliquett, *et al.*, 1995 [a]; Pliquett and Weaver, 1996 [a]) the scatter in Figure 8.1 was to be expected.

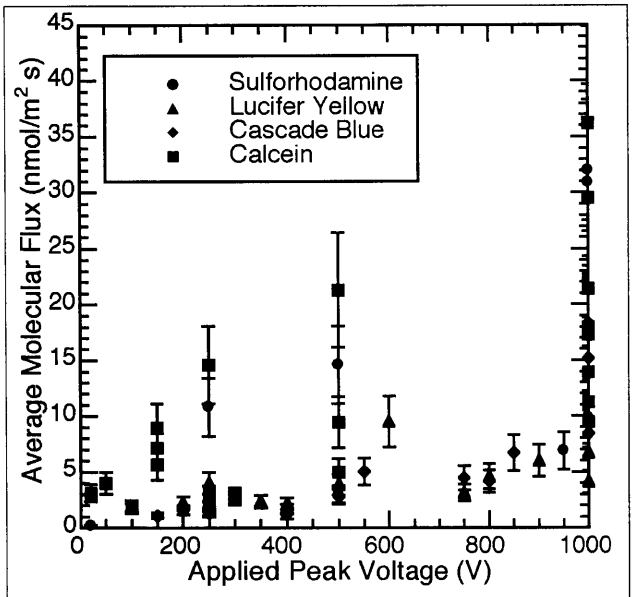

Figure 8.1. The average molecular flux plotted versus the average peak applied voltage. Four different molecules were used in the donor solution: sulforhodamine, lucifer yellow, cascade blue, and calcein. There does not seem to be a clear relationship between the average peak applied voltage and the average molecular flux.

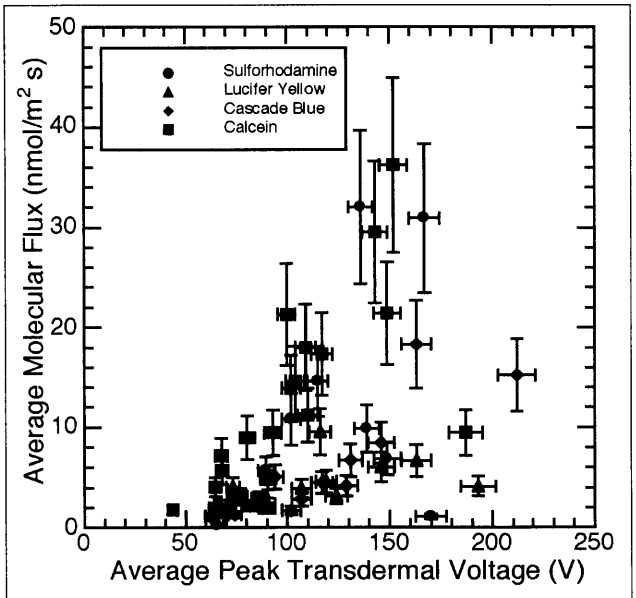

Figure 8.2. The average molecular flux plotted versus the average peak transdermal voltage. This figures is based on the same experiments and data shown in Figure 8.1. Although a generally increasing trend can be seen for the average molecular flux versus the average peak transdermal voltage, there still is not a clear relationship.

More evidence of this can be seen in Figure 8.3, where the average transdermal voltages were plotted versus the applied voltages, showing a poor relationship between the two voltages. However, the average fluxes plotted against the average transdermal voltage in Figure 8.2 also show a poor relationship.

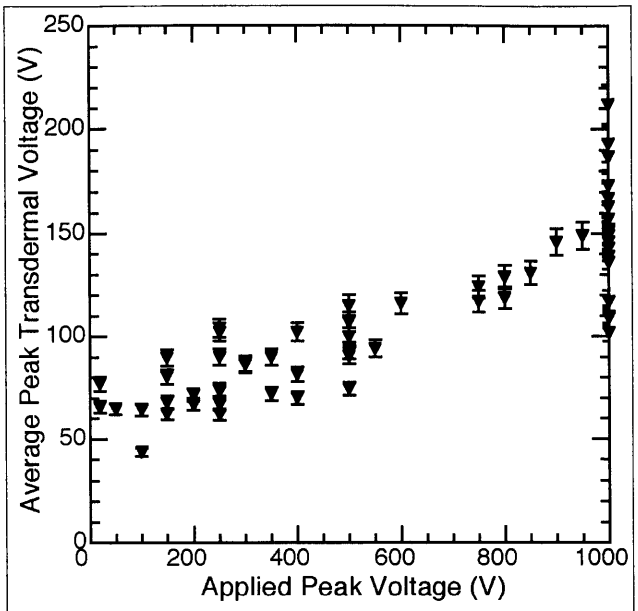

Figure 8.3. The average peak transdermal voltage versus the peak applied voltage. Although a generally increasing trend can be seen between the applied voltage and the resulting transdermal voltage, there is still a lot of scatter. For example, 18 experiments were conducted at an applied voltage of 1000 V, and the resulting peak transdermal voltages ranged from 102 V to 213 V.

Thus, by using average measurements of either the molecular flux or the transdermal voltage, significant errors can be introduced into the analyses, which motivates the use of a flow-through system in the current set of experiments.

Others have reported molecular flux versus either the average peak applied voltage (Prausnitz, *et al.*, 1993 [a]; Vanbever, *et al.*, 1994; Prausnitz, *et al.*, 1995 [b]; Vanbever and Préat, 1995; Vanbever, *et al.*, 1996 [a]; Vanbever, *et al.*, 1996 [b]; Vanbever, *et al.*, submitted) or the average peak transdermal voltage (Zewert, *et al.*, 1995; Pliquett and Weaver, 1996 [a]; Pliquett and Weaver, 1996 [b]). Many authors have reported only the average molecular flux after 1 h of pulsing (Prausnitz, *et al.*, 1993 [a]; Bommannan, *et al.*, 1994; Vanbever, *et al.*, 1994; Prausnitz, *et al.*, 1995 [b]; Riviere, *et al.*, 1995; Vanbever and Préat, 1995; Zewert, *et al.*, 1995; Prausnitz, *et al.*, 1996 [b]; Vanbever, *et al.*, 1996 [a]; Vanbever, *et al.*, 1996 [b]; Jadoul and Préat, 1997 [a]; Vanbever, *et al.*, 1997; Weaver, *et al.*, 1997; Vanbever, *et al.*, submitted). Those methods, while easier to apply, do not properly account for the time-varying nature of both the molecular flux and the transdermal voltage, and can be misleading, as was demonstrated here.

8.2.2. Molecular Flux and Transdermal Voltage Vary with Repeated Pulsing.

Time resolutions for the data recorded in these experiments were ~14 s for the molecular flux and ~1 μs for the transdermal voltage. This time resolution allowed the direct measurement of the instantaneous molecular flux versus the applied voltage for each pulse. With a time resolution of ~14 s, the molecular flux was actually averaged over ~3 pulses (one pulse is applied every 5.56 s). However, this is very close to a flux-per-pulse basis and a vast improvement over the traditional 1 h measurements.

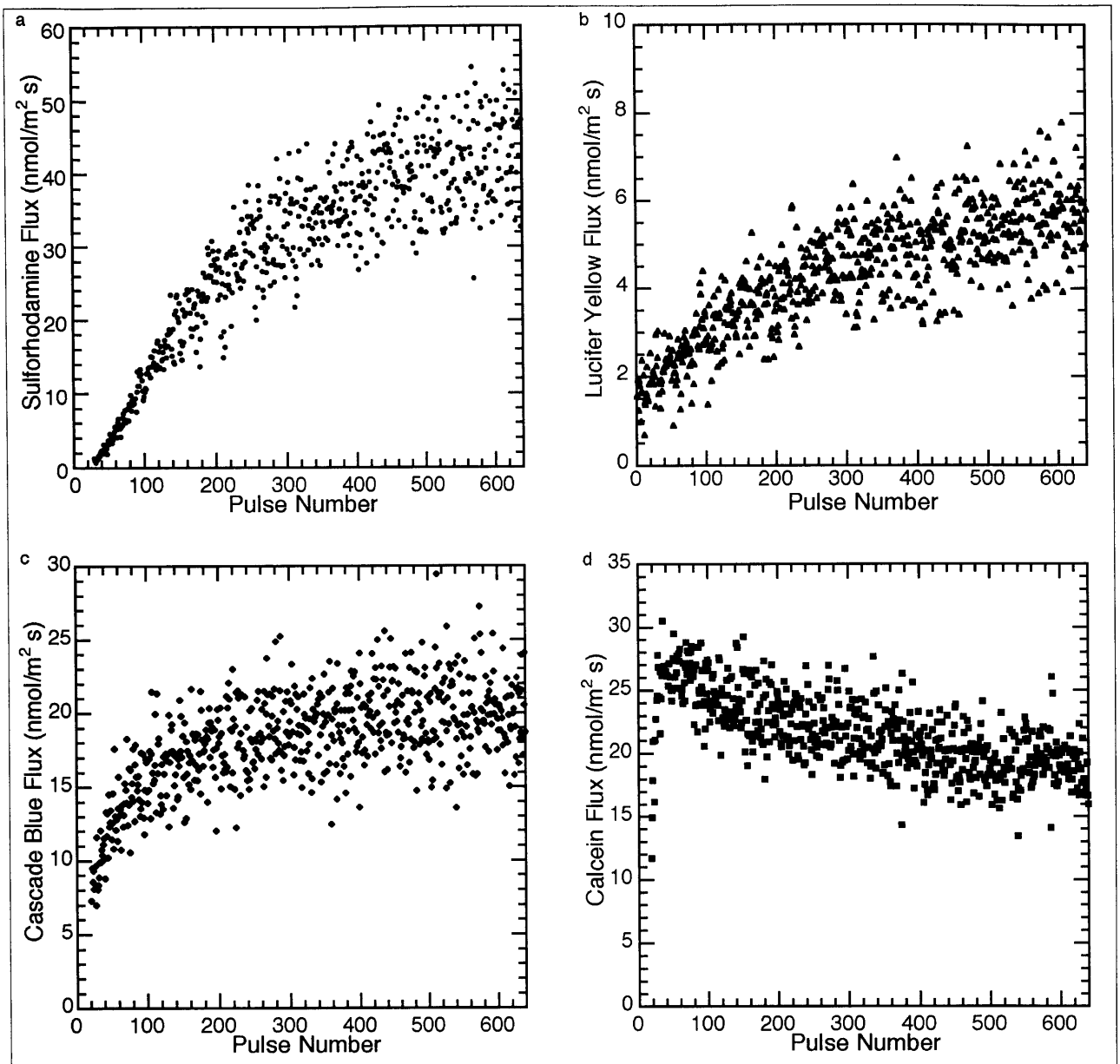

Figure 8.4. The molecular flux as a function of pulse number for four fluorescent compounds. Representative experiments shown; error bars removed for clarity. In all cases, 640 pulses were applied to the skin for 1 h, one pulse every 5.56 s. A flow-through system was used to measure the molecular flux through the skin in real time, with a time resolution of ~14 s. Even though the four donor molecules had similar properties, very different behaviors were observed. (a) The flux of sulforhodamine increased throughout the course of the experiment. (b) The flux of lucifer yellow increased to steady state. (c) The flux of cascade blue also went to steady state. (d) The flux of calcein quickly reached a maximum, then began decreasing with repeated pulsing.

Figure 8.4 shows the molecular flux through human skin, plotted for each pulse during a typical experiment (1000 $V_{applied}$, corresponding to 150 V_{skin}, τ = 1 ms, one pulse every 5.56 s for 1 h), for each of the four fluorescent donor molecules (8.4a, sulforhodamine; 8.4b, lucifer yellow; 8.4c, cascade blue; and 8.4d, calcein). The molecular flux the deconvoluted flux through the skin during pulsing.

Even though the four donor molecules had roughly similar molecular weights (457 Da to 623 Da) and were all hydrophilic and negatively charged, several different profiles of molecular flux versus

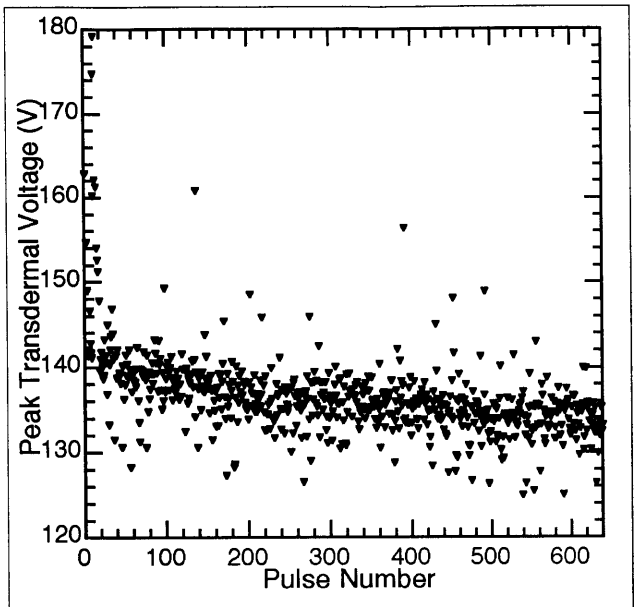

Figure 8.5. The transdermal voltage for each pulse in a typical experiment. Error bars have been removed for clarity. The peak transdermal voltage quickly drops (from ~180 V to ~140 V) with repeated pulsing, then continues decreasing at a slower rate afterwards (from ~140 V to ~130 V). Note that the peak transdermal voltage does not reach steady state, even after 1 h.

pulse number were observed. The flux of sulforhodamine (Figure 8.4a) increased steadily, without reaching a steady-state plateau. Longer experiments indicated that the molecular flux does not reaches a steady-state plateau, even after 7 h of pulsing (see Section 11.3). However, the fluxes of lucifer yellow (Figure 8.4b) and cascade blue (Figure 8.4c) did reach steady state within an hour (verified in later experiments involving pulsing over several hours; see Figures 11.3 and 11.4, for lucifer yellow and cascade blue, respectively). The flux of calcein (Figure 8.4d) first increased quickly during pulsing, then decreased with additional pulsing. This decrease is not an artifact, since PBS flow-protection of the pulsing electrodes was used to prevent contamination of the donor and receptor compartments by electrochemical by-products or pH changes from the electrodes. Other controls (including iontophoresis and passive exposure to calcein, see Section 4.1) have confirmed that calcein does not react with the skin. This decrease in calcein flux has also previously been reported (Prausnitz, *et al.*, 1994; Pliquett, *et al.*, 1995 [b]; Pliquett and Weaver, 1996 [a]; Pliquett and Weaver, 1996 [b]; Chen, *et al.*, 1998 [c]; Vanbever, *et al.*, submitted).

Figure 8.5 shows that $U_{skin,\,0}$ for each pulse drops quickly with the first few pulses, decreases more slowly with repeated pulsing, and does not reach steady state. This behavior was observed regardless of the tracer used. This is in agreement with earlier measurements of the transdermal voltage, made at 15 min intervals, that showed a generally decreasing trend in the transdermal voltage with repeated pulsing (see Section 7.4.1).

Thus, both the molecular flux and the transdermal voltage vary considerably with repeated pulsing. More experiments will be needed to better understand why different behaviors in the transdermal fluxes of similar molecular compounds was observed.

8.2.3. Formation of Localized Transport Regions.

Previously, many authors have reported the formation of "localized transport regions" (LTRs) after high-voltage pulsing (Zewert, *et al.*, 1995; Pliquett, *et al.*, 1996 [b]; Prausnitz, *et al.*, 1996 [a]; Chen,

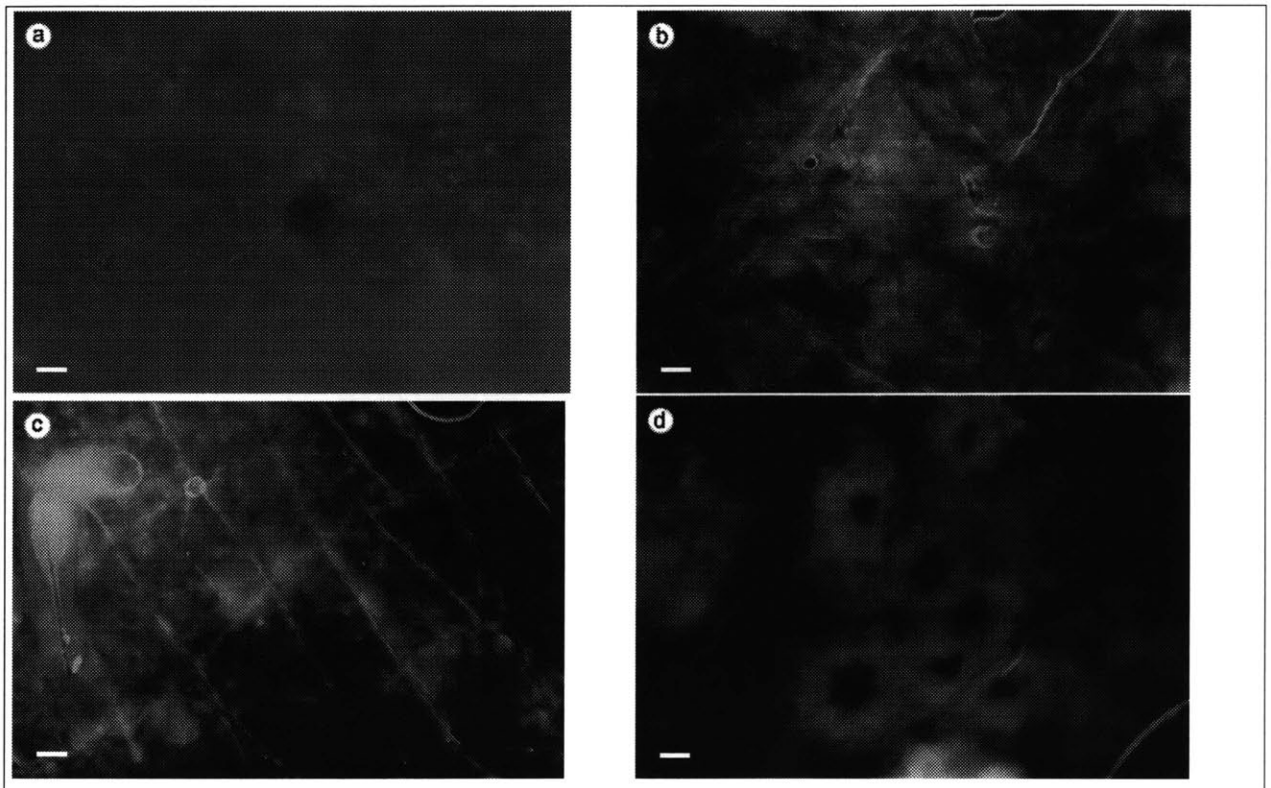

Figure 8.6. Photomicrographs of human skin after pulsing for four fluorescent compounds. Representative fields shown. Scale bar = 50 μ. Each fluorescent tracer shows a different pattern of staining, possibly indicating that different transport pathways are involved. (a) Sulforhodamine appears only in the interiors of the LTRs. (b) Lucifer yellow uniformly stains the entire surface of the skin, with the exception of the interiors of the LTRs, which appear darker. (c) Cascade blue uniformly stains the entire surface of the skin. No LTRs were identified. (d) Calcein forms "rings" around each LTR. The edges of the LTRs are brightly stained, but the interiors do not stain with calcein.

et al., 1998 [b]; Vanbever, *et al.*, submitted). However, in nearly all of these cases, either calcein or sulforhodamine (but usually both, simultaneously) was used in the donor solution.

In the current set of experiments, each of the four fluorescent tracers (sulforhodamine, lucifer yellow, cascade blue, and calcein) was used independently in the donor solution. The fluorescent regions observed in human stratum corneum after pulsing indicates those regions where molecular transport took place through the skin (Pliquett, *et al.*, 1996 [b]). Since molecular transport and ionic transport (electrical current) occur in the same regions in the skin (Pliquett, *et al.*, 1996 [b]), the same pattern of fluorescent staining of the skin would be expected for all four tracers.

In this study, however, each fluorescent tracer produced a different pattern of staining of the skin after 1 h of high-voltage pulsing. Calcein (Figure 8.6d) produced the LTR "ring" patterns previously observed in human skin (Pliquett, *et al.*, 1996 [b]). Sulforhodamine (Figure 8.6a) stained the interiors of the LTRs. The LTRs with lucifer yellow (Figure 8.6b) appeared as dark spots, although the background of the skin, not near the LTRs, appeared somewhat brighter. Cascade blue (Figure 8.6c) did not show any LTR formation.

Thus, the pathways for molecular transport may not necessarily be the same ones used for ionic transport (electrical current). Each molecule may have a different set of transport pathways available to

it, that are not necessarily available to other molecules. Partitioning of each compound into the skin, facilitated by electroporation, may be as important as the electrical driving forces (electrical drift, electroosmosis). Other unidentified molecular properties may also be important.

8.2.4. Onset of Molecular Transport at ~50 V_{skin}.

Combining Figures 8.4 and 8.5 for each experiment yields a plot of the molecular flux versus the peak transdermal voltage, as can be seen in Figure 8.7 (8.7a, sulforhodamine; 8.7b, lucifer yellow; 8.7c, cascade blue; and 8.7d, calcein). These data were plotted as the molecular flux versus $U_{skin,\,0}$ for each pulse, irrespective of pulse number, for every experiment. These data are from the same experiments shown in Figures 8.1, 8.2 and 8.3.

For each molecule, a nearly linear relationship was observed between the molecular flux and $U_{skin,\,0}$ for voltages > ~50 V (indicated by dotted lines in Figures 8.7a through 8.7d). However, in each case, the molecular flux tapered off for transdermal voltages < ~50 V. Although the molecular flux varied both in time, and from molecule to molecule, a transdermal voltage of at least ~50 V was necessary to cause significant molecular transport across the skin, regardless of the fluorescent tracer used.

Theoretical calculations and supporting experimental evidence in the literature have predicted electroporation predominantly at the appendages at $U_{skin,\,0}$ < 30 V, and electroporation of the lipid-corneocyte matrix at $U_{skin,\,0}$ > 30 V (Chizmadzhev, *et al.*, 1998 [a]). Although those calculations were based on a different system than the one used in the current study (for example, full-thickness instead of heat-stripped skin, 25 °C instead of 37 °C, rectangular pulses instead of exponential pulses), the value of 30 V for a transition to lipid-corneocyte electroporation (based primarily on electrical measurements) is reasonably close to the value determined in this study of ~50 V for the onset of significant molecular transport (based primarily on fluorescence measurements). Based on those calculations, the transcellular pathway through the skin, accessible primarily at higher transdermal voltages, allows significantly more molecular transport than the appendageal pathways that predominate at lower transdermal voltages. Most of the molecular transport takes place through the stratum corneum, not through the appendages.

8.3. Snake Skin Results.

In similar experiments involving shed snake skin instead of human skin, somewhat different results were obtained for the molecular flux on a per-pulse basis and the formation of LTRs. However, the drop in the transdermal voltage with repeated pulsing was very similar to human skin.

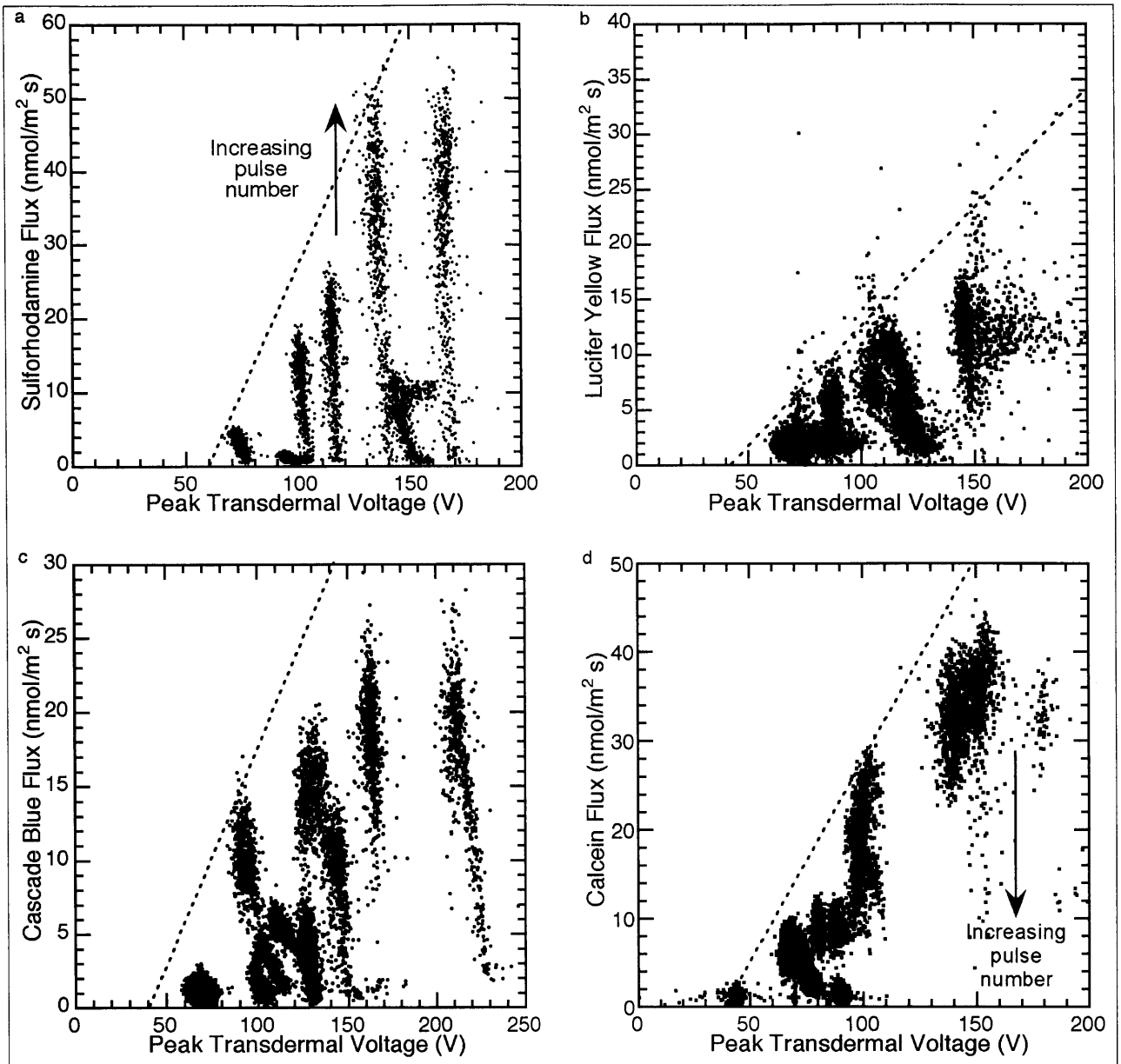

Figure 8.7. The instantaneous molecular flux versus the peak transdermal voltage. The instantaneous molecular flux for each of the four donor molecules (sulforhodamine, lucifer yellow, cascade blue, and calcein) is plotted for each experiment for every single pulse. Error bars have been removed for clarity. In all four cases an almost linear relationship can be seen between the flux and the peak transdermal voltage, with an intercept at ~50 V. This is indicated by the dotted line (this is not a quantitative determination; it is simply for illustrative purposes only). (a) Sulforhodamine flux. Data from 7 experiments shown. Since the flux of sulforhodamine continually rises throughout the experiment (see Figure 8.4a), the flux on a per-pulse basis starts towards the bottom of the graph and continuous to rise throughout the course of the experiment. The peak transdermal voltage slowly decreases with repeated pulsing, causing the "track" of data points to lean slightly to the left. (b) Lucifer yellow flux. Data from 13 experiments shown. The flux of lucifer yellow reaches a steady-state profile (Figure 8.4b), resulting in a "cloud" of points at the top of each track. Each track leans slightly to the left, due to the decrease in peak transdermal voltage with continued pulsing. (c) Cascade blue flux. Data from 13 experiments shown. The flux of cascade blue reaches steady state with repeated pulsing (Figure 8.4c), causing a "cloud" of points at the top of each track. Each track leans slightly to the left, since the peak transdermal voltage decreases with repeated pulsing. (d) Calcein flux. Data from 14 experiments shown. The flux of calcein quickly increases during pulsing initially, then begins to slowly decline with repeated pulsing (see Figure 8.4d). Hence, the tracks of calcein fluxes on this figure actually start towards the top of the figure, then head downwards with repeated pulsing. Since the peak transdermal voltage also decreases with repeated pulsing, each track leans towards the right.

8.3.1. Molecular Flux Changes with Repeated Pulsing.

Figure 8.8 shows the instantaneous molecular flux through shed snake skin in a typical experiment, plotted versus the pulse number for the same four fluorescent compounds (8.8a, sulforhodamine; 8.8b, lucifer yellow; 8.8c, cascade blue; and 8.8d, calcein). The molecular flux reported here is the deconvoluted average flux through the skin.

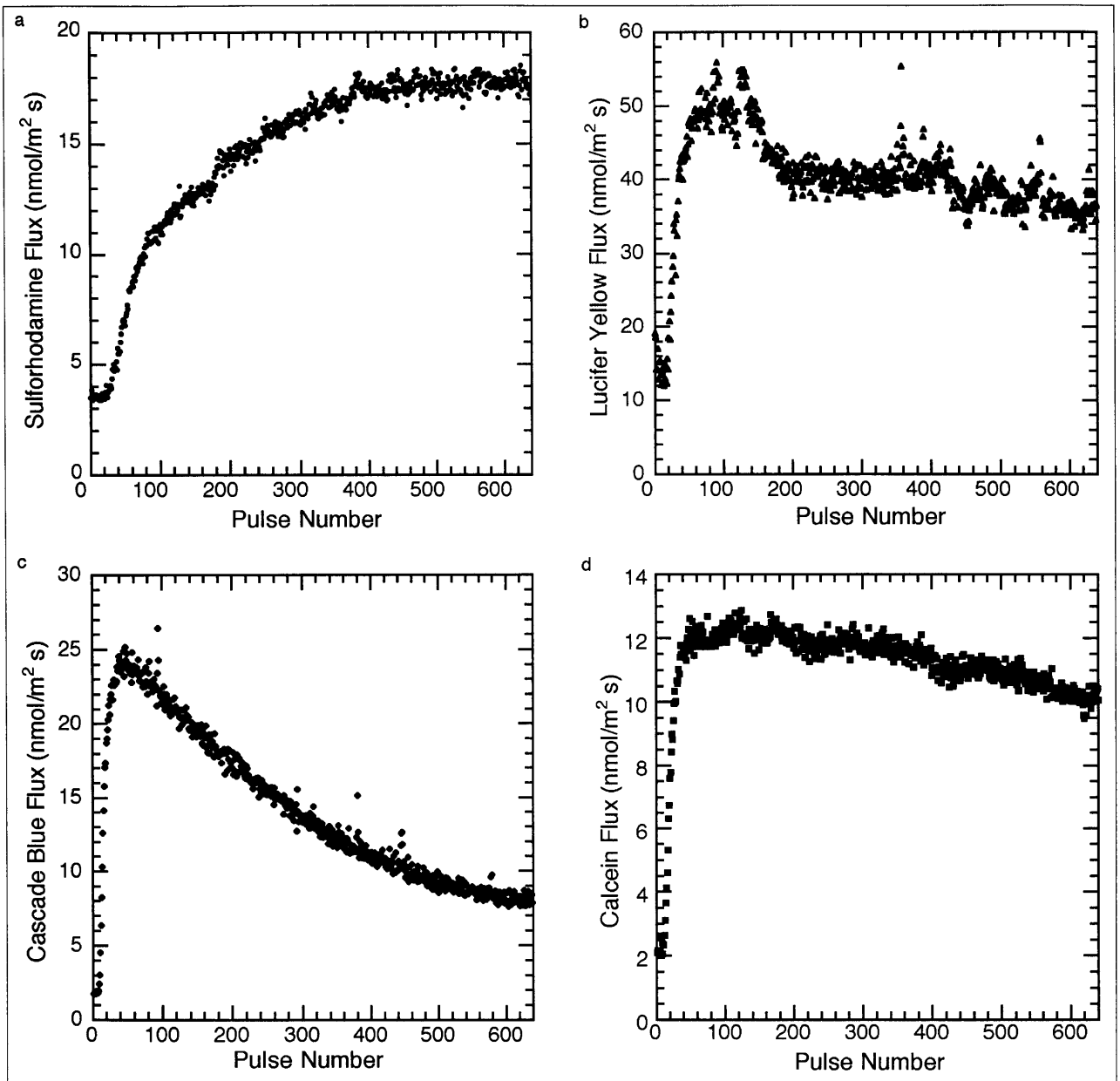

Figure 8.8. The molecular flux through snake skin as a function of pulse number. Representative experiments shown. Error bars have been removed for clarity. In all cases, 640 pulses were applied, 1 pulse every 5.56 s. A flow-through system was used to measure the flux in real time, with a time resolution of ~14 s. (a) The flux of sulforhodamine increased throughout the experiment, similar to in human skin (Figure 8.4a). (b) The flux of lucifer yellow quickly increased then decreased with additional pulsing. (c) The flux of cascade blue also increased quickly, then decreased with repeated pulsing. (d) The flux of calcein quickly reached a maximum, then began decreasing with repeated pulsing. This behavior was similar to human skin (see Figure 8.4d).

The behaviors of the sulforhodamine flux (gradual increase in the flux with repeated pulsing) and the calcein flux (quick rise, followed by a slow decrease in the flux) through snake skin were similar to human skin (compare Figure 8.8a versus 8.4a and Figure 8.8d versus 8.4d). However, very different behaviors were observed for the lucifer yellow and cascade blue fluxes (compare Figure 8.8b versus 8.4b and Figure 8.8c versus 8.4c). In human skin, both lucifer yellow and cascade blue rose to a steady-state plateau with repeated pulsing. However, the molecular flux of both lucifer yellow and cascade blue in snake skin quickly increased, then decreased with continued pulsing, similar to the behavior of calcein.

Decreases in the molecular flux with repeated pulsing have previously been observed for calcein (Prausnitz, *et al.*, 1994; Pliquett, *et al.*, 1995 [b]; Pliquett and Weaver, 1996 [a]; Pliquett and Weaver, 1996 [b]; Chen, *et al.*, 1998 [c]; Vanbever, *et al.*, submitted), but this is the first time that this drop has been observed with other fluorescent tracers. The pulsing electrodes were well-protected by polyacrylamide gels and streams of PBS (see discussion in Section 4.1), so it seems more likely that the drop in molecular flux, measured for three different fluorescent molecules in snake skin, is a real effect and not an artifact of the experimental system.

8.3.2. Transdermal Voltages Drop with Repeated Pulsing.

Figure 8.9 shows the voltage drop across shed snake skin during each pulse in a typical experiment. The transdermal voltage dropped quickly with the first few pulses, then decreased more slowly with additional pulsing. In particular, it did not go to steady state. This behavior was observed regardless of the fluorescent tracer used in the donor compartment.

The rate at which the transdermal voltage dropped in snake skin was similar to that of human skin (compare Figure 8.9 to Figure 8.5). The magnitude of the transdermal voltage created across snake skin during pulsing was also similar to human skin. Thus, in skin electroporation, shed black rat snake skin is a good model of the electrical properties of human skin.

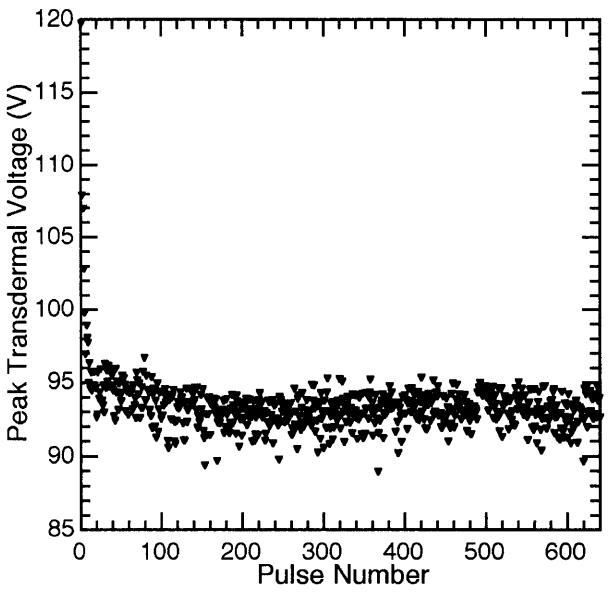

Figure 8.9. The transdermal voltage across snake skin versus pulse number. Error bars have been removed for clarity. Like human skin, in snake skin, the transdermal voltage initially drops rapidly, then continues decreasing at a slower rate afterwards.

8.3.3. *Localized Transport Regions in Snake Skin.*

Although LTR formation was also observed in snake skin, both the formation of LTRs and the molecular fluxes in time with repeated pulsing were quite different in snake skin than in human skin. Representative LTRs that formed on snake skin are shown in Figure 8.10. Unlike with human skin, the pattern of LTR staining was very similar for all four molecules (8.10a, sulforhodamine; 8.10b, lucifer yellow; 8.10c, cascade blue; and 8.10d, calcein). In all four cases, the LTRs appeared as rings with slightly darker interiors, similar to calcein in human skin (Figure 8.6d). The rest of the skin, away from the LTRs, showed very poor staining. Thus, in the electroporation of snake skin, molecular transport occurs through the LTRs, with the same transport pathways being used in all four cases. There does not appear to be any significant transport through the skin away from the LTRs.

8.3.4. *Transport Pathways are through Corneocytes.*

As there are no sweat ducts or hair follicles in snake skin, and since the mesos layer covers the entire snake, including underneath the scales (Roberts and Lillywhite, 1980; Itoh, *et al.*, 1990 [a]),

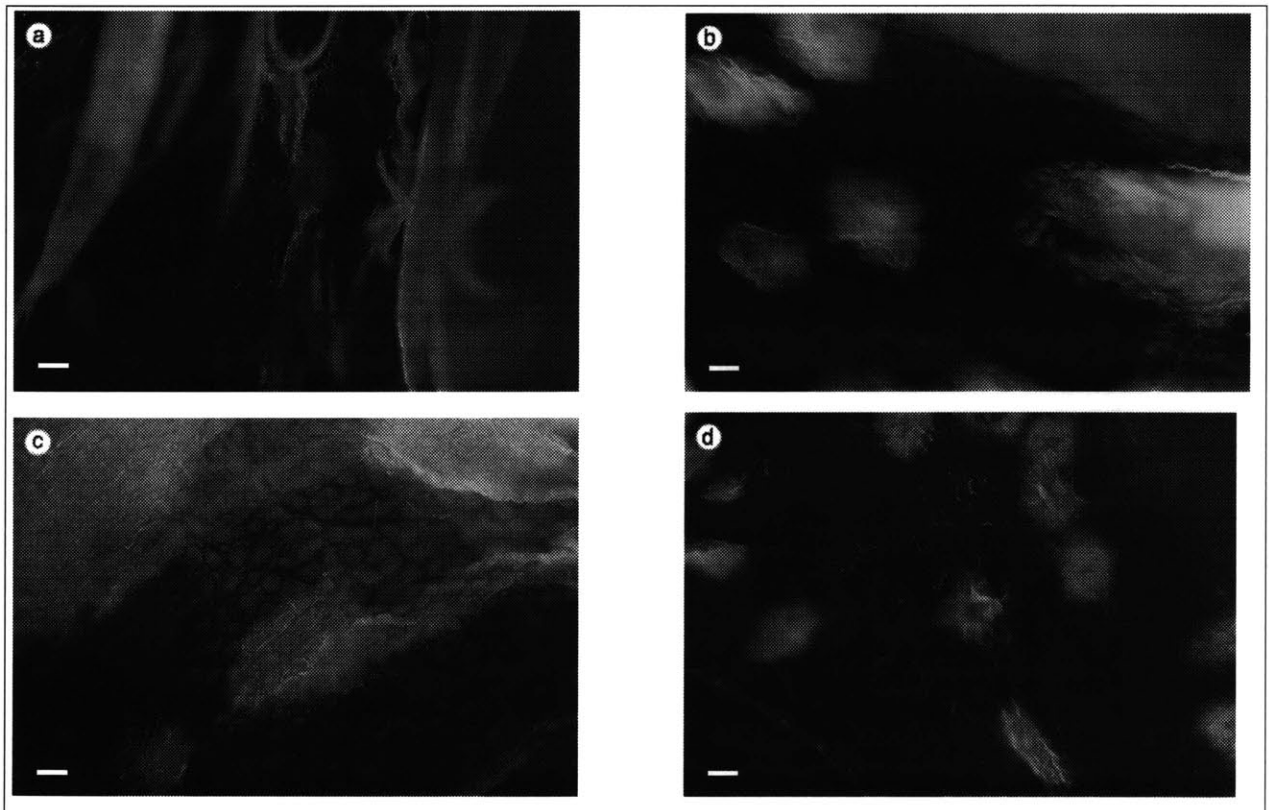

Figure 8.10. Photomicrographs of snake skin after pulsing for four fluorescent compounds. Scale bar = 50 μ. Representative fields shown. After 1 h of high-voltage pulsing, the appearance of the LTRs was very similar with all four tracers: (a) sulforhodamine, (b) lucifer yellow, (c) cascade blue, and (d) calcein.

then molecular transport through snake skin during high-voltage pulsing must be occurring through either the corneocytes, or the intercellular spaces.

However, the LTRs in both human (Figures 8.6a through 8.6d) and snake skin (Figures 8.10a through 8.10d) appear to be much bigger than the corneocytes (typically, an LTR is ~100 μ in diameter, versus ~30 μ in diameter for a corneocyte [Elias, 1983]). The LTRs only form during high-voltage pulsing, along with significant molecular transport (Pliquett, *et al.*, 1996 [b]; see also Sections 8.2.3 and 8.3.3). Thus, molecular transport during high-voltage pulsing occurs through the corneocytes of snake skin. With the large similarity in the results of human and snake skin, the corneocytes in human stratum corneum are probably also involved in molecular transport.

8.3.5. Transport Profiles.

In snake skin, the transport pathways across the skin used by lucifer yellow and cascade blue are probably the same pathways as for calcein, given the similarity of the molecular fluxes (compare Figures 8.9b, 8.9c, and 8.9d), and the similarity of the LTRs (compare Figures 8.10b, 8.10c, and 8.10d). This is in contrast to the human skin results, which showed very different behaviors for the fluxes of calcein, lucifer yellow, and cascade blue. Additional transport pathways, away from the LTRs and the appendages, may be used during molecular transport through human skin, causing different patterns of staining and different molecular flux profiles.

For sulforhodamine, a different mechanism may be involved in molecular transport than for the other three molecules, as sulforhodamine is significantly less hydrophilic than the others (Table 4.1). In both human and snake skin. the molecular flux of sulforhodamine increased slowly with repeated pulsing and did not reach steady state. Staining of the LTRs after pulsing in human skin was unlike the other molecules. Sulforhodamine appears to stain the centers of the LTRs, possibly indicating hydrophobic regions within the LTRs. This would account for the lack of fluorescence in the centers of the LTRs observed with calcein and lucifer yellow.

8.4. Conclusions.

This study showed that during high-voltage pulsing of the skin, both the molecular flux and the peak transdermal voltage need to be measured with high time resolutions, on the order of seconds, not hours, due to the changing nature of both the transdermal voltage and the resultant molecular flux. Molecules which are very similar (similar molecular weights, similar charges, etc.) can pass through the skin at significantly different rates, and cause quite different patterns of staining in the skin. Careful

measurements during repeated pulsing (exponential pulses, 1 ms time constant, 1 pulse every 5.56 s) have shown that the transdermal molecular flux increases markedly at transdermal voltages >50 V, possibly indicating the onset of electroporative molecular transport through the skin.

9. Time Course of Skin Electroporation.*

In skin electroporation, a series of short (~1 ms), high-voltage (~100 V_{skin}) pulses are typically applied to the skin, causing dramatic increases in molecular transport, potentially useful for drug delivery (Prausnitz, *et al.*, 1993 [a]). Many molecules have been successfully transported across the skin *in vitro*, including low molecular weight compounds such as sulforhodamine (Pliquett and Weaver, 1996 [a]; Pliquett, *et al.*, 1996 [b]; Chen, *et al.*, 1998 [b]; Chen, *et al.*, 1998 [c]; Vanbever, *et al.*, submitted) and calcein (Prausnitz, *et al.*, 1993 [a]; Prausnitz, *et al.*, 1993 [c]; Prausnitz, *et al.*, 1994; Pliquett, *et al.*, 1995 [b]; Pliquett and Weaver, 1996 [a]; Pliquett and Weaver, 1996 [b]; Pliquett, *et al.*, 1996 [b]; Prausnitz, *et al.*, 1996 [b]; Chen, *et al.*, 1998 [b]; Chen, *et al.*, 1998 [c]; Vanbever, *et al.*, submitted). Larger compounds have also been successfully transported across human skin as well, including luteinizing hormone releasing hormone (LHRH) (Bommannan, *et al.*, 1994; Riviere, *et al.*, 1995), oligonucleotides (Zewert, *et al.*, 1995; Regnier, *et al.*, in press [a]), and heparin (Prausnitz, *et al.*, 1995 [b]; Vanbever, *et al.*, 1997; Weaver, *et al.*, 1997).

Molecular transport across the skin is believed to take place across spontaneously forming "localized transport regions" (LTRs), distributed randomly on the surface of the skin, and are specifically not hair follicles or sweat ducts (Zewert, *et al.*, 1995; Pliquett, *et al.*, 1996 [b]; Prausnitz, *et al.*, 1996 [a]; Chen, *et al.*, 1998 [b]; Vanbever, *et al.*, submitted).

Pulses are typically applied to the skin at the rate of one pulse every 5 s (Prausnitz, *et al.*, 1993 [a]; Prausnitz, *et al.*, 1994; Prausnitz, *et al.*, 1995 [b]; Zewert, *et al.*, 1995; Pliquett and Weaver, 1996 [a]; Pliquett and Weaver, 1996 [b]; Prausnitz, *et al.*, 1996 [b]; Weaver, *et al.*, 1997; Chen, *et al.*, 1998 [b]; Chen, *et al.*, submitted [b]) or one pulse every minute (Kost, *et al.*, 1989; Vanbever, *et al.*, 1994; Pliquett, *et al.*, 1995 [b]; Vanbever and Préat, 1995; Pliquett and Weaver, 1996 [a]; Pliquett and Weaver, 1996 [b]; Prausnitz, *et al.*, 1996 [b]; Vanbever, *et al.*, 1996 [a]; Vanbever, *et al.*, 1996 [b]; Vanbever, *et al.*, 1997; Vanbever, *et al.*, 1998 [a]). However, in most of these experiments, measurements of the condition of the skin, or the amount of transport across the skin, are typically made once an hour. In essence, each measurement is the average of 60 to 720 pulses.

Recent experiments have shown that many dramatic changes occur in the skin on the time scale of a few pulses. For instance, the transdermal voltage can drop rapidly during the first few pulses (Chen, *et al.*, 1998 [c]). Also, the impedance of the skin can vary with repeated pulsing (Pliquett, *et al.*, 1995 [a]; Pliquett and Weaver, 1996 [a]). The molecular flux across the skin in time can also vary dramatically (Pliquett, *et al.*, 1995 [b]; Pliquett and Weaver, 1996 [a]; Chen, *et al.*, 1998 [c]; Chen, *et al.*, in press [a]), even for similar compounds (Chen, *et al.*, 1998 [c]).

---

*Some of the material in this chapter has also been published in Chen, *et al.*, (submitted) [b].

Much work has been done on individually measuring some of these properties of the skin during high-voltage pulsing. However, the combination of all these measurements would be useful in gaining a better understanding of the mechanism behind molecular transport during skin electroporation, as many of these factors undoubtedly could affect each other. The investigation of this subject is the topic for this chapter.

9.1. Real-Time Measurements and Time Resolutions.

In the skin electroporation experiments in this chapter, high-voltage, exponentially-decaying pulses with a time constant of ~1 ms were applied to the skin once every ~5 s, to facilitate comparison with previous experiments from the literature (Prausnitz, *et al.*, 1993 [a]; Prausnitz, *et al.*, 1994; Prausnitz, *et al.*, 1995 [b]; Zewert, *et al.*, 1995; Pliquett and Weaver, 1996 [a]; Pliquett and Weaver, 1996 [b]; Prausnitz, *et al.*, 1996 [b]; Weaver, *et al.*, 1997; Chen, *et al.*, 1998 [b]; Chen, *et al.*, in submitted [b]). While high-voltage pulses were being applied to the skin, several measurements were taken as rapidly as possible: the molecular flux, the transdermal voltage, the impedance of the skin between pulses, the amount of material loaded into the skin (the so-called "reservoir" effect) (Prausnitz, *et al.*, 1993 [a]), and the formation of LTRs (Table 9.1).

The molecular flux was measured with a time resolution of ~14 s (Chen, *et al.*, 1998 [c]; Chen, *et al.*, in press [a]), using a flow-through system in the receptor compartment, connected to a spectrofluorimeter. In this system, the contents of the receptor compartment were continuously pumped to a spectrofluorimeter and replaced with fresh PBS. The residence or "mixing" time of the receptor compartment (Fogler, 1992) was taken to be the time resolution for this system. Key factors governing this time are the volume of the receptor compartment, and the flowrate of PBS.

The transdermal voltage for every single pulse was recorded on a per-pulse basis while the pulses were applied once every ~5 s. Besides just the peak transdermal voltage, the entire waveform during the pulse was also measured and recorded, with a time resolution of 10 μs. As this was mostly an electrical measurement, the time resolution was limited only by the time needed to download and store the data, which had to be kept under 5 s.

Inter-skin impedance measurements gave a useful indication of the condition of the skin between pulses. Like the transdermal voltage measurements, the time resolution was limited only by the time

Table 9.1. Available Time Resolutions.

Measurement	Technique	Time Resolution
Molecular flux	Flow-through system, ~400 μl	14 s
Transdermal voltage	Differential high-voltage probe/computer	10 μs
Inter-pulse impedance	Impedance meter/computer	200 ms
Material transported into skin	Removal of donor followed by additional pulsing	1 pulse
LTR formation	Fluorescence microscopy	1 pulse (4 ms)

needed to download and save the impedance data, and this could be as little as 200 ms between measurements. The impedance measurements were a surrogate for the DC resistance of the skin, since directly measuring the DC resistance could potentially cause iontophoresis of the skin to occur. Thus, measuring the impedance of the skin at a low frequency, rather than the DC resistance, ensures that the net current is zero.

The amount of material (the fluorescent tracer) loaded into the skin during pulsing could not be determined in real time. To determine the amount of material present within the skin, after applying a series of high-voltage pulses, the donor and receptor compartments were then emptied, and additional pulses applied to remove the remaining material within the skin ("extraction"). Thus, to determine the amount of material in the skin with respect to the pulse number, a new experiment had to be conducted for each pulse number. The time resolution for this technique is therefore theoretically one pulse, although to conduct enough experiments for that great of a time resolution would be impractical.

Like the extraction experiments, to monitor the formation of LTRs in the stratum corneum during pulsing, the experiment needed to be stopped, and the skin removed from the chamber, prepared on a microscope slide, and studied under fluorescence microscopy. After mounting the skin on the microscope slide, the skin could not be reused, due to potential mechanical sheering; thus, a new experiment had to be conducted for each pulse number. This limited the time resolution to one pulse.

Others have successfully built chambers that could be examined under fluorescence microscopy during pulsing (Pliquett, *et al.*, 1996 [b]). By connecting a VCR to the microscope, the formation of LTRs could be monitored in real time during the experiment, giving an effective time resolution of 4 ms (VCRs typically record images at 24 frames per second). However, this technique was not used for the experiments described in this paper.

9.2. Materials and Methods.

The experimental apparatus used in these experiments has been modified from the ones previously described in the literature (Chen, *et al.*, 1998 [c]; Chen, *et al.*, in press [a]). The major additions include the skin impedance measurement system and the donor extraction system.

This system is described in greater detail in Appendix V. Human skin was placed in a diffusion chamber, equipped with independent flow-through systems in both the donor and the receptor compartments. A PBS solution containing 1 mM of a fluorescent tracer (sulforhodamine, lucifer yellow, cascade blue, or calcein; see discussion in Chapter 4) was used as the donor solution. The pulsing electrodes were surrounded by polyacrylamide gel and washed in a steady stream of PBS, to protect the donor and receptor compartments from chemical by-products produced by the electrodes during pulsing. The transdermal voltage during each pulse was measured separately using a different set of

inner "measuring" electrodes. The inter-pulse impedance of the skin was measured using an impedance meter that was disconnected from the chamber whenever a high-voltage pulse was applied. Data stored in real time from the spectrofluorimeter (flux measurements), the oscilloscope (voltage measurements), and the impedance meter were calibrated and processed to give information about the conditions of the experiment. After pulsing, the skin was removed, mounted on a microscope slide, and examined by fluorescence microscopy. Alternatively, the donor solution was flushed out and replaced with fresh PBS. Additional pulses were then applied to extract the material still within the skin.

9.2.1. Skin Preparation.

Human cadaver skin was prepared by the heat-stripping method, described in Appendix I. Briefly, stored cadaver skin at -80 °C (Gummer, 1989) was thawed to room temperature, then submerged in de-ionized water for 2 min at 60 °C. The epidermis (including the stratum corneum) was gently scraped off of the dermis, cut into 3/4 inch diameter circles, and stored at 4 °C, 95% humidity for up to 10 d (Gummer, 1989).

9.2.2. Permeation Chamber and Electrodes.

Phosphate-buffered saline (PBS) was prepared as described in Section 3.2. The donor solution consisted of a fluorescent tracer (either sulforhodamine, lucifer yellow, cascade blue, or calcein), dissolved in PBS at a concentration of 1 m<u>M</u>. The solution was gently stirred for >30 min (Nutator, Clay Adams, Becton Dickinson).

The flow-through system is described more fully in Appendix V (see Figure V.2). The permeation chambers were specially designed, side-by-side chambers, with a skin exposure area of 0.64 cm^2 (circular opening, 0.9 cm in diameter) (Crown Bio Scientific) (Friend, 1992). The chamber consisted of an outer water jacket and an inner compartment. Ports from the inner compartment allowed direct access to the inner compartment. Each chamber half had one large port near the skin (for the measuring electrodes and the flow-through system) and two small ports away from the skin (for the pulsing electrode and the electrode flow-protection system). To keep the skin and the donor and receptor solutions at 37 °C, water heated by a thermostated water bath (Neslab) was continually pumped through both outer jackets.

The flow-protected electrodes were constructed by soldering a piece of 0.040 inch diameter silver wire, ~0.5 cm long, to copper bell wire. The solder and exposed wire were covered by nonconducting silicone rubber (General Electric), so that only the silver wire was exposed. A piece of Tygon tubing,

1/32 inch ID, and the electrode were inserted through a truncated 200 µl pipette tip. The top of the pipette was sealed with epoxy (Devcon).

The two measurement/flow-through electrodes were constructed as follows. A piece of 0.040 inch diameter silver wire, ~0.5 cm long, was soldered to copper bell wire. The solder and exposed wire were covered by nonconducting silicone rubber, so that only the silver wire was exposed. Teflon tubing, 1/16 inch ID, was used for the outflow and Tygon tubing, 1/32 inch ID, was used for the inflow. The wire and the two tubes were inserted through a truncated 1 ml pipette tip. A hole was drilled into the side of the pipette tip and the Teflon tube was extended out through the hole. All of the tubes and wires were sealed in place with epoxy.

Next, the top of a 2 ml centrifuge tube was removed and two holes were drilled the tube: one in the bottom and one in the side. Tygon tubing, 1/32 inch ID, was epoxied to the bottom hole. The Teflon tube from the pipette was extended through the side hole in the centrifuge tube. The centrifuge tube was held in place to the side of the pipette with Parafilm (American National Can).

Before each experiment, plastic tubes were inserted through both compartments and sealed in place with Parafilm. The measuring/flow-through electrodes were also inserted into both compartments and sealed in place with Parafilm. The tubing within both compartments was wired in place with stainless steel wire. Both compartments was turned sideways, and polyacrylamide solution was poured in, completely immersing everything, leaving empty a volume of ~450 µl in each compartment. The polyacrylamide solution was composed of 0.75 g of 19:1 acrylamide:bis(N,N'-methylene-bis-acrylamide) powder (Bio-Rad), 43.75 µl of 440 m<u>M</u> $(NH_4)_2S_2O_8$ solution, and 3 µl of N,N,N',N'-tetramethyl-ethylenediamine (Bio-Rad) in 5 ml of PBS.

The polyacrylamide solution was allowed to harden (~10 min). After the solution solidified, the outer plastic tubing and the Parafilm were removed from the outer ports, leaving behind an empty channel through the gel. The flow-protected electrodes were inserted into this channel. During an experiment, PBS was pumped through each outer channel at a flowrate of ~6 ml/min, using two peristaltic pumps (VWR). The stainless steel wire was removed from each compartment, since the tubing was now immobilized in place by the gel.

9.2.3. Fluorescence Measurements.

Fluorescence measurements were taken with a spectrofluorimeter (Fluorescence Master Series Spectrometer, Photon Technology, Brunswick, NJ). Excitation and emission wavelengths for each fluorescent compound are given in Table 4.1.

The cuvette in the spectrofluorimeter was constructed by drilling two holes into a polystyrene microcuvette (VWR), to allow for inflow and outflow. One hole was drilled approximately 1/4 inch from

the bottom of the cuvette to allow liquid outflow, and the other hole was drilled higher in the cuvette to allow liquid inflow. Both holes were connected by Tygon tubing to a peristaltic pump ("Sarah" Cassette Peristaltic Pump, Barnant).

The final volume of the cuvette was ~200 μl, and was the minimum amount needed by the spectrofluorimeter for accurate detection and quantification of the receptor solution. Mixing within the cuvette was accomplished by the dripping of liquid into the cuvette. The performance of this system was close to an idealized continuous-stirred tank reactor (Fogler, 1992), and the residence time for the combined chamber-tubing-pump-cuvette system (volume of ~400 μl) was measured to be ~14 s. This was taken to be the time resolution for the flux measurements.

9.2.4. Electrical Equipment.

High-voltage exponential pulses were delivered by a high-voltage pulser (Electroporation System 600, BTX), specially modified to deliver 1 pulse every ~5 s (U. Pliquett, personal communication). Since the fluorescent tracers were all negatively charged, the negative terminal of the pulser was connected to the pulsing electrode in the donor compartment, and the positive terminal to the receptor compartment, to provide a favorable driving force.

The time constant on the high-voltage pulser was set to 1 ms. Pulses with peak transdermal voltages between 0 V and ~150 V across the skin were applied for 1 h, one pulse every 5.56 ± 0.01 s (640 pulses total).

Current delivered across the skin during each pulse was measured by measuring the voltage drop across a 1.2 Ω noninductive resistor placed in series with the permeation chamber. The voltage drop across the resistor was measured by a 10× voltage probe (HP 10071A, Hewlett Packard) connected to an oscilloscope (Hewlett Packard 54601, Hewlett Packard). The oscilloscope was connected through an RS-232 interface card (54641A RS-232 Interface Module, Hewlett Packard) to the serial port on a personal computer.

The voltage drop from the receptor to the donor compartment was measured by connecting a differential high-voltage probe (Active Differential Probe B9017RT, Yokogawa) to the immobilized silver wire measuring electrodes in each compartment. This probe was also connected to the same oscilloscope.

The computer was programmed using Turbo C++ (Borland), running a program that would count and record both voltage waveforms recorded by the oscilloscope for every pulse. The program is given in Section V.4.5. The program recorded the waveform data as ASCII characters and did not do any mathematical processing.

Between pulses, the impedance of the skin was measured using an impedance meter (Model 5R715 LCR Meter, Stanford Research Systems), connected to a personal computer via a RS-232 cable (not the

same one as before). The impedance meter was connected to the permeation chamber, via an electro-mechanical relay switch, connected to the timing circuit of the pulser (E. Gift, personal communication). Whenever a pulse was applied to the skin, the impedance meter would be physically disconnected from the pulser as a safety precaution.

This computer was also programmed in Turbo C++. It ran a program to continuously download and save the data from the impedance meter. This program is listed in Section V.4.2. Impedance measurements were taken once every ~200 ms.

9.2.5. Skin Experimental Protocol.

Prepared, stored skin was floated in PBS for ~1 min to remove the wax paper backing. The skin was loaded into the permeation chambers, with the stratum corneum facing the donor compartment. PBS was then pumped into each compartment.

The condition of the skin was checked by measuring its electrical impedance. A 100 Hz, 0.1 V bipolar sine wave (peak-to-peak) was applied across the skin and the resulting impedance measured using the LCR meter. The skin was considered bad and was discarded if its electrical impedance was <25 $k\Omega\,cm^2$ at a frequency of 100 Hz (or <40 $k\Omega$ for this apparatus). Previous experiments have shown that this impedance value compares favorably with the accepted DC resistance of <50 $k\Omega\,cm^2$ (Gowrishankar, personal communication). The resistances and impedances of the PBS and the polyacrylamide gel were neglected, since their combined resistances were previously measured to be 260 Ω (see Section 3.7), compared to ~30 $k\Omega$ for the skin.

After determining if the skin was acceptable or not, the apparatus was allowed to sit for 1 h to fully hydrate the skin (Prausnitz, *et al.*, 1993 [a]) and check for leaks. Leaky skin (passive flux above the detection limit, ~10^{-8} M, or ~10^{-10} $mol / m^2\,s$ for this experimental apparatus), was discarded.

9.2.6. High-Voltage Pulsing Protocol.

High-voltage exponential pulses, with a time constant of 1 ms and transdermal voltages between 0 V and ~150 V across the skin (applied voltages between 0 V and 1000 V) were applied for 1 h at the rate of one pulse every 5.56 s. PBS was pumped through the flow-protection system (across the electrodes) at ~6 ml/min using a peristaltic pump (VWR). PBS was also pumped through the receptor flow-through system at the rate of 0.0322 ml/s. The donor compartment flow-through system was initially set to recycle the donor solution in the donor compartment. The three computers (spectrofluorimeter, voltage waveforms, and impedance meter) were set to begin recording data.

In the extraction experiments, after pulsing was stopped, the flow-through system in the donor compartment was changed from the recycling mode to a flow-through mode (see Figure V.3), where fresh PBS was continuously pumped through the donor to a waste beaker (the other measuring systems, such as for the impedance of the skin or the fluorescence, were not shut down). After waiting for 30 min to allow the donor and receptor compartments to be fully flushed out with fresh PBS, ≥1 h of high-voltage pulsing was then applied to the skin.

After the experiment, the skin was removed from the chamber for fluorescence microscopy analysis. All of the data from the three computers (spectrofluorimeter data, impedance data, and voltage data) were downloaded onto a Sun Sparc 10 (Sun, Palo Alto, CA) workstation for analysis.

9.2.7. Fluorescence Microscopy.

A biocular fluorescence microscope (Olympus BH-2, Olympus) allowed simultaneous fluorescence and light illumination of the specimen at 4× and 10× magnifications. Pictures were taken using a camera (Olympus OM2, Olympus) mounted on the microscope (Pliquett, *et al.*, 1996 [b]).

Immediately after pulsing, the skin was carefully removed and gently placed onto a microscope

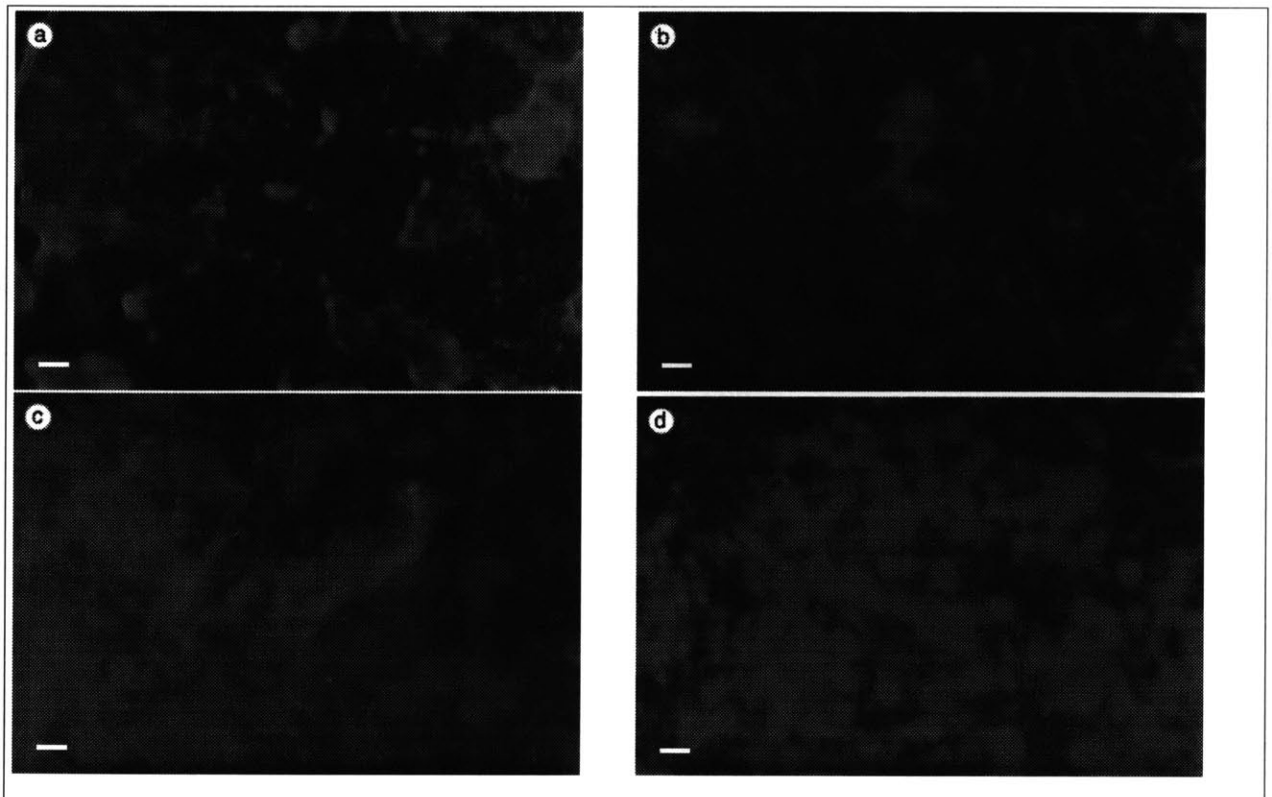

Figure 9.1. Time sequence of photomicrographs after pulsing with sulforhodamine. Scale bar = 50 μ. The number of applied pulses were: (a) 3 pulses, (b) 10 pulses, (c) 100 pulses, and (d) 680 pulses. The LTRs for sulforhodamine were well-defined regions that formed early during high-voltage pulsing, then grew in size with additional pulsing.

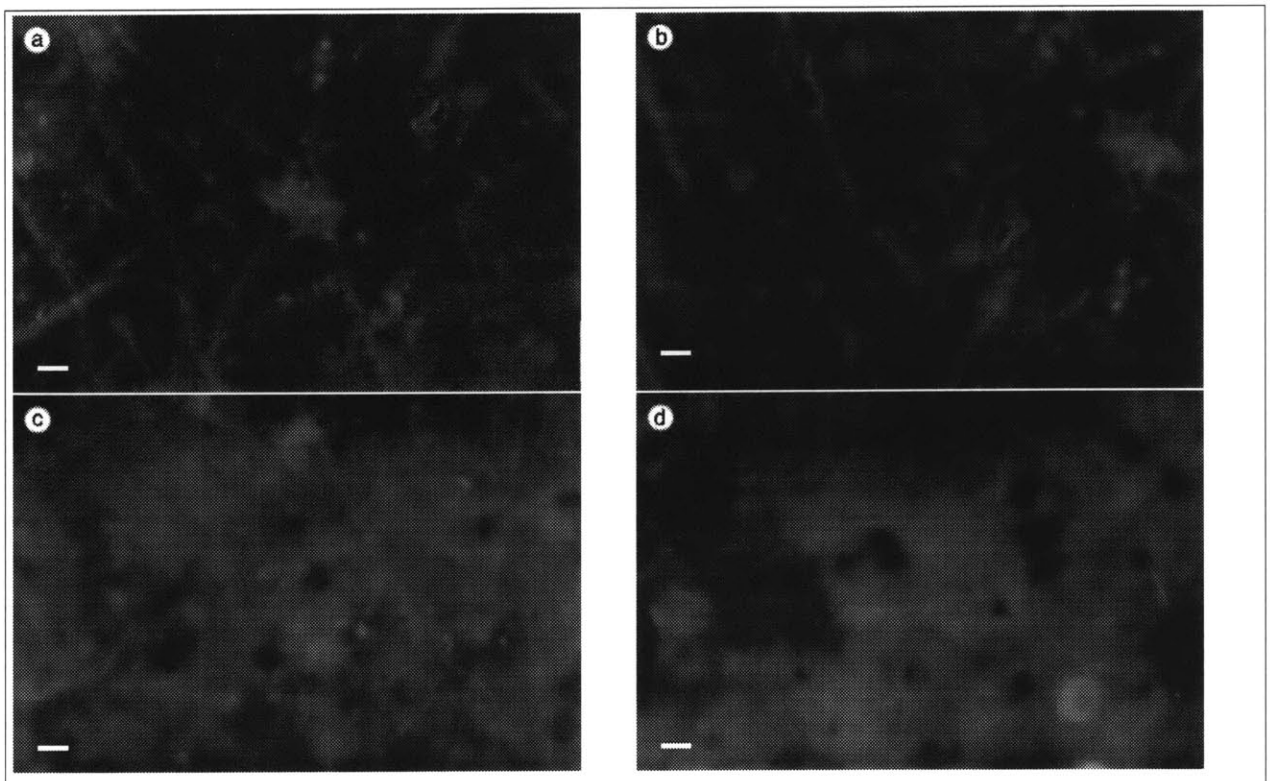

Figure 9.2. Time sequence of photomicrographs after pulsing with lucifer yellow. Scale bar = 50 μ. The number of high-voltage pulses were: (a) 3 pulses, (b) 10 pulses, (c) 100 pulses, and (d) 680 pulses. The LTRs for lucifer yellow appeared as dark regions on the surface of the skin. No fluorescence was seen in the interiors of the LTRs. However, the regions of the skin away from the LTRs were brightly fluorescent, and that fluorescence appeared to increase with pulse number.

slide (Gold Seal Rite-On, No. 3050, Clay Adams, Becton Dickenson). Excess liquid was gently blotted off with a paper towel. A drop of staining solution was added and a 22×22 No. 1 cover slip (Clay Adams, Becton Dickenson) was placed on top and sealed in place with clear nail polish (Hard as Nails, Sally Hensen, Del) (Prausnitz, *et al.*, 1996 [a]).

9.2.8. Numerical Analysis.

All of the fluorescence, voltage, impedance, and calibration data were first downloaded onto a Sun Sparc 10 workstation (Sun). A program written in MatLab 5 (Mathworks), running on a Sun Sparc 10, used these data to determine the flux, voltage, and impedance for each pulse during the experiment. This program can be seen in Section V.11.2. The program first loaded the voltage and current waveforms and fitted each curve to an exponential to determine voltages. Since the resistance of the chamber without any skin was 260 kΩ, the voltage across the skin could then be calculated by Ohm's Law. Next, the program loaded in the impedance data and calculated the impedance with respect to time for each pulse. The program then loaded the calibration and fluorescence data, and, using deconvolution

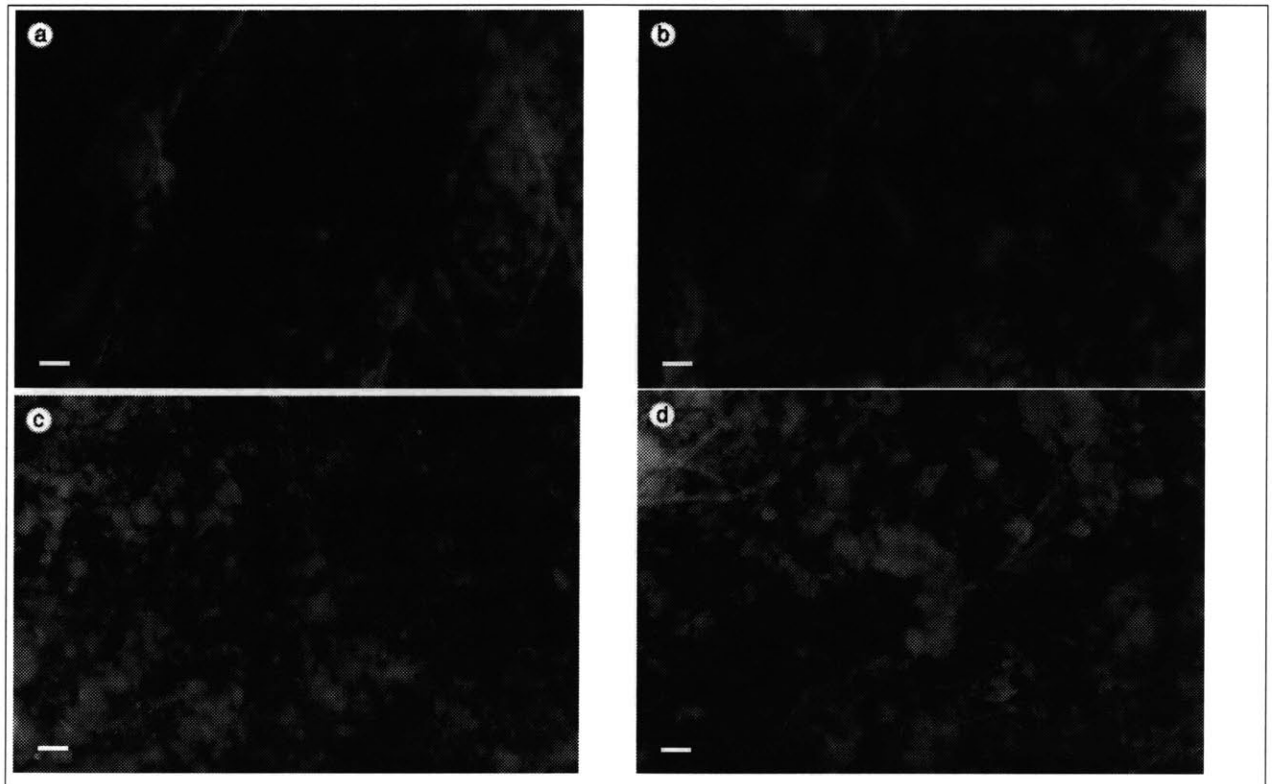

Figure 9.3. Time sequence of photomicrographs after pulsing with cascade blue. Scale bar = 50 μ. The number of applied pulses were: (a) 3 pulses, (b) 10 pulses, (c) 100 pulses, and (d) 680 pulses. No LTRs were observed for cascade blue during the entire pulsing protocol.

routines (Pliquett, *et al.*, 1995 [b]), calculated the molecular flux across the skin for each pulse. The three sets of data (flux, impedance, and voltage) were then synchronized together in time. In the extraction experiments, the flux measurements made during the extraction phase (with only PBS in the donor compartment) were integrated to determine the amount of material released from the skin.

9.3. Molecular Fluxes and Peak Transdermal Voltages.

The molecular fluxes for all four compounds (sulforhodamine, lucifer yellow, cascade blue, and calcein) were similar to those discussed in Section 8.2.2 (see Figures 8.4a through 8.4d). The flux of sulforhodamine increased throughout the entire experiment; lucifer yellow and cascade blue both achieved steady state; and the flux of calcein increased rapidly at the start of pulsing, then began decreasing afterwards.

The peak transdermal voltages were also similar to the previous experiments, also discussed in Section 8.2.2 (Figure 8.5). The transdermal voltages initially dropped quickly with the first few pulses, then leveled out with additional pulsing.

9.4 Localized Transport Region Formation.

After applying 3, 10, 100, and 680 pulses, the skin was removed and examined under fluorescence microscopy. Four donor solutions were used: sulforhodamine (Figures 9.1a through 9.1d), lucifer yellow (Figures 9.2a through 9.2d), cascade blue (Figures 9.3a through 9.3d), and calcein (Figures 9.4a through 9.4d). The pattern of staining observed on the surface of the skin was different for each donor solution used.

9.4.1. Observations of the Skin.

Sulforhodamine showed the formation of bright red fluorescent spots, randomly distributed on the surface of the skin, which were the LTRs (Figures 9.1a through 9.1d). These areas appeared within the first 1 to 10 pulses (Figures 9.1a and 9.2b), then grew larger with additional pulsing, although the

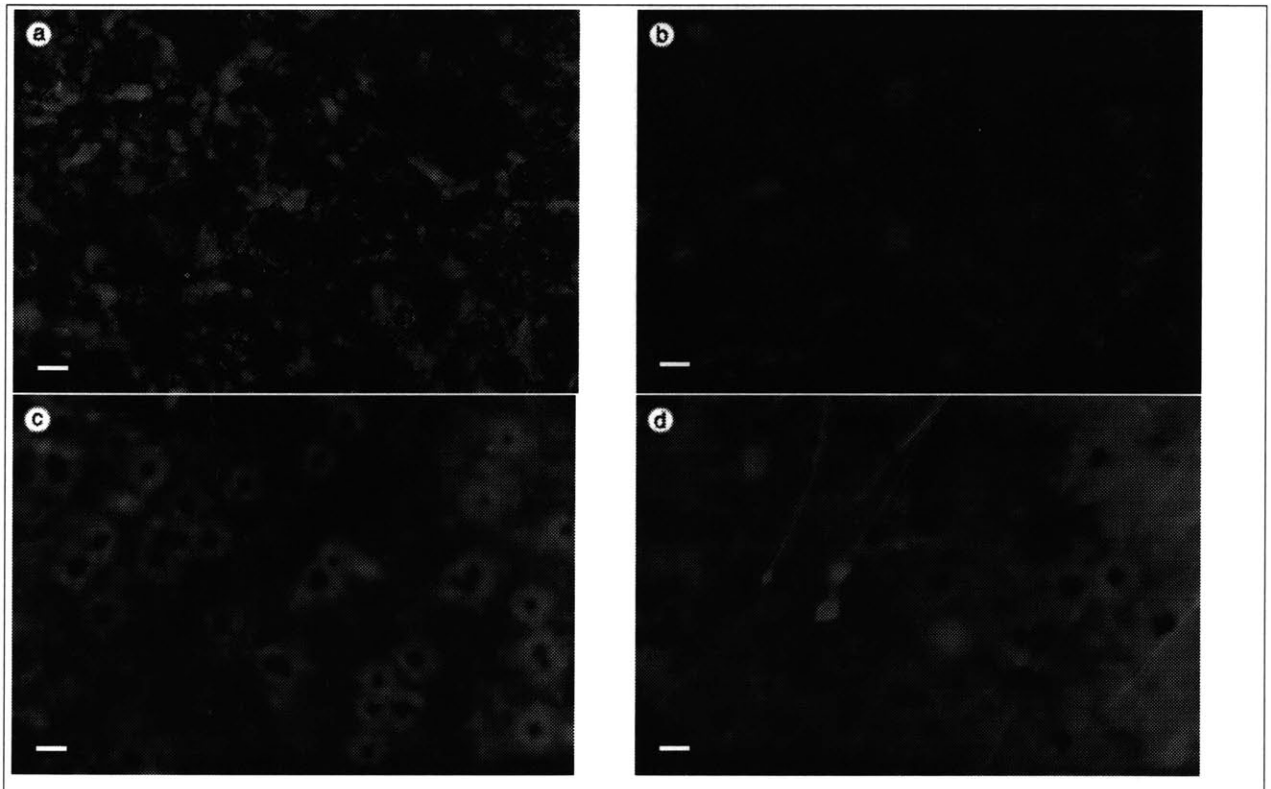

Figure 9.4. Time sequence of photomicrographs after pulsing with calcein. Scale bar = 50 μ. The number of pulses were: (a) 3 pulses, (b) 10 pulses, (c) 100 pulses, and (d) 680 pulses. Like the photomicrographs taken with lucifer yellow (see Figure 9.2), the LTRs after 1 h of pulsing appeared as dark centers surrounded by brightly fluorescent background staining of the skin. However, the LTR staining process appeared to be somewhat different than with lucifer yellow. With calcein, the centers of the LTRs initially appeared very bright (a and b), then darkened with additional pulsing, so that the LTRs appeared as "rings" (c). With additional pulsing, the "rings" enlarged and the fluorescence of the skin away from the LTRs increased, resulting in a more uniform staining pattern of the skin. However, the LTRs still remained dark.

number of spots on the surface of the skin did not appear to change significantly (Figures 9.1c and 9.1d). The behavior of these LTRs was consistent with the LTRs previously observed during pulsing with sulforhodamine (Pliquett, *et al.*, 1996 [b]).

In contrast, no readily identifiable brightly fluorescent regions were observed for lucifer yellow (Figures 9.2a through 9.2d). Instead, the entire skin appeared to be uniformly stained, with the exception of small, dark spots, randomly distributed on the surface of the skin, in the manner of the LTRs. Like the LTRs, these dark spots appeared to be randomly distributed, and not associated with the sweat ducts or hair follicles, which themselves were more brightly stained. The dark spots first become noticeable at around pulse 10, as the fluorescence intensity of the background increased (Figure 9.2b). The dark spots did not appear to grow in size or number with additional pulsing (Figures 9.2c and 9.2d). However, the dark spots themselves appeared to become more well-defined with additional pulsing. The background fluorescence of the skin also appeared to steadily brighten during the first half hour of pulsing (roughly 300 pulses), then leveled off with additional pulsing.

The staining of the skin with cascade blue was similar to that of lucifer yellow, except that no dark spots were observed (Figures 9.3a through 9.3d). The skin appeared to be uniformly stained. The background staining of cascade blue increased steadily with pulsing for the first half hour of pulsing (~300 pulses), then leveled off with additional pulsing (Figures 9.3c and 9.3d)

During pulsing with calcein, small, brightly green fluorescent spots formed on the surface of the skin, randomly distributed (Figure 9.4a). These spots appeared to enlarge with additional pulsing, in the manner of LTRs (Pliquett, *et al.*, 1996 [b]). However, the centers of the LTRs began to darken with additional pulsing, and by pulse 10, the centers of the LTRs appeared noticeably darker (Figure 9.4b). Meanwhile, the fluorescence of the skin, away from the LTRs, appeared to increase in intensity. By pulse 300, the skin appears to be covered by "rings" of fluorescence (Figure 9.4c). By pulse 680 (1 h of pulsing), the rings had spread out and the intensity of the skin away from the LTRs had increase enough so that the staining of the skin away from the LTRs appeared uniform, while the LTRs themselves appeared dark, similar to the results with lucifer yellow (Figure 9.4d).

9.4.2. Molecular Transport away from the LTRs.

These observations are in general agreement with other observations of LTRs (Zewert, *et al.*, 1995; Pliquett, *et al.*, 1996 [b]; Prausnitz, *et al.*, 1996 [a]; Chen, *et al.*, 1998 [b]; Vanbever, *et al.*, submitted). However, the staining of the skin observed with lucifer yellow and cascade blue appeared quite different than the staining of the skin previously observed with sulforhodamine and calcein (compare Figures 9.2 and 9.3 with Figures 9.1 and 9.4).

Lucifer yellow, cascade blue, and calcein all had shown significant staining of the skin, away from the LTRs. This observation has not been previously recorded in the literature. Measurements of the current through the skin during pulsing, however, have indicated that most of the ionic transport (electric current) appears to cross the skin through the LTRs (Pliquett, *et al.*, 1996 [b]). Thus, the driving force for the transport of fluorescent tracers into the skin, away from the LTRs, does not appear to be either electroosmosis (convection) or electrical drift, as these driving forces would follow the electric field lines through the skin at the LTRs. The driving force could be facilitated diffusion, if electroporation of the skin away from the LTRs is occurring, which would allow easier passage of these molecules into the skin away from the LTRs.

9.4.3. Centers of LTRs are Hydrophobic.

The centers of the LTRs appear to brightly stain with sulforhodamine, although with calcein and lucifer yellow, the centers of the LTRs stain poorly or not at all. Sulforhodamine can partition significantly into a lipophilic environment, unlike the other fluorescent tracers (see Section 4.2.1). Assuming that the LTRs form regardless of the fluorescent tracer present, then cascade blue appears to be able to stain both the LTRs and the non-LTR regions equally well, since no LTRs were ever directly observed with cascade blue.

In addition, Nile red, a lipophilic stainer, also brightly stains the LTR centers (Prausnitz, *et al.*, 1996 [a]; also see Section II.3), as do the polystyrene particles used in Chapter 5. The polystyrene particles, despite their high negative charge, in fact prefer hydrophobic environments over hydrophilic ones. Thus, the difficulty in cleaning them off of the glassware with only water; chloroform, an organic solvent, was necessary for cleaning (Section 5.5).

In conclusion, despite the molecular transport that occurs through the LTRs, the centers of the LTRs are probably very hydrophobic in nature.

9.5 Extraction of Compounds from the Skin after Pulsing.

The goal of these experiments was to determine how much material was transported into (not through) the stratum corneum during high-voltage pulsing. After applying a certain number of pulses to the skin with a fluorescent tracer as the donor, pulsing was stopped and the donor solution was replaced by fresh PBS (no fluorescent tracer). Pulsing was then started to extract the tracers still present within the skin.

There are two important confounding factors in these experiments. First, not all of the material can be extracted out of the skin simply by applying additional pulsing. Photomicrographs of the skin taken after lengthy extraction experiments (>2 h of additional pulsing) were identical to those where no extraction pulsing had been applied. The skin in both cases remained brightly fluorescent compared to the passive controls. Thus, a large amount of material still remained bound to the skin (either specifically or non-specifically), even after much additional extraction pulsing.

The second confounding factor is the epidermis. These experiments were conducted with the epidermis present, even though the epidermis is roughly 5× thicker than the stratum corneum and can also bind fluorescent compounds. Thus, even if the extraction of compounds from the stratum corneum took place, the compounds might become remain trapped within the epidermis instead. Alternatively, some extraction of materials from the epidermis instead of the stratum corneum may be occurring in these experiments.

9.5.1. Extraction Results.

The amount of material extracted versus the number of pulses applied to initially "load" the skin with fluorescent tracer is shown in Figure 9.5 (9.5a, sulforhodamine; 9.5b, lucifer yellow; 9.5c, cascade blue; and 9.5d, calcein). Most of these experiments were conducted with lucifer yellow, although a few experiments were conducted with the other fluorescent molecules for comparison purposes.

In general, the amount of material extracted from the skin was proportional to the number of pulses required to load the skin. There was a significant amount of sulforhodamine extracted from the skin. There was some loading of lucifer yellow and calcein, although not nearly as much as sulforhodamine. There was no measurable extraction of the skin with cascade blue.

9.5.2. Loading of the Epidermis, not only of the Stratum Corneum.

Assuming that the entire stratum corneum was completely filled with only donor solution (with an area of 0.64 cm^2, thickness of 10 μ, donor solution concentration of 1 m<u>M</u>), the maximum amount that could be extracted from the stratum corneum would be 0.64 nmol. The amount of material actually extracted from the skin was much larger, 1 to 50 nmol, indicating that loading within the epidermis may be playing an important role in these experiments.

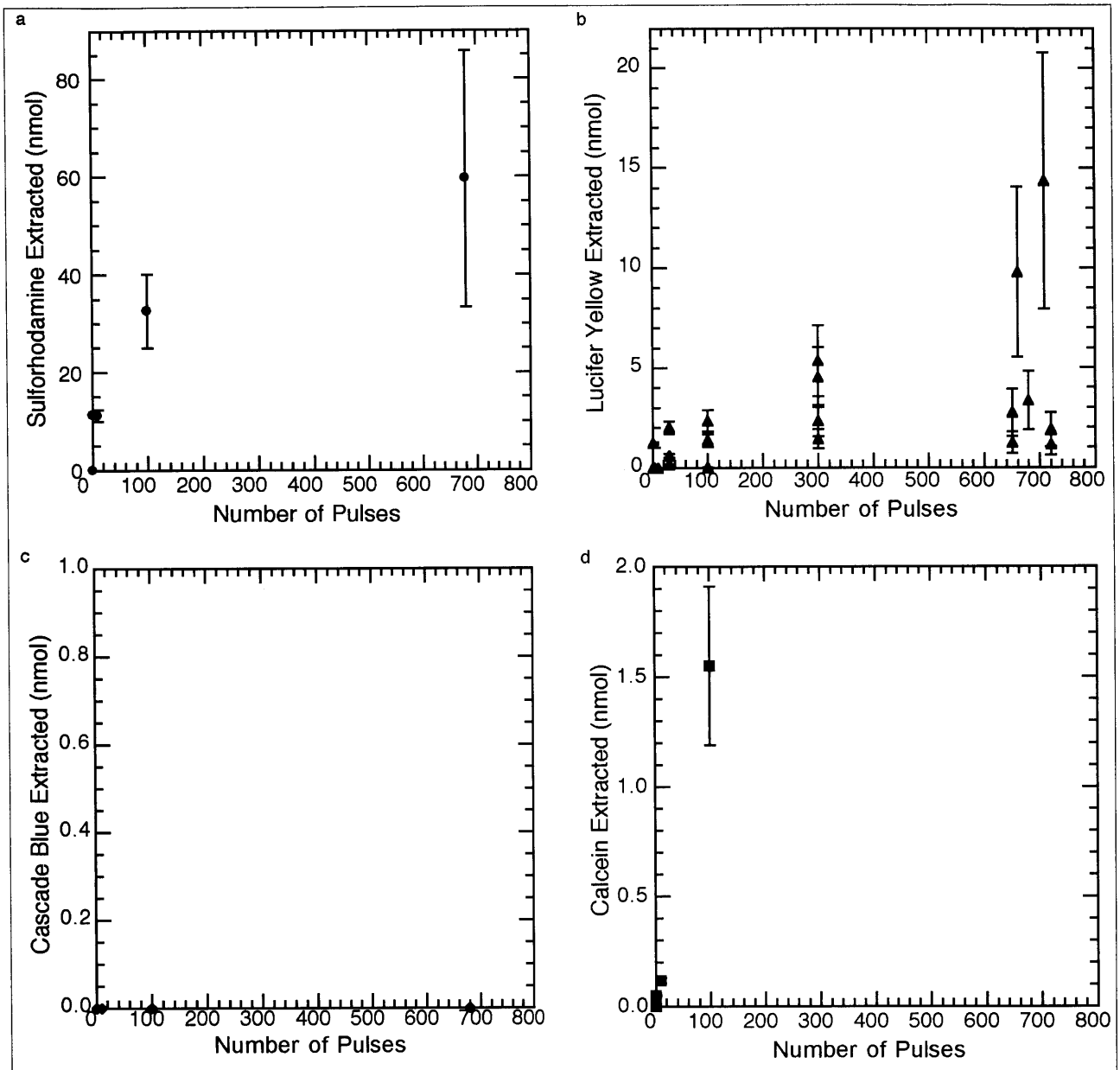

Figure 9.5. Extraction of fluorescent compounds from the skin after high-voltage pulsing. A given number of pulses were applied to the skin, with a fluorescent tracer as the donor. Afterwards, the donor compartment was flushed out with fresh PBS, and additional pulsing was applied to extract the materials trapped in the skin (the "reservoir" effect). In general, more pulses caused higher loadings. (a) Sulforhodamine showed the most loading. (b) Lucifer yellow showed some loading, although not as much as sulforhodamine. (c) Cascade showed no significant loading. (d) Calcein showed some loading for the conditions used.

Including the epidermis in this calculation (with a thickness of 100 μ), and assuming that the entire epidermis is filled with only donor solution (with a concentration of 1 mM), the maximum amount that could be extracted from the epidermis would be 6.4 nmol. This is consistent with the observed extractions for lucifer yellow and calcein, indicating that the epidermis has also been loaded with donor solution to some extent.

However, the amount of sulforhodamine extracted from the skin was nearly an order of magnitude larger (up to 50 nmol) than the maximum amount of sulforhodamine which could be loaded into the skin, based on this calculation. It is unclear why this much sulforhodamine was extracted from the skin; one possible explanation is that sulforhodamine somehow is concentrated into the lipid regions of the skin during pulsing, or strongly binds to the skin during transport.

9.5.3. Need for Further Experiments.

Given the limited number of experiments shown in Figures 9.5a through 9.5d, and the inconsistency between the amount of material actually extracted from the skin and the maximum amount that was estimated to be present, more experiments will undoubtedly be needed to understand these results. However, it appears that both the hydrophobicity of the molecule being transported, and the number of pulses applied are important factors in the loading of the skin. Other factors, such as the time constant or the inter-pulse spacing, should also be examined.

9.6. Electrical Impedances.

Rapid measurements of the impedance of the skin (time resolution of ~200 ms) were taken during the entire course of the experiment, including the 1 h passive control/skin hydration period. The impedance measurements were taken at a frequency of 100 Hz, using a bipolar sine wave with a peak-to-peak voltage of 0.1 V. Other experiments have shown a good correlation between the DC resistance of the skin, and the 100 Hz impedance (Gowrishankar, personal communication).

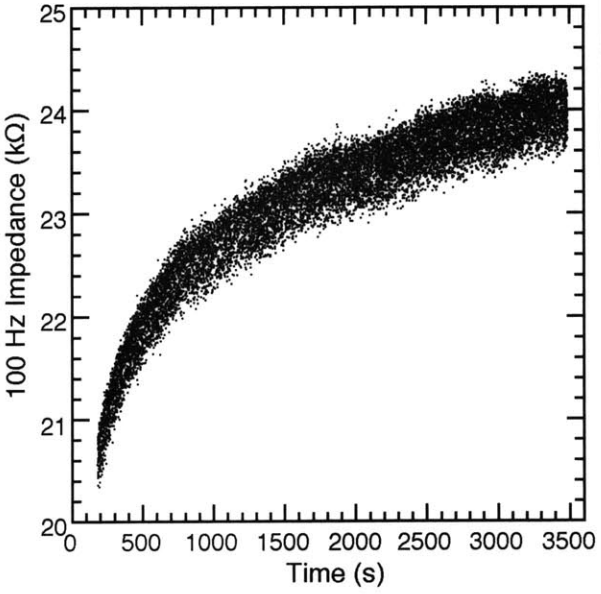

Figure 9.6. Passive 100 Hz impedance measurements of the skin during the 1 h passive control. The impedance of the skin in this particular case rose from ~21 kΩ to ~24 kΩ in 1 h.

9.6.1. Passive Impedances.

The 100 Hz impedance measurements of the skin during the initial 1 h hydration period typically show a rise in the impedance. A representative experiment is shown in Figure 9.6, where the

impedance of the skin was initially measured to be ~20 kΩ. After 1 h, the impedance of the skin had risen to ~24 kΩ.

This experiment was performed many times (~70 total), and rises in the impedance of the skin during the 1 h passive control period were observed in nearly all of these experiments, usually with increases of ~5 to ~20 kΩ.

It is unclear why the impedance (or the resistance) of the skin should increase as the skin becomes hydrated with PBS in that first hour. The addition of PBS (a highly conductive substance) to the skin should cause the impedance to drop, not increase. One possible explanation for the consistent increase in the impedance of the skin may be that the skin is already filled with water and ions, at a much higher concentration than in PBS (150 mM). Thus, hydration and equalization of the skin with the outside PBS solution would cause a net flux of ions out of the skin, with correspondingly higher impedance measurements.

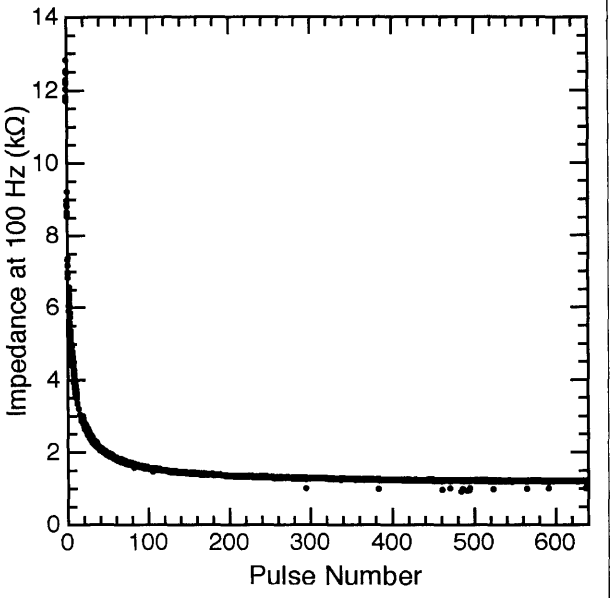

Figure 9.7. Impedance measurements at 100 Hz of the skin during pulsing. The impedance initially drops very quickly, then continues to decrease more slowly with additional pulsing. Pulses in the above experiment were given once every 5 s. The first 10 pulses from the above experiment can be seen in Figure 9.8.

9.6.2. *Impedances during Pulsing.*

The impedance of the skin quickly drops after the first few pulses, then continues to drop more slowly with additional pulsing (Figure 9.7). This is consistent with the skin electroporation hypothesis, where most of the aqueous pathways across the skin are initially formed in the first few pulses (Prausnitz, *et al.*, 1993 [a]; Chizmadzhev, *et al.*, 1995; Chizmadzhev, *et al.*, 1998 [a]). Additional pulses serve to keep these pathways open, and occasionally add new pathways as well, but at a much slower rate, thus the continuing drop in the

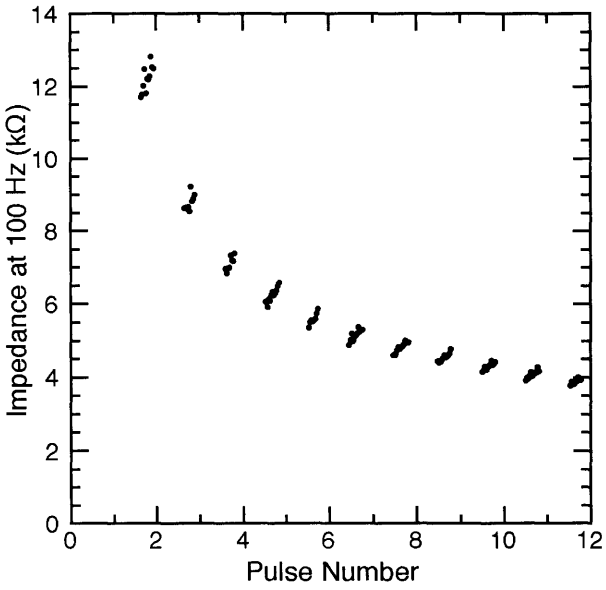

Figure 9.8. Impedance measurements at 100 Hz of the first 10 pulses. Impedance measurements were taken every ~200 ms, and pulses were applied to the skin every ~5 s. During high-voltage pulsing, the impedance meter was disconnected from the circuit, causing the gaps in the impedance measurements. After each pulse, the impedance of the skin started to rise, indicating that some recovery was taking place. However, the impedance of the skin after the pulse was lower than before. This trend continued throughout the entire experiment, as can be seen in Figure 9.7.

impedance of the skin with repeated pulsing.

An enlargement of the impedance measurements of the skin between the first several pulses can be seen in Figure 9.8. The gaps in the data were those regions where the impedance meter was disconnected from the chamber by the electromechanical relay, while the high-voltage pulse was being applied to the skin.

Between each of the pulses, the impedance of the skin begins to rise, indicating that some recovery (i. e., closing of the aqueous pathways) is occurring. However, the impedance of the skin after each pulse was lower than the pulse before it. This trend continued throughout the entire experiment.

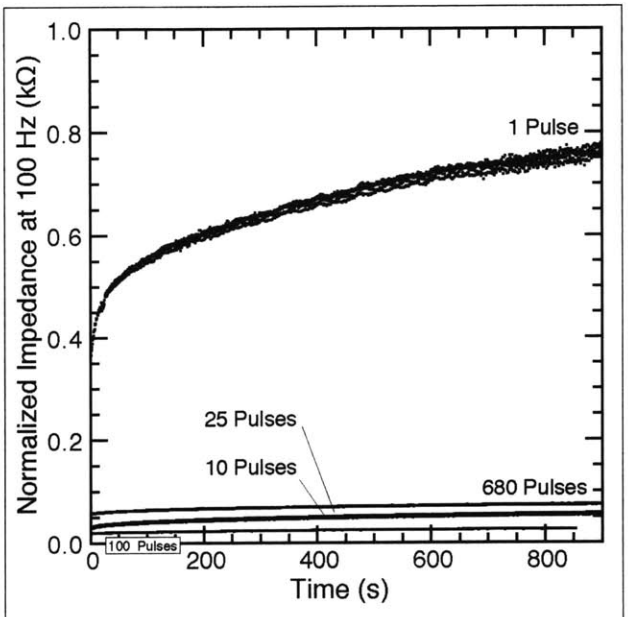

Figure 9.9. Normalized recovery of the impedance of the skin after pulsing. The impedance measurements have been normalized to pre-pulse values. The applied voltage was 1000 V, corresponding to a transdermal voltage of ~100 V (see Section 8.2.1). After one pulse, there was some recovery, to ~77%. However, after just 10 pulses, there was only poor recovery of the impedance of the skin.

The rise in the impedance of the skin continues after pulsing has stopped. Figure 9.9 shows the impedance of the skin after pulsing was stopped for 1, 10, 25, 100, and 640 pulses (normalized to the impedance of the skin before pulsing was started). In every case, the impedance of the skin increased after pulsing had been stopped, indicating that some recovery of the skin was taking place. However, the impedance did not rise to pre-pulsing levels.

The recovery of impedance of the skin appears to become increasingly difficult with additional pulsing. The impedance after 1 pulse recovers to ~77% of its pre-pulsing value, yet after 10 pulses, the impedance only recovers to ~5% of its pre-pulsing value. Thus, high-voltage pulsing appears to cause some irreversible changes in the structure of the skin, which accumulate with additional pulsing.

9.7. Course of a Typical Skin Electroporation Experiment.

The summation of all of the available data (transdermal voltage from Figure 8.5, molecular flux from Figure 8.4b, inter-pulse skin impedance from Figure 9.8, loading within the skin from Figure 9.5a, and LTR formation from Figure 9.2) for a typical experiment involving lucifer yellow as the donor is shown in Figure 9.10. The data are presented in this way to allow a side-by-side summary of the typical events that occur during skin electroporation.

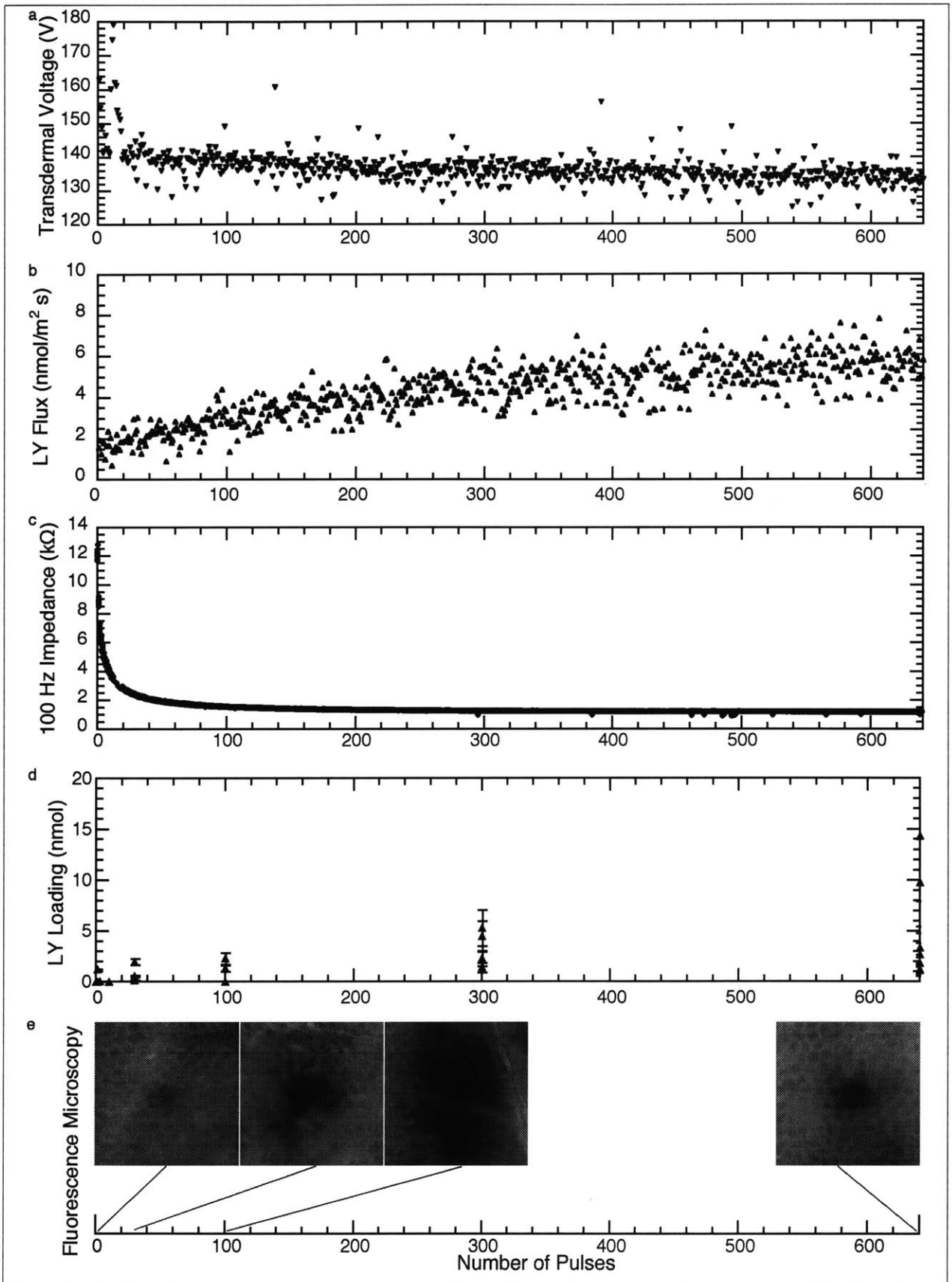

Figure 9.10. Skin electroporation parameters, measured in real time, during a typical experiment with lucifer yellow.

Many changes occur within the first few pulses. Significant transdermal fluxes can be measured after roughly 5 to 10 pulses. Loading of the donor within the skin is also significant during the first few pulses, which is consistent with the amount of molecular flux observed through the skin in the first few pulses; loading into the skin and transport through the skin should both be occurring simultaneously during high-voltage pulsing. The formation of LTRs on the surface of the skin can also be seen.

The peak transdermal voltage during pulsing drops significantly. The impedance of the skin during the first few pulses also drops quickly, going from a reversible regime to a less reversible one.

Even with many pulses, the system does not quite reach quasi-steady state. The peak transdermal voltages and the impedance of the skin continue to drop with continued pulsing, although much more slowly than in the first few pulses. In some cases the molecular flux reaches steady state (lucifer yellow, cascade blue), although in other cases it does not (sulforhodamine, calcein). Very few LTRs continue to form on the surface of the skin, although molecular transport through the skin away from the LTRs may also be significant.

Thus, to control transdermal transport for drug delivery purposes, the events that occur during skin electroporation must first be understood. Many things can happen within the first few pulses, and measurement of these parameters is necessary before control can be achieved.

10. Real-Time Iontophoresis of the Skin.

Although most of this thesis has dealt with the topic of skin electroporation, enough experiments have been conducted using iontophoresis (primarily as positive controls during the skin electroporation experiments) to warrant a separate discussion of skin iontophoresis.

Iontophoresis is the application of a small, usually constant DC current to the skin, which is commonly used to transport drugs and other molecules across the skin (Tyle, 1986; Banga and Chien, 1988; Burnette, 1989; Chien and Banga, 1989; Singh and Roberts, 1989; Cullander and Guy, 1992; Amsden and Goosen, 1995; Guy, 1996). Typically, currents are kept $<0.5\ mA / cm^2$, as higher currents stimulate nerves within the skin, causing irritation or pain (Banga and Chien, 1988; Burnette and Ongpipattanakul, 1988; Ledger, 1992). During iontophoresis, the resistance of the skin drops by an order of magnitude, to $\sim 10\ k\Omega\ cm^2$. This corresponds to a voltage drop across the skin of <5 V, which is not enough for electroporation to occur (Chizmadzhev, *et al.*, 1998 [a]).

Without a means to produce new transport pathways, molecular transport during iontophoresis occurs primarily through the pre-existing pathways across the skin, which are the sweat ducts and hair follicles (collectively called the "appendages" of the skin) (Abramson and Gorin, 1940; Abramson and Engel, 1942; Grimnes, 1984; Burnette and Marrero, 1986; Burnette and Ongpipattanakul, 1988; Cullander and Guy, 1991; Scott, *et al.*, 1993; Chen, *et al.*, 1998 [b]; Chen, *et al.*, in press [b]; also see Chapter 7, which discusses experiments involving the iontophoresis of human skin and shed black rat snake skin, a model of human skin which lacks hair follicles and sweat ducts).

10.1. Theory.

The driving force for molecular transport during iontophoresis is believed to be primarily through electrophoresis (sometimes called electrical drift), as governed by the Nernst-Planck equation:

$$J_i = -D_i \frac{\partial C_i}{\partial x} + \frac{z_i \mathcal{F} C_i}{\mathcal{R} T} \frac{\partial E}{\partial x}, \tag{10.1}$$

where $\mathcal{F}$ is the Faraday (96 484 C/mol), $\mathcal{R}$ is the molar gas constant (8.3144 J/mol K), T is the absolute temperature, E is the electric field, and x is the distance across the skin. For a species i, J_i is the molecular flux through the skin, D_i is the diffusion coefficient, C_i is the concentration, and z_i is the charge. The first term in the equation represents passive diffusion, and the second term represents electrophoresis.

However, the skin is a charged membrane, and some molecular transport may also be occurring via electroosmosis (Burnette, 1989; Singh and Maibach, 1996). Thus, a convective term can be added to the Nernst-Plank equation to account for electroosmosis:

$$J_i = -D_i \frac{\partial C_i}{\partial x} + \frac{z_i \mathcal{F} C_i}{\mathcal{R} T} \frac{\partial E}{\partial x} + u_b C_i, \tag{10.2}$$

where u_b represents the bulk velocity (in units of [length/time]) or solvent flow across the skin. During iontophoresis, bulk fluid flow will occur from the negative electrode to the positive electrode, since the skin is negatively charged (Singh and Maibach, 1996). An important application of this phenomenon is the transport of glucose out of the skin by iontophoresis, sometimes called "reverse iontophoresis."

With the development of an *in vitro* flow-through system that was able to measure molecular fluxes across the skin with a time resolution of ~14 s (Chen, *et al.*, in press [a]; see Section 8.1.3 and Appendix IV), and the availability of four hydrophilic, similarly charged fluorescent molecules, differing primarily in charge (calcein, cascade blue, lucifer yellow, and sulforhodamine) (see Chapter 4), a controlled study of the molecular transport during iontophoresis as a function of the molecular charge could be performed. The applied current was the same in each case, 1.0 mA / cm^2, chosen since it represented the maximum limit of what could be applied to human skin. The electrodes were encased in polyacrylamide gel and protected by a stream of PBS, so that any chemical by-products or pH changes produced by the electrodes would not react with the skin, or the donor and receptor compartments.

10.2. Materials and Methods.

The flow-through experimental apparatus used for iontophoresis was generally the same as the one that was used for the skin electroporation flow-through studies (see Appendix IV), with a few minor changes. Instead of a high-voltage pulser, a custom-built, constant current device was used that produced a steady current of 1.0 mA / cm^2 (0.64 mA total) (Prausnitz, *et al.*, 1993 [a]; U. Pliquett, personal communication). Transdermal voltages were not recorded during the experiments.

10.2.1. Skin Preparation.

Human cadaver skin was prepared by the heat-stripping method, described in Appendix I. Briefly, stored cadaver skin at -80 °C (Gummer, 1989) was thawed to room temperature and submerged in de-ionized water for 2 min at 60 °C. The epidermis (with the stratum corneum) was gently scraped off the dermis, cut into 3/4 inch diameter circles, and stored at 4 °C, 95% humidity for up to 10 d (Gummer, 1989).

10.2.2. Permeation Chamber with Four-Electrode System.

Phosphate-buffered saline (PBS) was prepared as described in Section 3.2. The donor solution consisted of a fluorescent tracer (one of either sulforhodamine, lucifer yellow, cascade blue, or calcein), dissolved in PBS to a concentration of 1 mM. The solution was gently stirred for >30 min (Nutator, Clay Adams, Becton Dickinson), to allow the tracer time to dissolve.

The flow-through system with the four-electrode design is described in more detail in Appendix IV. Briefly, the permeation chambers were specially designed, side-by-side chambers, with a skin exposure area of 0.64 cm^2 (circular opening, 0.9 cm in diameter) (Crown Bio Scientific) (Friend, 1992). The chamber consisted of an outer water jacket and an inner compartment. To keep the skin and the donor and receptor solutions constant at 37 °C, water heated by a thermostated water bath (Neslab) was continually pumped through both outer jackets.

The flow-protected electrodes were constructed by soldering a piece of 0.040 inch diameter silver wire, ~0.5 cm long, to copper bell wire. The solder and exposed wire were covered by nonconducting silicone rubber (General Electric), so that only the silver wire was exposed. A piece of Tygon tubing, 1/32 inch ID, and the electrode were inserted through a truncated 200 µl pipette tip. The top of the pipette was sealed off with epoxy (Devcon).

A ~2 inch long piece of Teflon tubing, 1/16 inch ID, was used for outflow and a longer piece of Tygon tubing, 1/32 inch ID, was used for inflow in the receptor compartment flow-through assembly. The two tubes were inserted through a truncated 1 ml pipette tip. A hole was drilled into the side of the pipette tip and the Teflon tube was extended out through the hole. All of the tubes and wires were sealed in place with epoxy.

The top of a 2 ml centrifuge tube was removed and two holes were drilled into the tube: one in the bottom and one in the side. Tygon tubing, 1/32 inch ID, was epoxied to the bottom hole. The Teflon tube from the pipette was extended through the side hole. The centrifuge tube was held in place to the side of the pipette with Parafilm (American National Can).

Before each experiment, plastic tubes were inserted through both compartments and sealed in place with Parafilm. In the receptor compartment, the flow-through assembly was inserted and sealed in place with Parafilm. The tubing within the receptor chamber was wired in place for the gel with stainless steel wire. Both compartments was turned sideways, and polyacrylamide solution was poured in, completely immersing everything, leaving empty a volume of ~2.1 ml for the donor compartment and ~450 µl for the receptor compartment. The polyacrylamide solution was composed of 0.75 g of 19:1 acrylamide:bis(N,N'-methylene-bis-acrylamide) powder (Bio-Rad), 43.75 µl of 440 m$\underline{M}$ $(NH_4)_2S_2O_8$ solution, and 3 µl of N,N,N',N'-tetramethylethylenediamine (Bio-Rad) in 5 ml of PBS.

The polyacrylamide solution was allowed to harden (~10 min). After the solution solidified, the outer plastic tubing and the Parafilm were removed from the outer ports, leaving behind an empty channel through the gel. The flow-protected electrodes were inserted into this channel. During an experiment, PBS was pumped through each outer channel at a flowrate of ~6 ml/min, using two peristaltic pumps (VWR). The stainless steel wire was removed from the receptor compartment, since the tubing in the receptor compartment was now immobilized in place by the gel.

10.2.3. Fluorescence Measurements.

Fluorescence measurements were taken with a spectrofluorimeter (Fluorescence Master Series Spectrometer, Photon Technology). Excitation and emission wavelengths for each compound are given in Table 4.1.

The cuvette in the spectrofluorimeter was constructed by drilling two holes into a polystyrene microcuvette (VWR), to allow for inflow and outflow. One hole was drilled approximately 1/4 inch from the bottom of the cuvette for the outflow, and the other hole drilled higher in the cuvette (approximately 1/2 inch from the bottom) for the inflow. Both holes were connected with Tygon tubing to a peristaltic pump ("Sarah" Cassette Peristaltic Pump, Barnant).

The final volume of the cuvette was ~200 µl, which was the minimum amount needed by the spectrofluorimeter for accurate detection and quantification of tracer concentration within the cuvette. Mixing within the cuvette was accomplished by dripping fluid into the cuvette. The performance of this system was modeled as an idealized continuous-stirred tank reactor (Fogler, 1992), and the residence time for the combined chamber-tubing-pump-cuvette system (volume of ~400 µl) was ~14 s.

10.2.4. Electrical Equipment.

A custom-built, constant current device was used that produced a steady current of 1.0 mA / cm^2 (0.64 mA total) (Prausnitz, *et al.*, 1993 [a]; U. Pliquett, personal communication). Since the fluorescent tracers were negatively charged, the negative terminal of the pulser was connected to the pulsing electrode in the donor compartment, and the positive terminal to the receptor compartment, to provide a favorable driving force (Figure 10.1). The current was monitored during the experiment by measuring the voltage drop across a 1.2 Ω resistor, placed in series with the chamber.

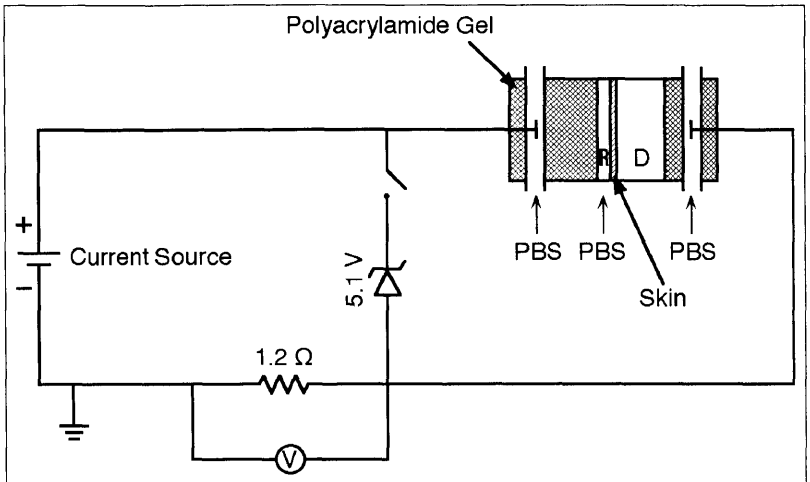

Figure 10.1. Iontophoresis circuit. Before the current source is activated, the switch next to the Zener diode initially is closed. After activating the current source, the switch is opened. This arrangement prevents any electrical transients caused by the activation of the current source from reaching the skin. Measuring the voltage drop across a 1.2 Ω resistor placed in series with the skin gives the current across the skin during the experiment.

The 5.1 V Zener diode, placed in parallel with the chamber, was used to prevent electrical transients from occurring across the skin (which could inadvertently cause electroporation to occur) when the constant current source was first activated. The switch was closed before turning on the constant current source, then opened afterwards.

10.2.5. Skin Protocol.

Prepared, stored skin was first floated in PBS for ~1 min to remove the wax paper backing. The skin was then loaded into the permeation chamber, with the stratum corneum facing the donor compartment. The donor compartment was filled with donor solution and the flow-through pumps started. The donor compartment was constantly stirred with a magnetic stir bar (Thermix Stirring Hot Plate Model 210T, Fischer Scientific; Spinbar, VWR).

The condition of the skin was checked by measuring its electrical impedance. A 100 Hz, 0.1 V bipolar sine wave (peak-to-peak) was applied across the skin and the resulting impedance measured using an LCR meter (Model 5R715 LCR Meter, Stanford Research Systems). Skin was considered bad and immediately discarded if its electrical resistance was <50 kΩ cm^2 (or <70 kΩ for this particular apparatus) (Prausnitz, *et al.*, 1993 [a]; M. R. Prausnitz, personal communication). For this apparatus,

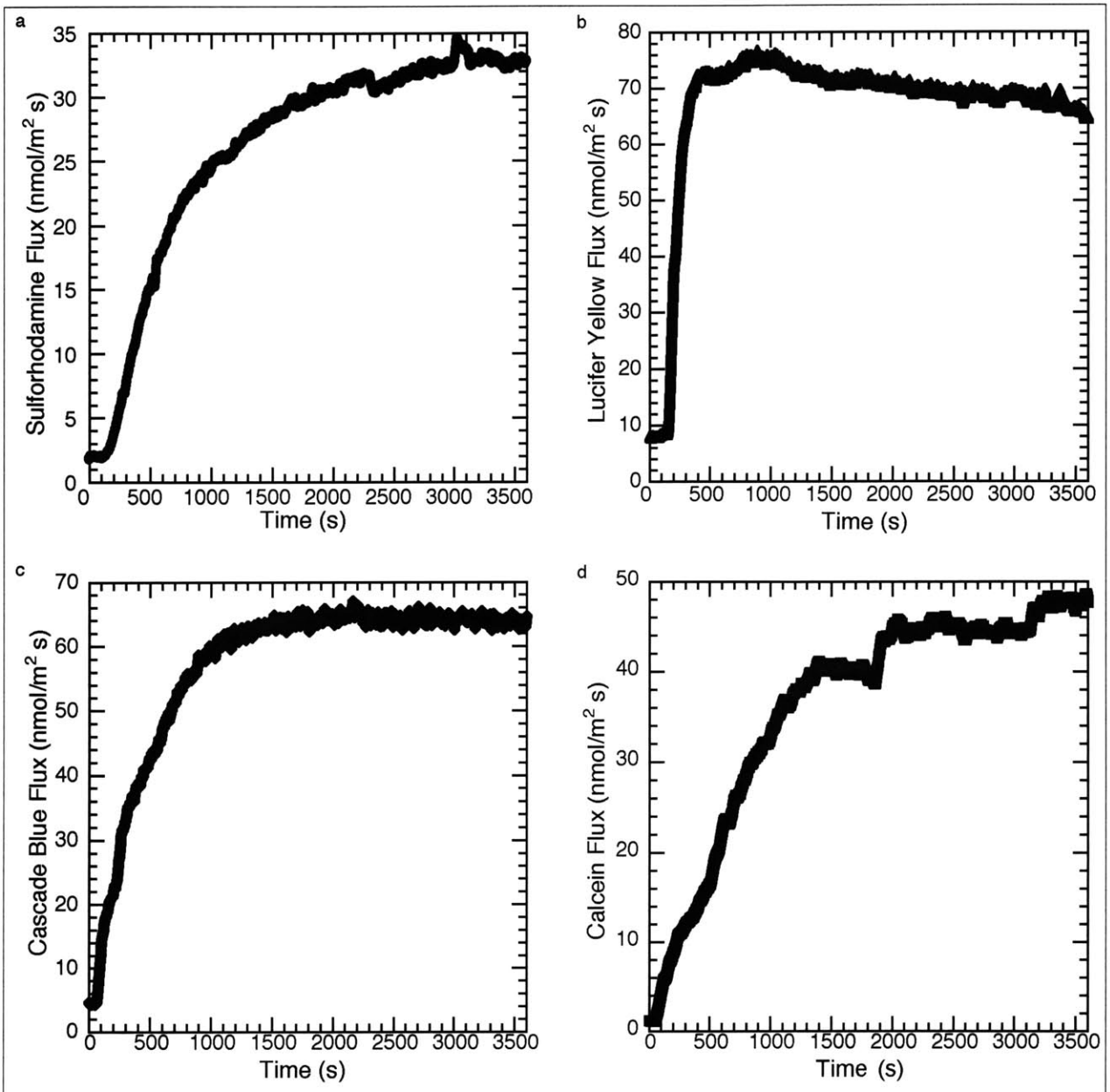

Figure 10.2. Real-time molecular fluxes of four fluorescent compounds during iontophoresis. A current of 1.0 mA / cm^2 was applied to the skin for 1 h. Typical experiments are shown. Error bars have been removed for clarity. Donor molecules used were (a) sulforhodamine, (b) lucifer yellow, (c) cascade, and (d) calcein. For all four fluorescent molecules, a rapid rise to near-steady state was observed in under 1 h. This behavior was different than skin electroporation, where the molecular flux often did not reach steady states (compare with Figure 8.8, where the same four fluorescent molecules were used under skin electroporation).

however, the impedance of the skin, not its resistance, was measured. Since the impedance of the skin decreases as the applied frequency increases, a value of <25 kΩ cm^2 of impedance at a frequency of 100 Hz (or <40 kΩ for this apparatus) was used as an indicator of bad skin. Previous experiments have shown that this value compares favorably with the accepted DC resistance of <50 kΩ cm^2 (Gowrishankar, personal communication).

The resistances and impedances of the PBS and the polyacrylamide gel were neglected, since their combined resistances were previously measured to be 251 Ω (see Section 3.6), compared to ~40 kΩ for the skin.

Next, the apparatus was allowed to sit for 1 h to fully hydrate the skin (Prausnitz, *et al.*, 1993 [a]) and check for leaks. Leaky skin (passive flux above the detection limit, $\sim 10^{-8}$ M, or $\sim 10^{-10}$ mol / m^2 s for this particular experimental apparatus), was discarded.

10.2.6. Iontophoresis Protocol.

Iontophoresis at 1.0 mA / cm^2 was applied for 1 h. PBS was pumped through the flow-protection system at ~6 ml/min using a peristaltic pump (VWR). PBS was also pumped through the flow-through system (through the receptor compartment and the spectrofluorimeter) at 0.0322 ml/s. The spectrofluorimeter was set to record ~1 h of data.

10.3. Iontophoresis Reaches Steady State within an Hour.

Unlike similar skin electroporation studies, with iontophoresis, steady-state molecular fluxes (or very nearly so) were achieved rapidly for all four fluorescence tracers, usually <1 h (Figures 10.2a, sulforhodamine; 10.2b, lucifer yellow, 10.2c, cascade blue; and 10.2d, calcein). Sulforhodamine (Figure 10.2a) and lucifer yellow (Figure 10.2b) did not quite reach steady state in 1 h, although they were more nearly so than comparable results obtained during skin electroporation (compare Figure 10.2a with Figure 8.4a and Figure 10.2b with Figure 8.4b). In addition, although neither protocol had been optimized, the molecular fluxes observed during iontophoresis compared favorably with the fluxes observed during skin electroporation.

In Figure 10.3, the steady-state molecular fluxes are plotted versus the molecular charge, where the molecular weight was kept approximately

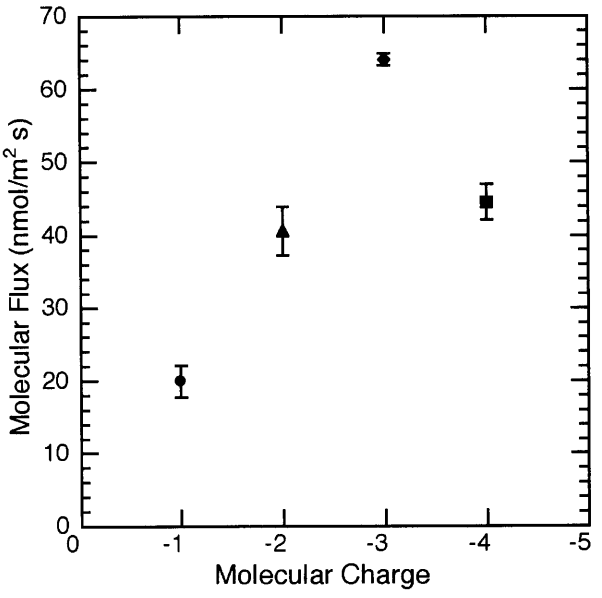

Figure 10.3. Molecular flux is proportional to change. In the above figure, sulforhodamine has a charge of -1, lucifer yellow is -2, cascade blue is -3, and calcein is -4. Although very few skin iontophoresis experiments were conducted (totally, only 8 flow-through experiments were performed), there still appeared to be a strong relationship between the charge of the donor molecule and the resulting molecular flux across the skin. This suggests that during iontophoresis, the predominant driving force is electrical drift, not electroosmosis or diffusion.

constant (~600 Da). There appears to be a reasonably good relationship between the molecular charge and the measured transdermal flux, in agreement with the Nernst-Planck equation (Equation 10.1).

Greater molecular fluxes were seen with the more highly charged species, which indicated that electrical drift appears to be a primary driving force. If electroosmosis (the convective term) was the primary driving force, then similar molecular fluxes would be observed for all four species, without this charge dependence. Thus, for the four species studied, it appears that electrical drift is the dominant transport mechanism.

10.4. Conclusions.

The main drawback in the use of iontophoresis is that larger currents, which would cause greater molecular transport under the Nernst-Planck equation (Equation 10.1), cannot be used since they could cause stimulation of the nerves within the skin (Banga and Chien, 1988; Burnette and Ongpipattanakul, 1988; Ledger, 1992). The electrical exposure of the skin (the voltage times the duration) during iontophoresis would typically be $\sim 1.8 \times 10^4$ V s (1 mA / cm^2 of current results in a voltage of about ~5 V_{skin}, applied for 1 h), whereas for electroporation the exposure would typically be ~64 V s (100 V pulse, 1 ms time constant, 640 pulses per h).

More experiments would obviously be needed to better understand the relationship between the charge of the donor molecule and its resultant molecular flux across the skin. As this was not the purpose of this thesis, only a limited subset of experiments were actually conducted under iontophoretic conditions. However, from these experiments, it does appear to be much easier to predict the molecular fluxes and the transport properties (see Section 7.3.3) during iontophoresis of the skin than during electroporation.

11. High-Voltage Pulsing Over Many Pulses.

The application of 1 mA / cm^2 iontophoresis to human cadaver skin *in vitro* resulted in steady-state molecular fluxes of small, hydrophilic fluorescent compounds in <1 h (see Figures 10.2a through 10.2d). Steady-state transdermal fluxes during iontophoresis (steady DC current) would be expected, given the constant applied driving force (electrical drift), as discussed in Section 10.1.

However, when a series of short (~1 ms), high-voltage pulses (~100 V_{skin}) are applied to the skin, causing electroporation in the skin, molecular fluxes across the skin of the same fluorescent compounds in many cases did not reach steady state within 1 h (see Figures 8.4a through 8.4d). However, the driving force across the skin should not be changing significantly in time, after the first ~20 pulses (see Figures 8.5 and 11.1). After the initial drop, the transdermal voltage does not change rapidly in time, presumably because the voltage drop across the skin is insufficient to create new aqueous pathways. Thus, the electrical driving forces experienced by the donor molecules should not be varying widely during these experiments (although there will still continue to be some decreases, as shown in Figures 8.5 and 11.1).

The purpose of this investigation was to determine when quasi-steady state molecular fluxes were reached during skin electroporation, using the same four compounds previously found to reach steady state during iontophoresis (Figures 10.2a through 10.2d). Knowing when steady state was reached and the molecular flux at steady state would be important observations in constructing a theory of molecular transport during skin electroporation.

11.1. Materials and Methods.

The flow-through system for measuring the contents of the receptor compartment is more fully discussed in Appendix IV. In these experiments, 1 mM of a fluorescent tracer (either sulforhodamine, lucifer yellow, cascade blue, or calcein; see Chapter 4) in PBS was used as the donor solution. During pulsing, PBS flow-protection was used around the pulsing electrodes. Data stored in real time from the spectrofluorimeter (flux measurements) and the oscilloscope (voltage measurements) were calibrated and processed to give information about the conditions of the experiment.

11.1.1. Skin Preparation.

Human cadaver skin was prepared by the heat-stripping method, described in Appendix I. Briefly, stored cadaver skin at -80 °C (Gummer, 1989) was thawed to room temperature. It was then submerged for 2 min in de-ionized water at 60 °C. The epidermis (including the stratum corneum) was gently scraped off of the dermis, cut into 3/4 inch diameter circles, and stored at 4 °C, 95% humidity for up to 10 d (Gummer, 1989). The epidermis was used in all of the experiments described here.

11.1.2. Permeation Chamber with Four-Electrode System.

Phosphate-buffered saline (PBS) was prepared using the method described in Section 3.2. PBS was used as the receptor solution in the permeation chamber. The donor solution consisted of a fluorescent tracer (either sulforhodamine, lucifer yellow, cascade blue, or calcein), dissolved in PBS to a concentration of 1 mM. The flow-through system is described more fully in Appendix IV.

The permeation chambers were custom-designed, side-by-side chambers, with a skin exposure area of 0.64 cm^2 (circular opening, 0.9 cm in diameter) (Crown Bio Scientific) (Friend, 1992). Each chamber half had one large port near the skin and two small ports away from the skin. The chamber was heated to 37 °C with a water bath.

The donor compartment measuring electrode was constructed by soldering a piece of silver wire to bell wire. The solder and wire were covered by nonconducting silicone rubber, so that only the silver wire was exposed. The wire was inserted through a truncated 1 ml pipette tip and sealed in place with epoxy.

The receptor compartment electrode was constructed by soldering a piece of silver wire to bell wire. The solder and wire were covered by nonconducting silicone rubber, so that only the silver wire was exposed. A piece of Teflon tubing was used for outflow and a longer piece of Tygon tubing was used for inflow. A hole was drilled into the side of the 1 ml pipette tip and the Teflon tube was extended out through the hole. All of the tubes and wires were sealed in place with epoxy.

The flow-protected electrodes were constructed by soldering a piece of silver wire to bell wire. The solder and wire were covered by nonconducting silicone rubber, so that only the silver wire was exposed. A piece of Tygon tubing and the electrode were inserted through a truncated 200 µl pipette tip. The top of the pipette was sealed off with epoxy.

The top of a 2 ml centrifuge tube was removed and two holes were drilled into the tube: one in the bottom and one in the side. Tygon tubing was epoxied to the bottom hole. The Teflon tube from the pipette was extended through the side hole in the centrifuge tube. The centrifuge tube was held in place to the side of the pipette with Parafilm (American National Can).

Before each experiment, plastic tubes were inserted through both compartments and sealed in place with Parafilm. In the receptor compartment, the measuring/flow-through electrode was inserted and sealed in place with Parafilm. The tubing within the receptor chamber was wired in place for the gel with stainless steel wire. Both compartments was turned sideways, and polyacrylamide solution was poured in, completely immersing everything. The polyacrylamide solution was composed of 0.75 g of 19:1 acrylamide:bis(N,N'-methylene-bis-acrylamide) powder (Bio-Rad), 43.75 µl of 440 m$\underline{M}$ $(NH_4)_2S_2O_8$ solution, and 3 µl of N,N,N',N'-tetramethylethylenediamine (Bio-Rad) in 5 ml of PBS.

The polyacrylamide solution was allowed to harden (~10 min). After the solution solidified, the outer plastic tubing and the Parafilm were removed from the outer ports, leaving behind an empty channel through the gel. The stainless steel wire was removed from the receptor compartment. During an experiment, PBS was pumped through each outer channel at a flowrate of ~6 ml/min.

11.1.3. Fluorescence Measurements.

Fluorescence measurements were taken with a spectrofluorimeter (Fluorescence Master Series Spectrometer, Photon Technology). Excitation and emission wavelengths for each compound are shown in Table 4.1.

The cuvette in the spectrofluorimeter was constructed by drilling two holes into a polystyrene microcuvette (VWR), to allow for inflow and outflow from the receptor compartment. One hole was drilled approximately 1/4 inch from the bottom of the cuvette for the outflow, and the other hole drilled higher in the cuvette (approximately 1/2 inch from the bottom) for the inflow. Both holes were connected to Tygon tubing to a peristaltic pump ("Sarah" Cassette Peristaltic Pump, Barnant).

The final volume of the cuvette was ~200 µl, and was the minimum amount needed by the spectrofluorimeter for accurate detection and quantification of the tracer concentration within the cuvette. Mixing within the cuvette was accomplished by dripping fluid down into the cuvette. The performance of this system was very close to an idealized continuous-stirred tank reactor (Fogler, 1992), and the residence time for the combined chamber-tubing-pump-cuvette system (volume of ~400 µl) was ~14 s. This was taken to be the time resolution for the flux measurements in these experiments.

11.1.4. Electrical Equipment.

High-voltage exponential pulses were delivered by a pulser (Electroporation System 600, BTX), custom-modified to deliver 1 pulse every ~5 s (U. Pliquett, personal communication). The time constant

was set to 1 ms. Exponential pulses with peak transdermal voltages between 0 V and ~150 V across the skin were applied for 1 h at the rate of one pulse every ~5 s.

Current delivered across the skin during the pulse was measured by measuring the voltage drop across a 1.2 Ω noninductive resistor, placed in series with the permeation chamber. The voltage drop across the resistor was measured by a voltage probe connected to a digital oscilloscope. The oscilloscope was connected to a personal computer.

The voltage drop from the receptor to the donor compartment was measured by connecting a differential high-voltage probe (Active Differential Probe B9017RT, Yokogawa) to the immobilized silver wire measuring electrodes in each compartment. This probe was also connected to the same oscilloscope.

The computer counted and recorded both voltage waveforms recorded by the oscilloscope for every pulse. The computer did not do any mathematical processing, since there was barely sufficient time to download the waveforms from the oscilloscope and record them onto the hard drive.

11.1.5. Skin Experimental Protocol.

Prepared, stored skin was floated in PBS for ~1 min to remove the wax paper backing. The skin was loaded into the permeation chamber, with the stratum corneum facing the donor compartment. The donor compartment was then filled with the donor solution and the flow-through pumps started. The donor compartment was constantly stirred by a magnetic stir bar.

The condition of the skin was checked by measuring its electrical impedance. A 100 Hz, 0.1 V bipolar sine wave (peak-to-peak) was applied across the skin and the resulting impedance measured using an LCR meter (Model 5R715 LCR Meter, Stanford Research Systems). Skin was considered bad and was discarded if its impedance was <25 $k\Omega\ cm^2$ at a frequency of 100 Hz (or <40 kΩ for this apparatus). Previous experiments have shown that this value compares favorably with the accepted DC resistance of <50 $k\Omega\ cm^2$ (Gowrishankar, personal communication). The resistances and impedances of the PBS and the polyacrylamide gel were neglected, since their combined resistances were previously measured to be 251 Ω (see Section 3.6), compared to ~40 kΩ for the skin.

After determining if the skin was acceptable or not, the apparatus was allowed to sit for 1 h to fully hydrate the skin (Prausnitz, *et al.*, 1993 [a]) and check for leaks. Leaky skin (passive flux above the detection limit, $\sim 10^{-8}$ M, or $\sim 10^{-10}\ mol / m^2\ s$ for this experimental apparatus), was discarded.

11.1.6. Pulsing Protocol.

High-voltage exponential pulses, with a time constant of 1 ms and transdermal voltages between 0 V and ~150 V across the skin (applied voltages between 0 V and 1000 V) were applied for 1 h at the rate of one pulse every ~5 s. PBS was pumped through the flow-protection system and the flow-through system during pulsing. Both the spectrofluorimeter computer and the computer recording voltage waveforms were set to record ~1 h of data.

After the experiment, the skin was removed from the chamber for microscopy analysis. All of the data from the two computers (spectrofluorimeter data and voltage data) were downloaded onto a workstation for analysis.

11.1.7. Numerical Analysis.

All of the fluorescence, voltage and calibration data were first downloaded onto a Sun Sparc 10 workstation (Sun). A program was in MatLab 5 (Mathworks) used these data to determine the flux versus voltage for each pulse. The program loaded in the voltage and current waveforms for each pulse and fitted each curve to an exponential to determine voltages. Since the resistance of the chamber without any skin was 251 Ω, the voltage across the skin could be calculated by Ohm's Law. The program then loaded the calibration and fluorescence data and used deconvolution routines (Pliquett, *et al.*, 1995 [b]; also see Section IV.13.2) to calculate the molecular flux across the skin. The two data files were then synchronized together in time, allowing the program to determine the measured flux for each pulse.

11.2. The Peak Transdermal Voltage Continues to Decline.

After pulsing for 1 h (~680 pulses, one pulse every ~5 s), the transdermal voltage was noted to decrease dramatically within the first ~20 pulses, then continue to decline more slowly afterwards (see Figure 8.5). The same trend was observed here, when more pulses were applied to the skin. The peak transdermal voltage dropped rapidly within the first several pulses, then continue to decline more slowly afterwards (see Figure 11.1). Experiments performed for up to 7 h (>5 000 pulses) continued to show this same trend (data not shown).

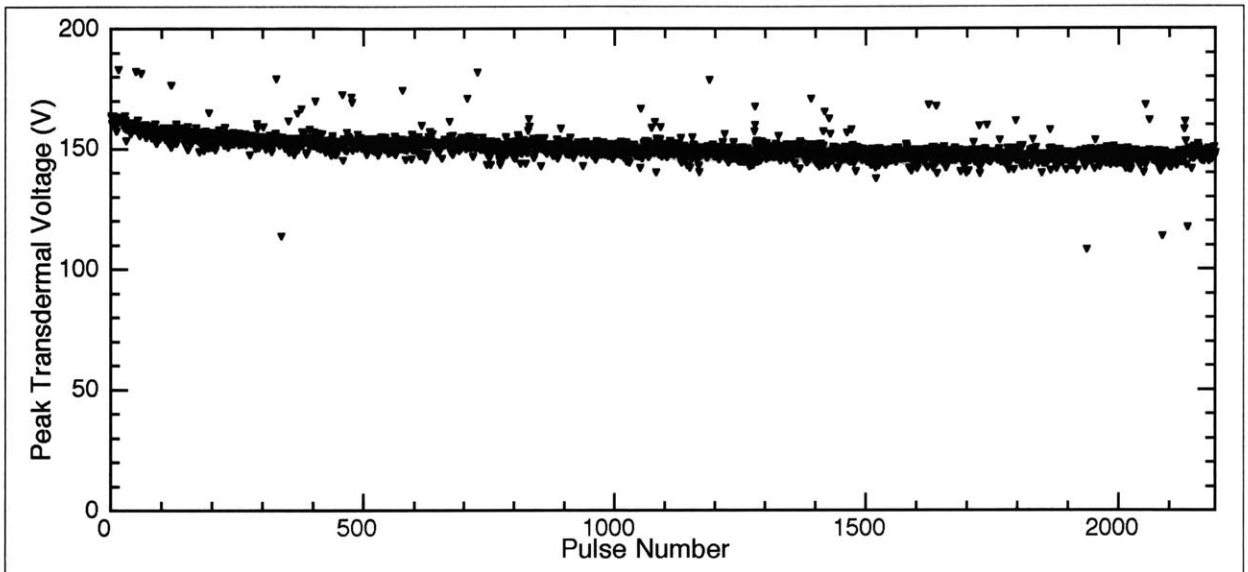

Figure 11.1. The transdermal voltage versus pulse number for 2 190 pulses. Although a large drop in the transdermal voltage occurs within the first several pulses, the transdermal voltage still continues to decline slowly afterwards with additional pulsing. Compare with Figure 8.5.

Thus, a steady-state plateau of the peak transdermal voltage is not reached during skin electroporation, but instead the transdermal voltage continuously declines with repeated pulsing. However, the rate of decrease is very slow, typically ~1 to 5 V/h. This continued decline could be due to several causes, including new pathway formation, enlargement of already existing pathways through the skin, or irreversible changes in the structure of the skin.

In typical 1 h high-voltage pulsing experiment, once pulsing has been stopped, the molecular flux

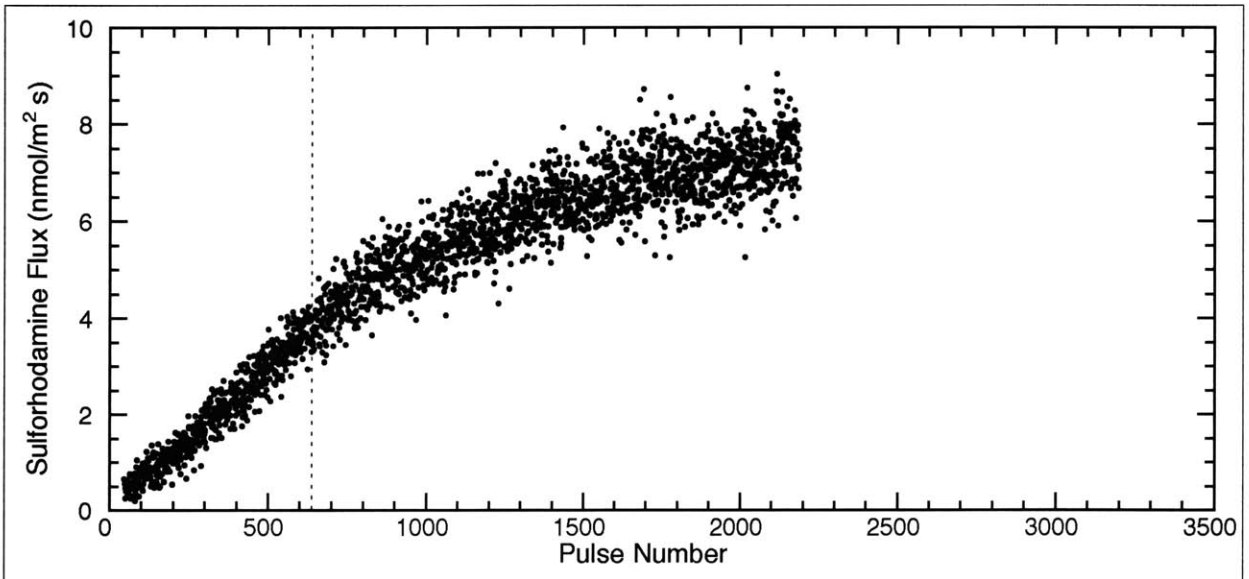

Figure 11.2. The molecular flux of sulforhodamine through human skin for 2 190 pulses. The flux of sulforhodamine did not reach steady state, even after pulsing for several hours. High-voltage pulses were applied at the rate of one pulse every ~5 s for over 3.5 h (2 190 pulses total). During that time, the flux of sulforhodamine across the skin increased monotonically. Dotted line in figure indicates first hour. The X-axis in this figure has been extended to 3 500 pulses, for easier comparison with Figures 11.3, 11.4, and 11.5. Even longer experiments have been performed (data not shown), lasting over 7 h (5 000 pulses total), without reaching steady state.

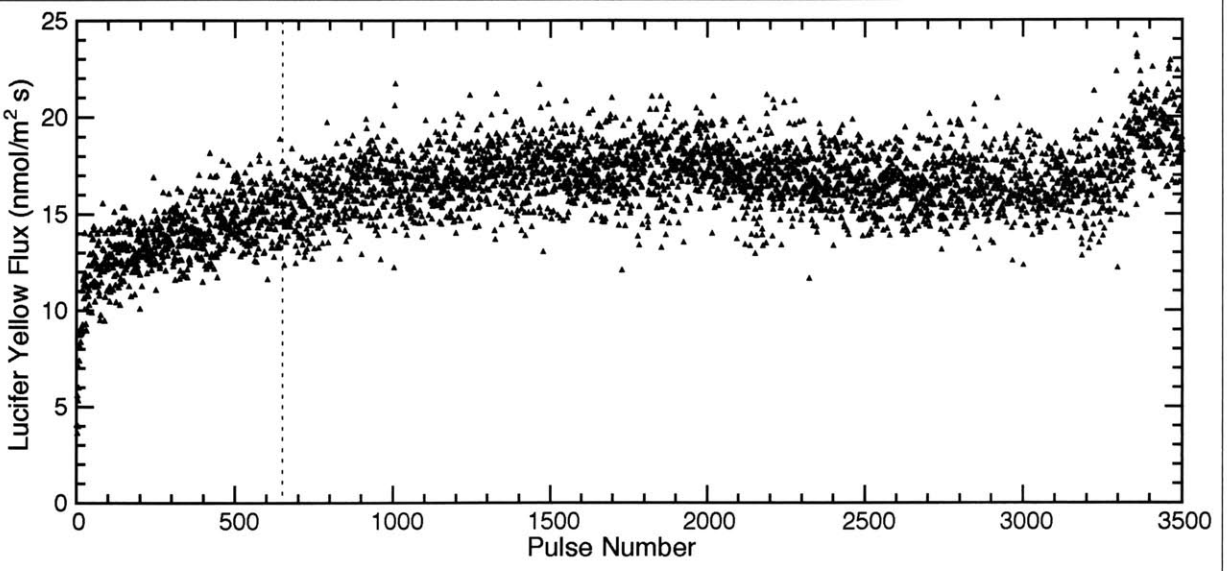

Figure 11.3. The molecular flux of lucifer yellow through human skin for 3 500 pulses. The flux of lucifer yellow reached steady state within 1 h (dotted line in figure). The averaged steady-state flux in this experiment was ~15 nmol / m^2 s. High-voltage pulses were applied to the skin at the rate of one pulse every ~5 s for over 5 h (3 500 pulses total). Compare with Figures 11.2, 11.4, and 11.5.

across the skin typically falls to below background levels in under 15 min (except for sulforhodamine). However, after several hours of pulsing, it takes much longer for the molecular flux across the skin to drop to below background levels, sometimes >2 h (data not shown). This could indicate that irreversible or only partially reversible changes are occurring in the structure of the skin during pulsing.

11.3. Some Molecules Reach Steady State; Others Do Not.

Unlike in skin iontophoresis, where steady-state molecular fluxes were reached in <1 h (see Figures 10.2a through 10.2d), steady-state molecular fluxes during skin electroporation were not always reached, even after pulsing for 7 h (corresponding to >5 000 pulses).

Figure 11.2 shows that the molecular flux of sulforhodamine across the skin during repeated pulsing continues to rise, without reaching a steady -state plateau. Longer experiments (up to 7 h) also showed this continued rise in the molecular flux (data not shown). It thus appears unlikely that the flux of sulforhodamine across the skin would reach steady state in a reasonable amount of time during skin electroporation.

Both lucifer yellow (Figure 11.3) and cascade blue (Figure 11.4) reached steady state relatively quickly, within 1 h of pulsing. Additional pulsing did not appear to significantly alter the molecular flux across the skin. Earlier experiments (see Figures 8.4b and 8.4c, respectively) have also shown

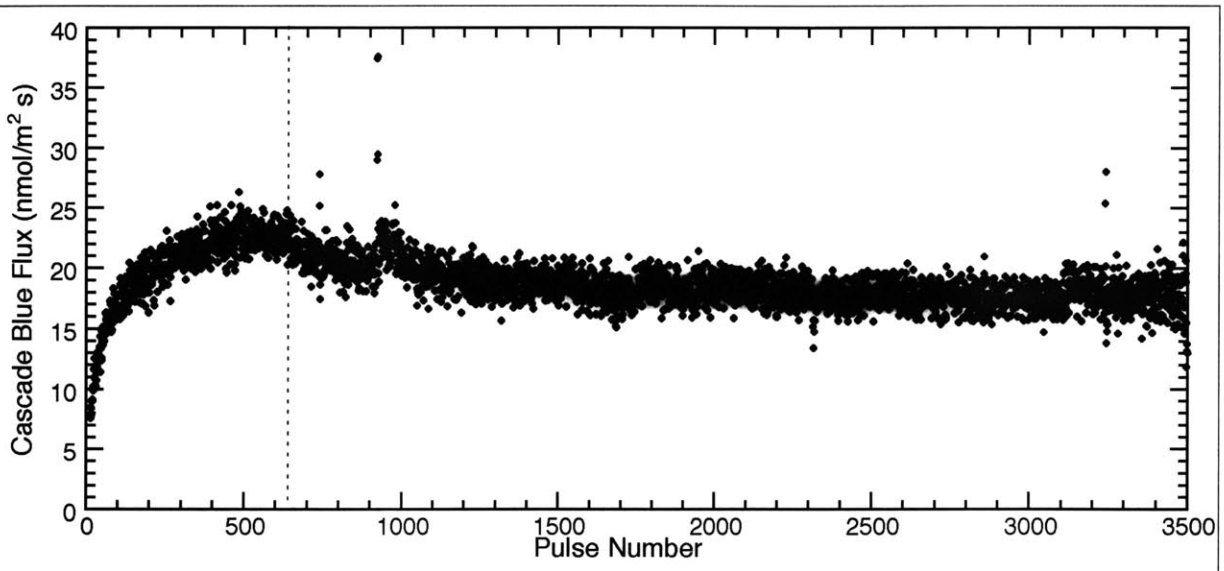

Figure 11.4. The molecular flux of cascade blue through human skin for 3 500 pulses. In the experiment shown here, high-voltage pulses were applied at the rate of one pulse every ~5 s to the skin for over 5 h (3 500 pulses total), reaching an averaged steady-state flux of ~20 nmol / m^2 s. Dotted line indicates the first hour (~680 pulses). Compare with Figures 11.2, 11.3, and 11.4.

that these two molecules reach steady state in <1 h, unlike sulforhodamine or calcein (Figures 8.4a and 8.4d, respectively).

The flux of calcein (Figure 11.5) was less predictable. The molecular flux of calcein generally peaked within the first 10 min of pulsing, then began decreasing afterwards (see Figure 8.4d). However, in some cases, the flux of calcein varied erratically with additional pulsing, as shown in Figure 11.5.

11.4. Conclusions.

The application of repeated high-voltage pulsing to the skin for very long periods of time (several hours), involving many thousands of pulses, had different effects on the molecular transport of different molecules. With some molecules such as sulforhodamine, the molecular flux continued to increase with repeated pulsing. Other molecules, such as lucifer yellow and cascade blue, reached a steady-state plateau within 1 h of pulsing. Some molecules, such as calcein, were unpredictable. These same four molecules were previously observed to reach steady-state molecular fluxes in <1 h during iontophoresis (see Section 10.2).

With repeated pulsing, the peak transdermal voltage initially dropped very quickly, during the first ~20 pulses, and continued to decrease slowly afterwards. This decrease may indicate that small, irreversible changes are occurring to the structure of the skin with each pulse. However, the electrical

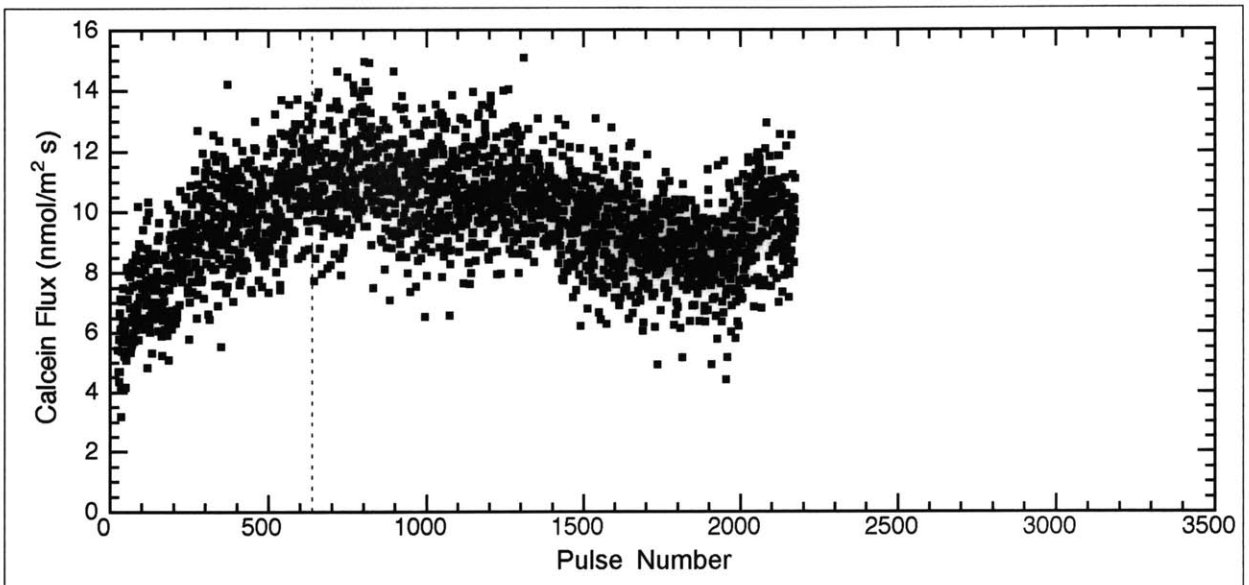

Figure 11.5. The molecular flux of calcein through human skin for 2 175 pulses. The flux of calcein did not reach steady state, and behaved unpredictably. In this experiment, high-voltage pulses were applied to the skin at the rate of one pulse every ~5 s for over 3.5 h (2 175 pulses total). Dotted line indicates first hour. The X-axis has been extended to 3 500 pulses, for comparison with other experiments (Figures 11.2, 11.3, and 11.4).

driving forces experienced by the donor molecules did not vary widely during these experiments (Figure 11.1).

Very different molecular flux profiles in time were recorded for each of the four fluorescent tracer molecules used (sulforhodamine, lucifer yellow, cascade blue, and calcein), although they were originally chosen due to their similarities (hydrophilicity, size, negative charge, fluorescence). Each molecule may be using different molecular transport pathways across the skin during skin electroporation, as previously discussed (see Section 8.2.3 and Figure 8.6).

12. Summary.

Applying a series of short (~1 ms), high-voltage (~100 V_{skin}) electrical pulses to the skin causes molecular transport to occur by a mechanism related to electroporation, hence the name of this phenomenon, "skin electroporation." Transport occurs through aqueous pathways that form as a result of pulsing. This technique can potentially be used for the delivery of drugs directly through the skin, without the use of needles.

During high-voltage pulsing, molecular transport occurs through or near "localized transport regions," or "LTRs." The LTRs form randomly and spontaneously on the surface of the skin, away from the sweat ducts and hair follicles. The LTRs grow in size, but not in number, with additional pulsing.

Molecular transport during skin electroporation occurs via a different process than iontophoresis, where a low-voltage, constant electrical current is applied to the skin (typically <0.5 mA / cm^2), which causes transport through the sweat ducts and hair follicles in the skin. No new pathways form during iontophoresis. Skin that lacks sweat ducts or hair follicles (such as snake skin) does not permit transport during iontophoresis, as there are no pathways available for transport.

The peak transdermal voltage during skin electroporation, the electrical impedance of the skin (a surrogate for the electrical resistance of the skin), and the molecular flux, all can change rapidly (of order seconds) with repeated pulsing. These parameters thus need to be rapidly measured in real time, since using aliquots or averages can lead to erroneous measurements and conclusions. The transdermal voltage generally decreases rapidly with the first few pulses, then continues decreasing more slowly afterwards. The impedance of the skin drops with repeated pulsing, with the amount of recovery of the impedance after pulsing also declining with additional pulsing. However, between each pulse, there is some recovery of the impedance, indicating that some recovery of the skin's barrier properties is taking place.

Molecular transport is thus very sensitive to the electrical conditions that are applied to the skin, especially the transdermal voltage and the number of pulses already delivered. In general, molecular transport increases with the voltage, the duration (time constant), and the frequency of the applied pulses. However, since the transdermal voltage can vary in time, it should be carefully monitored during delivery, possibly involving regulatory real-time feedback to the high-voltage supply. The monitoring of the transdermal voltage, as well as the number and type of pulses that can be applied reliably, in turn will be a function of the actual electrode/delivery reservoir configuration used to apply pulsing.

The molecular flux across the skin is also a function of the specific molecule being transported. Some molecules (such as lucifer yellow and cascade blue) will quickly reach steady-state fluxes within 1 h of pulsing; some molecules (such as sulforhodamine) do not reach steady state, but their molecular

fluxes continue to increase with additional pulsing; and other molecules (such as calcein) initially have large molecular fluxes, but then the flux begins to decrease with repeated pulsing. Even molecules with similar physicochemical properties appear to exhibit large differences in molecular flux behaviors during pulsing.

Given the observed inconsistencies in the molecular fluxes across the skin for similar compounds, a general theory of molecular transport during skin electroporation was not developed here. In general, however, the instantaneous molecular flux appears to be proportional to the transdermal voltage, although both can change with repeated pulsing. In skin electroporation, peak transdermal voltages of >50 V_{skin} are needed for molecular transport to occur.

Molecular transport thus depends on physicochemical parameters of the molecule, which have not yet been identified. Knowledge of the electronic charge and the molecular weight, by themselves, were not reliable predictors of molecular transport. Some parameters that may be important in predicting transport include hydrophobicity, size, 3D conformation, surface changes, pKa's, or ionization energies. Further work will be needed here to determine the relevant physicochemical parameters.

In conclusion, skin electroporation is a highly dynamic process, where the driving forces involved with molecular transport can change rapidly and somewhat unpredictably with repeated pulsing. Measurement, control, and prediction of these rapidly changing forces will be essential before skin electroporation can move from the lab to the clinic.

Bibliography.

Abidor, I. G., V. B. Arakelyan, L. V. Chernomordik, Y. A. Chizmadzhev, V. F. Pastushenko, and M. R. Tarasevich. "Electrical Breakdown of Bilayer Membranes. I. The Main Experimental Facts and Their Qualitative Discussion." Bioelectrochem. Bioenerget., **6**:37-52, 1979.

Abramson, H. A. "Skin Reactions. X. Preseasonal Treatment of Hay Fever by Electrophoresis of Ragweed Pollen Extracts in to the Skin: Preliminary Report." *J. Allergy*, **12**:169-175, 1941.

Abramson, H. A., and M. G. Engel. "Skin Reactions. XII. Patterns Produced in the Skin by Electrophoresis of Dyes." *Arch. Dermatol. Syphilol.*, **44**:190-200, 1942.

Abramson, H. A., and M. H. Gorin. "Skin Reactions. IX. The Electrophoretic Demonstration of the Patent Pores of the Living Human Skin; Its Relation to the Charge of the Skin." *J. Phys. Chem.*, **44**:1094-1102, 1940.

Ackerman, A. B. "Structure and Function of the Skin." In: *Dermatology*, Volume I. S. L. Moschella, D. M. Pillsbury, and H. J. Herley, Editors. Philadelphia: W. B. Saunders, 1978.

Amsden, B. G., and M. F. A. Goosen. "Transdermal Delivery of Peptide and Protein Drugs: An Overview." *AIChE J.*, **41**:1972-1997, 1995.

Arvidsson, S. B., R. H. Ekroth, A. M. C. Hansby, A. H. Lindholm, and G. William-Olsson. "Painless Venipuncture. A Clinical Trial of Iontophoresis of Lidocaine for Venipuncture in Blood Donors." *Acta Anaesth. Scand.*, **28**:209-210, 1984.

Banerjee, T. K., and A. K. Mittal. "Histochemistry of Snake Epidermis." In: *The Skin of Vertebrates*, R. I. C. Spearman, and P. A. Riley, Editors. London: Academic, 1978.

Banga, A. K., and Y. W. Chien. "Iontophoretic Delivery of Drugs: Fundamentals, Developments, and Biomedical Applications." *J. Control. Release*, **7**:1-24, 1988.

Banga, A., and M. R. Prausnitz. "Delivery of Protein and Gene-Based Drugs by Skin Electroporation." *Trends Biotech.*, in press.

Barnett, A., and J. C. Weaver. "Electroporation: A Unified, Quantitative Theory of Reversible Electrical Breakdown and Mechanical Rupture in Artificial Planar Bilayer Membranes." *Bioelectrochem. Bioenerget.*, **25**:163-182, 1991.

Belehradek, M., C. Domenge, B. Luboinski, S. Orlowski, J. Belehradek, and L. M. Mir. "Electrochemotherapy, a New Antitumor Treatment: First Clinical Phase I-II Trial." *Cancer*, **72**:3694-3700, 1993.

Benz, R., and U. Zimmermann. "Relaxation Studies on Cell Membranes and Lipid Bilayers in the High Electric Field Range." *Bioelectrochem. Bioenerg.*, **7**:723-739, 1980.

Blair, C. "Morphology and Thickness of the Human Stratum Corneum." *Brit. J. Dermatol.*, **80**:430-436, 1968.

Boddé, H. E., M. A. M. Kruithof, J. Brussee and H. K. Koerten. "Visualisation of Normal and Enhanced $HgCl_2$ Transport through Human Skin *in Vitro*." *Int. J. Pharm.*, **53**:13-24, 1989.

Boddé, H. E., I. van der Brink, H. K. Koerten and F. H. N. de Haan. "Visualization of *in Vitro* Percutaneous Penetration of Mercuric Chloride: Transport through Intercellular Spaces Versus Cellular Uptake through Desmosomes." *J. Control. Release*, **15**:227-236, 1991.

Bommannan, D., G. K. Menon, H. Okuyama, P. M. Elias, and R. H. Guy. "Sonophoresis. II. Examination of the Mechanisms of Ultrasound-Enhanced Transdermal Drug Delivery." *Pharm. Res.*, **9**:1043-1047, 1992 [a].

Bommannan, D., H. Okuyama, P. Stauffer, and R. H. Guy. "Sonophoresis. I. The Use of Ultrasound to Enhance Transdermal Drug Delivery." *Pharm. Res.*, **9**:559-564, 1992 [b].

Bommannan, D., J. Tamada, L. Leung, and R. O. Potts. "Effect of Electroporation on Transdermal Iontophoretic Delivery of Luteinizing Hormone Releasing Hormone (LHRH) *in Vitro*." *Pharm. Res.*, **11**:1809-1814, 1994.

Bose, V. G. *Electrical Characterization of Electroporation of Human Stratum Corneum.* M. S. Thesis. Massachusetts Institute of Technology, Cambridge, MA, 1994.

Bouclier, M., D. Cavey, N. Kail, and C. Hensby. "Experimental Models in Skin Pharmacology." *Pharmacol. Rev.*, **42**:127-154, 1990.

Bronaugh, R. L. and H. I. Maibach, Editors. *Percutaneous Absorption. Mechanisms — Methodology — Drug Delivery.* New York: Marcel Dekker, 1989.

Bronaugh, R. L., R. F. Stewart, and E. R. Congdon. "Methods for *in Vitro* Percutaneous Absorption Studies. II. Animal Models for Human Skin." *Tox. Appl. Pharm.*, **62**:481-488, 1982.

Burnette, R. R. "Iontophoresis." In: *Transdermal Drug Delivery: Developmental Issues and Research Inititatives*, J. Hadgraft, and R. H. Guy, Editors. New York: Marcel Dekker, 1989.

Burnette, R. R., and D. Marrero. "Comparison Between the Iontophoretic and Passive Transport of Thyrotropin Releasing Hormone across Excised Nude Mouse Skin." *J. Pharm. Sci.*, **75**:738-743, 1986.

Burnette, R. R., and B. Ongpipattanakul. "Characterization of the Pore Transport Properties and Tissue Alteration of Excised Human Skin during Iontophoresis." *J. Pharm. Sci.*, **77**:132-137, 1988.

Champion, R. H., J. L. Burton, and F. J. G. Ebling, Editors. *Textbook of Dermatology*. London: Blackwell, 1992.

Chang, D. C., B. M. Chassy, J. A. Saunders, and A. E. Sowers, Editors. *Guide to Electroporation and Electrofusion*. New York: Academic, 1992.

Chang, D. C., and T. S. Reese. "Changes in Membrane Structure Induced by Electroporation as Revealed by Rapid-Freezing Electron Microscopy." *Biophys. J.*, **58**:1-12, 1990.

Chattaraj, S. C., and R. B. Walker. "Penetration Enhancer Classification." In: *Perucutaneous Penetration Enhancers*, E. W. Smith, and H. I. Maibach, Editors. Boca Raton, Florida: CRC, 1995.

Chen, T. "Skin Electroporation for the Therapeutic Delivery of Drugs." *Pharm. News.*, **5**:21-24, 1998 [a].

Chen, T., R. Langer, and J. C. Weaver. "An *in Vitro* System for Measuring the Transdermal Voltage and Molecular Flux across the Skin in Real Time." In: *Electrically Mediated Delivery of Molecules to Cells: Electrochemotherapy, Electrogenetherapy, and Transdermal Drug Delivery by Electroporation, Methods in Molecular Medicine* (series), M. J. Jaroszeski, R. Gilbert, and R. Heller, Editors. Totowa, NJ: Humana, in press [a].

Chen, T., R. Langer, and J. C. Weaver. "Charged Microbeads Are Not Transported Across the Human Stratum Corneum *in Vitro* by Short High-Voltage Pulses." *Bioelectrochemistry*, submitted [a].

Chen, T., R. Langer, and J. C. Weaver. "Iontophoresis Causes Molecular Transport through Hair Follicles and Sweat Ducts in the Skin." *Proceedings of the Second World Congress for Electricity and Magnetism in Biology and Medicine*, F. Bersani, Editor. New York: Plenum, in press [b].

Chen, T., R. Langer, and J. C. Weaver. "Transdermal Drug Delivery by Skin Electroporation." In: Handbook of Pharmaceutical Controlled Release Technology, A. M. Klibanov, R. Langer, A. G. Mikos, N. A. Peppas, D. J. Trantolo, D. L. Wise, G. E. Wnek, and M. J. Yaszemski, Editors. New York: Marcel Dekker, submitted [b].

Chen, T., R. Langer, and J. C. Weaver. "Skin Electroporation Causes Molecular Transport across the Stratum Corneum through Localized Transport Regions." *J. Invest. Dermatol. Symp. Proc.*, **3**:159-165, 1998 [b].

Chen, T., E. M. Segall, R. Langer, and J. C. Weaver. "Skin Electroporation: Rapid Measurements of the Transdermal Voltage and Flux of Four Fluorescent Molecules Show a Transition to Large Fluxes Near 50 V." *J. Pharm. Sci.*, **37**:1368-1374, 1998 [c].

Cheng, K. L., K. Ueno, and T. Imamura. "Calcein." In: *CRC Handbook of Organic Analytical Reagents*. Boca Raton, Florida:CRC, 1982.

Chien, Y. W., and A. K. Banga. "Iontophoretic (Transdermal) Delivery of Drugs: Overview of Historical Development." *J. Pharm. Sci.*, **78**:353-354, 1989.

Chien, Y. W., O. Siddiqui, W.-M. Shi, P. Lelawongs, and J. C. Liu. "Direct Current Iontophoretic Transdermal Delivery of Peptide and Protein Drugs." *J. Pharm. Sci.*, **78**:376-383, 1989.

Chizmadzhev, Y. A., A. V. Indenbom, P. I. Kuzmin, S. V. Galichenko, J. C. Weaver, and R. O. Potts. "Electrical Properties of Skin at Moderate Voltages: Contribution of Appendageal Macropores." *Biophys. J.*, **74**:843-856, 1998 [a].

Chizmadzhev, Y. A., P. I. Kuzmin, J. C. Weaver, and R. O. Potts. "Skin Appendageal Macropores as Possible Pathways for Electric Current." *J. Invest. Dermatol. Symp. Proc.*, **3**: 1998 [b].

Chizmadzhev, Y. A., V. G. Zarnytsin, J. C. Weaver, and R. O. Potts. "Mechanism of Electroinduced Ionic Species Transport through a Multilamellar Lipid Bilayer System." *Biophys. J.*, **68**:749-765, 1995.

Craane-Van Hisberg, W. H. M., J. C. Verhoef, H. E. Junginger, and H. Boddé. "Thermoelectric Analysis of the Human Skin Barrier." *Thermochim. Acta*, **248**:303-318, 1994.

Cullander, C. "What are the Pathways of Iontophoretic Current Flow through Mammalian Skin?" *Adv. Drug Deliv. Rev.*, **9**:119-135, 1992.

Cullander, C., and R.H. Guy. "Sites of Iontophoretic Current Flow into the Skin: Identification and Characterization with the Vibrating Probe Electrode." *J. Invest. Dermatol.*, **97**:55-64, 1991.

Cullander, C., and R. H. Guy. "Transdermal Delivery of Peptides and Proteins." *Adv. Drug Deliv. Rev.*, **8**:291-329, 1992.

Duvanel, T., M. Harms, and J. Saurat. "New Technique to Perform Local Anesthesia: Pulse Iontophoresis." *Dermatologica*, **177**:30, 1988.

Edwards, D. A., M. R. Prausnitz, R. Langer, and J. C. Weaver. "Analysis of Enhanced Transdermal Transport by Skin Electroporation." *J. Control. Rel.*, **34**:211-221, 1995.

Elias, P. "Epidermal Lipids, Barrier Function, and Desquamation." *J. Invest. Dermatol.*, **80** (Suppl.):44s-49s, 1983.

Elias, P. M. "Structure and Function of the Stratum Corneum Permeability Barrier." *Drug Dev. Res.*, **13**: 97-105, 1988.

Friend, D. R. "*In Vitro* Skin Permeation Techniques." *J. Control. Release*, **18**:235-248, 1992.

Fogler, H. S. *Elements of Chemical Reactor Engineering.* Englewood Cliffs, New Jersey: Prentice Hall, 1992.

Freeman, S. A., M. A. Wang, and J. C. Weaver. "Theory of Electroporation of Planar Bilayer Membranes: Prediction of the Aqueous Area, Change in Capacitance, and Pore-Pore Separation." *Biophys. J.*, **67**:42-56, 1994.

Galichenko, S. V., P. I. Kuzmin, and Y. A. Chizmadzhev. "Electroporation of Skin Appendages under Iontophoretic Conditions: Theoretical Approach." *Membr. Cell. Biol.*, **13**:430-437, 1996.

Gallo, S. A., A. R. Oseroff, P. G. Johnson, and S. W. Hui. "Characterization of Electric-Pulse-Induced Permeabilization of Porcine Skin Using Surface Electrodes." *Biophys. J.*, **72**:2805-2811, 1997.

Glaser, R. W., S. L. Leikin, L. V. Chernomordik, V. F. Pastushenko, and A. I. Sokirko. "Reversible Electrical Breakdown of Lipid Bilayers: Formation and Evolution of Pores." *Biochim. Biophys. Acta*, **940**:275-287, 1988.

Gray, H. and C. D. Clemente. *Gray's Anatomy.* Malvern, Pennsylvania: Lea & Febiger, 1985.

Grasso, R. J., R. Heller, J. C. Cooley, and E. M. Haller. "Electrofusion of Individual Animal Cells Directly to Intact Corneal Epithelial Tissue." *Biochim. Biophys. Acta*, **980**:9-14, 1989.

Grimnes, S. "Pathways of Ionic Flow through Human Skin *in Vivo*", *Acta. Derm. Venereol. (Stockh.)*, **64**:93-98, 1984.

Gummer, C. L. "The *in Vitro* Evaluation of Transdermal Delivery." In: *Transdermal Drug Delivery: Developmental Issues and Research Inititatives*, J. Hadgraft and R. H. Guy, Editors. New York: Marcel Dekker, 1989.

Guy, R. H. "Current Status and Future Prospects of Transdermal Drug Delivery." *Pharm. Res.*, **13**:1765-1769, 1996.

Guy, R. H., and J. Hadgraft. "Selection of Drug Candidates for Transdermal Drug Delivery." In: *Transdermal Drug Delivery: Developmental Issues and Research Initiatives*, J. Hadgraft, and R. H. Guy, Editors. New York: Marcel Dekker, 1989.

Hadgraft, J. "Prodrugs and Skin Absorption." In: *Design of Prodrugs*, H. Bundgaard, Editor. Amsterdam, Elsevier, 1985.

Hadgraft, J. and R. H. Guy, Editors. *Transdermal Drug Delivery: Developmental Issues and Research Initiatives.* New York: Marcel Dekker, 1989.

Hancock, W. S. and J. T. Sparrow. *HPLC Analysis of Biological Compounds: A Laboratory Guide.* New York and Basel: Marcel Dekker, 1984.

Haugland, R. P. *Handbook of Fluorescent Probes and Research Chemicals.* Eugene, Oregon: Molecular Probes, 1992.

Henschen, A., K.-P. Hupe, F. Lottspeich, and W. Voelter, Eds. *High Performance Liquid Chromatography in Biochemistry.* Weinheim, Germany: VCH Verlagsgesellschaft, 1985.

Hofmann, G. A., W. V. Rustrum, and K. S. Suder. "Electro-incorporation of Microcarriers as a Method for the Transdermal Delivery of Large Molceules." *Bioelectrochem. Bioenerg.*, **38**:209-222, 1995.

Hrushesky, W. J. M. "Temporally Optimizable Delivery Systems — *Sine Qua Non* for Molecular Medicine." Ann. N. Y. Acad. Sci., **618**:xi-xvii, 1991.

Inada, H., A. H. Ghanem, and W. I. Higuchi. "Studies on the Effects of Applied Voltage and Duration on Human Epidermal Membrane Alteration/Recovery and the Resultant Effects upon Iontophoresis." *Pharm. Res.*, **11**:687-697, 1994.

Indenbom, A. V., P. I. Kuzmin, and Y. A. Chizmadzhev. "Changes in the Electrical Properties of the Skin Outermost Layer during Pulse Electrotreatment." *Membr. Cell. Biol.*, **11**:367-380, 1997.

Itoh, T., R. Magavi, R. L. Casady, T. Nishihata, and J. H. Rytting. "A Method to Predict the Percutaneous Permeability of Various Compounds: Shed Snake Skin as a Model Membrane." *Pharm. Res.*, **7**:1302-1306, 1990 [a].

Itoh, T., J. Xia, R. Magavi, T. Nishihata, and J. H. Rytting. "Use of Shed Snake Skin as a Model Membrane for *in Vitro* Percutaneous Studies: Comparison with Human Skin." *Pharm. Res.*, **7**:1042-1047, 1990 [b].

Jadoul, A., J. Bouwstra, and V. Préat. "Skin Integrity after Electrically Enhanced Transdermal Drug Delivery." *Adv. Drug Deliv. Rev.*, in press.

Jadoul, A., N. Lecouturier, J. Mesens, W. Caers, and V. Préat. "Electrically Enhanced Transdermal Delivery of Alnitidan." *J. Control. Rel.*, **54**:265-272, 1998.

Jadoul, A., and V. Préat. "Electrically-Enhanced Transdermal Delivery of Domperidone." *Int. J. Pharm.*, **154**:229-234, 1997 [a].

Jadoul, A., V. Regnier, J. Doucet, D. Durand, and V. Préat. "X-ray Scattering Analysis of the Stratum Corneum Treated by High Voltage Pulses." *Pharm. Res.*, **14**:1275-1277, 1997 [b].

Jadoul, A., H. Tanajo, V. Préat, F. Spies, and H. Boddé. "Electroperturbation of Human Stratum Corneum Fine Structure by High Voltage Pulses: A Freeze Fracture Electron Microscopy and Differential Thermal Analysis Study." *J. Invest. Dermatol. Symp. Proc.*, **3**:153-158, 1998.

Johnson, M. E. *Biophysical Aspects of Transdermal Drug Delivery and Chemical Enhancement*, Ph. D. Thesis. Cambridge, Massachusetts: Massachusetts Institute of Technology, 1996.

Johnson, P. G., S. A. Gallo, S. W. Hui, and A. R. Oseroff. "A Pulsed Electric Field Enhances Cutaneous Delivery of Methylene Blue in Excised Full-Thickness Porcine Skin." *J. Invest. Dermatol.*, submitted.

Kasting, G. B. and L. A. Bowman. "*D. C. Electrical Properties of Frozen, Excised Human Skin.*" *Pharm. Res.*, **7**:134-143, 1990.

Kost, J., D. Levy, and R. Langer. "Ultrasound as a Transdermal Enhancer." In: *Percutaneous Absorption: Mechanisms — Methodolgy — Drug Delivery*, R. L. Bronaugh, and H. I. Maibach, Editors. New York: Marcel Dekker, 1989.

Kost., J., U. Pliquett, S. Mitragotri, A. Yamamoto, R. Langer, and J. Weaver. "Synergistic Effect of Electric Field and Ultrasourd on Transdermal Transport." *Pharm. Res.*, **13**:633-638, 1996.

Lampe, M. A., A. L. Burlingame, J. Whitney, M. L. Williams, B. E. Brown, E. Roitman, and P. M. Elias. "Human Stratum Corneum Lipids: Characterization and Regional Variations." *J. Lip. Res.*, **24**:120-130, 1983 [a].

Lampe, M. A., M. L. Williams, and P. M. Elias. "Human Epidermal Lipids: Characterization and Modulations during Differentiation." J. Lip. Res., **24**:131-140, 1983 [b].

Landmann, L. "Keratin Formation and Barrier Mechanisms in the Epidermis of *Natrix natrix* (*Reptilia*: *Serpentes*): An Ultrastructural Study." *J. Morph.*, **162**:93-126, 1979.

Landmann, L., C. Stolinski, and B. Martin. "The Permeability Barrier in the Epidermis of the Grass Snake during the Resting Stage of the Sloughing Cycle." *Cell Tissue Res.*, **215**:369-382, 1981.

Langer, R. "New Methods of Drug Delivery." *Science*, **249**:1527-1533, 1990.

Lanegr, R. "Drug Delivery and Targeting" Nature, **392**:5-10, 1998.

Leblond, C. P. "Histological Structure of Hair, with a Brief Comparison to Other Epidermal Appendages and Epidermis Itself." *Ann. N. Y. Acad.. Sci.*, **53**:464-475, 1951.

Lillywhite, H. B., and P. F. A. Maderson. "Skin Structure and Permeability." In: *Biology of the Reptilita. Volume 12: Physiological Ecology*, C. Gans, and F. H. Plough, Editors. New York: Academic, 1982.

Ledger, P. W. "Skin Biological Issues in Electrically Enhanced Transdermal Delivery." *Adv. Drug Deliv. Rev.*, **9**:289-307, 1992.

Lide, D. R., Editor. *CRC Handbook of Chemistry and Physics*, 71st Edition. Boca Raton, Florida: CRC, 1991.

Lombry, C., N. Dujardin, and V. Préat. "Influence of Molecular Weight on Transdermal Drug Delivery by Skin Electroporation." In preparation.

Maderson, P. F. A., A. H. Zucker, and S. I. Roth. "Epidermal Regeneration and Percutaneous Water Loss Following Cellophane Stripping of Reptile Epidermis." *J. Exp. Zool.*, **204**:11-32, 1978.

Malkova, O. N., P. I. Kuzmin, Y. A. Chizmadzhev, and R. Potts. "A Theoretical Study of Outermost Skin Layer Electroporation." *Membr. Cell. Biol.*, **10**:601-611, 1997.

Mansbridge, J. N., and A. M. Knapp. "Penetration of Lucifer Yellow into Human Skin: A Lateral Diffusion Channel in the Stratum Corneum." *J. Histochem. Cytochem.*, **41**:909-914, 1993.

Martin, G. T., U. Pliquett, and J. C. Weaver. "Theoretical Analysis of Localized Heating in Human Skin Subjected to "High-Voltage" Pulses." In Preparation.

Metcalfe, H. C., J. E. Williams, and J. F. Castka. *Modern Chemistry*, Teacher's Edition. New York: Holt, Rinehart and Winston, 1986.

Meyer, B. R., W. Kries, J. Eschbach, V. O'Mara, S. Rosen and D. Sibalis. "Transdermal versus Subcutaneous Leuprolide: A Comparison of Acute Pharmacodynamic Effect." *Clin. Pharm. Ther.*, **48**:340-345, 1990.

Mitragotri, S., D. Blankenstein, and R. Langer. "Ultrasound-Mediated Transdermal Protein Delivery." *Science*, **269**:850-853, 1995 [a].

Mitragotri, S., D. A. Edwards, D. Blankenstein, and R. Langer. "A Mechanistic Study of Ultrasonically-Enhanced Transdermal Drug Delivery." *J. Pharm. Sci.*, **84**:697-706, 1995 [b].

Mir, L. M., M. Belehradek, C. Domenge, S. Orlowski, B. Poddevin, J. Belehradek, G. Schwaab, B. Luboinski, and C. Paoletti. "Electrochemotherapy, a Novel Antitumor Treatment: First Clinical Trial." *C. R. Acad. Sci. Paris Sérle. III*, **313**:613-618, 1991.

Montagna, W., A. Kligman, and K. Carlisle. *Atlas of Norman Human Skin*. New York: Springer-Verlag, 1992.

Monteiro-Riviere, N. A. "Comparative Anatomy, Phsyiology, and Biochemistry of Mammalian Skin." In: *Dermal and Ocular Toxicology*, D. W. Hobson, Editor. Boca Raton, Florida: CRC, 1991.

Monteiro-Riviere, N. A., A. O. Inman, and J.E. Riviere. "Identification of the Pathway of Iontophoretic Drug Delivery: Light and Ultrastructure Studies using Mercuric Chloride in Pigs." *Pharmacol. Res.*, **11**:251-256, 1994.

Morimoto, Y., T. Hatanaka, K. Sugibayashi, and H. Omipa. "Prediction of Skin Permeability of Drugs: Comparison of Human and Hairless Rat Skin." *J. Pharm. Pharmacol.*, **44**:634-639, 1992.

Neumann, E., M. Schaefer-Ridder, Y. Wang, and P. H. Hofschneider. "Gene Transfer into Mouse Lyoma Cells by Electroporation in High Electric Fields." *EMBO J.*, **1**:841-845, 1982.

Neumann, E., A. E. Sowers, and C. A. Jordan, Editors. *Electroporation and Electrofusion in Cell Biology*. New York: Plenum, 1989.

Okino, M., H. Tomie, H. Kanesade, M. Marumoto, K. Esata, and H. Suzuki. "Optimal Electric Conditions in Electrical Impulse Chemotherapy." *Jpn. J. Cancer Res.*, **83**:1095-1101, 1992.

Orlowski, S., and L. M. Mir. "Cell Electropermeabilization: A New Tool for Biochemical and Pharmacological Studies." *Biochim. Biophys. Acta*, **1154**:51-63, 1993.

Pliquett, U. "Mechanistic Studies of Molecular Transdermal Transport due to Skin Electroporation." *Adv. Drug Deliv. Rev.*, in press.

Pliquett, U., E. A. Gift, and J. C. Weaver. "Determination of the Electric Field and Anomalous Heating Caused by Exponential Pulses in Electroporation Experiments." *Bioelectrochem. Bioenerg.*, **39**:39-53, 1996 [a].

Pliquett, U., and C. A. Gusbeth. "Calcein as Model for Hydrophilic Drugs: Avoiding Artifacts." In preparation.

Pliquett, U., R. Langer, and J. C. Weaver. "Changes in the Passive Electrical Properties of Human Stratum Corneum due to Electroporation." *Biochim. Biophys. Acta*, **1239**:111-121, 1995 [a].

Pliquett, U., G. T. Martin, and J. C. Weaver. "Experimental Measurement of Localized Heating in Human Skin Subjected to "High-Voltage" Pulses." In Preparation.

Pliquett, U., and M. R. Prausnitz. "Electrical Impedance Spectroscopy for Rapid and Non-invasive Analysis of Skin Electroporation" In: *Electrically Mediated Delivery of Molecules to Cells: Electrochemotherapy, Electrogenetherapy, and Transdermal Drug Delivery by Electroporation, Methods in Molecular Medicine* (series), M. J. Jaroszeski, R. Gilbert, and R. Heller, Eds., Totowa, NJ: Humana Press, in press.

Pliquett, U., M. R. Prausnitz, Y. A. Chizmadzhev, and J. C. Weaver. "Measurement of Rapid Release Kinetics for Drug Delivery." *Pharm. Res.*, **12**:549-555, 1995 [b] (Errata in *Pharm. Res.*, **12**:1244, 1995).

Pliquett, U. F., R. Vanbever, G. T. Martin, V. Préat, and J. C. Weaver. "Molecular Transport across Stratum Corneum due to Electric Pulses: Behavior of Localized Transport Regions (LTRs)." In: *Electricity and Magnetism in Biology and Medicine*, New York: Plenum, in press.

Pliquett, U., R. Vanbever, V. Préat, and J. C. Weaver. "Local Transport Regions in Human Stratum Corneum due to Short and Long High-Voltage Pulses. Submitted.

Pliquett, U., and J. C. Weaver. "Electroporation of Human Skin: Simultaneous Measurement of Changes in the Transport of Two Fluorescent Molecules and in the Passive Electrical Properties." *Bioelectrochem. Bioenerg.*, **39**:1-12, 1996 [a].

Pliquett, U., and J. C. Weaver. "Transport of a Charged Molecule across the Human Epidermis due to Electroporation." *J. Control. Rel.*, **38**:1-10, 1996 [b].

Pliquett, U., T. E. Zewert, T. Chen, R. Langer, and J. C. Weaver. "Imaging of Fluorescent Molecule and Small Ion Transport through Human Stratum Corneum during High Voltage Pulsing: Localized Transport Regions are Involved." *Biophys. Chem.*, **58**:185-204, 1996 [b].

Potter, H. "Electroporation in Biology: Methods, Applications, and Instrumentation." *Anal. Biochem.*, **174**:361-373, 1988.

Potts, R. O., D. Bommannan, O. Wang, and J. A. Tamada. "Transdermal Peptide Delivery using Electroporation." In: *Protein Delivery, Physical Systems*, L. M. Sanders and R. W. Hendren, Eds., New York: Plenum Press, in press.

Potts, R. O., D. Bommannan, O. Wang, J. A. Tamada, J. E. Riviere, and N. A. Monteiro-Riviere. "Transdermal Peptide Delivery using Electroporation." *Pharm. Biotechnol.*, **10**:213-238, 1997.

Potts, R. O., and R. H. Guy. "Routes of Ionic Permeability through Mammalian Skin." *Solid State Ionics*, **53**:165-169, 1992.

Potts, R. O., R.H. Guy, and M.L. Francouer. "Routes of Ionic Permeability through Mammalian Skin." *Solid State Ionics*, **53**:165-169, 1992.

Powell, K. T., A. W. Morgenthaler and J. C. Weaver. "Tissue Electroporation: Observation of Reversible Electrical Breakdown in Vaible Frog Skin." *Biophys. J.*, **56**:1163-1171, 1989.

Prausnitz, M. R. "A Practical Assessment of Transdermal Drug Delivery by Skin Electroporation." *Adv. Drug Deliv. Rev.*, in press.

Prausnitz, M. R. "Do High-Voltage Pluses Cause Changes in Skin Structure?" *J. Control. Rel.*, **40**:321-326, 1996 [a].

Prausnitz, M. R. "Electroporation." In: *Electronically Controlled Drug Delivery*, B. Berner, and S. M. Dinh, Eds., Boca Raton, FL: CRC Press, 1998.

Prausnitz, M. R. *Electroporation of Tissue and Cells for Drug Delivery Applications.* Ph. D. Thesis, Massachusetts Institute of Technology, Cambridge, MA, 1994.

Prausnitz, M. R. "Reversible Skin Permeabilization for Transdermal Delivery of Macromolecules." *Crit. Rev. Ther. Drug Carrier Syst.*, **14**:455-483, 1997.

Prausnitz, M. R. "The Effects of Electric Current Applied to the Skin: A Review for Transdermal Drug Delivery." *Adv. Drug Deliv. Rev.*, **18**:395-425, 1996 [b].

Prausnitz, M. R. "Transdermal Delivery of Macromolecules: Recent Advances by Modification of Skin's Barrier Properties." In: *Stability, Formulation and Delivery of Peptides and Proteins.*, Z. Shahrokh, S. Shire, T. Randolph, J. Cleland, and V. Sluzky, Eds., Washington, DC: American Chemical Society, 1997 [b].

Prausnitz, M. R., V. G. Bose, R. Langer, and J. C. Weaver. "Electroporation." In: *Percutaneous Penetration Enhancers*, E. W. Smith and H. I. Maibach, Eds., Boca Raton, FL: CRC Press, 1995 [a].

Prausnitz, M. R., V. G. Bose, R. Langer, and J. C. Weaver. "Electroporation of Mammalian Skin: A Mechanism to Enhance Transdermal Drug Delivery." *Proc. Natl. Acad. Sci. USA*, **90**:10504-10508, 1993 [a].

Prausnitz, M. R., E. R. Edelman, J. A. Gimm, R. Langer, and J. C. Weaver. "Transdermal Delivery of Heparin by Skin Electroporation." *Bio/Technology*, **13**:1205-1209, 1995 [b].

Prausnitz, M. R., V. G. Bose, R. S. Langer, and J. C. Weaver. "Transtissue Molecular Transport due to Electroporation of Skin." In: *Electricity and Magnetism in Biology and Medicine*, M. Blank, Ed., San Francisco: San Francisco Press, 1993 [b].

Prausnitz, M. R., J. A. Gimm, R. H. Guy, R. Langer, J. C. Weaver, and C. Cullander. "Imaging of Transport Pathways across Human Stratum Corneum during High-Voltage and Low-Voltage Electrical Exposures." *J. Pharm. Sci.*, **85**:1363-1370, 1996 [a].

Prausnitz, M. R., C. S. Lee, C. H. Liu, J. C. Pang, T.-P. Singh, R. Langer, and J. C. Weaver. "Transdermal Transport Efficiency during Skin Electroporation and Iontophoresis." *J. Control. Release*, **38**:205-217, 1996 [b].

Prausnitz, M. R., U. Pliquett, R. Langer, and J. C. Weaver. "Rapid Temporal Control of Transdermal Drug Delivery by Electroporation." *Pharm. Res.*, **11**:1834-1837, 1994.

Prausnitz, M. R., D. S. Seddick, A. A. Kon, V. G. Bose, S. Frankenburg, S. N. Klaus, R. Langer, and J. C. Weaver. "Methods for *in Vivo* Tissue Electroporation Using Surface Electrodes." *Drug Deliv.*, **1**:125-131, 1993 [c].

Prausnitz, M. R., U. Pliquett, and R. Vanbever. "Mechanistic Studies of Skin Electroporation using Biophysical Methods." In: *Electrically Mediated Delivery of Molecules to Cells: Electrochemotherapy, Electrogenetherapy, and Transdermal Drug Delivery by Electroporation, Methods in Molecular Medicine* (series), M. J. Jaroszeski, R. Gilbert, and R. Heller, Eds., Totowa, NJ: Humana Press, in press.

Prausnitz, M., R. Vanbever, and V. Préat. "Macromolecules as Novel Transdermal Transport Enhancer for Skin Electroporation." In: *Electricity and Magnetism in Biology and Medicine*, F. Bersani, Ed., New York: Plenum Press, in press.

Préat, V. "Skin Electroporation." In: *Transdermal Drug Delivery*, 2nd Edition, R. Guy and J. Hadgraft, Eds., Marcell Dekker, in preparation.

Préat, V., and R. Vanbever. "Transdermal Drug Delivery by Electroporation." In: *Prediction of Percutaneous Penetration*, Volume 4, K. Brain, V. James, and K. Walters, Eds., 1996.

Préat, V., R. Vanbever, A. Jadoul, and V. Regnier. "Comparison of Iontophoresis and Electroporation: Mechanisms and Tolerance." In: *Electricity and Magnetism in Biology and Medicine*, F. Bersani, Ed., New York: Plenum Press, in press.

Raykar, P. V., M.-C. Fung, and B. D. Anderson. "The Role of Protein and Lipid Domains in the Uptake of Solutes by Human Stratum Corneum." *Pharm. Res.*, **5**:140-150, 1988.

Regnier, V., T. Le Doan, and V. Préat. "Parameters Controlling Topical Delivery of Oligonucleotides by Electroporation." *J. Drug Target.*, **5**:275-289, 1998.

Regnier, V., T. Le Doan, and V. Préat. "Topical Delivery of Phosphorothioate Oligonucleotides to the Skin by Electroporation." *J. Drug Target.*, in press [a].

Regnier, V., and V. Préat. "Localisation of a FITC-labelled Phosphorothioate Oligodeoxynucleotide in the Skin after Topical Delivery by Iontophoresis or Electroporation." *Pharm. Res.*, in press [b].

Regnier, V., and V. Préat. "Mechanisms of a Phosphorothioate Oligonucleotide Delivery by Skin Electroporation." *Int. J. Pharm.*, in press [c].

Regnier, V., A. Tahiri, N. André, M. Lemaître, T. Le Doan, and V. Préat. "Electroporation Mediated Delivery of 3'-Protected Phosphodiester Oligodeoxynucleotides to the Skin. Submitted.

Rigg, P. C., and B. W. Barry. "Shed Snake Skin and Hairless Mouse Skin as Model Membranes for Human Skin during Permeation Studies." *J. Invest. Dermatol.*, **94**:235-240, 1990.

Riviere, J. E., and M. C. Heit. "Electrically-Assisted Transdermal Drug Delivery." *Pharm. Res.*, **14**:687-697, 1997.

Riviere, J. E., N. A. Monteiro-Riviere, R. A. Rogers, D. Bommannan, J. A. Tamada, and R. O. Potts. "Pulsatile Transdermal Delivery of LHRH Using Electroporation: Drug Delivery and Skin Toxicology." *J. Control. Rel.*, **36**:229-233, 1995.

Roberts, J. B., and H. B. Lillywhite. "Lipid Barrier to Water Exchange in Reptile Epidermis." *Science*, **207**:1077-1079, 1980.

Roberts, J. B., and H. B. Lillywhite. "Lipids and the Permeability of Epidermis from Snakes." *J. Exp. Zool.*, **228**:1-9, 1983.

Rougier, A., D. Dupuis, C. Lotte, R. Rouguet, and H. Schaefer. "*In Vivo* Correlation between Stratum Corneum Reservoir Function and Percutaneous Absorption." *J. Invest. Dermatol.*, **81**:275-278, 1983.

Salford, L. G., B. R. R. Persson, A. Brun, C. P. Ceberg, P. C. Kongstad, and L. M. Mir. "A New Brain Tumour Therapy Combining Bleomycin with *in Vivo* Electropermeabilization." *Biochem. Biophys. Res. Com.*, **194**: 938-943, 1993.

Santus, G. C., and R. W. Baker. "Transdermal Enhancer Patent Literature." *J. Control. Release* , **25**:1-20, 1993.

Schaefer, H., and T. E. Redelmeier, Editors. *Skin Barrier: Principles of Percutaneous Absorption.* Basel: Karger, 1996.

Schwarz, V., C. H. Sutcliffe, and P. P. Style. "Some Hazards of the Sweat Test." *Arch. Dis. Childh.*, **43**: 695-701, 1968.

Scott, E. R., A. I. Laplaza, H. S. White, and J. B. Phipps. "Transport of Ionic Species in Skin: Contribution of Pores to the Overall Skin Conductance." *Pharm Res*, **10**:1699-1709, 1993.

Scott, E. R., H. S. White, and J. B. Phipps. "Direct Imaging of Ionic Pathways in Stratum Corneum Using Scanning Electrochemical Microscopy." *Solid State Ionics*, **53**:176-183, 1992.

Sears, F. W., M. W. Zemansky, and H. D. Young. *University Physics.* Reading, Massachusetts: Addison-Wesley, 1987.

Singh, P., and H. I. Maibach. "Iontophoresis: An Alternative to the Use of Carriers in Cutaneous Drug Delivery." *Adv. Drug Deliv. Rev.*, **18**:379-394, 1996.

Singh, J., and M. S. Roberts. "Transdermal Delivery of Drugs by Iontophoresis: A Review." *Drug Design Deliv.*, **4**:1-12, 1989.

Sloan, J. B., and K. Soltani. "Iontophoresis in Dermatology." *J. Am. Acad. Dermatol.*, **15**:671-684, 1986.

Stryer, L. *Biochemistry*, 3rd Edition. New York: W. H. Freeman, 1988.

Sukharev, S. I., A. V. Titomirov and V. A. Klenchin. "Electrically-Induced DNA Transfer into Cells. Electrotransfection *in Vivo*." *Gene Therapeutics: Methods and Applications of Direct Gene Transfer*, J. A. Wolff, Editor. Boston: Birkhäuser, 1994.

Swartzendruber, D. C., P. W. Wertz, K. C. Madison, and D. T. Downing. "Evidence that the Corneocyte has a Chemically Bound Lipid Envelope." *J. Inv. Dermatol.*, **88**:709-713, 1987.

Takahashi, K., S. Tamagawa, T. Katagi, J. H. Rytting, T. Nishihata, N. Mizuno. "Percutaneous Permeation of Basic Compounds through Shed Snake Skin as a Model Membrane." *J. Pharm. Pharmacol.*, **45**:882-886, 1993.

Tyle, P. "Iontophoretic Devices for Drug Delivery." *Pharm. Res.*, **3**:318-326, 1986.

Vanbever, R. *Skin Electroporation for Transdermal Drug Delivery.* Ph. D. Thesis, Université Catholique de Louvain, Brussels, Belgium, 1997.

Vanbever, R., N. De Morre, and V. Préat. "Transdermal Delivery of Fentanyl by Electroporation. II. Mechanisms Involved in Drug Transport." *Pharm. Res.*, **13**:1359-1365, 1996 [a].

Vanbever, R., D. Fouchard, A. Jadoul, N. De Morre, V. Préat, and J.-P. Marty. "*In Vivo* Non-Invasive Evaluation of Hairless Rat Skin after High-Voltage Pulse Exposure." *Skin Pharmacol. Appl. Skin Physiol.*, **11**:23-34, 1998 [a].

Vanbever, R., G. Langers, S. Montmayeur, and V. Préat. "Transdermal Delivery of Fentanyl: Rapid Onset of Analgesia Using Skin Electroporation." *J. Control. Rel.*, **50**:225-235, 1998 [b].

Vanbever, R., E. Le Boulengé, and V. Préat. "Transdermal Delivery of Fentanyl by Electroporation. I. Influence of Electrical Factors." *Pharm. Res.*, **13**:559-565, 1996 [b].

Vanbever, R., N. Lecouturier, and V. Préat. "Transdermal Delivery of Metoprolol by Electroporation." *Pharm. Res.*, **11**:1657-1662, 1994.

Vanbever, R., M.-A. Leroy, and V. Préat. "Transdermal Permeation of Neutral Molecules by Electroporation." *J. Control. Rel.*, in press.*J. Control. Rel.*, **54**:243-250, 1998 [c].

Vanbever, R., U. F. Pliquett, V. Préat, and J. C. Weaver. "Transdermal Transport and Changes in Skin Electrical Properties due to Short and Long High-Voltage Pulses." Submitted.

Vanbever, R., M. R. Prausnitz, and V. Préat. "Macromolecules as Novel Transdermal Transport Enhancers for Skin Electroporation." *Pharm. Res.*, **14**:638-644, 1997.

Vanbever, R., and V. Préat. "Factors Affecting Transdermal Delivery of Metoprolol by Electroporation." *Bioelectrochem. Bioenerg.*, **38**:223-228, 1995.

Vanbever, R., and V. Préat. "*In Vivo* Efficacy and Safety of Skin Electroporation." *Adv. Drug Deliv. Rev.*, in press. In: *Electrically Mediated Delivery of Molecules to Cells: Electrochemotherapy, Electrogenetherapy, and Transdermal Drug Delivery by Electroporation, Methods in Molecular Medicine* (series), M. J. Jaroszeski, R. Gilbert, and R. Heller, Eds., Totowa, NJ: Humana Press, in press.

Vanbever, R., and V. Préat. "Skin Electroporation for Transdermal Drug Delivery." In preparation.

Vanbever, R., D. Skrypczak, A. Jadoul, and V. Préat. "Comparison of Skin Electropertubations Induced by Iontophoresis and Electroporation." In: *Prediction of Percutaneous Penetration*, Volume 4, K. Brain, V. James, and K. Walters, Eds., 1996 [c].

Vanbever, R., J. C. Weaver, and V. Préat. "Skin Electroporation for Transdermal Drug Delivery." In: *Electricity and Magnetism in Biology and Medicine*, F. Bersani, Ed., New York: Plenum Press, in press.

Walters, K. A. "Penetration Enhancers and Their Use in Transdermal Therapeutic Systems." In: *Transdermal Drug Delivery: Developmental Issues and Research Inititatives*, J. Hadgraft and R. H. Guy, Editors. New York: Marcel Dekker, 1989.

Wang, S., M. Kara, and R. R. Krishnan. "Transdermal Delivery of Cyclosporin-A Using Electroporation." *J. Control. Rel.*, 50:61-70w 1998.

Wearley, L., J.-C. Liu, and Y. W. Chien. "Iontophoresis-Faciliated Transdermal Delivery of Verapamil. II. Factors Affecting the Reversibility of Skin Permeability." *J. Control. Release*, **9**:231-242, 1989.

Weaver, J. C. "Electroporation: A Dramatic Nonthermal Electric Field Phenomenon." *Electricity and Magnetism in Biology and Medicine*, M. Blank, Editor. San Francisco, California: San Francisco, 1993 [a].

Weaver, J. C. "Electroporation: A General Phenomenon for Manipulating Cells and Tissues." *J. Cell. Biochem.*, **51**:426-435, 1993 [b].

Weaver, J. C. "Electroporation in Cells and Tissues: A Biophysical Phenomenon due to Electromagnetic Fields." *Radio Sci.*, **30**:205-21, 1995 [a].

Weaver, J. C. "Electroporation Theory: Concepts and Mechanisms." In: *Molecular Biology: Methods*, J. A. Nickoloff, Ed., 1995 [b].

Weaver, J. C., and Y. A. Chizmadzhev. "Electroporation." In: *CRC Handbook of Biological Effects of Electromagnetic Fields*, 2nd Edition, C. Polk, and E. Postow, Editors. Boca Raton, Florida: CRC, 1996 [a].

Weaver, J. C., and Y. A. Chizmadzhev. "Theory of Electroporation: A Review." *Bioelectrochem. Bioenerg.*, **41**:135-160, 1996 [b].

Weaver, J. C., R. Langer, and R. O. Potts. "Tissue Electroporation for Localized Drug Delivery." In: *Electromagnetic Fields*, Washington, DC: American Chemical Society, 1995.

Weaver, J. C., R. Vanbever, T. E. Vaughan, and M. R. Prausnitz. "Heparin Alters Transdermal Transport Associated with Electroporation." *Biochem. Biophys. Res. Com.*, **234**:637-640, 1997.

Weaver, J. C., T. E. Vaughan, and Y. Chizmadzhev. "Theory of Electrical Creation of Aqueous Pathways across Skin Transport." *Adv. Drug Deliv. Rev.*, in press.

Weaver, J. C., T. E. Vaughan, and Y. Chizmadzhev. "Theory of Skin Electroporation: Implications of Straight-Through Aqueous Pathway Segments that Connect Adjacent Corneocytes." *J. Invest. Dermatol. Symp. Proc.*, **3**:143-147, 1998.

Wertz, P. W. and D. T. Downing. "Stratum Corneum: Biological and Biochemical Considerations." In: *Transdermal Drug Delivery: Developmental Issues and Research Initiatives*, J. Hadgraft and R. H. Guy, Editors. New York: Marcel Dekker, 1989.

Wester, R. C., and H. I. Maibach. "Animal Models for Percutaneous Absorption." In: *Models in Dermatology*, H. Maibach, and N. Lowe, Editors. Basel: Karger, 1985.

Wester, R. C., and H. I. Maibach. "Animal Models for Percutaneous Absorption." In: *Topical Drug Bioavailability, Bioequivalence, and Penetration*, V. P. Shah, and H. I. Maibach, Editors. New York: Plenum, 1993.

Whitaker, J. E., R. P. Haugland, P. L. Moore, P. C. Hewitt, M. Reese, and R. P. Haugland. "Cascade Blue Derivatives: Water Soluble, Reactive, Blue Emission Dyes Evaluated as Fluorescent Labels and Tracers." *Anal. Biochem.*, **198**:119-130, 1991.

Williams, A. R. *Ultrasound: Biological Effects and Potential Hazards*. New York: Academic, 1983.

Williams, A. C., and B. W. Barry. "Skin Absorption Enhancers." *Crit. Rev. Ther. Drug Carrier Syst.*, **9**:305-353, 1992.

Zewert, T. E., U. F. Pliquett, R. Langer, and J. C. Weaver. "Transdermal Transport of DNA Antisense Oligonucleotides by Electroporation." *Biochem. Biophys. Res. Com.*, **212**:286-292, 1995.

Zewert, T. E., U. Pliquett, R. Vanbever, T. Chen, R. Langer, and J. C. Weaver. "Electrical Creation of Very Large, Straight Through Aqueous Pathways across Human Skin: Chemical Enhancement Allows Rapid Transdermal Delivery of Macromolecules." In preparation.

Zhang, L., L. Li, Z. L. An, R. M. Hoffman, and G. A. Hofmann. "*In vivo* Transdermal Delivery of Large Molecules by Pressure-Mediated Electroincorporation and Electroporation: A Novel Method for Drug and Gene Therapy." *Bioelectrochem. Bioenerg.*, **42**:283-292, 1997.

Zlotogorski, A. "Iontophoresis in Dermatology." *J. Am. Acad. Derm.*, **17**:690, 1987.

The Appendices.*

In these appendices are detailed, step-by-step instructions on how to perform most of the experiments described in this thesis. Many technical problems have been addressed since the first skin electroporation experiments (Prausnitz, *et al.*, 1993 [a]), which have led to more complicated equipment, more rigorous procedures, and much more data to collect. Although these experiments are extremely time-consuming (preparing an experiment can take 2 to 3 h, the experiment itself can take another 2 to 5 h, and calibration and disassembly can take an additional 1 to 2 h; a single experiment can thus take up to 10 h to complete), it has been shown (see Section 7.2) that these careful techniques are, in fact, necessary for accurate measurements of the skin electroporation phenomenon.

The raw data has not been presented in this thesis, owing to the sheer volume of the data gathered. The computer data files take up approximately 425 MB of space; if printed out, even at roughly 5 000 closely spaced numbers per page, to show all of the data would still require over 86 000 pages!

*Many of these protocols and descriptions have also been reported in Chen, *et al.* (in press [a]).

I. Preparation of Human Skin.

Most of the human skin *in vitro* experiments are performed with a stratum corneum/epidermis preparation (no dermis). Since the stratum corneum is the main barrier for transport, the other layers of the skin are not important for studying transdermal drug delivery. The epidermis can usually be left on the stratum corneum without affecting either molecular transport or the electrical properties of the stratum corneum. However, the dermis can affect molecular transport, since it is much thicker (1 to 3 mm) than the stratum corneum (10 to 20 μ). Thus, the dermis is usually removed, leaving behind the epidermis and the stratum corneum.

In some experiments, the epidermis needs to also be removed, leaving behind just the stratum corneum. This can be done by using a dilute trypsin solution to digest away the epidermis. However, stratum corneum is very difficult to work with. It can tear very easily. Just picking up the stratum corneum can sometimes cause it to tear. Thus, it is usually simpler to leave the epidermis on as a mechanical support for the stratum corneum.

I.1. Preparation of the Epidermis (with the Overlying Stratum Corneum).

The procedure for removing the epidermis (including the overlying stratum corneum) from the dermis by heating the skin to 60 °C is commonly called "heat-stripping" (Gummer, 1989).

1. Cadaver skin should be stored at -80 °C for up to 6 months before use (Gummer, 1989). Cadaver skin should be fresh-frozen within 24 h post-op or post-mortem. It should be as hairless as possible. Good areas are the abdomen, thighs, or back. The skin should not be dermatomed or frozen with any preservative media.
2. To thaw the skin to room temperature, take the skin from the freezer and place it on an undisturbed counter for approximately 2 to 3 h (longer if the piece is large). Wait until the skin has been completely thawed.
3. Heat a bath of de-ionized water to 60 °C. It is very important that the temperature be as close to 60 °C as possible. The water bath should be sufficiently large that the addition of the skin will not significantly change the temperature of the water bath. Note that the temperature "window" at which the skin can be heat-stripped is very small. If the temperature is too low (<57 °C), the epidermis will not easily separate from the dermis. If the temperature is too high (>62 °C), the lipids in the stratum corneum will start to disorder, which permanently reduces the electrical resistance of the stratum corneum (Craane-Van Hisberg, *et al.*, 1994).

4. Immediately place the skin (removing any packaging) into the 60 °C water bath for 2 min.
5. Remove the skin and place it on a sheet of wax paper.
6. Using a blunt metal object (such as a rounded spatula), gently scrape away the epidermis from the stratum corneum. Hold the dermis firmly in place with a pair of tweezers while gently scraping away the epidermis. The epidermis can be folded up and moved aside during this process, but it should not be stretched or touched with anything sharp or metal. Try to keep the hair follicles with the epidermis.
7. Once the epidermis has been completely removed from the dermis, place the epidermis in a tray of clean, de-ionized water (do not use the 60 °C water bath).
8. At this point, the epidermis is probably folded up. Gently open the epidermis until it is floating as a flat sheet on top of the water. Metal objects of any kind should not be used. The stratum corneum (which is hydrophobic) should now be on top, and the epidermis (which is hydrophilic) is on the underside. For stratum corneum-only preparations, skip to Section I.2.
9. Take a sheet of wax paper, place it underwater, under the epidermis, and gently lift up the wax paper out of the water so the epidermis attaches to it and remains flat. Place the wax paper and skin on a cutting board. Note that several brands of wax paper will curl when soaked in water, which makes it very difficult to slide the paper under the floating epidermis. One type of wax paper that works well and does not curl is the 4 inch × 4 inch weighing paper that can be obtained from VWR.
10. Using a 3/4 inch diameter hole punch (Small Parts, Miami Lakes, FL) and a hammer, cut the skin and wax paper into 3/4 inch discs. Even with a new, sharp hole punch, it can be very difficult to cut completely through both the skin and the wax paper. The hole punch should be hit very hard, several times, to ensure a clean cut through both the skin and the wax paper. Keep the punches as close together as possible. Avoid any regions that are discolored or torn. Place the discs into a weigh boat.
11. The skin should be stored in a 4 °C, 95% humidity environment before use. Fill the bottom of a sealed glass chamber (such as a desiccation chamber) with a saturated solution of K_2SO_4 in water, which will maintain the chamber at 95% humidity. There should be a level within this chamber, away from the water, where the weigh boats will remain dry. Place the weigh boats containing the skin into this chamber. Under these conditions, the skin can last for 10 to 14 d before use (Gummer, 1989).

I.2. Preparation of Isolated Sheets of Stratum Corneum.

The stratum corneum can be isolated from the epidermis by soaking them overnight in a 0.25 wt% trypsin solution. This can be done either after the epidermis has been heat-stripped off of the dermis, or with the dermis still intact. However, with the dermis still in place, it will take much longer (up to several days) for the trypsin to soak through the dermis and the epidermis.

1. Prepare a solution of 0.25 wt% trypsin (Gibco BRL) in a sealable glass jar.
2. Place the heat-stripped epidermis (from Section I.1, Step 8, before punching out the circles) or the dermis into this solution and seal the jar shut.
3. Leave overnight (>12 h) at 4 °C.
4. Remove the skin from the jar, and rinse the skin gently with de-ionized water.
5. The epidermis should now have a "slime"-like consistency. This can be gently sloughed off either by hand or under a stream of PBS (Raykar, *et al.*, 1988). Be careful not to tear the stratum corneum.
6. Place the stratum corneum in a tray of clean, de-ionized water. Take a sheet of wax paper, place it underwater, under the stratum corneum, and gently lift up the wax paper out of the water so the stratum corneum attaches to it and remains flat. Place the wax paper and skin on a cutting board.
7. Using a 3/4 inch diameter hole punch (Small Parts, Miami Lakes, FL) and a hammer, cut the skin and wax paper into 3/4 inch discs. Keep the punches as close together as possible. Avoid any regions that are discolored or torn. Place the discs into a weigh boat.
8. The stratum corneum should be stored at 4 °C, 95% humidity before use. Fill the bottom of a sealed glass chamber (such as a desiccation chamber) with a saturated solution of K_2SO_4 in water, which will maintain the chamber at 95% humidity. There should be a level within this chamber, away from the water, where the weigh boats will remain dry. Place the weigh boats containing the stratum corneum into this chamber. Under these conditions, the stratum corneum can last for up to 10 d before use (Gummer, 1989).

II. The Original Skin Electroporation System of Prausnitz, *et al.* (1993 [a]).

This appendix describes the preparation of the original experimental system for studying skin electroporation. Although this system (shown in Figure II.1) was not actually used in this thesis, most of the equipmental designs and techniques used in this thesis were originally based on this system, which consisted of the following: a high-voltage pulser, a permeation chamber, two Ag/AgCl pulsing electrodes, and a 37 °C water bath. Many modifications were added later to address some of the inadequacies of this original system.

Some problems of this system include: no protection of the skin from the pulsing electrodes (pH changes and chemical by-products from the pulsing electrodes can contaminate the donor and receptor compartments), no direct measurement of the transdermal voltage, 1 h aliquot fluorescence measurements, DC skin resistance measurements (which causes iontophoresis of the skin), exponential pulsing time constants of 1.2 ms (which were reported as ~1 ms), uncertainty in the 5 s pulse spacing (the uncertainty was estimated at 5.0 ± 0.5 s), no degassing of PBS (oxygen dissolved in PBS can quench some of the fluorescent tracers), and multiple experiments using the same pulser performed simultaneously (which prevented accurate estimation of the transdermal voltage). Many of these problems were corrected in later "generations" of the equipment; the original system is described here for comparison purposes.

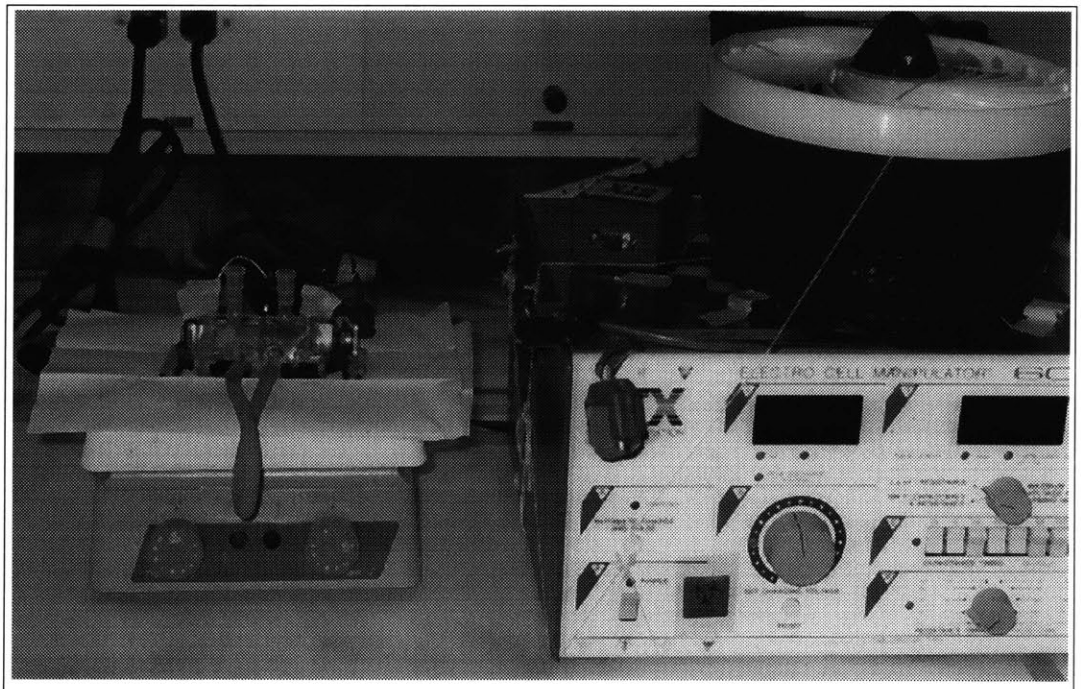

Figure II.1. The original skin electroporation system of Prausnitz, *et al.* (1993 [a]). The skin is placed within the side-by-side permeation chamber on the left (only one chamber shown here; there could be up to 10 different chambers in parallel). Ag/AgCl electrodes, connected to the custom-modified high-voltage pulser on the right, are placed on either side of the skin. The fan on top of the pulser is used to cool the circuitry within the pulser.

II.1. Modifying the High-Voltage Pulser.

In a commonly used protocol (Prausnitz, *et al.*, 1993 [a]; Prausnitz, *et al.*, 1995 [b]; Pliquett and Weaver, 1996 [a]; Prausnitz, *et al.*, 1996 [b]), the high-voltage pulser delivers a high-voltage, exponentially-decaying pulse to the permeation chamber once every ~5 s. There are no presumably no commercially available devices that can produce 1000 V exponentially-decaying voltage pulses into a load of ~500 Ω, at the rate of 1 pulse every ~5 s. Instead, a commercial pulser has to be internally modified to be able to deliver pulses at that rate (U. Pliquett, personal communication).

The procedure for modifying the internal workings of a high-voltage pulser will depend mainly on the pulser being modified. Modifying high-voltage equipment is extremely dangerous. Any modifications to the pulser should only be undertaken by a qualified electrical engineer, thoroughly familiar with high-voltage electronics. This work should be done in close consultation with the pulser manufacturer.

Briefly, the pulser needs to be modified so that it immediately begins recharging its capacitors after discharging each pulse (some pulsers require a button to be pressed to reset the pulser between pulses). A flip-flop timing circuit can be used to cause the pulser to discharge itself at a fixed frequency (here, 1 pulse every ~5 s). This timing circuit should be located near the pulse activation button, so as to avoid the high-voltage areas of the pulser (E. A. Gift, personal communication).

II.2. Typical Experimental Protocol from Prausnitz, *et al.* (1993 [a]).

The original permeation chamber design is shown schematically in Figure II.2 (Prausnitz, *et al.*, 1993 [a]; M. R. Prausnitz, personal communication). The permeation chambers are modified side-by-side glass diffusion chambers (Crown Bio Scientific), with an outer water jacket, and an inner compartment (Friend, 1992). Two or three ports extend from the inner compartment, through the water jacket, to the outside, allowing direct access to the inner compartment. The volume of the inner compartment is ~3.1 ml, and the area of the main opening is 0.63 cm^2 (0.9 cm in diameter).

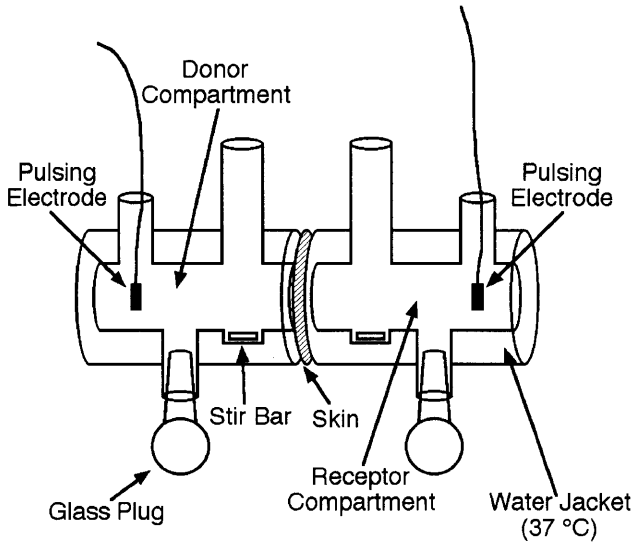

Figure II.2. Schematic diagram of the original permeation chamber.

1. Phosphate-buffered saline, PBS: 1.1 mM KH_2PO_4, 2.7 mM KCl, 8.1 mM Na_2HPO_4, 138 mM NaCl (total of 150 mM) in 500 ml de-ionized H_2O. Adjust to pH 7.4 with HCl and NaOH as necessary.

2. A typical donor solution consists of 1 mM of a hydrophilic fluorescent tracer in PBS. Examples of hydrophilic fluorescent tracers include lucifer yellow (457 Da) (Prausnitz, *et al.*, 1993 [a]; Chen, *et al.*, 1998 [c]), calcein (623 Da) (Prausnitz, *et al.*, 1993 [a]; Pliquett and Weaver, 1996 [a]; Vanbever, *et al.*, submitted), and sulforhodamine (607 Da) (Pliquett and Weaver, 1996 [a]) (all from Molecular Probes). Wrap the donor solution immediately in aluminum foil to protect it from light. Gently shake on a Nutator (Clay Adams, Becton Dickinson) for >30 min to ensure complete dissolution. This solution should be made immediately before use, right after the PBS solution has been made.

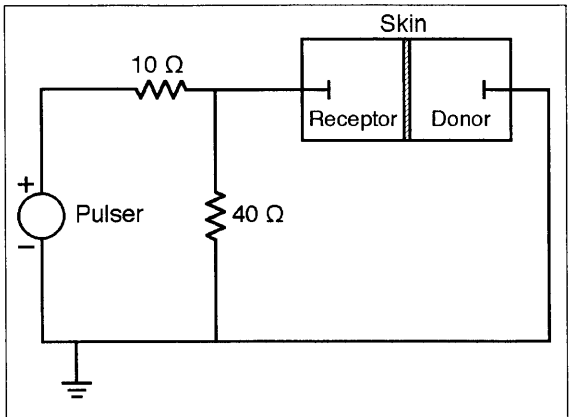

Figure II.3. Circuit diagram of the original experimental apparatus. There is a 40 Ω shunt pathway around the skin. The 10 Ω resistor is a safety device to protect the pulser in the event of a short circuit.

3. Assemble 1 to 10 chambers together. Connect each set to a 37 °C water bath.

4. In each chamber half, insert a Ag/AgCl pulsing electrode (In Vivo Metrics, Heraldsburg, CA). The electrodes may be too large to fit in the sampling port, so they must be inserted "tail-first" from the large opening where the skin belongs. Once inserted, they should be secured in place with tape, facing the opening for the skin.

5. The electrical circuit is shown in Figure II.3. The chamber is connected to the circuit so that the receptor pulsing electrode is positive and the donor electrode is grounded. This provides a favorable driving force for a negatively charged molecule. However, for a positively charged molecule, the positive and negative terminals to the chamber should be interchanged. This circuit will provide exponential pulses with a time constant of ~1.2 ms. The 10 Ω resistor is a safety device used to protect the system in the event of a short circuit.

6. Float a piece of skin (see Appendix I) in a dish of PBS for ~1 min.

7. Gently remove the wax paper backing. Do not use tweezers. The skin should float on the surface, with the stratum corneum side facing upwards.

8. Position the skin in the chamber so that the stratum corneum faces the donor compartment and the epidermis faces the receptor compartment. Clamp the chamber shut.

9. Fill the donor and receptor compartments with PBS.

10. Check the condition of the skin with a commercial ohmmeter. The resistance of "good skin" should be >50 kΩ cm^2 (70 kΩ for this chamber) (Prausnitz, *et al.*, 1993 [a]; M. R. Prausnitz, personal communication). The passive flux of the donor solution across the skin should be

negligible (below the detection limit of the spectrofluorimeter). Low resistances or large passive fluxes indicate that the integrity of the skin has been compromised in some way, and thus the skin should be discarded.

11. Add a 1.5 mm "flea"-type magnetic stir bar (VWR) to each compartment.
12. Connect the chamber to the pulsing circuit as shown in Figure II.3, verifying that the electrodes are properly connected.
13. Turn on the stirring plate and the water bath. Set the temperature of the water bath to 4 °C and leave the system running overnight (~12 h).
14. Flush the donor and receptor compartments 3× with PBS. Check the resistance of the skin again to verify that the skin is still good (the resistance of the skin may have drifted some from its previous reading). If the resistance has dropped below 50 kΩ cm^2 (70 kΩ), the skin should be discarded.
15. Wait 1 h, then empty the receptor compartment into a disposable polystyrene cuvette (VWR) for analysis, and flush the receptor compartment 3×with PBS.
16. Set the pulser to deliver the appropriate types of pulses, and start the pulser. Record the time. Verify that the pulses are being applied at the rate of 1 pulse every 5 s with a stopwatch.
17. After 1 h, stop the pulser. Empty the receptor compartment into a cuvette. Flush the receptor compartment 3×with PBS.
18. For the post-pulsing measurements, wait 1 h, then empty the receptor compartment into a cuvette. Flush the receptor compartment 3×with PBS. Repeat this step 3×(3 h total).
19. After 24 h, take a final measurement of the receptor compartment.

II.3. Mounting the Skin for Microscopy.

This procedure is from Prausnitz, *et al.*, (1996 [a])). The skin is mounted in a solution of glycerol/water and Nile Red, which prominently stains the lipid regions of the stratum corneum (Prausnitz, *et al.*, 1996 [a]). The skin can then be examined under fluorescence or confocal microscopy.

Note that fluorescence microscopy does not directly indicate the regions involved in molecular transport. The fluorescence observed under the microscope could be coming from either the surface or inside the skin (Pliquett, *et al.*, 1996 [b]; Chen, *et al.*, submitted [a]; also see Section 5.7). Some authors have established a correlation between the regions of fluorescence on the surface of the skin and the regions where molecular transport occurs (Pliquett, *et al.*, 1996 [b]).

1. To make the stock mounting solution, mix 10 mg Nile Red (Molecular Probes) in 20 ml acetone (Prausnitz, *et al.*, 1996 [a]). Wrap in aluminum foil to protect from light. This solution can be stored indefinitely if protected from light.
2. To make the final mounting solution, thoroughly mix 7.5 ml glycerol in 2.5 ml de-ionized water. Add 250 µl of the stock mounting solution (from above). Wrap in aluminum foil to protect from light. This solution can also be stored indefinitely if protected from light.
3. After the experiment has been finished, empty the donor compartment. Flush it out 3×with PBS.
4. Open the permeation chamber and carefully remove the skin. Place it carefully on a microscope slide. Gently spread the skin out so it lies flat, and lightly blot it dry with a paper towel. Do not rub the skin.
5. Add a drop of mounting solution (from Step 2).
6. Gently put a cover slip on top. This will cause the mounting solution to spread out and cover the skin. Seal in place with clear nail polish.

III. Chamber with Flow-Protected Electrodes.

The electrode flow-protection system, as described in this appendix, is designed to solve the problem of gas production and pH changes from the pulsing electrodes. Further refinements include the addition of a system for directly measuring the transdermal voltage, irrespective of any polarization effects at the pulsing electrodes.

The application of an electrical current to water causes the formation of O_2 gas at the positive electrode and H_2 gas at the negative electrode. Within a metal wire, the current is carried by free electrons, but within a hydrolytic solution such as PBS, the current is carried by free ions (H^+, OH^-, Na^+, Cl^-, etc.). The conversion between electrons and ions in solution are chemical reactions that occur at the electrode-electrolyte interface. At the positive electrode*, the following half-cell reaction occurs:

$$2H_2O \rightarrow 4H^+ + O_2\uparrow + 4e^-, \qquad \text{(III.1)}$$

leading to the production of oxygen gas and an increase in pH. At the negative electrode, the following half-cell reaction occurs:

$$2H_2O + 2e^- \rightarrow 2OH^- + H_2\uparrow, \qquad \text{(III.2)}$$

causing the formation of hydrogen gas and a drop in pH. Together, these two half-cell reactions form the hydrolytic or "water-splitting" electrochemical reaction that can be found in any elementary chemistry textbook (Metcalfe, *et al.*, 1986):

$$2H_2O \rightarrow 2H_2 + O_2. \qquad \text{(III.3)}$$

Therefore, the design of the permeation chamber should not be to prevent the formation of gas, which is unavoidable, but to prevent these gases and chemical by-products from reaching the donor and receptor chambers.

The electrodes are encased in polyacrylamide gel, protected by a stream of fresh PBS continuously flowing past the electrodes. Polyacrylamide gel was chosen since it was electrically conducting, chemically inert, and easy to prepare. The electrical resistance of polyacrylamide gel was similar to that of PBS, since its structure is largely composed of polymer strands, surrounded by bulk solution. It is frequently used in polyacrylamide gel electrophoresis, where proteins on a polyacrylamide gel are

*The terms "cathode" and "anode" are not always used consistently in the electrochemistry literature, so the unambiguous terms "positive electrode" and "negative electrode" are used here instead. The positive electrode (usually colored red) is the high-voltage line; the negative electrode (usually colored black) is grounded. The electrons flow from the negative electrode to the positive electrode; however, the current nonintuitively flows from the positive electrode to the negative electrode (by convention).

placed in a strong electrical field to separate them on the basis of their charge (in addition, sodium dodecyl sulfate is often added to separate proteins on the basis of their size) (Stryer, 1988).

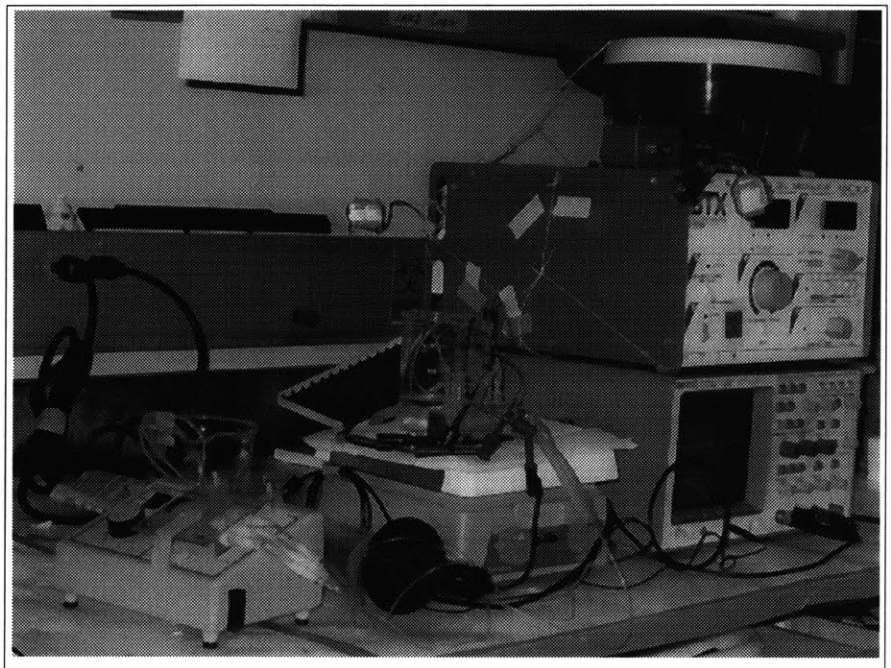

Figure III.1. Permeation chamber with flow-protected electrodes. The small pump on the left pumps fresh PBS from the PBS reservoir (behind the pump), through the permeation chamber and around the pulsing electrodes, to the waste beaker (behind the chamber). Pulses are applied with the custom-modified high-voltage pulser (top right), connected to silver wire electrodes within the chamber. The high-voltage probe (behind the pump), connected to the oscilloscope on the lower right, goes to two additional measurement electrodes within the chamber. A second voltage probe (not visible behind the stirring plate) is connected to a 1.2 Ω resistor in series with the chamber, to measure the current during pulsing.

Chemical by-products that are produced at the pulsing electrodes cross a stream of PBS (~6 ml/min, or ~0.6 cm/s), and 2 cm of solid polyacrylamide gel before reaching the inner compartments. The transit time for this process takes several hours (Section 4.1.8), much longer than the experiment itself. Note that all of these measurements and tests were conducted with the short pulses ($\tau \sim 1$ ms). Most of the experiments in this thesis used short pulses. For long pulses ($\tau \geq 100$ ms), the volume of gas production exceeds the capacities of this system, and can cause the polyacrylamide gel within the chamber to fracture. Thus, the experimental system, as described in this appendix, cannot be used to protect the pulsing electrodes when long pulses are used.

The pulsing electrodes are silver wire electrodes instead of the Ag/AgCl electrodes. Since a high-voltage probe is used to directly measure the transdermal voltage, any electrode polarization that may be occurring at the electrode-electrolyte interface can thus be ignored. In addition, with the Ag/AgCl electrodes, after only a few pulses, enough of the AgCl plating is removed so that the silver becomes directly exposed to the solution. Using Ag/AgCl electrodes to avoid polarization effects is not an effective solution; therefore, a system to directly measure the transdermal voltage was added here.

III.1. Solutions.

The day before the experiment, prepare Solutions 1 through 5 (Solution 5, PBS, is needed to prepare Solution 1). On the day of the experiment, prepare Solutions 5 (again) and 6, since these solutions can not be stored and have to be used immediately.

1. Acrylamide monomer solution: 7.5 g of 19:1 acrylamide:bis(N,N'-methylene-bis-acrylamide) powder (Bio-Rad, Hercules, CA) in 50 ml PBS (Solution 5, below). Prepare and mix together in a fume hood (the monomer is carcinogenic). Let the solution stand for >12 h before using, to allow the monomer to fully dissolve. This solution can be prepared well in advance of the experiment; it will not polymerize without addition of the catalyst.
2. Stock mounting solution: 10 mg Nile Red (Molecular Probes) in 20 ml acetone (Prausnitz, *et al.*, 1996 [a]). Wrap in aluminum foil to protect from light. This solution can be stored indefinitely if protected from light.
3. Final mounting solution: 7.5 ml glycerol in 2.5 ml de-ionized water and mix thoroughly. Add 250 µl of the stock mounting solution (Solution 2). Wrap in aluminum foil to protect from light. This solution can also be stored indefinitely if protected from light.
4. Acrylamide initiator solution: 0.3 g $(NH_4)_2S_2O_8$ in 3 ml H_2O. This solution can be stored for only a week.
5. Phosphate-buffered saline, PBS: 1.1 m$\underline{M}$ KH_2PO_4, 2.7 m$\underline{M}$ KCl, 8.1 m$\underline{M}$ Na_2HPO_4, 138 m$\underline{M}$ NaCl (total of 150 m$\underline{M}$) in 500 ml de-ionized H_2O. Stir under vacuum for >30 min to remove dissolved gases from solution. Both light and O_2 can cause the quenching of fluorescent molecules, but this effect can be reduced by removing the dissolved gases from PBS, and protecting the solution from light whenever possible. Adjust to pH 7.4 with HCl and NaOH. This solution should be degassed immediately before use.
6. A typical donor solution consists of 1 m$\underline{M}$ of a hydrophilic fluorescent tracer in PBS (see Chapter 4). Examples of hydrophilic fluorescent tracers include lucifer yellow (457 Da) (Prausnitz, *et al.*, 1993 [a]; Chen, *et al.*, 1998 [c]), calcein (623 Da) (Prausnitz, *et al.*, 1993 [a]; Pliquett and Weaver, 1996 [a]; Vanbever, *et al.*, submitted), and sulforhodamine (607 Da) (Pliquett and Weaver, 1996 [a]) (all from Molecular Probes; see Chapter 4). Wrap the donor solution immediately in aluminum foil to protect it from light. Gently shake on a Nutator (Clay Adams, Becton Dickinson) for >30 min to ensure complete dissolution. This solution should be made immediately before use, right after preparing the PBS solution.

III.2. Electrode Fabrication.

The permeation chambers are custom-designed, side-by-side glass diffusion chambers (Crown Bio Scientific), with an outer water jacket (to maintain the temperature at 37 °C) and an inner compartment (Figure III.2) (Friend, 1992). Side-by-side permeation chambers (where the skin is mounted vertically), are preferable to vertical permeation chambers (where the skin is mounted horizontally) for two reasons. First, any bubbles produced by the electrodes can easily be removed from the system, before they reach the skin. In a vertical chamber, the bubbles would float upwards towards the skin. Second, mounting the skin vertically eliminates gravity as a possible driving force, which is important for mechanistic studies. Here, gravity includes effects such as the weight of the liquid pushing down on the skin.

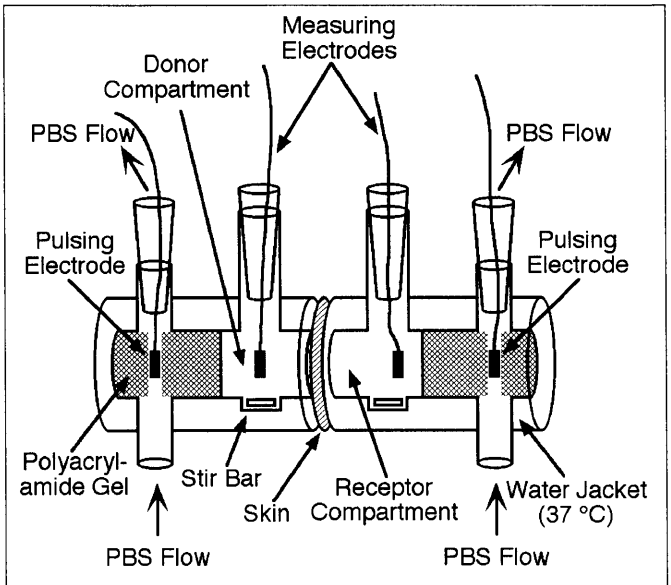

Figure III.2. Schematic diagram of chamber with flow-protected electrodes. PBS is pumped around the outer electrodes to remove any chemical by-products produced by the electrodes.

Ports extend from the inner compartment, through the water jacket, to the outside, allowing direct access to the inner compartment. Each chamber half has one large port (for sampling) and two smaller additional ports on the far ends (for placement of the pulsing electrodes and the flow-protection system around the electrodes). The volume of the inner compartment is ~3.1 ml, and the area of the circular opening is 0.64 cm^2 (0.9 cm diameter).

There are four electrodes in this system (Figures III.2, III.3, and III.4). The two outer electrodes are used for pulsing, and the two inner electrodes for measuring the transdermal voltage. There are two sets of electrodes: the inner measuring electrodes, and the outer pulsing electrodes.

The electrodes are made from silver wire, and the connectors are made from 200 µl pipette tips, with assorted amounts of tubing, all held in place by epoxy (Devcon). While the electrodes are generally reusable between experiments if sufficiently cleaned with fine-grain sandpaper, they should be periodically examined. Worn-out or broken electrodes should be discarded. The pulsing electrodes can typically survive about a month of intense use before wearing out; the measurement electrodes can last somewhat longer.

III.2.1. Measurement Electrode Fabrication.

The main requirement for the measurement electrodes are that they should not be able to move once they are snugly placed within the chamber (Figure III.3).

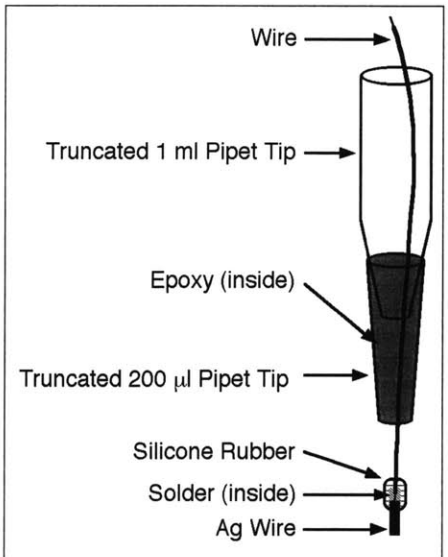

Figure III.3. Measurement electrode fabrication. Only the silver wire electrode is exposed to the donor solution; the solder is encased in nonconducting silicone rubber.

1. Cut off a piece of pure silver wire, ~0.040 inch diameter, ~0.5 cm long.
2. Solder the end of the silver wire to a piece of copper bell wire, as shown in Figure III.3.
3. Once the solder hardens, cover the solder (but not the silver wire) with nonconducting silicone rubber (General Electric). Use as little silicone rubber as possible, but make sure that the solder is completely covered. Wait for the silicone rubber to harden (~1 d).
4. Cut the end off a 200 µl pipette tip. The hole at the end of the pipette should be just large enough to accommodate the wire.
5. Insert the wire with the silver electrode up through the end of the pipette tip. The silver electrode should be placed so that when the pipette tip is placed snugly into the large port of the permeation chamber, the silver electrode is positioned in the middle of the chamber.
6. If the 200 µl pipette tip is smaller than the large port, it could get stuck inside. Thus, a "handle" is needed, so that there is a way to remove the pipette tip from the chamber (Figure III.3). Cut the end off a 1 ml pipette tip so that the copper bell wire will just fit through the opening. Slide the electrode wire through this pipette tip.
7. Completely fill the 200 µl pipette with epoxy. Immediately insert the 1 ml pipette tip into the epoxy at the top of the 200 µl pipette tip. Hold everything in place until the epoxy cures, and verify that the silver wire does not move while the epoxy is curing.

III.2.2. Pulsing Electrode Fabrication.

Each pulsing electrode is designed to allow electrical pulses to be applied, as well as allowing a stream of PBS to flow around the electrode and out to a waste beaker (Figure III.4). A separate port in the permeation chamber supplies fresh PBS to the pulsing electrode (see Figure III.2).

1. Cut off a piece of pure silver wire, ~0.040 inch diameter, ~0.5 cm long.
2. Solder the end of the silver wire to a piece of copper bell wire, as shown in Figure III.4. Keep the solder to a minimum, since the entire electrode, when completed, must still fit within the small port of the permeation chamber.
3. Once the solder hardens, cover the solder (but not the silver wire) with nonconducting silicone rubber. Use as little silicone rubber as possible, but make sure that the solder is completely covered. This will ensure that the electrical pulses are delivered by only the silver, not the solder. Wait for the silicone rubber to harden (~1 d).
4. Cut the end off a 200 µl pipette tip. The hole at the end of the pipette should be slightly larger than the bell wire, so that there is room for PBS to flow around the wire.

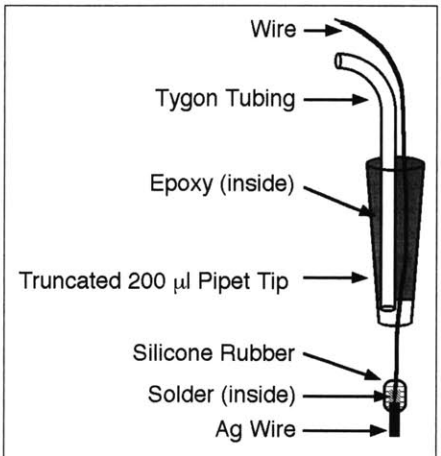

Figure III.4. Pulsing/flow-protection electrode fabrication. This electrode is similar to the previous electrode (see Figure III.3), except an additional tube permits the continuous flow of PBS around the electrode, to control the pH and allow for the removal of chemical by-products.

5. Insert the wire with the silver electrode up through the end of the pipette tip, as shown above in Figure III.4. The silver electrode should be placed so that when the pipette tip is placed snugly into the small port of the permeation chamber, the silver electrode is positioned in the middle of the chamber.
6. Cut off a piece of Tygon tubing, 1/32 inch ID, ~3 inches long. Insert it into the wider end of the pipette as far as possible, wedging the bell wire into place.
7. Fill the wider end of the pipette with epoxy, to fix both the tubing and the wire in place. The epoxy should completely seal off the end of the pipette. Make sure that the epoxy does not flow far enough into the pipette tip so that it covers the opening of the tubing, and verify that the wire and the tubing do not move while the epoxy is curing.

III.3. Electrode Flow-Protection System.

Each of the two pulsing electrodes is continuously washed in a stream of PBS, pumped by a peristaltic pump. For each of the pulsing electrodes, PBS is pumped from a reservoir into each compartment through the side ports, up around the electrode (channeled by the polyacrylamide gel), and then up through the tubing connected to the pulsing electrodes. From there, the PBS flows into a waste flask (Figure III.5).

Since the purpose of the flow-protection system is to wash any chemical by-products out of the system, the pumps for this system do not need to be very precise. A good flowrate is ~6 ml/min per

electrode. Tygon tubing should be used to connect the reservoir, the pumps, and the permeation chamber together. The tube fittings needed to connect the tubing to the pump and the chamber will vary, depending on the type of equipment available. If a connector to the chamber is not available, a good one can be made by epoxying a piece of Tygon tubing to a pipet tip.

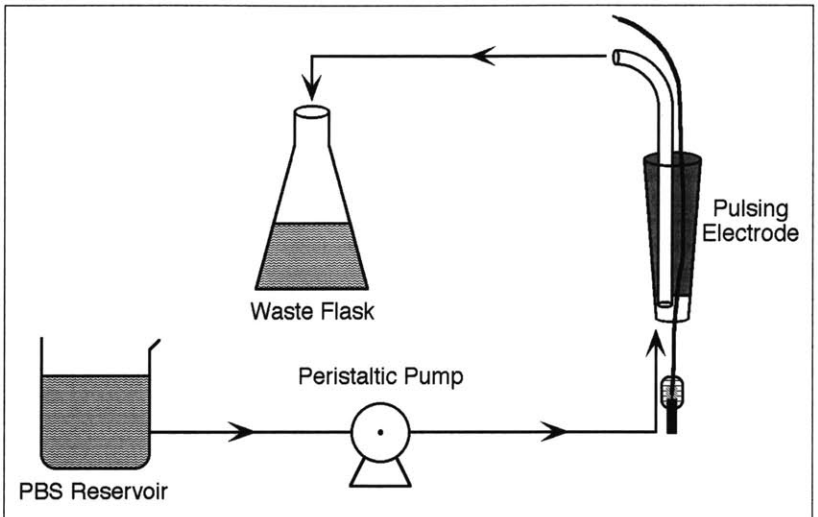

Figure III.5. Liquid circuit for a flow-protected pulsing electrode. There are two pulsing electrodes, so this arrangement is used twice. PBS is pumped into the permeation chamber from the PBS reservoir, up through the pulsing electrode, to a waste flask.

III.4. The Electrical Circuit.

All of the components in the electrical circuit (shown in Figure III.6), including the wires and the clip leads, should be able to withstand high voltages and positioned with safety in mind. The electrical circuitry should be set up in a protected area away from the permeation chamber (e. g., on a different bench), so that any fluid leaks or spills cannot reach the electrical components. Modifications to the high-voltage pulser have previously been discussed in Section II.1.

The chamber is connected to the circuit so that the receptor pulsing electrode is positive and the donor electrode is grounded (Figure III.6). This arrangement provides a favorable driving force for a negatively charged molecule. However, for a positively charged species, the positive and negative terminals to the chamber should be interchanged.

The 9.8 Ω resistor is a safety device used to protect the system in the event of a short circuit. It should

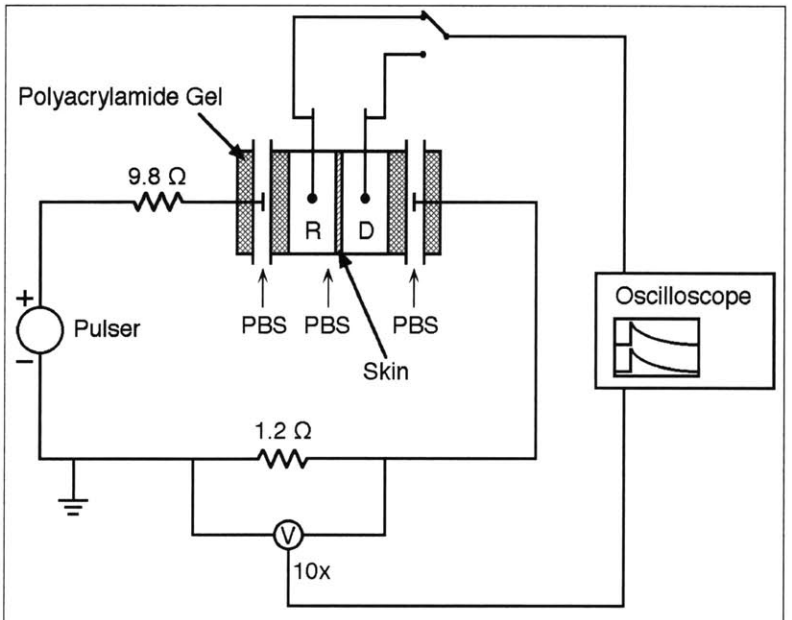

Figure III.6. Circuit diagram for transdermal voltage measurements. The 9.8 Ω resistor is a safety device in the event of a short circuit. The transdermal voltage is measured by a high-voltage probe, and the current is measured by a 10× voltage probe across a 1.2 Ω resistor placed in series with the chamber. R indicates the receptor compartment and D indicates the donor compartment. The two outer PBS streams and the polyacrylamide gel around the pulsing electrodes are used to prevent chemical contamination of the donor and receptor compartments by the electrodes.

be a 50 W (or higher) noninductive power resistor.

Since the 1.2 Ω resistor is in series with the skin, it can be used to measure the current across the skin during pulsing. It should be a 50 W (or higher) noninductive power resistor. A 10× voltage probe from the digital oscilloscope should be connected across the 1.2 Ω resistor. Once the voltage drop across the resistor is known, the current can be determined by applying Ohm's law (Equation 3.2)..

The donor and receptor compartments each contain a measuring electrode. A grounded high-voltage probe (Tektronix) is sequentially used to measure the voltages on either side of the skin.

III.5. Impedance Measurement Circuit.

The resistance of the skin should be checked to make sure the skin is in good condition. However, an ohmmeter or other DC source should not be used to measure the resistance of the skin, since it may cause iontophoresis during the measurement. Some commercial ohmmeters can apply voltages up to ~5 V during ordinary resistance measurements. In "good" skin, these ohmmeters can generate very large current densities in the skin, sometimes more than ~0.5 mA / cm^2. A current density of 0.5 mA / cm^2 is also the maximum current density that can be applied to the skin in humans during iontophoresis. Thus, such ohmmeters should never be used to measure the resistance of the skin.

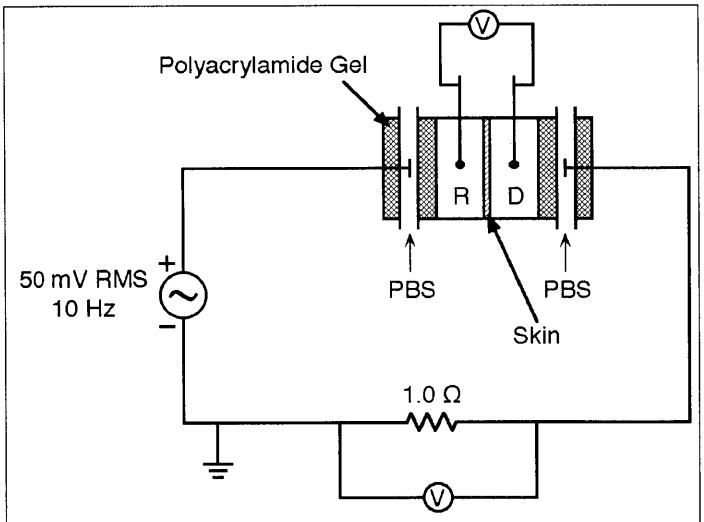

Figure III.7. Circuit diagram for measuring the impedance of the skin. The AC source produces a 50 mV RMS, 10 Hz bipolar sine wave. The current across the skin can be determined by measuring the RMS voltage across the 1.0 Ω resistor in placed series with the skin. The voltage across the skin can be determined with the voltmeter placed across the permeation chamber (ignoring the contribution due to PBS, which is negligible compared to the skin). The impedance of the skin can then be found by Ohm's Law.

A bipolar sinusoidal AC voltage source does not deliver a net current to the skin, and should be used instead of a DC source. However, using an AC voltage source gives the impedance, not the resistance, of the skin. At low frequencies (<1 kHz), the skin's impedance approximates its resistance, but at higher frequencies, the capacitance of the skin can introduce errors. Thus, besides low RMS voltages (<0.1 V), low frequencies (10 Hz or 100 Hz) should be used.

Although commercial test equipment is available (e. g., Model 5R715 LCR Meter, Stanford Research Systems), a skin impedance tester can also be set up using an AC sinewave generator. This circuit is

shown in Figure III.7. The AC source should be able to produce a 10 Hz, 50 mV (peak-to-peak) bipolar sine wave. For a good piece of skin, the maximum RMS current this system will produce is ~1 μA.

In this circuit, the impedance of the skin can be determined by measuring the RMS voltage across the 1.0 Ω resistor. From this value, Ohm's Law gives the current (which should be <1 μA). The voltage drop across the skin, divided by the current, gives the skin's impedance.

III.6. Resistance of PBS.

The skin, PBS, and some polyacrylamide gel are located between the two measurement electrodes. The resistivities of the PBS and the polyacrylamide gel are constant, but should be measured.

1. Make up a solution of PBS (Solution 5 in Section III.1).
2. Prepare the permeation chamber, with the four electrodes and the polyacrylamide gel (described below in Section III.7).
3. Fill the chamber with PBS.
4. Connect the high-voltage pulser and the flow-protection system to the chamber (see Figure III.6). Heat the chamber to 37 °C using the water jacket (the resistivity of PBS is a function of temperature).
5. Manually apply pulses to the chamber, starting from 0 V and increasing in units of 100 V, up to 1000 V. Apply 5 to 10 pulses per setting. For each pulse, record the voltage drops appearing across the inner measurement electrodes (U_{inner}) and the 1.2 Ω resistor (U_{curr}, given that $R_{curr} = 1.2\ \Omega$).
6. To find the current (I), apply Ohm's law to the 1.2 Ω resistor:

$$I = \frac{U_{curr}}{R_{curr}} = \frac{U_{curr}}{1.2\ \Omega}. \qquad \text{(III.4)}$$

7. Plot the voltage drop across the inner measurement electrodes (U_{inner}) versus the current (I). The slope of the line is the resistance of the PBS and the polyacrylamide gel (lumped together in one variable, R_{PBS}) between the two measurement electrodes:

$$R_{PBS} = \frac{U_{inner}}{I}. \qquad \text{(III.5)}$$

III.7. Permeation Chamber Preparation.

The polyacrylamide gel around each pulsing electrode directs PBS in and out of the chamber, without contacting the donor or receptor solutions (this is the hollowed-out regions that run around each of the two pulsing electrodes in Figure III.2).

III.7.1. Preparation of the Mold.

Acrylamide in solution takes approximately 10 min to polymerize into polyacrylamide gel. In this time, the acrylamide solution has to poured into the chamber. To create the channels that run through the polyacrylamide gel, plastic tubes are inserted into the chamber, which are then removed once the acrylamide has polymerized. Preparing the mold for the permeation chambers can be done the day before the experiment.

1. Find two flexible plastic tubes, approximately 9 inches long, that will fit through the two small ports on each chamber half.
2. Slide the plastic tubes through these ports (use tweezers as needed), so that roughly 1 to 2 inches of tubing protrudes out on either side. These tubes are the mold for the electrode flow-protection channel.
3. Place Parafilm (American National Can) around each opening tightly. Use two layers of Parafilm. This should create a watertight seal around the openings, so the acrylamide solution does not leak out.
4. Position each of the two chambers sideways, so that the large opening (where the skin is located) is on top. The chambers should be braced in some fashion (propping them up on pencils or test tubes) so that they can not tip or move when filled with liquid.

III.7.2. Adding the Polyacrylamide Gel.

Acrylamide monomer in solution (Solution 1, from Section III.1) will polymerize into a gel in approximately 10 min upon addition of a catalyst (N,N,N',N'-tetramethylethylenediamine) (Bio-Rad) and a free radical initiator (Solution 4). Synthesis of the polyacrylamide gel should be performed just before the experiment (the chambers should already be prepared), since the polyacrylamide gel will begin dehydrating after a few hours.

1. Thoroughly mix together 10 ml of acrylamide solution (Solution 1 from Section III.1), 87.5 µl of the initiator (Solution 4), and 6 µl of N,N,N',N'-tetramethylethylenediamine in a 15 ml test tube.
2. For each chamber half, immediately pour in the acrylamide solution so that it reaches the level of the large port. This should leave a donor volume of ~2.1 ml.
3. Do not disturb the chambers while the gel is polymerizing, as disturbances will cause the gel to take longer to harden, and the gel will set poorly as a result. It takes ~10 min for the gel to harden. Any leftover acrylamide solution can be used to monitor the gelling process.
4. After the gel forms, carefully remove the Parafilm around the each of the plastic tubes of the electrode flow-protection system. Remove the plastic tubes through one of the small ports.
5. Before using, fill the permeation chambers with PBS to keep the polyacrylamide gel from drying out.

III.8. Preparing the Equipment.

On the day of the experiment, the following should have already been prepared and assembled: Solutions 1 through 4 (Section III.1), the permeation chamber and the electrodes (Sections III.2 and III.7.1), the electrode flow-protection system (Section III.3), the electrical circuit (Section III.4), the high-voltage pulser (Section II.1), the skin (Section I.1), and the impedance meter (Section III.5). Immediately before the experiment, Solutions 5 and 6 (Section III.1), and the polyacrylamide gel in the chamber (Section III.7.2) need to be prepared. Once the gel in the chamber is ready, place the chamber on a magnetic stirring plate and connect it to a 37 °C water bath.

III.9. Loading the Skin into the Chamber.

The condition of the skin is checked by measuring its electrical impedance and monitoring the passive flux of the donor solution. The impedance of "good skin" should be >25 $k\Omega\,cm^2$ at 100 Hz (Prausnitz, *et al.*, 1993 [a]; Chen, *et al.*, 1998 [b]; M. R. Prausnitz, personal communication; Gowrishankar, personal communication). The passive flux of the donor solution across the skin after 1 h should be negligible (below the detection limit of the spectrofluorimeter). Low impedances or large passive fluxes indicate that the skin's integrity has been compromised in some way. This could be due to a hole in the skin, shearing of the skin during the loading process, or the poor quality of skin's preservation *post mortum*.

The impedance is measured across the two measurement electrodes in the permeation chamber. However, besides the skin, this measurement also includes PBS and the polyacrylamide gel. The other

impedances can be neglected, though, since the impedance of the skin is much larger than PBS (see Section 3.5).

1. Float a piece of skin (see Section I.1) in a dish of PBS for ~1 min.
2. Gently remove the wax paper backing. Do not use tweezers. The skin should float on the surface, with the stratum corneum side facing upwards.
3. Position the skin in the chamber so that the stratum corneum faces the donor compartment and the epidermis faces the receptor compartment. Clamp the chamber shut.
4. Fill the donor and receptor compartments with PBS.
5. Connect the impedance meter (see Section III.5) to the measurement electrodes. Good skin has an impedance >25 $k\Omega\ cm^2$ at 100 Hz. Poor skin should be discarded.
6. Disconnect the impedance meter.
7. Remove PBS from the donor compartment and add donor solution (Solution 6 from Section III.1). Add 1.5 mm "flea"-type magnetic stir bars to the donor and receptor compartments.
8. Connect the chamber to the pulsing circuit as shown in Figure III.6.
9. Turn on the stirring plate and the water bath.

III.10. Applying Pulsing.

High-voltage pulses should be applied to the skin at the rate of 1 pulse every ~5 s. Both the time constant and the applied voltage should be set on the pulser as needed before pulsing is started. The transdermal voltage is a nonlinear function of the applied voltage (see Figures 7.10 and 8.3) (Pliquett, *et al.*, 1995 [a]; Chen, *et al.*, 1998 [c]). Thus, given a desired transdermal voltage, a guess of the applied voltage should be made at this time.

1. After 1 h (passive control), make a measurement of the receptor chamber fluorescence. If the fluorescence is significantly higher than the background, then the skin is leaking and should be discarded.
2. Set the pulser to deliver the appropriate types of pulses.
3. Gradually start the pumps for the electrode flow-protection system. Make sure that the polyacrylamide gel in the chamber does not crack or break when this is turned on. If the gel breaks, new gel will have to be made, and the experiment will have to be aborted.
4. Start the pulser. Record the time the experiment was started, and monitor the pulses to make sure they are being applied at the correct rate (i. e., 1 pulse every 5 s).

5. Every 15 min (starting at time 0), record the voltage in the donor and receptor compartments. With a grounded high-voltage probe, these measurements should be made on subsequent pulses. Also record the current through the 1.2 Ω resistor.
6. After pulsing, turn off the pumps. Make a measurement of the receptor chamber fluorescence.
7. Mount the skin for fluorescence microscopy, as described in Section II.3.

III.11. Calculating Transdermal Voltages.

The voltage drop across the skin can be determined by applying Ohm's Law to the current and the voltage. The resistance of the intervening PBS (R_{PBS}) should already be known (see Sections 3.5 and III.6).

1. Ohm's Law is used to convert the average voltage drop (U_{curr}) across the 1.2 Ω resistor (R_{curr} = 1.2 Ω):

$$I = \frac{U_{curr}}{R_{curr}} = \frac{U_{curr}}{1.2\ \Omega}. \qquad \text{(III.6)}$$

2. The current across the skin (I) and the voltage drop across the measurement electrodes (U_{inner}) should now be known. To calculate the transdermal voltage (U_{skin}), use the following equation:

$$U_{skin} = U_{inner} - I\,R_{PBS}. \qquad \text{(III.7)}$$

IV. Chamber with Flow-Through System for Real-Time Measurements.

Although this is not the first flow-through system for studying skin permeation, with a working volume of only 400 μl, it has one of the highest time resolutions of any flow-through system — 14 s (Figure IV.1). This is necessary for studying skin electroporation phenomenon, where many dramatic changes can occur after only a few of pulses (Prausnitz, *et al.*, 1994; Pliquett and Weaver, 1996 [a]; Chen, *et al.*, 1998 [c]).

In addition to the flow-protected electrodes and the transdermal voltage measurement system described in Appendix III, the system in this appendix will also measure both the molecular flux and the transdermal voltage on an almost per-pulse basis (if pulses are applied at the rate of 1 pulse every 5.56 s, a time resolution of ~14 s covers a little less than 3 pulses).

IV.1. Solutions.

The day before the experiment, prepare Solutions 1 through 5 (Solution 5, PBS, is needed to prepare Solution 1). On the day of the experiment, prepare Solutions 5 (again) and 6, since these solutions can not be stored and have to be used immediately.

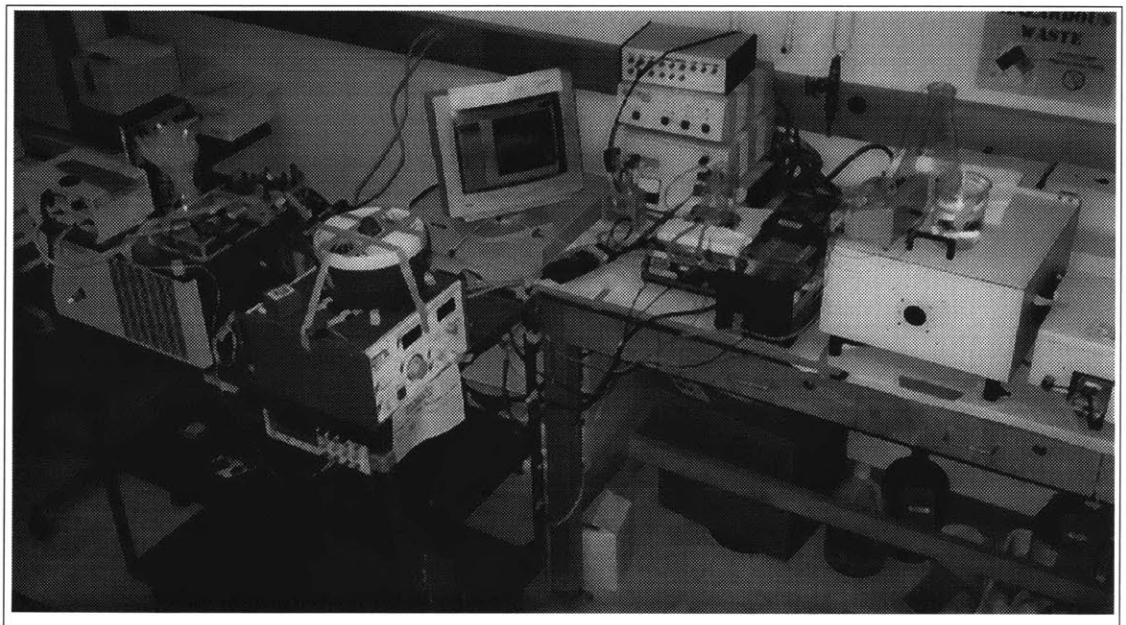

Figure IV.1. Flow-through experimental apparatus. The permeation chamber is in the middle of the picture, on top of the stirring plate. To its right are the flow-through pumps (black). To the right of that is the fluorimeter, containing the flow-through cuvette for real-time fluorescence measurements. On top of the fluorimeter are the flow-protection pumps, the PBS reservoir, and the waste beaker. To the left of the stirring plate is the differential high-voltage probe (flat black box). On the cart on the left are the pulser (blue), the water bath, the electronic circuitry (on top and behind the water bath), and the computer and oscilloscope which are connected to the high-voltage probe (middle level).

1. Acrylamide monomer solution: 7.5 g of 19:1 acrylamide:bis(N,N'-methylene-bis-acrylamide) powder (Bio-Rad) in 50 ml PBS (Solution 5, below). Prepare and mix together in a fume hood (the monomer is carcinogenic). Let the solution stand for >12 h before using, to allow the monomer to fully dissolve. This solution can be prepared well in advance of the experiment; it will not polymerize without addition of the catalyst.
2. Stock mounting solution: 10 mg Nile Red (Molecular Probes) in 20 ml acetone (Prausnitz, *et al.*, 1996 [a]). Wrap in aluminum foil to protect from light. This solution can be stored indefinitely if protected from light.
3. Final mounting solution: 7.5 ml glycerol in 2.5 ml de-ionized water and mix thoroughly. Add 250 µl of the stock mounting solution (Solution 2). Wrap in aluminum foil to protect from light. This solution can also be stored indefinitely if protected from light.
4. Acrylamide initiator solution: 0.3 g $(NH_4)_2S_2O_8$ in 3 ml H_2O. This solution can be stored for only a week.
5. Phosphate-buffered saline, PBS: 1.1 m<u>M</u> KH_2PO_4 (0.40 g per 2.0 l H_2O), 2.7 m<u>M</u> KCl (0.40 g), 8.1 m<u>M</u> Na_2HPO_4 (2.30 g), 138 m<u>M</u> NaCl (16 g) (total of 150 m<u>M</u>) in de-ionized H_2O. Although the volume of the receptor compartment is very small (~400 µl), a typical experiment can consume a surprisingly large volume of PBS, since both the flow-through fluorescence measurements and the electrode flow-protection systems are continuously pumping PBS through the chamber. One experiment can consume up to 2.0 l of PBS. Stir the PBS solution under vacuum for >30 min to remove dissolved gases from solution. Both light and O_2 can cause the quenching of fluorescent molecules, but this can be reduced by removing the dissolved gases from PBS, and protecting the solution from light whenever possible. Adjust to pH 7.4 with HCl and NaOH. This solution should be degassed immediately before use.
6. A typical donor solution consists of 1 m<u>M</u> of a hydrophilic fluorescent tracer in PBS (see Chapter 4). Examples of hydrophilic fluorescent tracers include lucifer yellow (457 Da) (Prausnitz, *et al.*, 1993 [a]; Chen, *et al.*, 1998 [c]), calcein (623 Da) (Prausnitz, *et al.*, 1993 [a]; Pliquett and Weaver, 1996 [a]; Vanbever, *et al.*, submitted), and sulforhodamine (607 Da) (Pliquett and Weaver, 1996 [a]) (all from Molecular Probes). Wrap the donor solution immediately in aluminum foil to protect it from light. Gently shake on a Nutator (Clay Adams, Becton Dickinson) for >30 min to ensure complete dissolution. This solution should be made immediately before use, right after preparing the PBS solution.

IV.2. Receptor Measurement Electrode Fabrication.

The permeation chambers are custom-designed, side-by-side glass permeation chambers (Crown Bio Scientific), with an outer water jacket (to maintain the temperature at 37 °C) and an inner compartment (Figure IV.2) (Friend, 1992).

Ports extend from the inner compartment, through the water jacket, to the outside, which allows direct access to the inner compartment. Each chamber half has one large port (for the measuring electrodes and the flow-through sampling system), with two smaller additional ports on the far ends (for placement of the electrodes and the flow-protection system around the electrodes). The volume of the inner compartment is ~3.1 ml, and the area of the circular opening is 0.64 cm^2 (0.9 cm diameter).

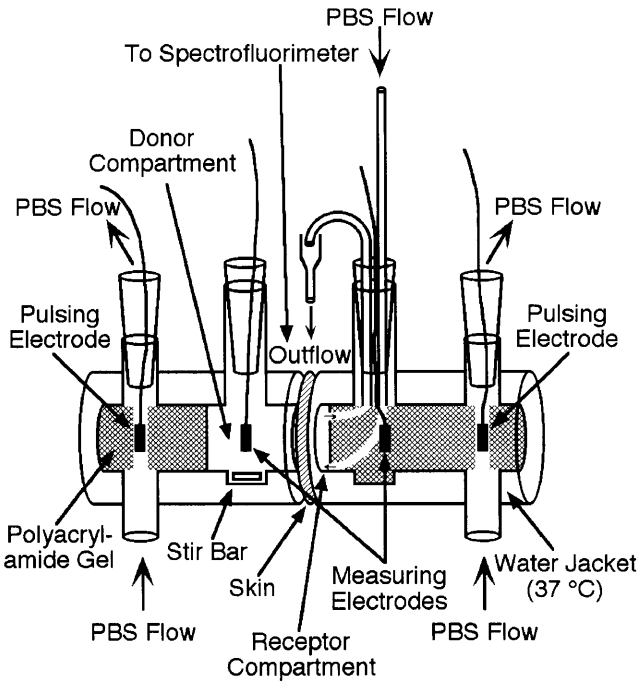

Figure IV.2. Skin permeation chamber with flow-through sampling system. The two outer electrodes are used for pulsing, and the two inner electrodes are used to measure the voltage drop across the skin. PBS is pumped around the pulsing electrodes to remove any chemical by-products generated during pulsing. PBS is also pumped through the receptor compartment to a spectrofluorimeter for real-time detection.

There are four electrodes in this system (Figures IV.2). The two outer electrodes are used to apply pulses, and the two inner electrodes are used to measure the transdermal voltage. Due to limitations of space within the donor and receptor compartments, the electrodes are constructed to allow both electrical access and liquid flow to the chamber. Thus, there are three types of electrodes in this system: the donor measurement electrode, the receptor measurement electrode, and the pulsing electrodes (the same design is used in both the donor and the receptor compartments).

The electrodes are made from silver wire, and the connectors are made from 200 µl pipette tips, with assorted amounts of tubing. The fabrication of the donor measurement electrodes has been previously described in Section III.2.1 (it was used for both compartments in Appendix III, but for this system only one of these electrodes is needed in the donor compartment). The fabrication of the two outer pulsing electrodes has been previously described in Section III.2.2.

While the electrodes are generally reusable between experiments if sufficiently cleaned with fine-grain sandpaper, they should be periodically examined. Worn-out or broken electrodes should be discarded. The pulsing electrodes can typically survive about a month of intense use before wearing out; the measurement electrodes can last somewhat longer.

The receptor measurement electrode must allow PBS to flow into and out of the receptor compartment, as well as detecting pulses (Figure IV.3).

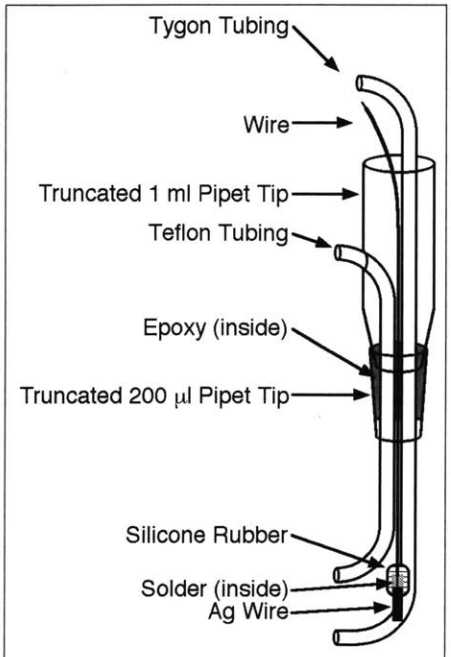

Figure IV.3. Receptor side measurement electrode. Two tubes allow the flow of PBS into and out of the receptor compartment.

1. Cut off a piece of pure silver wire, ~0.040 inch diameter, ~0.5 cm long.
2. Solder the end of the silver wire to a piece of copper bell wire, as shown in Figure IV.3.
3. Once the solder hardens, cover the solder (but not the silver wire) with nonconducting silicone rubber. Use as little silicone rubber as possible, but make sure that the solder is completely covered. Wait for the silicone rubber to harden (~1 d).
4. Cut off a piece of Tygon tubing, 1/32 inch ID, ~9 inches long. This will be used for the inflow into the receptor compartment. Cut off a piece of Teflon tubing, 1/16 inch ID, ~5 inches long. This will be used for outflow. In general, Tygon tubing is more flexible than Teflon tubing and is easier to manipulate. Thus, most of the tubing in this system is made from Tygon tubing. However, Tygon tubing is not strong enough to support the venting system; thus, Teflon tubing is used instead.
5. Cut the end off a 200 µl pipette tip. The hole at the end of the pipette should be large enough to accommodate the wire and the two tubes. Cut the end off a 1 ml pipette tip so that the wire and the two tubes will fit through that hole as well.
6. A hole needs to be drilled into the side of the 1 ml pipette for the Teflon outflow tubing. This hole must be placed high enough so that the tubing clears the side of the port, and large enough to accommodate the Teflon tubing. Insert the 200 µl pipette tip and the 1 ml pipette tip into the large port of the permeation chamber. Mark the level where the 1 ml pipette tip just clears the side of the port. Take the pipette tips out, and drill the hole in the side of the 1 ml pipette tip, just above this level.
7. Insert the Teflon outflow tubing through the 200 µl pipette tip, through the opening of the 1 ml pipette tip, and out through the hole on the side of the 1 ml pipette tip. Insert the Tygon inflow tubing and the wire through the 200 µl pipette tip and the 1 ml pipette tip (see Figure IV.3). The silver electrode should be placed so that when the 200 µl pipette tip is placed snugly into the large port of the permeation chamber, the silver electrode is positioned in the middle of the chamber. The two tubes should extend about 2 inches from the bottom of the 200 µl pipette tip.

8. Fill the 200 µl pipette with epoxy, to immobilize the wire and the two tubes in place. Next, insert the 1 ml pipette tip into the epoxy at the top of the 200 µl pipette tip (keeping the tubes and wires properly positioned inside) and hold everything in place until the epoxy cures. Verify that the wires and the tubing do not move while the epoxy is curing.
9. Completely insert the electrode through the large port of the receptor compartment, such that the two tubes come out through the side. The silver wire electrode should be positioned in the middle of the compartment. Mark both tubes where they emerge from the chamber. Take the electrode out of the compartment and cut both tubes on those marks. The tubes should now be the proper size for the receptor compartment.

IV.3. Flow-Through Sampling System.

In the receptor compartment, PBS is pumped from a reservoir, through the long Tygon tube of the receptor measurement electrode, into the receptor compartment (Figure IV.4). It then flows back up through the short Teflon tube of the electrode into a collection tube on the side of the electrode. From there, the PBS is pumped to a cuvette inside the spectrofluorimeter, and then out to a waste flask.

IV.3.1. Fabrication of the Receptor Venting System.

In a sealed receptor compartment with such a small volume (~400 µl), the minute pressure differences introduced by the peristaltic action of the pump can build up within the chamber. The receptor compartment design allows these pressure differences to be eliminated.

Figure IV.4 shows a small collection tube (made from a centrifuge tube) near the outflow of the receptor compartment. Liquid from the receptor compartment drips down into the collection tube, which is pumped into the spectrofluorimeter detector. Transient pressure differences from the receptor compartment are eliminated by venting the system at this location. The collection tube is not permanently fixed to the receptor measurement electrode, to allow for easier assembly and cleaning.

1. Cut the lid off of a 2 ml centrifuge tube.
2. Cut off a piece of Tygon tubing, 1/32 inch ID, ~3 inches long.
3. Drill a hole in the bottom of the centrifuge tube. The piece of Tygon tubing should just fit inside this hole.
4. Drill a second hole near the midpoint of the centrifuge tube. This hole should be just large enough to accommodate the Teflon tube from the receptor measurement electrode.

5. Attach the piece of Tygon tubing to the hole with epoxy. This tube should be flush with the bottom of the centrifuge tube and should not protrude into it (Figure IV.4).

IV.3.2. Cuvette Fabrication.

The cuvette in the spectrofluorimeter has to accommodate both the inflow and outflow of liquid to and from the permeation chamber. The volume of the liquid within the cuvette should be the smallest volume needed to obtain an accurate fluorescence measurement. In addition, the apparatus described in this appendix can be assembled and disassembled as needed.

The spectrofluorimeter cuvette is a 1 ml polystyrene semi-micro cuvette with two holes drilled into the side (Figure IV.4). Liquid enters through the upper hole and exits through the lower hole. Since the outflow rate of the cuvette is higher than the inflow rate, the level of liquid stays at a constant height, immediately below the level of the outlet. The height of liquid within the cuvette depends on the minimum volume of liquid in the cuvette that yields a sufficiently accurate signal in the spectrofluorimeter.

However, there is a cyclical rise and fall in the height of liquid within the cuvette, due to the differences between the inflow rate and the outflow rate. Since liquid leaves the cuvette faster than it enters, the level of liquid within the cuvette will drop. However, the liquid in the cuvette cannot be drawn out unless the outlet is

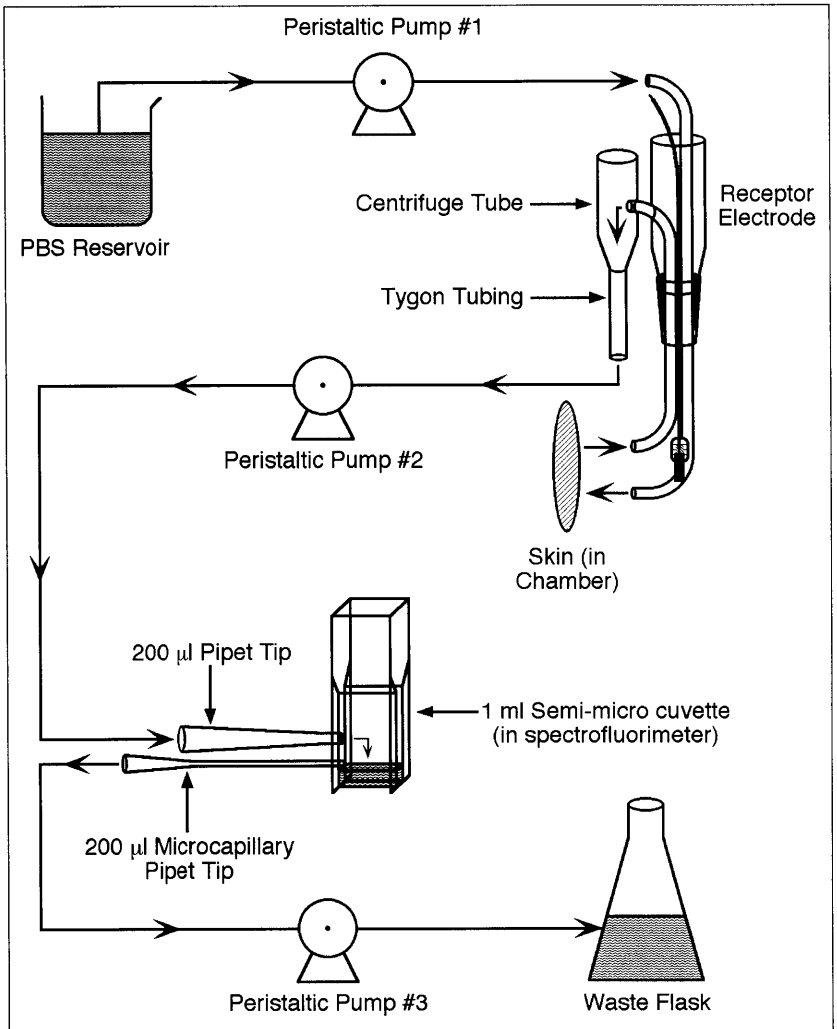

Figure IV.4. Liquid circuit for flow-through measurements of the receptor compartment. PBS is pumped from a reservoir into the receptor measurement electrode, down into the permeation chamber. PBS then exits the receptor compartment into a collection (centrifuge) tube. From there, it is pumped into a cuvette in the spectrofluorimeter for real-time detection. Finally, PBS from the cuvette is pumped out into a waste flask. The arrangement of pumps and tubing allow this system to maintain a constant throughput.

completely submerged. Once the outlet is exposed, the pump begins to draw in air instead of liquid. When this occurs, the level of liquid in the cuvette will rise, since liquid is still entering the cuvette. This level will rise until the outlet is submerged again, causing the cycle to repeat.

The cyclic rise and fall of the height of liquid within the cuvette systematically varies from the bottom to the top of the outlet. This cycling pattern can be detected on relatively sensitive spectrofluorimeters. To minimize this effect, the outlet size must be kept as small as possible. A problem with using very small tubing is that it can frequently become blocked by stray bits of dirt and debris, especially from the skin. The amount of dirt and debris can be minimized by continuously flushing the system (during the passive controls, and between experiments), and by very thorough washing of the entire system before shutting it down. To clear a blocked tube, the system should be backflushed to remove the clog.

Using a 200 µl microcapillary pipet tip (the inner diameter of the tip opening is roughly 500 µ) keeps the level reasonably constant. A diameter of only 500 µ for the outlet may not seem particularly worrisome, but that size is significant compared to the working volume of the cuvette. With an outlet this small, the cyclic changes in the height of the liquid in the cuvette are not significant compared to the shot noise of the spectrofluorimeter.

Mixing within the cuvette is accomplished by the dripping of liquid into the cuvette. The height of the inlet should be high enough to allow the falling liquid to form droplets. The volume of the cuvette is small enough that the splashing of the drops into the liquid will cause adequate mixing to occur.

Before making the cuvette, the minimum volume of liquid that the spectrofluorimeter needs for an accurate signal has to first be determined. Most spectrofluorimeters pass a vertical beam of light through the cuvette. The beam of light is probably centered inside the cuvette, so that the liquid above and below this beam do not contribute to the fluorescence measurement.

1. Make up a solution of an easily obtainable highly fluorescent molecule.
2. Add 1 ml of this test solution to a 1 ml semi-micro cuvette and place the cuvette in the spectrofluorimeter.
3. Pipet small amounts of liquid out of the cuvette until the readings on the spectrofluorimeter begin to respond.
4. Attach a clamp to the top of the cuvette. This clamp will keep the cuvette from sliding down fully into its holder; thus, the cuvette will sit higher in the incident beam of light.
5. Adjust the position of this clamp downward on the cuvette (forcing the cuvette to rise higher and higher in the incident beam of light) until the readings on the spectrofluorimeter begin to respond.

6. Repeat Steps 3 to 5 until no more adjustments are needed. This is the minimum amount of liquid needed for an accurate signal in the spectrofluorimeter. Lightly mark these levels on the side of the cuvette.
7. Obtain two 200 µl microcapillary pipet tips. The openings of these pipet tips are approximately 500 µ in diameter, smaller than the openings on the standard 200 µl pipet tips.
8. Two holes now should be drilled into the side of the cuvette to allow for inflow and outflow. These holes should allow the two microcapillary pipette tips to just fit through. These holes should be drilled on the same side of the cuvette, on a side that will not interfere with either the excitation beam or the fluorescence emission from the cuvette. The first hole (for outflow) should be drilled just above the first mark, and the second hole (for inflow) should be drilled approximately 1/4 inch above that.
9. The two microcapillary pipet tips should be attached to Tygon tubing with epoxy, for attachment to the peristaltic pumps. However, they should not be attached to the cuvette. This allows the entire system to be removed from the spectrofluorimeter for cleaning between experiments.

IV.3.3. Pump Balancing.

There are three pumps that are used in the flow-through sampling system. It is vital that these pumps be properly "balanced," to avoid any accumulations or leakage within the flow-through system. The three pumps should all have flowrates of ~0.03 ml/s, and should provide consistent flowrates over very long times. However, these flowrates will not be identical. These differences cannot be avoided, and in fact can be used advantageously to maintain the flow-through system at steady state. The differences in the flowrates of the various pumps may be on the order of 0.3 µl / s (±1% of the flowrate) or less. While minuscule, these differences can still quickly build up in a system as small as this one over time.

The pumps (see Figure IV.4) should be set up such that the fastest pump is Peristaltic Pump #3, followed by Peristaltic Pump #2, with Peristaltic Pump #1 being the slowest. The differences in flowrates will cause air to be drawn into the flow-through system in two places: the collection tube and the spectrofluorimeter cuvette. This is necessary to keep the throughput of the system constant. Determining which pump is the fastest requires very careful measurements of the flowrates of each of the three pumps (up to three significant digits).

IV.3.4. Flow-Through System Characteristics.

At this point, all of the components should now be in place, correctly connected by tubing. The lengths of the tubing used to connect all of the components in the flow-through system probably will vary. While most of the tubing lengths are relatively unimportant, the length of the tubing between the chamber and the spectrofluorimeter should be minimized.

Although there is mixing within the tubing, the pump, and in the cuvette, the chamber/tubing/pump/cuvette system is modeled as having two components: a plug flow region, where no mixing occurs, and a continuous stirred tank reactor region, where instant perfect mixing occurs (Fogler, 1992).

Several parameters needed for this model: the cuvette volume (V_{cuv}), the liquid bulk flowrate (Q), the reaction time (t_{react}), and the residence time (τ_{cuv}). The reaction time, t_{react}, is the time it takes for a molecule leaving the receptor compartment to reach the spectrofluorimeter (the plug flow region). The residence time, τ_{cuv}, of the cuvette is the average time it takes for a molecule entering the cuvette to leave (the continuous stirred tank reactor region) (Fogler, 1992). For an ideal continuous stirred tank reactor, the residence time distribution of this system can be predicted as an exponentially decaying function. The time constant for this decay gives τ_{cuv}, or the time resolution of the system. If this system is properly set up, its performance should be reasonably close to ideal.

To measure t_{react} and τ_{cuv}, a technique known as a "pulse-chase" experiment is used, where a drop of tracer (the "pulse") is added to the system, and then flushed through it (the "chase"). The drop should be as small and as narrow as possible (ideally, it should be a δ function).

1. Make up a tracer solution of an easily obtainable highly fluorescent molecule.
2. Partially assemble the flow-through system, from the receptor measurement electrode onwards.
3. Pump water through the system until the spectrofluorimeter reads a constant background.
4. Add an aliquot of tracer to the receptor measurement electrode. (By selectively turning on and off the pumps, this drop can be made reasonably small.)
5. Turn on the pumps and measure the time it takes for the spectrofluorimeter to first detect the spike of tracer. This is the reaction time (t_{react}).
6. Pump water through the system until the spectrofluorimeter reads a constant background again.
7. Add another pulse of the tracer to the receptor measurement electrode.
8. Record the fluorescence on the spectrofluorimeter. If the system is behaving close to an ideal system, after a short delay (t_{react}), the fluorescence in the cuvette should quickly peak, then decay exponentially afterwards.
9. Save the data from the spectrofluorimeter and import the data into a graphing program.

10. Fit the decay of fluorescence to an exponential curve. The time constant for the exponential decay of the curve is τ_{cuv}. This is also the time resolution of the system.
11. Assemble the rest of the flow-through system. This includes the polyacrylamide gel within the permeation chamber (described below in Section IV.6).
12. Measure the average flowrate through the entire system ($\mathcal{Q}$), using the waste stream. Ignore the air getting pumped through the system.
13. The cuvette volume can be calculated by multiplying the residence time (τ_{cuv}) by the flowrate ($\mathcal{Q}$) (Fogler, 1992):

$$V_{cuv} = \tau_{cuv}\, \mathcal{Q}. \tag{IV.1}$$

IV.4 The Electrical Circuit.

The electrical circuit (shown in Figure IV.5) has to perform two functions. First, it must deliver high-voltage pulses to the permeation chamber once every 5 s. Second, it has to measure and record the transdermal voltage and the current across the skin in real time. Since pulses are being applied to the skin every 5 s, there is very little time to manually record data or make adjustments between

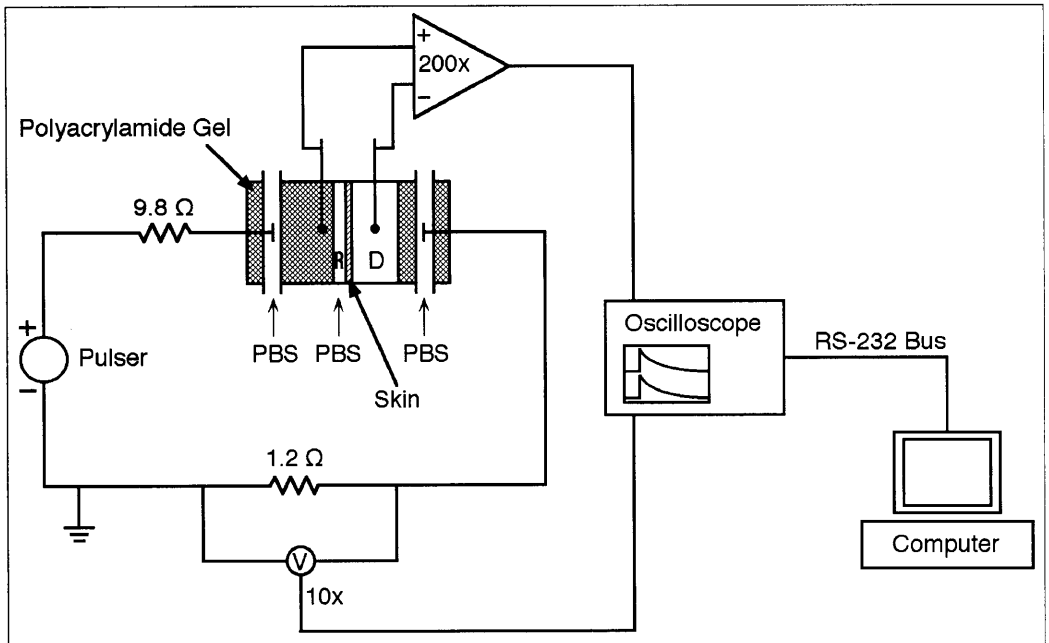

Figure IV.5. Electrical circuit for measuring voltages and currents on a per-pulse basis. The 9.8 Ω resistor is a safety device in the event of a short circuit. The transdermal voltage is measured by a 200× differential voltage probe, and the current is measured by a 10× voltage probe across a 1.2 Ω resistor placed in series with the chamber. Both voltage probes are connected to an oscilloscope, which downloads the data into a computer for later analysis. R indicates the receptor compartment and D indicates the donor compartment. The two outer PBS streams and the polyacrylamide gel around the pulsing electrodes are used to prevent chemical contamination of the donor and receptor compartments by the electrodes. The inner PBS stream flows from the receptor compartment to a spectrofluorimeter for detection.

pulses. Thus, all of these operations have to be completely automated.

All of the components in the electrical circuit (shown in Figure IV.5), including the wires and the clip leads, should be able to withstand high voltages and positioned with safety in mind. The electrical circuitry should be set up in a protected area away from the permeation chamber (on a different bench), so that any fluid leaks or spills cannot reach the electrical components. Modifications to the high-voltage pulser have previously been discussed in Section II.1.

In a commonly used protocol (Prausnitz, *et al.*, 1993 [a]; Prausnitz, *et al.*, 1995 [b]; Pliquett and Weaver, 1996 [a]; Prausnitz, *et al.*, 1996 [b]), the pulser delivers a high-voltage exponential pulse to the permeation chamber once every ~5 s. The current and the voltage during the pulse are detected by two high-voltage probes connected to a digital oscilloscope. The data are then immediately downloaded from the oscilloscope into a computer for later processing. The system stores all of the data and is ready to download the next pulse in less than 5 s.

IV.4.1. The Pulsing Circuit.

The chamber is connected to the circuit so that the receptor pulsing electrode is positive and the donor electrode is grounded (Figure IV.5). This provides a favorable driving force for a negatively charged molecule. However, for a positively charged species, the positive and negative terminals to the chamber should be interchanged.

The 9.8 Ω resistor is a safety device used to protect the system in the event of a short circuit. It should be a 50 W (or higher) noninductive power resistor.

Since the 1.2 Ω resistor is in series with the skin, it can be used to measure the current across the skin during pulsing. It should also be a 50 W (or higher) noninductive power resistor. A 10× voltage probe from the digital oscilloscope should be connected across the 1.2 Ω resistor. Once the voltage drop across the resistor is known, the current can be determined by applying Ohm's law.

The donor and receptor compartments each contain a measuring electrode. Connected across these electrodes is a 200× differential high-voltage probe (B9017RT Active Differential Probe, Yokogawa). Using a high-voltage probe in the receptor compartment that measures with respect to ground instead of a differential probe is not recommended, since the grounded high-voltage probe can potentially introduces other voltages, such as the polarization voltage of the pulsing electrodes.

Between the two measurement electrodes are the skin and PBS, where the resistivity of PBS is constant for a given temperature. The differential probe is also connected to the oscilloscope.

IV.4.2. Real-Time Data Acquisition and Storage.

The digital oscilloscope records data simultaneously from two channels, and uploads the acquired data to a computer for subsequent analysis. The computer downloads the data from the oscilloscope and stores it on disk. All of these operations must be completed in less than 5 s, before the next pulse arrives.

One digital oscilloscope that has worked well is a Hewlett Packard 54601 with an 54641A RS-232 Interface Module (Hewlett Packard), which can be connected with an RS-232 cable to the serial port of a personal computer.

The program the computer is running will be machine-specific, depending on which serial port the oscilloscope is connected to, as well as the programming languages used by the computer and the oscilloscope (see Section IV.4.3). In general, though, the computer program should be in a low-level programming language, and the computer itself should be reasonably fast. The oscilloscope should be transferring data in the most compact format available (i. e., as unformatted ASCII characters instead of formatted arrays of numbers).

The computer program needs to direct the oscilloscope to transfer data to the computer once a pulse has been triggered, and it should store the raw data on the hard drive (or on a ramdisk if enough memory is available). No mathematical processing needs to be done during the experiment. The computer has to be able to complete the transfer and save the data in under 5 s.

The 5 s spacing between pulses allows very little time for the correction of problems, so care must be taken in setting up this system. Examples of problems that can occur include loose serial plugs, line noise due to faulty or excessively long cables, errors in the proper recording of an NL ("New Line" command, ASCII string #0A) or an EOT ("End of Transmission" command, ASCII string #04), improper triggering of the oscilloscope by line noise in either voltage probe, and failure of the oscilloscope and the computer to properly synchronize headers and data streams.

A transfer rate of 9600 baud between the oscilloscope and the computer allows roughly 1 kb of raw data to be transferred in 5 s, which corresponds to a time resolution of approximately 10 μs for each pulse waveform. Before starting, verify that there is adequate space on the hard drive, since one experiment can consume nearly 1 MB of space.

IV.4.3. `SAVEWAVE.CPP`.

The following is the source code for `SAVEWAVE.CPP`, a computer program that measures and records the transdermal voltage and current from the digital oscilloscope for each pulse. It is in Turbo C++ (Borland, Scotts Valley, CA).

```
/* SAVEWAVE.CPP */
/* Program stores pulse waveform and current waveform for every pulse.    */
/*   Program can store up to 1 pulse every 5 s.  Data saved in 4 files.   */
/*   The 2 preamble files contain data about the x and y settings on the  */
/*   oscilloscope, saved in MatLab format (PREAMB1.M and PREAMB2.M).  The */
/*   2 data files contain the actual waveform data, stored in ascii       */
/*   (WAVE1.DAT and WAVE2.DAT).  Each wave is stored as a block of 500    */
/*   bytes (no separators).                                               */
/* Oscilloscope RS-232 module (HP 54651A) should be connected to serial   */
/*   port 1 on computer.  Oscilloscope settings:  Hit [Print/Utility],    */
/*   then <RS-232 Menu>, and check these settings before running program: */
/*     Connect to <Computer>, Factors <Off>, Resolution <Low>,            */
/*     Baud Rate <9600>, Handshake <Xon>                                  */
/* Tani Chen, 3/17/1997 */

#include <stdio.h>
#include <dos.h>
#include <string.h>
#include <bios.h>
#include <conio.h>

/* Bioscom port 0 = serial port 1 */
#define OscPort 0
/* Bioscom send = 1, read = 2, status = 3 */
#define Send 1
#define Read 2
#define Status 3
#define DataReady 0x0100


InitCom1()  /* Initialize serial port 1 */
{
  union REGS r;

  r.h.ah = 0x00;
  r.h.al = 0xE3;
  r.x.dx = 0x00;
  int86(0x14, &r, &r);
  printf("  Serial port 1 initialized.\n");
}


OscCom(char *command)  /* Send command to oscilloscope */
{
  int i;

  delay(100);  /* Do not change!  Timing necessary for oscilloscope to */
               /*   take readings correctly!                           */
  for(i=0; i<strlen(command); ++i)  /* 1 character at a time */
  {
    bioscom(Send, command[i], OscPort);
  }
  bioscom(Send, 0x0A, OscPort);  /* Line feed */
  printf("  Command: %s\n", command);
}


int ReadOsc()  /* Wait for ready signal (?) */
{
  int data;
  int i = 0;
  union REGS r;

  while((data=bioscom(Status, 0, OscPort) & DataReady != 0x001 && i<10))
  {
    i++;
  }
  data = bioscom(Read, 0, OscPort);
  data = data&0x00FF;
  return(data);
}


Preamble(int channel, char *filename)
/* Preamble format: 1(byte), 1(nrm), 4000(pnts), 1(dummy) */
/*   xincr, xorig, xref(dummy), yincr, yorig, yref(dummy) */
/* Stored as MatLab file */
{
  int i;
  char preamble[125];
  char preamble2[125];
  char *command;
  FILE *fp;

  if(channel == 1)  /* Select channel */
  {
    OscCom(":WAV:SOUR CHAN1");
  }
  else if(channel == 2)
  {
    OscCom(":WAV:SOUR CHAN2");
  }
```

```
  delay(500);  /* Reset port for signaling...  don't ask me why!  Removing */
  bioscom(Read, 0, OscPort);  /* these lines will cause bytes to be lost!! */
  command = ":WAV:PRE?";  /* No time to jump to subroutine... */
    /* Using OscCom here causes bytes to be lost! */
  printf("  Command: %s\n", command);
  for(i=0; i<strlen(command); ++i)  /* 1 character at a time */
  {
    bioscom(Send, command[i], OscPort);
  }
  bioscom(Send, 0x0A, OscPort);  /* Line feed */

  i = 0;  /* Enter data */
  while((preamble[i]=ReadOsc()) != 10 && i<100)
  {
    i++;
  }
  preamble[i] = '\0';  /* Add line feed to end of data */
  printf("  Channel %d data: %-.57s...\n", channel, preamble);

  for(i=0; i<strlen(preamble); i++)  /* Erase commas from preamble */
  {
    if(preamble[i] == ',')
    {
      preamble[i] = ' ';
    }
  }

  sprintf(preamble2, "preamble%d = [ %s ];", channel, preamble);  /* Save */
  fp = fopen(filename, "write");               /*   data in Matlab format */
  fprintf(fp, "%s\n", preamble2);
  fclose(fp);
  printf("  Preamble from channel %d stored in %s.\n", channel, filename);
}


Waveform(char *filename1, char *filename2)  /* Dump both channels to disk */
{
  int i;
  char *command;
  char wave1[511];  /* (header=10 bytes)(data=500 bytes)(EOF=1 byte) */
  char wave1a[501];  /* 500 data bytes + EOF */
  char wave2[511];  /* Same for channel 2 */
  char wave2a[501];
  FILE *fp;

  OscCom(":DIG CHAN1,CHAN2");  /* Store both traces in oscilloscope */
  OscCom(":WAV:SOUR CHAN1");  /* Select channel 1 */
  command = ":WAV:DATA?";  /* No time to jump to subroutine... */
  printf("  Command: %s\n", command);
  for(i=0; i<strlen(command); ++i)  /* 1 character at a time */
  {
    bioscom(Send, command[i], OscPort);
  }
  bioscom(Send, 0x0A, OscPort);  /* Line feed */

  /* Waiting for pulse.  ReadOsc spits out 0's until the oscilloscope      */
  /*   is ready to send data (which means the oscilloscope was triggered,  */
  /*   which means a pulse was detected.)  The 0's are not part of the DIG */
  /*   header and really screw up data transferring (510 bytes from DIG)!! */
  printf("  Waiting");
  while(i=ReadOsc() == 0)
  {
    printf(".");
  }

  printf("\n  Pulse detected.\n");
  for(i=0; i<511; i++)  /* Pulse detected, reading data */
  {
    wave1[i] = ReadOsc();
    if(wave1[i] == 0)  /* 0 (no data) causes string to terminate early     */
    {                  /*   making a real mess of the rest of the program! */
      wave1[i] = 1;
    }
  }
  wave1[i] = '\0';  /* End of file */

  OscCom(":WAV:SOUR CHAN2");  /* Then select channel 2 */
  command = ":WAV:DATA?";  /* No time to jump to subroutine... */
  printf("  Command: %s\n", command);
  for(i=0; i<strlen(command); ++i)  /* 1 character at a time */
  {
    bioscom(Send, command[i], OscPort);
  }
  bioscom(Send, 0x0A, OscPort);  /* Line feed */

  for(i=0; i<511; i++)  /* Read data, I hope */
  {
    wave2[i] = ReadOsc();
    if(wave2[i] == 0)  /* 0 (no data) causes string to terminate early */
    { wave2[i] = 1;
    }
```

```
 }
 wave2[i] = '\0';  /* End of file */

 for(i=0; i<511; i++)  /* Patch up data so this stupid PC can process it */
 {
   if(wave1[i] == 26)  /* 26 = EOF, change to 25 to avoid crashing! */
   {
     wave1[i] = 25;
   }
   if(wave1[i] == 7)  /* Turn off that stupid bell! */
   {
     wave1[i] = 8;
   }
   if(wave1[i] == 10)  /* Character 10 messes up byte count on disk!! */
   {                    /*   Don't ask me why, just don't change this! */
     wave1[i] = 11;
   }
   if(wave2[i] == 26)  /* And of course, repeat for channel 2 waveform */
   {
     wave2[i] = 25;
   }
   if(wave2[i] == 7)
   {
     wave2[i] = 8;
   }
   if(wave2[i] == 10)
   {
     wave2[i] = 11;
   }
 }

 i = 0;  /* Delete useless header info (channel 2) */
 while((wave2a[i] = wave2[i+10]) != '\0')
 {
   i++;
 }

 i = 0;  /* Delete useless header info (channel 1) */
 while((wave1a[i] = wave1[i+10]) != '\0')
 {
   i++;
 }

 printf("  Channel 1 data (%d): %-.50s... \n", strlen(wave1a), wave1a);
 printf("  Channel 2 data (%d): %-.50s... \n", strlen(wave2a), wave2a);
 OscCom(":RUN");  /* Resume oscilloscope readings */

 fp = fopen(filename1, "append");  /* Save channel 1 as block of 500 */
 fprintf(fp, "%.500s", wave1a);    /*   bytes                        */
 fclose(fp);
 printf("  Channel 1 data stored in %s.\n", filename1);

 fp = fopen(filename2, "append");  /* And channel 2 also */
 fprintf(fp, "%.500s", wave2a);
 fclose(fp);
 printf("  Channel 2 data stored in %s.\n", filename2);
}


main()
{
  FILE *fp;
  int pulseno = 1;
  int choice;
  char *preamble1 = "PREAMB1.M";  /* Preamble data file for channel 1 */
  char *preamble2 = "PREAMB2.M";  /* Preamble data file for channel 2 */
  char *waveform1 = "WAVE1.DAT";  /* Waveform data file for channel 1 */
  char *waveform2 = "WAVE2.DAT";  /* Waveform data file for channel 2 */

  printf("*** Program Initialization ***\n");
  printf("Initializing serial port 1....\n");
  InitCom1();

  printf("Setting up oscilloscope....\n");
  OscCom("*RST");  /* Reset oscilloscope */
  OscCom(":SYST:LOCK ON");  /* Prevents user from messing with settings */
  OscCom(":VIEW CHAN2");  /* Turn on channel 2 */
  OscCom(":DITH OFF");  /* Turn off errors (oscilloscope *adds* errors!) */
  OscCom(":WAV:POIN 500");  /* 500-byte data blocks.  Limit of what can */
                            /*   be saved in under 5 s!                 */
  OscCom(":WAV:FORM BYTE");  /* Data goes from 0 to 255 */
  OscCom(":ACQ:COMP 40");  /* Mininum threshold to trigger storage */
  OscCom(":ACQ:TYPE NORM");  /* Normal acquisition (no averaging) */

  /* Channel 1 = Uskin (high voltage probe, 1000x) */
  /* Channel 2 = I (10x probe)                     */
  OscCom(":TIM:RANG 5 MS");  /* Set x-axis to 5 ms across */
  OscCom(":TIM:REF LEFT");  /* Align pulse with left side */
  OscCom(":CHAN2:PROB X10");  /* 10x probe for current (channel 2) */
  OscCom(":CHAN2:BWL ON");  /* Clean up channel 2's signal */
  OscCom(":CHAN1:BWL ON");  /* Clean up channel 1's signal */
  OscCom(":TRIG:MODE NORM");  /* Set up oscilloscope to respond to pulses */
```

```
                          /*   on channel 2 (Current)                */
  OscCom(":TRIG:NREJ ON");  /* Turn on noise rejection */

  printf("Enter voltage settings:\n");  /* Select ranges to display/record */
  printf("  1. High voltage    (600 V/2.5 A)\n");
  printf("  2. Medium voltage (240 V/1 A)\n");
  printf("  3. Low voltage     (120 V/0.5 A)\n");
  printf("Choice?");
  scanf("%d", &choice);
  if(choice == 1)
  {
    OscCom(":CHAN1:RANG 4V");
    OscCom(":CHAN1:OFFS 1.5V");
    OscCom(":CHAN2:RANG 4V");
    OscCom(":CHAN2:OFFS 1.5V");
    OscCom(":TRIG:SOUR CHAN1");
    OscCom(":TRIG:LEV 500MV");
  }
  else if(choice == 2)
  {
    OscCom(":CHAN1:RANG 1.6V");
    OscCom(":CHAN1:OFFS 600MV");
    OscCom(":CHAN2:RANG 1.6V");
    OscCom(":CHAN2:OFFS 600MV");
    OscCom(":TRIG:SOUR CHAN1");
    OscCom(":TRIG:LEV 250MV");
  }
  else if(choice == 3)
  {
    OscCom(":CHAN1:RANG 800MV");
    OscCom(":CHAN1:OFFS 300MV");
    OscCom(":CHAN2:RANG 800MV");
    OscCom(":CHAN2:OFFS 300MV");
    OscCom(":TRIG:SOUR CHAN1");
    OscCom(":TRIG:LEV 400MV");
  }

  printf("Getting preambles...\n");
  Preamble(1, preamble1);  /* Get preamble data for channel 1 */
  Preamble(2, preamble2);  /* Get preamble data for channel 2 */

  fp = fopen(waveform1, "write");  /* Delete data files from disk   */
  fclose(fp);                      /*   so new files can be written */
  fp = fopen(waveform2, "write");
  fclose(fp);
  printf("*** Initialization Completed ***\n\n");

  printf("*** Receiving Waveforms ***\n");
  printf("Press any key AFTER pulse to stop recording!\n");

  while(kbhit() == 0)  /* Stop reading waveforms when key is pressed */
  {
    printf("Pulse #%d...\n", pulseno);
    pulseno++;
    Waveform(waveform1, waveform2);  /* Get waves */
  }

  printf("*** All Waveforms Recorded ***\n");
  OscCom(":SYST:LOCK OFF");  /* Allow use of oscilloscope again */
  printf("\n*** End of Program ***\n");
  delay(1000);
}
```

IV.5. Resistance of PBS.

The skin, PBS, and some polyacrylamide gel are located between the two measurement electrodes. The resistivities of the PBS and the polyacrylamide gel are constant, but should be measured.

1. Make up a solution of PBS (Solution 5 from Section IV.1).
2. Prepare the permeation chamber, with the four electrodes and the polyacrylamide gel (described below in Section IV.6).
3. Fill the chamber with PBS.

4. Connect the high-voltage pulser and the flow-protection system to the chamber (see Figure IV.5). Heat the chamber to 37 °C using the water jacket.
5. Manually apply pulses to the chamber, starting from 0 V and increasing in units of 100 V, up to 1000 V. Apply 5 to 10 pulses per setting. For each pulse, record the voltage drops appearing across the inner measurement electrodes (U_{inner}) and the 1.2 Ω resistor (U_{curr}, given that $R_{curr} = 1.2\ \Omega$).
6. To find the current (I), apply Ohm's law to the 1.2 Ω resistor:

$$I = \frac{U_{curr}}{R_{curr}} = \frac{U_{curr}}{1.2\ \Omega}. \tag{IV.2}$$

7. Plot the voltage drop across the inner measurement electrodes (U_{inner}) versus the current (I). The slope of the line is the resistance of the PBS and the polyacrylamide gel (lumped together in one variable, R_{PBS}) between the two measurement electrodes:

$$R_{PBS} = \frac{U_{inner}}{I}. \tag{IV.3}$$

IV.6. Permeation Chamber Preparation.

The polyacrylamide gel around each pulsing electrode directs PBS in and out of the chamber, without contacting the donor or receptor solutions (this is the hollowed-out regions that run around each of the two pulsing electrodes in Figure IV.2). On the receptor side, the polyacrylamide also keeps the volume of the receptor compartment at a minimum (on the right half of Figure IV.2). Embedded in this side are the tubes entering and leaving the receptor chamber, and the measurement electrode.

IV.6.1. Preparation of the Mold.

Acrylamide in solution takes approximately 10 min to polymerize into polyacrylamide gel. In this time, the acrylamide solution has to poured into the chamber. To create the channels that run through the polyacrylamide gel, plastic tubes are inserted into the chamber, which are then removed once the acrylamide has polymerized. Preparing the mold within the permeation chambers can be done the day before the experiment.

1. Find two flexible plastic tubes, approximately 9 inches long, that will fit through the two small ports on each chamber half.
2. Slide the plastic tubes through these ports (use tweezers as needed), so that roughly 1 to 2 inches of the tube protrudes out on either side. These tubes are the mold for the electrode flow-protection channel.
3. Place Parafilm around each opening tightly. Use two layers of Parafilm. This should create a watertight seal around the openings, so the acrylamide solution will not leak out.
4. Insert the receptor measuring electrode into the receptor compartment. Make sure the two tubes that lead to the receptor compartment are angled toward the opening. Place Parafilm tightly around this electrode as well.
5. Due to the elasticity of the tubing, however, the two tubes of the electrode are probably stuck next to each other instead of on opposite sides of the chamber as shown in Figure IV.2. Using a thin stainless steel wire, attach the outlet tubing to the top of the chamber. This wire will be removed after the polyacrylamide gel has been added.
6. Position each of the two chambers sideways, so that the large opening (where the skin is located) is on top. The chambers should be braced in some fashion (propping them up on pencils or test tubes) so that they can not tip or move when filled with liquid.

IV.6.2. Adding the Polyacrylamide Gel.

Acrylamide monomer in solution (Solution 1 from Section IV.1) will polymerize into a gel in approximately 10 min upon addition of a catalyst (N,N,N',N'-tetramethylethylenediamine) (Bio-Rad) and a free radical initiator (Solution 4). Most of the gel is still liquid (PBS, in this case), surrounded by cross-linked polymer. Thus, the conductivity and the electrical properties of the polyacrylamide gel are essentially the same as PBS.

Synthesis of the polyacrylamide gel should be performed just before the experiment (the chambers should already be prepared), since polyacrylamide gel will begin dehydrating after a few hours.

1. Thoroughly mix together 10 ml of acrylamide solution (Solution 1 from Section IV.1), 87.5 µl of the initiator (Solution 4), and 6 µl of N,N,N',N'-tetramethylethylenediamine in a 15 ml test tube.
2. On the donor side, immediately pour in the acrylamide solution so that it reaches the level of the large port (embedding the plastic tube for the flow-protection system). This should leave a donor volume of ~2.1 ml.
3. On the receptor side, immediately pour in the acrylamide solution, completely filling the chamber. The top of the solution should be perfectly flush with the top of the chamber, and there should

not be a meniscus above the chamber. The acrylamide solution will completely cover the plastic tubing of the flow-protection system, and the silver measurement electrode. Make sure that the liquid does not enter the two tubes that form the receptor compartment. The solution will shrink slightly as it gels; this shrinkage is what forms the receptor compartment. Thus, to get a consistent, reproducible volume for the receptor compartment, the solution should always be poured so that it is flush with the top of the chamber.

4. Do not disturb the chambers while the gel is polymerizing, as disturbances will cause the gel to take longer to harden, and the gel will set poorly as a result. It will take approximately 10 min for the gel to harden. Any leftover acrylamide solution can be used to monitor the gelling process.
5. After the gel forms, carefully remove the Parafilm around the each of the plastic tubes of the electrode flow-protection system. Remove the plastic tubes through one of the small ports. Do not remove the receptor measurement electrode or the surrounding Parafilm.
6. Carefully remove the stainless steel wire holding the outlet tube of the receptor compartment in place, which should now be held in place by the polyacrylamide gel.
7. Using a syringe, force air through the inlet and outlet tubes of the receptor chamber to ensure that they are not blocked by stray bits of polyacrylamide gel.
8. Connect the collection tube (see Section IV.3.1) to the outlet tube on the side of the receptor electrode, as shown in Figure IV.4). Hold it in place with Parafilm.
9. Before using, fill the permeation chambers with PBS to keep the polyacrylamide gel from drying out.

IV.7. Preparing the Equipment.

On the day of the experiment, the following should have already been prepared and assembled: Solutions 1 through 4 (Section IV.1), the permeation chamber and the electrodes (Sections IV.2, III.2, and IV.6.1), the electrode flow-protection system (Section III.3), the flow-through system in the spectrofluorimeter (Section IV.3), the electrical circuit (Section IV.4), the high-voltage pulser (Section II.1), the skin (Section I.1), and the impedance meter (Section III.5). Immediately before the experiment, Solutions 5 and 6 from Section IV.1, and the polyacrylamide gel in the chamber (Section IV.6.2) need to be prepared. Once the gel in the chamber is ready, place the chamber on a magnetic stirring plate and connect it to a 37 °C water bath.

All of the tubes in the flow-through and the electrode flow-protection system should be flushed through with PBS. Use a piece of Parafilm instead of human skin in the permeation chamber. There should be a steady stream of air bubbles entering the flow-through system at the collection tube and the spectrofluorimeter cuvette. The flushing should continue until the spectrofluorimeter gives stable

readings for the fluorescence. This can take up to an hour in some cases, especially if the lines were not sufficiently cleaned and flushed the last time the equipment was used.

IV.8. Loading Skin into the Chamber.

The condition of the skin is checked by measuring its electrical impedance and monitoring the passive flux of the donor solution. The impedance of "good skin" should be >25 $k\Omega\,cm^2$ at 100 Hz (Prausnitz, *et al.*, 1993 [a]; Chen, *et al.*, 1998 [b]; M. R. Prausnitz, personal communication; Gowrishankar, personal communication). Low impedances or large passive fluxes indicate that the skin's integrity has been compromised in some way.

The impedance is measured across the two inner measurement electrodes in the permeation chamber. However, besides the skin, this measurement also includes PBS and the polyacrylamide gel. The other impedances can be neglected, though, since the impedance of the skin is much larger than PBS (see Section 3.6).

1. Float a piece of skin (see Section I.1) in a dish of PBS for ~1 min.
2. Gently remove the wax paper backing. Do not use tweezers. The skin should float on the surface, with the stratum corneum side facing upwards.
3. Fill the receptor compartment completely with PBS. There should not be any air bubbles present.
4. Position the skin in the chamber so that the stratum corneum faces the donor compartment and the epidermis faces the receptor compartment. Clamp the chamber shut. Verify that the receptor compartment is still completely filled with PBS.
5. Fill the donor with PBS.
6. Connect the impedance meter (see Section III.5) to the measurement electrodes. Good skin has an impedance >40 $k\Omega\,cm^2$ at 100 Hz. Poor skin should be discarded.
7. Disconnect the impedance meter.
8. Remove the PBS from the donor compartment and add the donor solution (Solution 6). Add a 1.5 mm "flea"-type magnetic stir bar to the donor compartment.
9. Connect the chamber to the pulsing circuit as shown in Figure IV.5, verifying that all four electrodes are properly connected.
10. Turn on the stirring plate and the water bath.

IV.9. Passive Control.

After the skin has been loaded in the chamber, the flow-through system should be activated. The skin should be left for at least 1 h to fully hydrate the skin and check for leaks (holes or tears in the skin). Leaks can be detected by observing large or increasing readings in the background fluorescence observed on the spectrofluorimeter. If the skin begins to leak, it should be discarded.

IV.10. Pulsing Conditions.

High-voltage pulses should be applied to the skin at the rate of 1 pulse every ~5 s. Both the time constant and the applied voltage should be set on the pulser as needed before pulsing is started. The transdermal voltage is a nonlinear function of the applied voltage (see Figures 7.10 and 8.3) (Pliquett, *et al.*, 1995 [a]; Chen, *et al.*, 1998 [c]). Thus, given a desired transdermal voltage, a guess of the applied voltage should be made at this time.

1. Set the pulser to deliver the appropriate types of pulses.
2. Gradually start the pumps for the electrode flow-protection system. Make sure that the polyacrylamide gel in the chamber does not crack or break when this is turned on. If the gel breaks, new gel will have to be made, which will cause the experiment to be aborted.
3. Turn on the oscilloscope and the computer. They should be set to start recording once the first pulse is applied. Make sure that all screen savers, energy savers, and any other software drivers that can cause process interrupts in the computer have been completely turned off. The computer should not be doing anything during the experiment besides downloading data. Any timing glitches between the computer and the oscilloscope could cause either the computer or the oscilloscope to crash.
4. Start the spectrofluorimeter for a time-based scan. The spectrofluorimeter should record fluorescence for the time of pulsing (typically 1 h), plus some additional time at the beginning to measure the baseline, and some time at the end to measure recovery. The time interval between successive measurements should be as short as possible (e. g., 0.5 s). Record about a minute of passive flux (control) to establish the baseline.
5. Start the pulser. The oscilloscope and the computer should start recording pulses immediately with the first pulse. Note the exact time when pulsing starts, on the clock and on the spectrofluorimeter (t_{start}). These times will be needed later to synchronize the pulsing data and the fluorescence data.

6. Since the spectrofluorimeter, the pulser, and the oscilloscope/computer are all automated, during the experiment, the equipment should simply be monitored at all times in case something goes wrong.

IV.11. Ending the Experiment.

After pulsing, the recovery of the skin can be measured by recording the fluorescence once the pulser has been turned off. Afterwards, the skin should be removed from the permeation chamber and mounted on a microscope side for analysis. Voltage and current data from the computer and data from the spectrofluorimeter should be saved on disk for later analysis. The standard curve should also be measured.

1. After pulsing, turn off the pulser, but leave the rest of the equipment running. Wait until the fluorescence reaches steady state to stop recording on the spectrofluorimeter.
2. Turn off all of the pumps.
3. Empty the donor compartment. Flush it out 3× with PBS.
4. Open the permeation chamber and carefully remove the skin. Place it carefully on a microscope slide. Gently spread the skin out so it lies flat, and lightly blot it dry with a paper towel. Do not rub the skin.
5. Add a drop of mounting solution (Solution 3 from Section IV.1).
6. Gently put a cover slip on top. This will cause the mounting solution to spread out and cover the skin. Seal in place with nail polish. Bring the slide to a fluorescence microscope for immediate analysis and photography (Section II.3).
7. Save the data from the computer and from the spectrofluorimeter. These should be copied to a workstation for later analysis (see Section IV.13).

IV.12. Measuring the Standard Curve.

The standard curve should be measured under exactly same conditions that the experiment was performed under, including the same flowrates, tubing, and the same measurement cuvette. Placing the calibration solutions in separate cuvettes and measuring their fluorescence will not work, since the volume of liquid within the cuvette needs to be exactly the same for each sample. Thus, each calibration solution needs to be separately pumped through the spectrofluorimeter.

Since the calibration curve is continually being pumped through the spectrofluorimeter, 10 ml will be needed for each concentration, to allow the fluorescence in the system to go to steady state.

1. Prepare a standard curve, starting at the donor concentration. Make up 10 ml of solution for each concentration.
2. Set up the spectrofluorimeter for a time-based scan.
3. Run each sample through the spectrofluorimeter. Start from the most dilute sample and increase to the most concentrated. Record the times that each solution passes through the spectrofluorimeter. With only 10 ml of solution per concentration, steady state for each concentration in this system will only last for a few minutes. It is usually simpler to let the spectrofluorimeter run continuously, than to start and stop the spectrofluorimeter between each concentration and risk missing the steady state regime.
4. Save the calibration curve onto disk for later analysis.

IV.13. Analysis of the Flux and Voltage Data.

All of the fluorescence, voltage, current, and calibration data needs to be downloaded into a computer for analysis. Due to the amount of data one experiment can generate, a workstation, rather than a PC, is recommended (e. g. Sun Sparc 10, Sun). A sample program, written in MatLab (MathWorks), is given in Section IV.13.4.

The first step in the analysis is to convert all of the flux and current data into the transdermal voltage data. The next step is to calibrate and deconvolute the fluorescence data into molecular flux data. The final step is to correlate the two sets of measurements, to determine the amount of molecular flux that occurs during each pulse.

IV.13.1. Transdermal Voltage Calculations.

The voltage drop across the skin can be determined by applying Ohm's Law to the current and the voltage. The resistance of the intervening PBS (R_{PBS}) should already be known (see Sections 3.6 and III.6).

1. Since the data from the oscilloscope has probably been transferred in a compacted format, the first step is to uncompress the data and convert it into voltage data.

2. Ohm's Law is used to convert the voltage drop (U_{curr}) across the 1.2 Ω resistor (R_{curr} = 1.2 Ω):

$$I = \frac{U_{curr}}{R_{curr}} = \frac{U_{curr}}{1.2\ \Omega}. \qquad \text{(IV.4)}$$

3. The current across the skin (I) and the voltage drop across the measurement electrodes (U_{inner}) for each pulse should now be known. To calculate the transdermal voltage (U_{skin}), use the following equation:

$$U_{skin} = U_{inner} - I\,R_{PBS}. \qquad \text{(IV.5)}$$

IV.13.2. Deconvolution of the Fluorescence Data.

The fluorescence measured in the spectrofluorimeter is the sum of two components: the molecular flux out of the skin, and the mixing that occurs in the tubing and the cuvette (see Section IV.3.4). With a model of the mixing that occurs in this system, the molecular flux across the skin can be determined.

1. Using the standard curve (Section IV.12), convert all of the fluorescence data into concentrations. These are molecular concentrations within the cuvette, not transdermal fluxes.
2. The molecular flux across the skin is determined by the following equation (Pliquett, *et al.*, 1995 [b]).

$$J = V_{cuv}\frac{C_2 - C_1}{A\,\Delta t} + \frac{Q}{A}\frac{C_1 + C_2}{2}. \qquad \text{(IV.6)}$$

In this equation, J is the molecular flux across the skin, V_{cuv} is the volume of the cuvette (see Section IV.3.4), A is the exposed area of the skin, C_1 and C_2 are two successive measurements on the spectrofluorimeter (expressed as concentrations), Δt is the length of time between two subsequent measurements of C_1 and C_2, and Q is the average flowrate through the cuvette (Section IV.3.4). C is assumed to be linear and J is assumed to be constant, both over the time interval Δt, which should be kept small (0.5 s). This equation has to be applied to every pair of measurements made on the spectrofluorimeter. Note that due to the mixing within the cuvette, the time resolution for these measurements is not more accurate than τ_{cuv}.

IV.13.3. Correlation of Fluxes and Voltages.

At this point, there are two arrays of data, representing the transdermal voltages during each pulse, and the molecular fluxes across the skin (at a time resolution of τ_{cuv}). These data need to be correlated in time with each other.

1. Define the first pulse to occur at a time 0. Then the nth pulse occurs at time t:

$$t = (n-1)\, t_{int}. \tag{IV.7}$$

2. To correlate the time on the spectrofluorimeter with the time of each pulse, the time on the spectrofluorimeter (t_{fluor}) needs to be corrected for the elapsed time before pulsing was started (t_{start}) and the plug flow time (t_{react}).

$$t = t_{fluor} - t_{start} - t_{react}. \tag{IV.8}$$

3. Now that the two measurements have been synchronized in time (t), the molecular flux during each pulse can be determined. Note, however, that the time resolution is still τ_{cuv}. If pulses were applied more rapidly than that ($t_{int} < \tau_{cuv}$), then the flux measurements will still be confounded by subsequent pulses.

IV.13.4. `JvsU.m`.

The following is the script file ("`*.m` file") for `JvsU.m`, a MatLab 5 program which calibrates and correlates the flux and voltage data to determine the molecular flux for each pulse.

```
% JvsU.m
% This program inputs raw voltage data (from 'savewave.cpp', files 'preamb1.m',
%   'preamb2.m', 'wave1.dat', and 'wave2.dat') and raw fluorescence data from
%   the Spex, outputed as ascii files, as 'calb.txt' and 'fluor.txt'.  See
%   parameter list for correct formats.  Program processes data, outputs a plot
%   of flux (in 'CorrFlux') and transdermal voltages (in 'Uskin'), and plots
%   those versus pulse number (in 'Number').  The results are saved in
%   'final.txt' as pulse number, skin voltage (in V), and flux (in mol/m2/s),
%   for use in further analysis.
% Tani Chen, 4/17/97
%   Modified on 6/9/97


clc
disp 'Intializing...'
clear
close all
format
NumPulse = input('  Enter number of pulses. ->');  % Number of pulses delivered
NumData = 500;     % Number of data points in each pulse
Rcur = 1.2;        % Resistance of current-measuring resistor (Ohm)
Rpbs = 251;        % Resistance of PBS in chamber (Ohm)

% SpexTime is for use with Bldg 20 (Runs F1-F26s).  Uncomment for those runs.
% SpexTime = 3900;  % Length of time data was recorded on the Spex, in seconds.
```

```
%                   %   Number of data points = 2 * SpexTime + 1 (have to include
%                   %   0 s).  Also see routines on entering calibration and flux
%                   %   data!  Unix routines cannot be adjusted with SpexTime!

SpexTime = 4500;  % Length of time data was recorded on the spectrofluorimeter,
                  %   in seconds.  Despite the changeover in equipment, this
                  %   variable is going to remain "SpexTime," even tho the Spex
                  %   is no longer being used (it should really be called
                  %   "PTITime"....)
 SpexTime = 13500;  % 3 h + 45 min run
% SpexTime = 28800;  % 7 h + 1 h run

DeltaT = .5;      % Sampling time on Spex (s)
                  % Sampling time on PTI (Also .5 s to preserve continuity)
ErrorV = 4.81;    % Error in voltage measurement of probe:  +/- 4.8 V  (SD)
ErrorI = ErrorV/Rcur/200;  % Error in current (voltage thru Rcur)

% PerErrFl = .045;  % Error in flux measurements:  +/- 4.5%  (SD)
%                   %   This is only for the Spex!
PerErrFl = .022;

Signal = 14 * 2;      % Number of points fluorescence signal is averaged over
Area = .64 / 100 / 100;  % Area of the skin (m2)
PulseIntv = ((1*3600+20*60+52)/(873-1) + (1*3600+6*60+37)/(720-1) + (1*3600+6*60+41)/(720-1)) / 3;
  % Time interval between pulses (s)
  %   *BTX autopulser only!!*  This needs to be very accurate!!
  %   Data:  873 pulses = 1:20:52, 720 pulses = 1:06:37, 720 pulses = 1:06:41
  %   Note that pulse #1 = 0:00:00
% PulseIntv = ((1*3600 + 0*60 + 17) - (0*3600 + 0*60 + 40)) / 740;
  %   740 pulses in 1 h (4.8338)
% PulseIntv = ((1*3600 + 0*60 + 27) - (0*3600 + 0*60 + 38)) / 710;
  %   710 pulses in 1 h (5.0549)
 PulseIntv = ((1*3600 + 0*60 + 53) - (0*3600 + 0*60 + 40)) / 730;
  %   730 pulses in 1 h (4.9493)

% Pump characteristics for Runs F27 - ?
%   (currently set to Pump Speed 99)
Pump = (.0301205 + .0295858 + .0285714) / 3 / 1000;    % Pump flowrate with
                                                       %   chamber (l/s)
PumpCuv = (.0303030 + .03125 + .0318471) / 3 / 1000; % Pump flowrate without
                                                       %   chamber (l/s)
TauCh = (19.0223 + 29.9944 + 18.3699) / 3;  % Residence time of whole system (s)
Tau = (18.2856 + 22.0411 + 23.4928) / 3;    % Residence time of chamber only (s)
Tdelay = (65 + 64 + 63) / 3;       % Time lag of entire system(s)
Toffset = (19 + 18 + 19) / 3;      % Time lag of cuvette only (s)
% Pump speed 99:  Pump =    .0301205, .0295858, .0285714
%                 PumpCuv = .0303030, .03125, .0318471
%                 TauCh =   19.0223, 29.9944, 18.3699
%                 Tau =     18.2856, 24.0411, 23.4928
%                 Tdelay =  65, 64, 63
%                 Toffset = 19, 18, 19
% Pump speed 77:  Pump =    .0214592, .0223214, .0221239
%                 PumpCuv = .0248756, .0239234, .0238095
%                 TauCh =   24.9851, 22.7287, 18.8472
%                 Tau =     30.7906, 35.5403, 28.0830
%                 Tdelay =  80, 75, 74
%                 Toffset = 26, 25, 26
% Pump speed 55:  Pump =    .0152905, .0192308, .0157233
%                 PumpCuv = .0165289, .0167364,.0165975
%                 TauCh =   40.8933, 35.7017, 20.0055
%                 Tau =     37.8878, 40.7751, 41.3692
%                 Tdelay =  107, 104, 108
%                 Toffset = 34, 30, 29
% Pump speed 33:  Pump =    .00874126, .00898876, .00904159
%                 PumpCuv = .00996016, .00961538, .00959233
%                 TauCh =   197.953, 180.041, 98.8818
%                 Tau =     53.5107, 62.2365, 60.1493
%                 Tdelay =  179, 196, 189
%                 Toffset = 64, 57, 56

% Pump characteristics for Runs F4 - F26s.  Uncomment for those runs.
% Pump = (.03238 + .03198 + .03212) / 3 / 1000;    % Pump flowrate with
%                                                    %   chamber (l/s)
% PumpCuv = (.03198 + .03191 + .03226) / 3 / 1000; % Pump flowrate without
%                                                    %   chamber (l/s)
% TauCh = (20.4 + 24.0 + 27.6) / 3;  % Residence time of whole system (s)
% Tau = (14.6 + 16.0 + 12.8) / 3;    % Residence time of chamber only (s)
% Tdelay = (46 + 50 + 48) / 3;       % Time lag of entire system(s)
% Toffset = (31 + 23 + 23) / 3;      % Time lag of cuvette only (s)

% Pump characteristics for Runs F1, F2, and F3.  Uncomment for those runs.
% Pump = (.06757 + .06281 + .07042) / 3 / 1000;    % Pump flowrate with
%                                                    %   chamber (l/s)
% PumpCuv = (.07042 + .07310 + .07788) / 3 / 1000; % Pump flowrate without
%                                                  %   chamber (l/s)
% TauCh = (14.5 + 14.5 + 12.0) / 3;   % Residence time of whole system (s)
% Tau = (5.5 + 5.0 + 8.0) / 3;        % Residence time of chamber only (s)
% Tdelay = (18.2 + 18.0 + 18.0) / 3;  % Time lag of entire system(s)
% Toffset = (8 + 9 + 7 + 7) / 4;      % Time lag of cuvette only (s)

Vcuv =  PumpCuv * Tau;             % Volume of cuvette (and tubing) (l)
Vch = PumpCuv * TauCh;             % Approx. volume of chamber (l)
```

```
Tstart = input('  Enter starting time (don''t add offset). ->') + Toffset;
MW = input('  Enter molecular weight of tracer. ->');
Charge = input('  Enter charge of tracer. ->');
Charge = abs(Charge);                % Ignore negative sign
NA = 6.0221367e23;                   % Avogadro's number (1 / mol)
Elc = 1.60217733e-19;                % Charge on the electron (C)
Thickn = 20 * 1e-6;                  % Thickness of the stratum corneum (m)
Condy = 1 / (67 / 100);              % Conductivity of PBS (Ohm m)


disp 'Entering preamble data from "preamb1.m"...'
preamb1  %  Preamble format:  1(byte), 1(norm), 400(#points), 1(dummy), Xincr,
         %    Xorig, Xref, Yincr, Yorig, Yref
Xincr = preamble1(5);    % Tick = (bucketnumber - Xref) * Xincr + Xorig
Xorig = preamble1(6);    %   Should be the same for both sets of data
Xref = preamble1(7);
Yincr1 = preamble1(8);   % Voltage = (data - Yref) * Yincr + Yorig
Yorig1 = preamble1(9);
Yref1 = preamble1(10);


disp 'Entering preamble data from "preamb2.m"...'
preamb2                  % Same format as above
Yincr2 = preamble2(8);   % Voltage = (data - Yref) * Yincr + Yorig
Yorig2 = preamble2(9);
Yref2 = preamble2(10);


disp 'Entering waveform data from "wave1.dat"...'  % Chamber voltage data
FileNo = fopen('wave1.dat', 'r');
Uch = fread(FileNo, [NumData, NumPulse], 'uchar');
Uch = ((Uch - Yref1) * Yincr1 + Yorig1) * 200;
  %  See preambles for equations.  200x high voltage probe


disp 'Entering waveform data from "wave2.dat"...'  %  Current voltage data
FileNo = fopen('wave2.dat', 'r');
Ucur = fread(FileNo, [NumData, NumPulse], 'uchar');
Ucur = (Ucur - Yref2) * Yincr2 + Yorig2;  % See preambles for equations
Ucur = Ucur .* (Ucur > 0);                % Get rid of negative current (noise)
Ucur = Ucur / Rcur;                       % Convert volts to amps


disp 'Deleting prepulse data from chamber voltages...'
for j = 1:NumPulse
  Utemp = Uch(:, j);              % Temporary matrix for each column
  if max(Utemp) > 7
    Loc(j) = min(find(Utemp > 7));  % Pulse detected when > 7 V.  "Find" lists
  else
     Loc(j) = 50;
  end
end                               %   all the locations > 7.  "Min" gives the
                                  %   location of the first pulse.


disp 'Deleting prepulse data from current measurements...'
for j = 1:NumPulse
  Utemp = Ucur(:, j);             % Temporary matrix
  Loc1 = min(find(Utemp > .05));  % Same routine as above.  Voltage > .1 V
                                  %  Change this for lower voltages...
  if Loc1 > Loc(j)
    Loc(j) = Loc1;
  end
  Ucur(1:(NumData - Loc(j) + 1), j) = Ucur(Loc(j):NumData, j);
  Ucur((NumData - Loc(j) + 2):NumData, j) = NaN;
  Uch(1:(NumData - Loc(j) + 1), j) = Uch(Loc(j):NumData, j);
    % Delete header and push data forward so 0 means start of pulse
  Uch((NumData - Loc(j) + 2):NumData, j) = NaN;  % Fill holes with "NaN"
end


disp 'Fitting chamber voltages (ignore log of zero errors)...'
Uch = log(Uch - Uch .* (Uch <= 0));
  % Take logs of only positive numbers.  Negative numbers are changed to 0's
  %   (since the log of a negative number is complex!), then -Inf.  NaN's
  %   reamain NaN's
Uch = isfinite(Uch) .* Uch;  % Convert -Inf to NaN (former negative numbers)

for j = 1:NumPulse
  Tick = ((1:500)' - Xref + Loc(j)) * Xincr + Xorig;
    %  Set up time vector for each pulse for curve fitting (s).  See preamble
  Utemp = Uch(1:150, j);
  if sum(isnan(Utemp)) == size(Utemp, 1)  % If Utemp empty, then no line fit
    Chamber(j, :) = [NaN NaN];
  else
    Chamber(j, :) = polyfit(Tick(isfinite(Utemp)), Utemp(isfinite(Utemp)), 1);
      % Linear fit (ln y = m * Time + b)
  end
end

Chamber(:, 1) = -1 ./ Chamber(:, 1);  % Tau(s) = -1 / m
TauPulse = Chamber(:, 1);
```

```
Chamber(:, 2) = exp(Chamber(:, 2));   % Uch(V) = exp(b)
  %  Chamber(:, 1) = TauPulse = Tau (s)
  %  Chamber(:, 2) = Peak voltage across differential electrodes (V)


disp 'Fitting current measurements (ignore log of zero errors)...'
Ucur = log(Ucur - Ucur .* (Ucur <= 0));  % Take logs of positives
Ucur = isfinite(Ucur) .* Ucur;           % Same routine as above

for j = 1:NumPulse  % Same routine as above, except for current now
  Tick = ((1:500)' - Xref + Loc(j)) * Xincr + Xorig;  % (s)
  Utemp = Ucur(1:150, j);
  Current(j, :) = polyfit(Tick(isfinite(Utemp)), Utemp(isfinite(Utemp)),1);
end

Current(:, 2) = exp(Current(:, 2));  % Ucur(V) = exp(b) (Don't need Tau)
  %  Current(:, 2) = Peak currents across measuring resistor, Rcur (A)


disp 'Finding transdermal voltages...'
Uskin = Chamber(:, 2) - Current(:, 2) * Rpbs;
  % Uskin = Uch - Upbs = Uch - I * Rpbs
Uskin = Uskin .* (Uskin<1e3) ./ (Uskin<1e3) .* (Uskin>0) ./ (Uskin>0);
  % Get rid of errors (negatives, too large)
Rskin = Chamber(:, 2) ./ Current(:, 2) - Rpbs;
  % Rskin = Uch / I - Rpbs  (Rskin = Uskin / I (Ohm)
Rskin = Rskin .* (Rskin<1e4) ./ (Rskin<1e4) .* (Rskin>0) ./ (Rskin>0);
  %  Get rid of errors (negatives, too large)
VoltTime = (0:(NumPulse - 1))' * PulseIntv;
  % Time vector for Uskin, same size as Uskin (s)

% DM3000F format load (Bldg 20).  Uncomment for Runs F1-F26s.
% disp('Loading fluorescence calibration data from "calb.txt" (ignore file errors)...')
% ! rm temp.txt
% ! rm temp2.txt
% % Delete header from calibration data.
% %   7802 = SpexTime * 2 + 1  (See initialization)
% ! tail -7802 calb.txt > temp2.txt
% % Delete trailer from calibration data
% %   7801 = SpexTime * 2 + 1  (See initialization)
% ! head -7801 temp2.txt > temp.txt
% ! rm temp2.txt
% FileNo = fopen('temp.txt', 'r');
% Calb = fscanf(FileNo, '%e  %e', [2 7801]);
% Calb = Calb';
% Calb = Calb(:, 2);  % Calibration curve (arbitrary x-axis)

% PTI format load (Bldg E25).
disp('Loading fluorescence calibration data from "calb.txt" (ignore file errors)...')
! rm temp.txt
% Delete header from calibration data (5 lines)
! tail +5 calb.txt > temp.txt
load temp.txt
Calb = temp(:, 2);  % Calibration curve (arbitrary x-axis)
! rm temp.txt


disp('Calibrating data...')  % Plot calibration data
Handle = semilogy(Calb);
set(figure(1), 'Position', [1160 6 1142 845])
set(Handle, 'Color', 'c')
xlabel('Point number')
ylabel('Fluorescence (counts/s)')
title('Raw Calibration Data from "calb.txt"')


disp('  Scaling graph (see page on right)...')
Choice = 1;
while Choice == 1
  disp('    Click on bottom left corner.')
  BotLeft = ginput(1);
  disp('    Click on top right corner.')
  TopRight = ginput(1);
  axis([BotLeft(1) TopRight(1) BotLeft(2) TopRight(2)])  % Scale graph
  Choice = input('    Enter 1 for re-scale, 2 to restart, 0 when done. ->');
  if Choice == 2
    axis auto
    Choice = 1;
  end
end


disp('  Entering calibration values...')
for j = 2:8    % Change the 8 to a 9 for the Bldg 20 runs (Runs F1 to F26s).
               %   Altho since 9 is usually less than the background level, it
               %   shouldn't really matter.
  Choice = 1;  % Get values for each calibration sample
  while Choice == 1
    disp('    Click on left-most region of sample #')
    disp(j)
    MouseLeft = ginput(1);
    Handle = line([MouseLeft(1);MouseLeft(1)], [BotLeft(2);TopRight(2)]);
```

```
    set(Handle, 'Color', 'r')
    disp('    Click on right-most region.')
    MouseRight = ginput(1);
    Handle = line([MouseRight(1);MouseRight(1)], [BotLeft(2);TopRight(2)]);
    set(Handle, 'Color', 'r')
    Choice = input('    Enter 1 to re-do, 0 when done. ->');
  end
  Coord(j) = mean(Calb(round(MouseLeft(1)):round(MouseRight(1))));
    % Coord contains the calibration curve values (2 thru 10) (cps).  Average
    %   of range selected by mouse
end


disp('  Figuring calibration equation (ignore log of zero errors)...')
Conc = log([NaN 1e-1 1e-2 1e-3 1e-4 1e-5 1e-6 1e-7 1e-8] * 1e-3);
  % Concentration values (M).  Sample #1 (= Donor = 1 mM) is ignored.
Coord = log(Coord);

close(1)
Handle = plot(Coord, 'co-');  % Plot calibration curve
set(figure(1), 'Position', [514 430 560 420])
set(Handle, 'MarkerSize', 4)
set(Handle, 'MarkerFaceColor', 'c')
ylabel('log(fluorescence intensity)')
xlabel('Sample #')
title('Standard Curve Data')
axis([2 8 floor(min(Coord(2:8))) ceil(max(Coord(2:8)))])
  % For the Bldg 20 runs (Runs F1-F26s), these 8's should all be 9's.  Again,
  %   it probably doesn't really matter....

Low = input('    Enter lowest sample number in linear region. ->');
High = input('    Enter highest sample number in linear region. ->');
CalbEqn = polyfit(Coord(Low:High), Conc(Low:High), 1);  % Get curve fit
                                                        %   parameters


% DM3000F format load (Bldg 20).  Uncomment for Runs F1-F26s.
% disp('Loading fluorescence flux data from "fluor.txt"...')
% ! rm temp.txt
% % Delete header from calibration data.
% %   7802 = SpexTime * 2 + 1 + tail(1)  (See initialization)
% ! tail -7802 fluor.txt > temp2.txt
% % Delete trailer from calibration data
% %   7801 = SpexTime * 2 + 1  (See initialization)
% ! head -7801 temp2.txt > temp.txt
% ! rm temp2.txt
% FileNo = fopen('temp.txt', 'r');
% Fluor = fscanf(FileNo, '%e  %e', [2 7801]);  % Fluorescence data
% Fluor = Fluor';
% Fluor = Fluor(:, 2);
% ! rm temp.txt

% PTI format load (Bldg E25).
disp('Loading fluorescence flux data from "fluor.txt"...')
! rm temp.txt
% Delete header from calibration data (5 lines)
! tail +5 fluor.txt > temp.txt
load temp.txt
Fluor = temp(:, 2);


disp('Glitch removal...')
Handle = plot(Fluor, 'g');
axis tight
ylabel('Fluorescence (counts/s)')
xlabel('Point Number')
title('Raw Fluorescence Data from "fluor.txt"')

Choice = input('  Enter 1 for glitch removal, 0 if OK. ->');
while Choice == 1
  Handle = plot(Fluor, 'go-');
  set(figure(1), 'Position', [1160 6 1142 845])
  set(Handle, 'MarkerSize', 4)
  set(Handle, 'MarkerFaceColor', 'g')
  axis tight
  ylabel('Fluorescence (counts/s)')
  xlabel('Point Number')
  title('Raw Fluorescence Data from "fluor.txt"')

  disp('  Scaling graph (see page on right)...')
  Choice = 1;
  while Choice == 1
    disp('    Click on bottom left corner.')
    BotLeft = ginput(1);
    disp('    Click on top right corner.')
    TopRight = ginput(1);
    axis([BotLeft(1) TopRight(1) BotLeft(2) TopRight(2)])  % Scale graph
    Choice = input('    Enter 1 for re-scale, 2 to restart, 0 when done. ->');
    if Choice == 2
      axis auto
      axis tight
      Choice = 1;
```

```
    end
  end

  disp('  Click on left-most region.')
  MouseLeft = ginput(1);
  Handle = line([MouseLeft(1); MouseLeft(1)], [BotLeft(2) TopRight(2)]);
  set(Handle, 'Color', 'r')
  disp('  Click on right-most region.')
  MouseRight = ginput(1);
  Handle = line([MouseRight(1); MouseRight(1)], [BotLeft(2) TopRight(2)]);
  set(Handle, 'Color', 'r')

  Choice = input('  Enter 1 to abort, 0 if correct. ->');
  if Choice == 0
    disp('  Deleting section...')
    Fluor(floor(MouseLeft):ceil(MouseRight)) = NaN;
  end
  Choice = input('  Enter 1 for more removals, 0 when done. ->');
end


disp('Converting fluorescences into concentrations (ignore dividing by zero errors)...');
Fluor = Fluor(:) .^ (CalbEqn(1) * (1 - isnan(Fluor(:)))) * exp(CalbEqn(2)) .* ((1 - isnan(Fluor(:))) ./ (1 -
isnan((Fluor(:)))));
  % Fluorescence in (M) (from Conc)


disp('Applying signal averaging...')
disp('  Number of points being averaged:')
disp(Signal)
for j = 1:(size(Fluor) - Signal)
  Fluor(j) = mean(Fluor(j:(j + Signal - 1)));
end
Fluor((size(Fluor) - Signal + 1):size(Fluor)) = NaN;


disp('Finding lag times (see page on right)...')
Handle = plot(Fluor, 'y');
set(figure(1), 'Position', [1160 6 1142 845])
axis tight
ylabel('Fluorescence (counts/s)')
xlabel('Point Number')
title('Raw Fluorescence Data from "fluor.txt"')

disp('  Scaling graph...')
Choice = 1;
while Choice == 1
  disp('    Click on bottom left corner.')
  BotLeft = ginput(1);
  disp('    Click on top right corner.')
  TopRight = ginput(1);
  axis([BotLeft(1) TopRight(1) BotLeft(2) TopRight(2)])  % Scale graph
  Choice = input('    Enter 1 for re-scale, 2 to restart, 0 when done. ->');
  if Choice == 2
    axis auto
    axis tight
    Choice = 1;
  end
end

disp('  Click on start of rise.')
Tlag = ginput(1);
Tlag = Tlag(1);        % Need only x coordinate
Handle = line([Tlag; Tlag], [BotLeft(2) TopRight(2)]);
set(Handle, 'Color', 'r')
if Tlag > size(Fluor, 1)  % Didn't reach steady state
  Tlag = NaN;
end
if Tlag < 0  % Didn't reach steady state
  Tlag = NaN;
end
Tlag = Tlag/2 - Tstart; % Subtract off time until first pulse (includes Toffset)

Choice = input('Type 0 to continue. ->');


disp('Finding rise times (see page on right)...')
Handle = plot(Fluor, 'y');
set(figure(1), 'Position', [1160 6 1142 845])
axis tight
ylabel('Fluorescence (counts/s)')
xlabel('Point Number')
title('Raw Fluorescence Data from "fluor.txt"')

disp('  Scaling graph...')
Choice = 1;
while Choice == 1
  disp('    Click on bottom left corner.')
  BotLeft = ginput(1);
  disp('    Click on top right corner.')
  TopRight = ginput(1);
  axis([BotLeft(1) TopRight(1) BotLeft(2) TopRight(2)])  % Scale graph
```

```
  Choice = input('    Enter 1 for re-scale, 2 to restart, 0 when done. ->');
  if Choice == 2
    axis auto
    axis tight
    Choice = 1;
  end
end

disp('  Click on end of rise.')
TSS = ginput(1);
TSS = TSS(1);        % Need only x coordinate
Handle = line([TSS; TSS], [BotLeft(2) TopRight(2)]);
set(Handle, 'Color', 'r')
if TSS > size(Fluor, 1)  % Didn't reach steady state
  TSS = NaN;
end
if TSS < 0  % Didn't reach steady state
  TSS = NaN;
end
TSS = TSS/2 - Tstart;  % Subtract off time until first pulse (includes Toffset)


disp('Deleting data below the detection limit...')
DetLmt = exp(Conc(High));
for j = 1:(size(Fluor))
  if Fluor(j) < DetLmt
    Fluor(j) = NaN;
  end
end


disp('Deconvoluting fluxes...')
  % Routine taken from Pliquett, U., M. R. Prausnitz, Y. A. Chizmadzhev, and
  %   J. C. Weaver.  "Measurement of Rapid Release Kinetics for Drug Delivery,"
  %   _Pharm Res_, 12(4):549-55, 1995, Equations (7) and (8).  With some
  %   additional modifications and simplifications.
for j = 1:(size(Fluor)-1)
  Flux(j) = Vcuv*(Fluor(j + 1) - Fluor(j))/Area/.5 + PumpCuv/Area*(Fluor(j + 1) + Fluor(j))/2;
  % Flux in (mol / m2 / s)
end


disp('Correlating fluxes with pulses...')
FluxTime = ((1:(SpexTime * 2 + 1))' - Tstart) / 2;  % Time vector for flux
                                                    %   data.
MaxNo = (floor(NumPulse - (VoltTime(NumPulse) - max(FluxTime)) / PulseIntv));
  % Figure out how many pulses correspond between flux data (which ends after
  %   SpexTime s) and voltage data (which = 720 * PulseIntv > SpexTime).
  %   Should be about 700 pulses.
if MaxNo > NumPulse
  MaxNo = NumPulse;
end

for j = 1:MaxNo
  CorrFlux(j) = Flux(max(find(sign(FluxTime - VoltTime(j)) < 0)) + 1);  % Phew!
    % CorrFlux contains the flux at the instant when a pulse is applied (Time
    %   lags have already been accounted for, above.
    %   sign(FluxTime - VoltTime(j)) gives -1 for FluxTime < VoltTime and +1
    %   for >.  find gives all the points where FluxTime < VoltTime and max
    %   gives the largest one (which is where FluxTime = VoltTime.  Then we
    %   record the flux at that point.
end
CorrFlux = CorrFlux .* (CorrFlux>0) ./ (CorrFlux>0); % Get rid of negatives
CorrFlux = CorrFlux';  % Put the matrix in the right orientation.  I don't know
                       %   why MatLab insists on transposing the matrix....


disp('Displaying flux vs voltage results (ignore negative data errors)...')
semilogy(Uskin, CorrFlux,  'w.');  % Plot flux vs transdermal voltage!
set(figure(1), 'Position', [1160 6 1142 845])
xlabel('Transdermal Voltage (V)')
ylabel('Instantaneous Flux (mol / m2 / s)')
title('Instantaneous Flux versus Transdermal Voltage')

disp('  Adding error bars (ignore negative data errors)...')
for j = 1:MaxNo
  Handle=line([(Uskin(j)-ErrorV) (Uskin(j)+ErrorV)],[CorrFlux(j), CorrFlux(j)]);
  set(Handle, 'Color', 'r')
  FluxErr = PerErrFl * CorrFlux(j);
  Handle = line([Uskin(j), Uskin(j)], [(CorrFlux(j) - FluxErr), (CorrFlux(j) + FluxErr)]);
  set(Handle, 'Color', 'r')
end

hold on
Handle = semilogy(Uskin, CorrFlux, 'wd');  % Plot flux vs transdermal voltage!
set(Handle, 'MarkerSize', 2)               %   This time, put dots on top of
set(Handle, 'MarkerFaceColor', 'w')        %   error bars so we can see them.
hold off


disp('Displaying flux vs current results (ignore negative data errors)...')
figure
```

```
semilogy(Current(:,2), CorrFlux,  'w.');  % Plot current vs transdermal voltage
set(figure(2), 'Position', [1160 -895 1142 845])
xlabel('Current (A)')
ylabel('Instantaneous Flux (mol / m2 / s)')
title('Instantaneous Flux versus Current')

disp('  Adding error bars (ignore negative data errors)...')
for j = 1:MaxNo
  Handle=line([(Current(j, 2) - ErrorI) (Current(j, 2 ) +ErrorI)], [CorrFlux(j), CorrFlux(j)]);
  set(Handle, 'Color', 'r')
  FluxErr = PerErrFl * CorrFlux(j);
  Handle = line([Current(j, 2), Current(j, 2)], [(CorrFlux(j) - FluxErr), (CorrFlux(j) + FluxErr)]);
  set(Handle, 'Color', 'r')
end

hold on
Handle = semilogy(Current(:,2), CorrFlux, 'wd');  % Plot current vs voltage
set(Handle, 'MarkerSize', 2)               %   This time, put dots on top of
set(Handle, 'MarkerFaceColor', 'w')        %   error bars so we can see them.
hold off


disp('Displaying time courses for flux and voltage...')
Number = (1:MaxNo)';
figure

subplot(2, 1, 1)  % Top plot is voltage versus time
Handle = plot(Number, Uskin, 'co');
axis tight
set(figure(3), 'Position', [514 430 560 420])
set(Handle, 'MarkerSize', 2)
set(Handle, 'MarkerFaceColor', 'c')
xlabel('Pulse Number')
ylabel('Transdermal Voltage (V)')
title('Transdermal Voltage during the Experiment')

subplot(2, 1, 2)  % Bottom plot (same figure) is flux versus time
Handle = plot(Number, CorrFlux, 'go');
axis tight
set(Handle, 'MarkerSize', 2)
set(Handle, 'MarkerFaceColor', 'g')
xlabel('Pulse Number')
ylabel('Instantaneous Flux (mol / m2 / s)')
title('Instantaneous Flux during the Experiment')


disp('Displaying cumulative flux...')
CumFlux(1) = CorrFlux(1);
if isnan(CorrFlux(1)) == 1;
  CumFlux = 0;
end

for j = 2:MaxNo
  if isnan(CorrFlux(j)) == 0;
    CumFlux(j) = CumFlux(j - 1) + CorrFlux(j);
  else
    CumFlux(j) = CumFlux(j - 1);
  end
end
CumFlux = CumFlux * Area * PulseIntv * MW * 1e6;

figure
Handle = plot(CumFlux, 'yd');
set(figure(4), 'Position', [514 6 560 369])
axis tight
set(Handle, 'MarkerSize', 3)
set(Handle, 'MarkerFaceColor', 'y')
xlabel('Pulse Number')
ylabel('Cumulative Transport (ug)')
title('Cumulative Transport across the Skin')


disp('Results of experiment:')
disp('  Starting time of spectrofluorimeter [Tstart-Toffset]:')
disp(Tstart-Toffset)
Count = sum(isnan(CorrFlux));  % Number of NaN's in the flux data
disp('  Number of pulses analyzed [MaxNo]:')
disp(MaxNo)
disp('  Number of flux data points analyzed [Nanal]:')
Nanal = MaxNo - Count;
disp(Nanal)
disp('  Length of experiment [Length] (min):')
Length = MaxNo * PulseIntv;   % Length in s (not min)
disp(Length / 60)
disp('  Detection limit [DetLmt] (_M_):')
disp(DetLmt)
disp('  Number of points used in signal averaging [Signal]:')
disp(Signal)
disp('  Time lag before detection [Tlag] (s):')
disp(Tlag)
disp('  Estimated number of pulses before detection [Ndt]:')
Ndt = min(find(CorrFlux > 0));
```

```
disp(Ndt)
disp('  Rise time [TSS] (s):')
format short g
disp(TSS);
format
disp('  Estimated number of pulses before steady state [Nss]:')
Nss = round(TSS / PulseIntv + 1);
disp(Nss);
disp('  Average transdermal voltage [Uskavg] (V):')
Uskavg = sort(Uskin);
Uskavg = mean(Uskavg(1:(size(Uskavg,1) - sum(isnan(Uskavg)))));
disp(Uskavg)
disp('  Average time constant [Tauavg] (ms):')
Tauavg = mean(TauPulse) * 1000;
disp(Tauavg)
disp('  Average resistance of the skin [Rskavg] (Ohm):')
Rskavg = sort(Rskin);
Rskavg = mean(Rskavg(1:(size(Rskavg,1) - sum(isnan(Rskavg)))));
disp(Rskavg)
disp('  Average flux [Javg] (mol / m2 / s):')
SortCF = sort(CorrFlux);
Javg = mean(SortCF(1:size(SortCF, 1) - Count));
disp(Javg)
disp('  Average flux (ug / cm2 / h):')
disp(Javg * MW * 1e6 / 100 / 100 * 3600)
disp('  Net transport (ug):')
disp(CumFlux(MaxNo))
disp('  Average transport number [Travg]:')
format short e
Tr = CorrFlux * Area * Length * NA * Charge * Elc ./ (NumPulse .* Uskin .* TauPulse ./ Rskin);
SortTr = sort(Tr);
Travg = SortTr(1:size(SortTr, 1) - Count);
Travg = sort(Travg);
Travg = mean(Travg(1:(size(Travg,1) - sum(isnan(Travg)))));
disp(Travg)
format
disp('  Fractional aqueous area for tracer [Fwavg]:')
Fwion = Thickn / Condy / Area ./ Rskin;
Fw = Fwion .* Tr / (Charge / 150);
SortFw = sort(Fw);
Fwavg = SortFw(1:size(SortFw, 1) - Count);
Fwavg = sort(Fwavg);
Fwavg = mean(Fwavg(1:(size(Fwavg,1) - sum(isnan(Fwavg)))));
disp(Fwavg)


disp('Displaying transport number and fractional aqueous area results...')
figure
subplot(2, 1, 1)  % Top plot is transport number graph
Handle = plot(Number, Tr, 'mo');
axis tight
set(figure(5), 'Position', [12 -470 560 420])
set(Handle, 'MarkerSize', 2)
set(Handle, 'MarkerFaceColor', 'c')
xlabel('Pulse Number')
ylabel('Transport Number')
title('Transport Number during the Experiment')

subplot(2, 1, 2)  % Bottom plot is fractional aqueous area graph
Handle = plot(Number, Fw, 'wo');
axis tight
set(Handle, 'MarkerSize', 2)
set(Handle, 'MarkerFaceColor', 'w')
xlabel('Pulse Number')
ylabel('Fractional Aqueous Area')
title('Fractional Aqueous Area during the Experiment')


disp('Saving results to "final.txt" (Pulse Number, Uskin, Current, Flux,')
disp('  Transport Number, Fractional Aqueous Area)...')
disp('  (To load, type "load final.txt -ascii")')
Uskin = Uskin(1:MaxNo);
CorrFlux = CorrFlux(1:MaxNo);
Tr = Tr(1:MaxNo);
Fw = Fw(1:MaxNo);
Current = Current(:,2);
Final = ([Number'; Uskin'; Current'; CorrFlux'; Tr'; Fw'])';
  % All those stupid transposes are giving me a headache!
save final.txt Final -ascii

disp('exit')
disp(' ')
disp('End of program.')
```

V. Chamber with Donor and Receptor Flow-Through Systems.

The flow-through system described in this appendix is similar to the one outlined in Appendix IV. The two major additions discussed in this appendix are a donor recycling flow-through system, and a real-time skin impedance measurement system. In all other respects, it is very similar to the one in Appendix IV (see Figure V.1 and V.2).

In the first flow-through system (Appendix IV), there was a slight pressure difference between the donor and receptor compartments. This pressure difference was created by the flow-through system on the receptor side, needed to cause the flow of liquid out of the receptor compartment. By placing a similar system on the donor side, this pressure difference between the two compartments was eliminated.

With a flow-through system on the donor side, the contents of the donor compartment could also be quickly changed at will, even during pulsing, simply by changing the tubing connected to it. Thus, the donor compartment could be quickly flushed with PBS. This system thus allowed the quantitative mea-

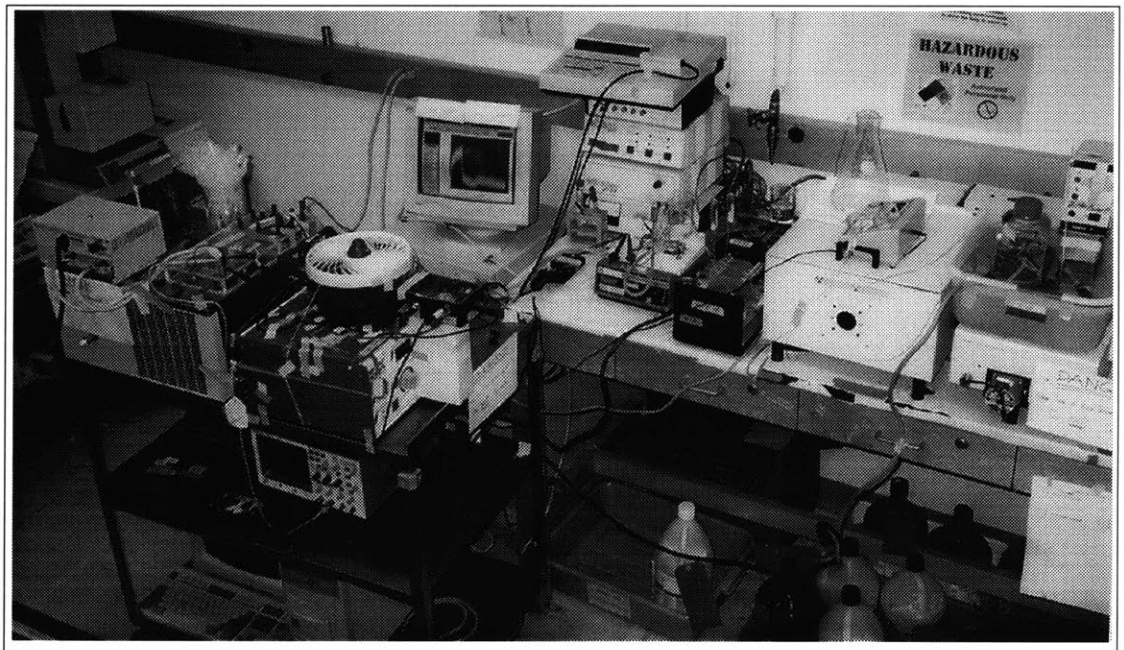

Figure V.1. Double flow-through experimental apparatus. This system allows the simultaneous, real-time recording of the transdermal voltage, molecular flux, and the impedance of the skin. The permeation chamber is in the center of the photograph, on the stirring plate (not used). To the right of the permeation chamber are the pumps (black) for the flow-through system and the donor recycling system. To the right of the pumps is the spectrofluorimeter (white boxes), containing the flow-through cuvette (not visible inside). On top of the spectrofluorimeter are the flow-protection pumps and the waste beaker. On the far right is a water bath which heats the PBS reservoirs to 37 °C. To the left of the permeation chamber is the differential high-voltage probe (flat black box). The top level of the cart holds the high-voltage pulser (blue box with fan), the timing relay (clear box with electronics, suspended in front of the pulser), the water bath (far left, used for heating the chamber to 37 °C), and various electronics (on top of and behind the water bath). On the middle level of the cart are the computer and oscilloscope that are used for recording voltages and currents. On the lower level of the cart is the computer used for recording skin impedances. It is connected to the impedance meter (box with red numbers, just above the permeation chamber) by a serial cable.

surement of compounds extracted from within the skin, during and after pulsing.

A system for measuring the impedance of the skin in real time was also needed, to allow the condition of the skin to be monitored at all times, even during high-voltage pulsing. Monitoring and recording the impedance of the skin in real time between pulses (time resolution of ~100 ms) has not been previously reported.

V.1. Solutions.

The day before the experiment, prepare Solutions 1 through 5 (Solution 5, PBS, is needed to prepare Solution 1). On the day of the experiment, prepare Solutions 5 (again) and 6, since these solutions can not be stored and have to be used immediately.

1. Acrylamide monomer solution: 7.5 g of 19:1 acrylamide:bis(N,N'-methylene-bis-acrylamide) powder (Bio-Rad) in 50 ml PBS (Solution 5, below). Prepare and mix together in a fume hood (the monomer is carcinogenic). Let the solution stand for >12 h before using, to allow the monomer to fully dissolve. This solution can be prepared well in advance of the experiment; it will not polymerize without addition of the catalyst.
2. Stock mounting solution: 10 mg Nile Red (Molecular Probes) in 20 ml acetone (Prausnitz, *et al.*, 1996 [a]). Wrap in aluminum foil to protect from light. This solution can be stored indefinitely if protected from light.
3. Final mounting solution: 7.5 ml glycerol in 2.5 ml de-ionized water and mix thoroughly. Add 250 µl of the stock mounting solution (Solution 2). Wrap in aluminum foil to protect from light. This solution can also be stored indefinitely if protected from light.
4. Acrylamide initiator solution: 0.3 g $(NH_4)_2S_2O_8$ in 3 ml H_2O. This solution can be stored for only a week.
5. Phosphate-buffered saline, PBS: 1.1 m<u>M</u> KH_2PO_4 (0.40 g per 2.0 l H_2O), 2.7 m<u>M</u> KCl (0.40 g), 8.1 m<u>M</u> Na_2HPO_4 (2.30 g), 138 m<u>M</u> NaCl (16 g) (total of 150 m<u>M</u>) in de-ionized H_2O. Although the volume of the receptor compartment is very small (~400 µl), a typical experiment can consume a surprisingly large volume of PBS, since the flow-through measurement and the two electrode flow-protection systems are continuously pumping PBS through the chamber. One experiment can consume more than 2.0 l of PBS. Stir the PBS solution under vacuum for >30 min to remove dissolved gases from solution. Both light and O_2 can cause the bleaching of fluorescent molecules, but this can be reduced by removing the dissolved gases from PBS, and protecting the solution from light whenever possible. Adjust to pH 7.4 with HCl and NaOH. This solution should be degassed immediately before use.

6. A typical donor solution consists of 1 mM of a hydrophilic fluorescent tracer in PBS (see Chapter 4). Examples of hydrophilic fluorescent tracers include lucifer yellow (457 Da) (Prausnitz, *et al.*, 1993 [a]; Chen, *et al.*, 1998 [c]), calcein (623 Da) (Prausnitz, *et al.*, 1993 [a]; Pliquett and Weaver, 1996 [a]; Vanbever, *et al.*, submitted), and sulforhodamine (607 Da) (Pliquett and Weaver, 1996 [a]) (all from Molecular Probes). Wrap the donor solution immediately in aluminum foil to protect it from light. Gently shake on a Nutator (Clay Adams, Becton Dickinson) for >30 min to ensure complete dissolution. This solution should be made immediately before use, right after preparing the PBS solution.

V.2. Electrode Placement.

The permeation chambers are custom-designed, side-by-side glass diffusion chambers (Crown Bio Scientific), with an outer water jacket and an inner compartment (Figure V.2) (Friend, 1992).

Ports extend from the inner compartment, through the water jacket, to the outside, which allows direct access to the inner compartment. Each chamber half has one large port (for the measuring electrodes and the flow-through system), with two smaller additional ports on the far ends (for placement of the electrodes and the flow-protection system around the electrodes). The volume of the inner compartment is ~3.1 ml, and the area of the circular opening is 0.64 cm^2 (0.9 cm diameter).

There are four electrodes in this system (Figures V.2). The two outer electrodes are used to apply pulses, and the two inner electrodes are used to measure the transdermal voltage and the impedance of the skin. Due to limitations of space within the donor and receptor compartments, the electrodes are constructed to allow both electrical access and liquid flow to the chamber. There are two types of electrodes in this system: the inner

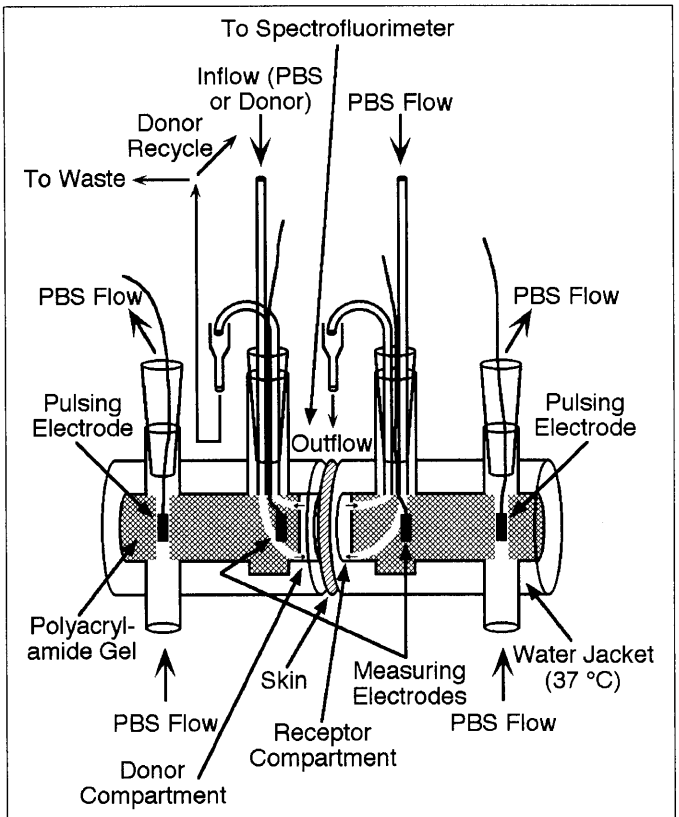

Figure V.2. Skin permeation chamber with double flow-through system. The two outer electrodes are used for pulsing, and the two inner electrodes are used to measure the voltage drop across the skin and the impedance of the skin. PBS is pumped around the pulsing electrodes to remove chemical by-products generated during pulsing. PBS is also pumped through the receptor compartment to a spectrofluorimeter for real-time detection. In the donor compartment, the donor solution (PBS by itself, or with a fluorescent tracer) can either be recycled or pumped to a waste beaker.

measurement/flow-through electrodes, and the outer pulsing electrodes.

The electrodes are made from silver wire, and the connectors are made from 200 µl pipette tips, with assorted amounts of tubing, all held in place by epoxy (Devcon). The fabrication of the measurement electrodes has been previously described in Section IV.2 (it was used only in the receptor compartments in Appendix IV, but for this system, the same design is used for both compartments). The fabrication of the two outer pulsing electrodes has been previously described in Section III.2.2.

V.3. Donor Recycling System.

In addition to the two pumps needed for the electrode flow-protection system (see Figure III.5) and the three pumps needed for the receptor flow-through system (see Figure IV.4) two additional pumps are also needed for the donor compartment recycling system (for a total of seven pumps). The two pumps of the donor recycling system also need to be properly "balanced" to avoid any leaks or accumulations within the donor compartment. However, the flowrates for this system do not need to be as accurate as the ones on the receptor side.

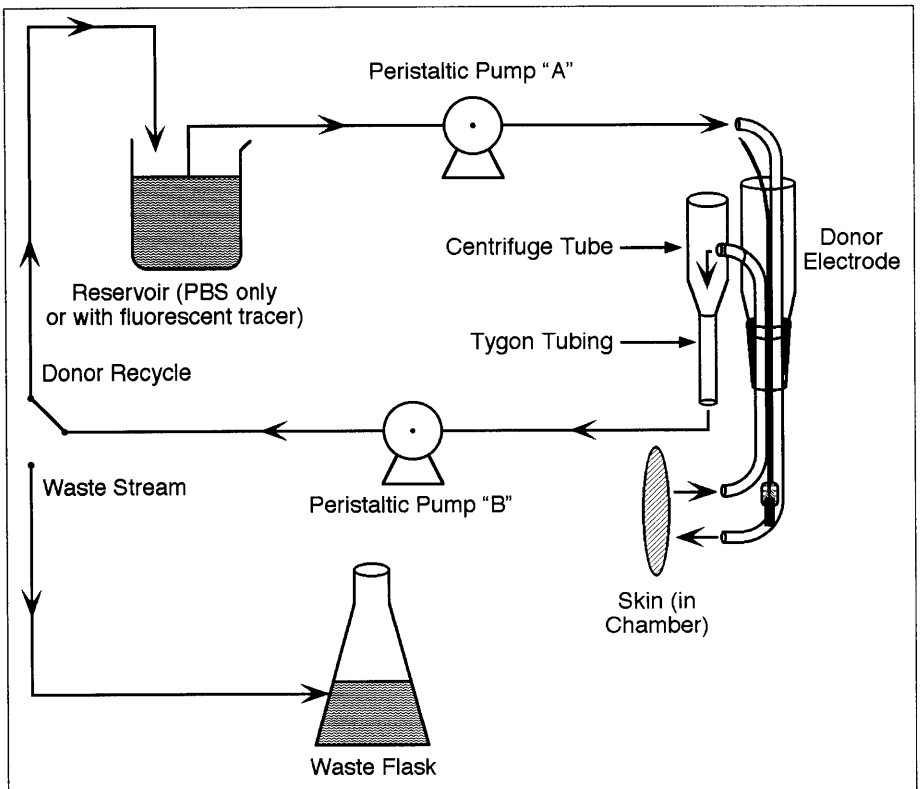

Figure V.3. Liquid circuit for the flow-through system in the donor compartment. This circuit can operate in two modes (switch on left). In the "recycle" mode (shown above), PBS (with or without a fluorescent tracer) is pumped from the reservoir, to the skin, and back to the reservoir. In the "flush" mode (with the switch down), PBS is pumped from the reservoir, to the skin, then out to a waste flask.

The two pumps (see Figure V.3) should be set up such that the faster pump is Peristaltic Pump "B" and the slower pump is Peristaltic Pump "A". The differences in flowrate will cause air to be drawn in through the collection tube. Since the liquid from the collection tube either gets recycled back into the donor reservoir or is removed as waste, the air bubbles will not contact the skin. This system can thus maintain a constant pressure within the donor compartment.

V.4. The Electrical Circuit.

The electrical circuit (shown in Figure V.4) has to perform three functions. First, it must deliver high-voltage pulses to the permeation chamber once every 5 s. Second, it has to measure and record the transdermal voltage and the current across the skin in real time. Third, it must record the impedance of the skin at all times, even between pulses. Since pulses are being applied to the skin every 5 s, there is very little time to manually record data or make adjustments between pulses. All of these operations must be completely automated.

All of the components, including the wires and the clip leads, should be able to withstand high-voltages and positioned with safety in mind. The electrical circuitry should be set up in a protected area away from the permeation chamber so that any fluid leaks or spills do not reach the electrical components.

The high-voltage pulsing circuit is the same one described in Section IV.4. Modifications to the pulser have already been discussed in Section II.1. Instructions on setting up and programming an impedance meter are described below in Section V.4.1. A new program, described in Section V.4.5,

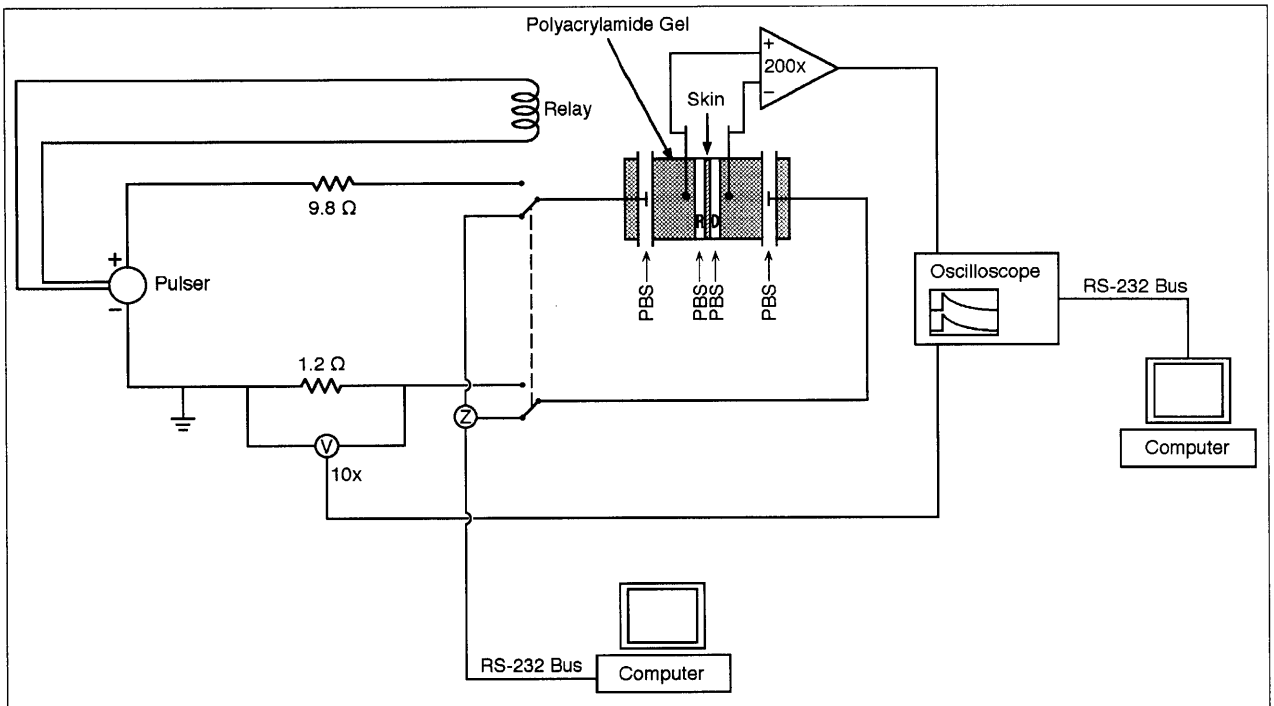

Figure V.4. The electrical circuit. The timing circuits of the high-voltage pulser (left) are connected to an electromechanical relay (top), which switches off the impedance meter (Z near center) whenever a pulse is applied. The impedance of the skin is measured continuously with a computer (bottom), except during a pulse. The 9.8 Ω resistor is a safety device in case of a short circuit. The transdermal voltage is measured by a 200× differential high-voltage probe, and the current is measured by a 10× voltage probe across a 1.2 Ω resistor placed in series with the chamber. Both voltage probes are connected to an oscilloscope, which downloads the data into another computer (right). R indicates the receptor compartment and D indicates the donor compartment. The two outer PBS streams and the polyacrylamide gel around the pulsing electrodes are used to prevent chemical contamination of the donor and receptor compartments by the electrodes.

also allows the transdermal voltage measurement system to record asynchronous or randomly spaced pulses, instead of pulses at a fixed interval.

V.4.1. The Skin Impedance Measurement Circuit.

The main requirements for the impedance meter are that it produce a very low bipolar sinusoidal current (<1 $\mu A / cm^2$ RMS) at a low frequency (<100 Hz), and that it has a way to download data in real time and at high speeds to a computer, for storage and processing. A sinusoidal current measures the impedance of the skin, not its resistance; but a true resistance measurement would require a DC current, which could potentially cause iontophoresis of the skin. Low frequency impedances of the skin compare favorably with actual skin resistances (Gowrishankar, personal communication), without causing iontophoresis of the skin.

There are several impedance meters available that meet these requirements; one such meter is the Model 5R715 LCR Meter (Stanford Research Systems). However, applying a 1000 V pulse to the impedance meter would probably seriously damage or destroy the LCR meter. Thus, the LCR meter has to be physically disconnected (using a electromechanical relay) from the high-voltage pulser whenever a pulse is about to be applied. This can be done by connecting the flip-flop timing circuit of the pulser (see Section II.1) to the electromechanical relay (Figure V.4), such that whenever a pulse is to be applied, the impedance meter is disconnected and the high-voltage pulser is connected to the permeation chamber (E. A. Gift, personal communication).

The impedance meter should also be connected to a computer for data storage. For example, the LCR Meter described above can be connected to a computer via an RS-232 cable to the serial port of a computer. The program the computer is running will be machine-specific, depending on which serial port the oscilloscope is connected to, and the programming languages of the computer and the oscilloscope (see Section V.4.2 and V.4.3). In general, though, the computer program should be in a low-level programming language, and the computer itself should be reasonably fast.

The impedance meter should be transferring data in the most compact format available (i. e., as unformatted ASCII characters instead of formatted arrays of numbers). The impedance meter should be programmed to dump impedance data to the computer, regardless of whether or not it is actually connected to the skin or not. Many impedance meters will start downloading an error flag (such as 9.9999×10^{20} Ω) if disconnected. These can be deleted in later processing steps.

The computer program should store the raw data, along with the time, on the hard drive (or on a ramdisk if enough memory is available). Before starting, verify that there is adequate space on the hard drive, since one experiment can consume over 2 MB. A sample program is listed in Sections V.4.2 and V.4.3.

No mathematical processing should be done during the experiment. Time resolutions of up to 100 ms can be obtained if care is taken in setting up the programs and connections. There is very little time for the correction of problems. Examples of problems that can occur include loose serial plugs, line noise due to faulty or excessively long cables or failure of the impedance meter and the computer to properly synchronize headers and data streams.

V.4.2. SKININT.CPP.

The following is the source code for SKININT.CPP, a program to interface with an LCR meter (Model 5R715 LCR Meter, Stanford Research Systems) and measure the impedance and the capacitance of the skin in real time. It is in Turbo C++ (Borland). Due to time constraints, this file simply stores the data in raw form; there is another file (convert.m) in Section V.4.3 that converts the raw data for processing.

```
/* SKININT.CPP */
/* Program downloads and saves data from the LCRmeter, even if the        */
/*   LCRmeter is just recording noise or off-scale readings.  The data is */
/*   saved to the file "INTRSKIN.DAT" for later processing.               */
/* The encoded data is as follows:                                        */
/*   Time:   Time in seconds since start of experiment                    */
/*   G/R/O:  Good/Out-of-Range/Overrange                                  */
/*   2:      Range set on instrument (useless)                            */
/*   C/R:    Capacitance/impedance at 100 Hz                              */
/*   value:  Value in exponential notation, in Farads or Ohms             */
/* The LCRmeter should be protected from the high voltage pulse.  The     */
/*    LCRmeter should be connected thru the RS-232 port to the back of    */
/*    COM1.  The settings should be 9600 baud, parity off, even parity, 8 */
/*    data bits.  On the back of the machine, it should look like:        */
/*                                                                        */
/*       +--Baud-+ of/n o/e 7/8                                           */
/*       *   |   *   |   *   *   *   *                                    */
/*       |   *   |   *   |   |   |   |                                    */
/*                                                                        */
/* Tani Chen, 5/19/1998 */

#include <stdio.h>
#include <dos.h>
#include <string.h>
#include <bios.h>
#include <conio.h>
#include <time.h>

/* Bioscom port 0 = serial port 1 */
#define LcrPort 0
/* Bioscom send = 1, read = 2, status = 3 */
#define Send 1
#define Read 2
#define Status 3
#define DataReady 0x0100

InitCom1()  /* Initialize serial port 1 */
{
  union REGS r;

  r.h.ah = 0x00;
  r.h.al = 0xE3;
  r.x.dx = 0x00;
  int86(0x14, &r, &r);
  printf("  Serial port 1 initialized.\n");
}

void LcrCom(char *command)  /* Send command to LCRmeter */
{
  int i;
  for(i=0; i<strlen(command); ++i)  /* 1 character at a time */
    bioscom(Send, command[i], LcrPort);
  bioscom(Send, 0x0A, LcrPort);  /* Line feed */
  /* printf("  Command: %s\n", command); */
}
```

```
main()
{
  printf("*** Program Initialization ***\n");
  FILE *fp;
  int i;
  int j;
  int Byte;
  char *ZFile = "INTRSKIN.DAT";  /* Data file */
  char ZData[30];   /* Holds data feed from LCRmeter */
  clock_t Zero, Timer;
  double Time;

  printf("Initializing serial port 1....\n");
  InitCom1();
  LcrCom(" ");

  printf("Setting up LCRmeter... ");
  LcrCom("*RST");       /* Reset LCRmeter */
  LcrCom("PMOD4");      /* Measure capacitance & resistance (impedance) */
  LcrCom("FREQ0");      /* Set frequence to 100 Hz */
  LcrCom("VOLT0.1");    /* Set drive voltage to 0.1 V */
  LcrCom("RNGH1");      /* Turn on range hold */

  LcrCom("RATE1");      /* Set measurement rate to fast */
  LcrCom("OUTF0");      /* Verbose ASCII data transmission */
  fp = fopen(ZFile, "write");  /* Delete data files from disk   */
  fclose(fp);                  /*   so new files can be written */
  printf("Done.\n\n");

  printf("Press any key to start.\n");
  while(kbhit() == 0)
  {
  }
  i = getch();  /* Clear keyboard buffer */

  printf("\n*** Receiving Data ***\n");
  printf("Double-tap Range Hold on LCRmeter!!\n");
  printf("Press any key to stop recording!\n\n");
  Zero = clock(); /* Reset timer */

  while(kbhit() == 0)  /* Stop reading waveforms when key is pressed */
  {
    LcrCom("STRT");     /* Start measurement */
    LcrCom("*WAI");     /* Wait until LCRmeter ready before getting data */
    LcrCom("XALL?");    /* Get capacitance */

    for(i=0; i<30; i++)  /* Read data, I hope */
    {
      /* No time to jump to a subroutine!  Doing so will lose bytes! */
      while((Byte=bioscom(Status, 0, LcrPort) & DataReady != 0x001 && i<10))
      {
        i++;
      }
      Byte = bioscom(Read, 0, LcrPort);
      Byte = Byte&0x00FF;
      ZData[i] = Byte;
    }
    Timer = clock();  /* Record time */
    ZData[30] = ' ';  /* I don't know where character #30 is coming from! */

    for (i=0; i<30; i++)
    {
      if (ZData[i] == 10 || ZData[i] == 0 || ZData[i] == 13)
        /* Delete the damn returns, carridge feeds, and null characters!! */
      {
        for (j=i; j<29; j++)
        {
          ZData[j] = ZData[j+1];
        }
        ZData[29] = ' ';
        i = i - 1; /* Now that the bad character has been deleted, have to
                      re-check the next character in line */
      }
    }
    ZData[29] = '\0';

    Time = (Timer - Zero) / CLK_TCK;  /* Calculate time in seconds */
    printf("Datastream (%.3f s):  %s\n", Time, ZData);
    sound(1000);
    delay(5);
    nosound();

    fp = fopen(ZFile, "append");
    fprintf(fp, "%.4f        ", Time);  /* Save the elapsed time */
    fprintf(fp, "%s\n", ZData);    /* And the data stream */
    fclose(fp);

  }
  printf("\n*** End of Program ***\n");
  nosound();
  delay(1000);
}
```

V.4.3. convert.m.

The following is the MatLab 5 script file for convert.m, a program which converts data from SKININT.CPP and the LCR meter (Model 5R715 LCR Meter, Stanford Research Systems) into three new files that can be read by the MatLab script file, JUZ.m (see Section V.11.2). This program filters out many of the noise errors and timing glitches that can occur while the data are being downloaded from the LCR meter; however, it requires a very long time to run, up to 5 h per file in some cases. There are several function calls to progress.m (Section V.4.4), a program that draws progress bars on the screen to keep track of progress.

```
% Convert.m
% Converts data files from the LRC meter into 3 columns to be read by MatLab.
%   This program takes a *long* time to convert the files!!  Run overnight!
% Tani Chen  6/12/98

% *** CLEAR OLD STUFF OUT ***
clc
disp 'Intializing...'
disp ' '
clear
close all
format
% errortrap on
disp 'Directory of ~/Working:'
!ls
disp ' '

Number = input('Enter number of files ->');
Filename(Number, 20) = ' ';
for k = 1:Number
  kstring = num2str(k);
  eval(['  disp ''Enter filename for file #', kstring, ' '' ']);
  Name = input('  ->', 's');
  StrLen(k) = size(Name, 2);
  Filename(k, 1:size(Name, 2)) = Name;
end
disp ' '
disp 'Files to convert:'
disp(Filename)
disp ' '

for FileNo = 1:Number
  FileString = num2str(FileNo);
  NumString = num2str(Number);
  eval(['disp(''Now converting file "', Filename(FileNo, 1:StrLen(FileNo)), '" (', FileString, '/', NumString,
')...'')']);
  !rm temp.txt
  eval([ '!wc -l ', Filename(FileNo, 1:StrLen(FileNo)),  ' > temp.txt']);
  File   = fopen('temp.txt', 'r');
  Temp   = fread(File, 8, 'char');
  Length = str2num(char(Temp'));
  fclose(File);


  File = fopen(Filename(FileNo, 1:StrLen(FileNo)), 'r');
%  Handle = progress(0, 'Converting electrical data from "intrskin.dat"...');
  eval(['Handle = progress(0, ''Converting electrical data from "', Filename(FileNo, 1:StrLen(FileNo)), '"...'');']);
  set(Handle, 'MenuBar', 'none');
  set(Handle, 'NumberTitle', 'off');
  for j = 1:Length
    Pos  = 1;
    Temp = 0;          % Null out previous reading
    while Temp ~= 13   % Read until a carriage return (^M) is detected
      Temp = fread(File, 1, 'char');  % Enter next byte
      String(Pos) = char(Temp);       % Store as string in String
      Pos = Pos + 1;                  % Move to next character
    end

    Flag = 0 ;  % Value flag (0 = Time, 1 = Capacitance, 2 = Impedance)
    TempCap  = 'NaN';
    TempImp  = 'NaN';
    TempTime = 'NaN';
    for i = 1:size(String, 2)

      if (String(i) == char(9) & Flag == 0)   % Time deliminated by a <tab>
```

```
      TempTime = String(1:i - 1);
      Pos      = i;   % Remember this location
      Flag     = 1;   % Increase flag
    end

    if (String(i) == ',' & Flag == 2)   % Impedance deliminated by a ,
      TempImp = String(Pos + 1:i - 1);
      Flag    = 3;
    end

    if (String(i) == ',' & Flag == 1)   % Capacitance deliminated by a ,
      TempCap = String(Pos + 1:i - 1);
      Pos     = i;   % Remember this location
      Flag    = 2;   % Increase flag
    end

    if (i == size(String, 2) & Flag == 2)
      TempImp = String(Pos + 1:i);
      Flag    = 4;
    end

  end

  if (TempCap(1) == 'G' | TempCap(1) == 'O')
    Cap(j) = str2num(TempCap(4:size(TempCap, 2)));
    if Cap(j) > 1e20
      Cap(j) = NaN;
    end
  else
    Cap(j) = NaN;
  end

  if (TempImp(1) == 'G' | TempImp(1) == 'O')
    Imp(j) = str2num(TempImp(4:size(TempImp, 2)));
    if Imp(j) > 1e20
      Imp(j) = NaN;
    end
  else
    Imp(j) = NaN;
  end

  ZTime(j) = str2num(TempTime);
  progress(j/Length)
 end
 fclose(File);
 close(Handle)

 eval(['disp ''  Saving capacitance data to "', Filename(FileNo, 1:StrLen(FileNo)), '.cap"...'' ']);
 eval(['save ', Filename(FileNo, 1:StrLen(FileNo)), '.cap Cap -ascii']);
 eval(['disp ''  Saving impedance data to "', Filename(FileNo, 1:StrLen(FileNo)), '.imp"...'' ']);
 eval(['save ', Filename(FileNo, 1:StrLen(FileNo)), '.imp Imp -ascii']);
 eval(['disp ''  Saving time data to "', Filename(FileNo, 1:StrLen(FileNo)), '.ztime"...'' ']);
 eval(['save ', Filename(FileNo, 1:StrLen(FileNo)), '.ztime ZTime -ascii']);
 disp ' '

 clear Cap
 clear Imp
 clear ZTime
end

disp('Done!')
% errortrap off
```

V.4.4. progress.m.

Many of the files in this appendix require long periods of time to run (hours to days). The following MatLab 5 script file draws a progress bar on the screen, to monitor progress.

```
function fout = waitbar2(x,name)
%WAITBAR2 Display wait bar (uses Tags to keep track of objects).
%       H = WAITBAR2(X,'title') creates and displays a wait bar of
%       fractional length X.  The handle to the waitbar figure is
%       returned in H.  X should be between 0 and 1.  Each
%       subsequent call to waitbar, WAITBAR2(X), extends the length
%       of the bar to the new position X.
%
%       WAITBAR2 is typically used inside a FOR loop that performs a
%       lengthy computation.  A sample usage is shown below:
%
```

```
%           h = waitbar2(0,'Please wait...');
%           for i=1:100,
%               % computation here %
%               waitbar2(i/100)
%           end
%           close(h)

%       Clay M. Thompson 11-9-92
%       Copyright (c) 1992-93 by The MathWorks, Inc.
%       $Revision: 1.9 $  $Date: 1993/09/24 18:57:13 $
x = max(0,min(100*x,100));

if nargin==2,
  pos = get(0,'ScreenSize');
  f = figure('position',[pos(3)/2-500 pos(4)/2-30 360 60], ...
             'resize','off');
  colormap([])

  h = axes('Xlim',[0 100],'Ylim',[0 1]);
  title(name)
  axis off
  set(h,'box','on')
  set(h,'position',[.05 .30 .9 .30])
  set(h,'YTickLabelMode','manual')
  set(h,'YTickLabel',[])

  xpatch = [0 x x 0];
  ypatch = [0 0 1 1];
  xline = [100 0 0 100 100];
  yline = [0 0 1 1 0];
  p = patch(xpatch,ypatch,'b','Edgecolor','b','EraseMode','none','tag','waitpatch');
  l = line(xline,yline,'eraseMode','none','tag','waitline');
  set(l,'Color',get(gca,'Xcolor'))


else
  p = findobj(gca,'tag','waitpatch');
  l = findobj(gca,'tag','waitline');
  if isempty(p) | isempty(l), error('Couldn''t find waitbar handles.'); end
  xpatch = get(p,'xdata');
  xpatch = [xpatch(2) x x xpatch(2)];
  set(p,'Xdata',xpatch)
  xline = get(l,'xdata');
  set(l,'xdata',xline)
end

drawnow

if nargout==1,
  fout = f;
end
```

V.4.5. WAVETIME.CPP.

The following is the source code for WAVETIME.CPP, a program to measure the transdermal voltage and current for each pulse. Rather than relying on a fixed pulse interval, it simultaneously records the time of the pulse. Randomly or irregularly spaced pulses can thus be recorded and correctly processed. It is in Turbo C++ (Borland).

```
/* WAVETIME.CPP */
/* Program stores pulse waveform and current waveform for every pulse.    */
/*   Program can store up to 1 pulse every 5 s.  Data saved in 4 files.   */
/*   The 2 preamble files contain data about the x and y settings on the  */
/*   oscilloscope, saved in MatLab format (PREAMB1.M and PREAMB2.M).  The */
/*   2 data files contain the actual waveform data, stored in ascii       */
/*   (WAVE1.DAT and WAVE2.DAT).  Each wave is stored as a block of 500    */
/*   bytes (no separators).                                               */
/* Oscilloscope RS-232 module (HP 54651A) should be connected to serial   */
/*   port 1 on computer.  Oscilloscope settings:  Hit [Print/Utility],    */
/*   then <RS-232 Menu>, and check these settings before running program: */
/*     Connect to <Computer>, Factors <Off>, Resolution <Low>,            */
/*     Baud Rate <9600>, Handshake <Xon>                                  */
/* Tani Chen, 3/17/1997 */

#include <stdio.h>
```

```
#include <dos.h>
#include <string.h>
#include <bios.h>
#include <conio.h>
#include <time.h>

/* Bioscom port 0 = serial port 1 */
#define OscPort 0
/* Bioscom send = 1, read = 2, status = 3 */
#define Send 1
#define Read 2
#define Status 3
#define DataReady 0x0100


InitCom1()  /* Initialize serial port 1 */
{
  union REGS r;

  r.h.ah = 0x00;
  r.h.al = 0xE3;
  r.x.dx = 0x00;
  int86(0x14, &r, &r);
  printf("  Serial port 1 initialized.\n");
}


OscCom(char *command)  /* Send command to oscilloscope */
{
  int i;

  delay(100);  /* Do not change!  Timing necessary for oscilloscope to */
        /*   take readings correctly!                                   */
  for(i=0; i<strlen(command); ++i)  /* 1 character at a time */
  {
    bioscom(Send, command[i], OscPort);
  }
  bioscom(Send, 0x0A, OscPort);  /* Line feed */
  printf("  Command: %s\n", command);
}


int ReadOsc()  /* Wait for ready signal (?) */
{
  int data;
  int i = 0;
  union REGS r;

  while((data=bioscom(Status, 0, OscPort) & DataReady != 0x001 && i<10))
  {
    i++;
  }
  data = bioscom(Read, 0, OscPort);
  data = data&0x00FF;
  return(data);
}


Preamble(int channel, char *filename)
/* Preamble format: 1(byte), 1(nrm), 4000(pnts), 1(dummy) */
/*   xincr, xorig, xref(dummy), yincr, yorig, yref(dummy) */
/* Stored as MatLab file */
{
  int i;
  char preamble[125];
  char preamble2[125];
  char *command;
  FILE *fp;

  if(channel == 1)  /* Select channel */
  {
    OscCom(":WAV:SOUR CHAN1");
  }
  else if(channel == 2)
  {
    OscCom(":WAV:SOUR CHAN2");
  }

  delay(500);  /* Reset port for signaling...  don't ask me why!  Removing */
  bioscom(Read, 0, OscPort);  /* these lines will cause bytes to be lost!! */
  command = ":WAV:PRE?";  /* No time to jump to subroutine... */
    /* Using OscCom here causes bytes to be lost! */
  printf("  Command: %s\n", command);
  for(i=0; i<strlen(command); ++i)  /* 1 character at a time */
  {
    bioscom(Send, command[i], OscPort);
  }
  bioscom(Send, 0x0A, OscPort);  /* Line feed */

  i = 0;  /* Enter data */
  while((preamble[i]=ReadOsc()) != 10 && i<100)
  {
```

```
    i++;
  }
  preamble[i] = '\0';  /* Add line feed to end of data */
  printf("  Channel %d data: %-.57s...\n", channel, preamble);

  for(i=0; i<strlen(preamble); i++)  /* Erase commas from preamble */
  {
    if(preamble[i] == ',')
    {
      preamble[i] = ' ';
    }
  }

  sprintf(preamble2, "preamble%d = [ %s ];", channel, preamble);  /* Save */
  fp = fopen(filename, "write");                /*   data in Matlab format */
  fprintf(fp, "%s\n", preamble2);
  fclose(fp);
  printf("  Preamble from channel %d stored in %s.\n", channel, filename);
}


Waveform(char *filename1, char *filename2, char *filename3, int Zero)
   /* Dump both channels and the time to disk */
{
  int i;
  char *command;
  char wave1[511];  /* (header=10 bytes)(data=500 bytes)(EOF=1 byte) */
  char wave1a[501];  /* 500 data bytes + EOF */
  char wave2[511];  /* Same for channel 2 */
  char wave2a[501];
  clock_t Timer;
  double Time;
  FILE *fp;

  OscCom(":DIG CHAN1,CHAN2");  /* Store both traces in oscilloscope */
  OscCom(":WAV:SOUR CHAN1");  /* Select channel 1 */
  command = ":WAV:DATA?";  /* No time to jump to subroutine... */
  printf("  Command: %s\n", command);
  for(i=0; i<strlen(command); ++i)  /* 1 character at a time */
  {
    bioscom(Send, command[i], OscPort);
  }
  bioscom(Send, 0x0A, OscPort);  /* Line feed */

  /* Waiting for pulse.  ReadOsc spits out 0's until the oscilloscope      */
  /*   is ready to send data (which means the oscilloscope was triggered,  */
  /*   which means a pulse was detected.)  The 0's are not part of the DIG */
  /*   header and really screw up data transferring (510 bytes from DIG)!! */
  printf("  Waiting");
  while(i=ReadOsc() == 0)
  {
    printf(".");
  }

  printf("\n  Pulse detected.\n");

  sound(2048);  /* Beep every time there's a pulse... */
  delay(5);
  nosound();
  Timer = clock();

  for(i=0; i<511; i++)  /* Pulse detected, reading data */
  {
    wave1[i] = ReadOsc();
    if(wave1[i] == 0)  /* 0 (no data) causes string to terminate early     */
    {                  /*   making a real mess of the rest of the program! */
      wave1[i] = 1;
    }
  }
  wave1[i] = '\0';  /* End of file */

  OscCom(":WAV:SOUR CHAN2");  /* Then select channel 2 */
  command = ":WAV:DATA?";  /* No time to jump to subroutine... */
  printf("  Command: %s\n", command);
  for(i=0; i<strlen(command); ++i)  /* 1 character at a time */
  {
    bioscom(Send, command[i], OscPort);
  }
  bioscom(Send, 0x0A, OscPort);  /* Line feed */

  for(i=0; i<511; i++)  /* Read data, I hope */
  {
    wave2[i] = ReadOsc();
    if(wave2[i] == 0)  /* 0 (no data) causes string to terminate early */
    { wave2[i] = 1;
    }
  }
  wave2[i] = '\0';  /* End of file */

  for(i=0; i<511; i++)  /* Patch up data so this stupid PC can process it */
  {
    if(wave1[i] == 26)  /* 26 = EOF, change to 25 to avoid crashing! */
```

```
    {
      wave1[i] = 25;
    }
    if(wave1[i] == 7)  /* Turn off that stupid bell! */
    {
      wave1[i] = 8;
    }
    if(wave1[i] == 10)  /* Character 10 messes up byte count on disk!! */
    {                    /*   Don't ask me why, just don't change this! */
      wave1[i] = 11;
    }
    if(wave2[i] == 26)  /* And of course, repeat for channel 2 waveform */
    {
      wave2[i] = 25;
    }
    if(wave2[i] == 7)
    {
      wave2[i] = 8;
    }
    if(wave2[i] == 10)
    {
      wave2[i] = 11;
    }
  }

  i = 0;  /* Delete useless header info (channel 2) */
  while((wave2a[i] = wave2[i+10]) != '\0')
  {
    i++;
  }

  i = 0;  /* Delete useless header info (channel 1) */
  while((wave1a[i] = wave1[i+10]) != '\0')
  {
    i++;
  }

  printf("  Channel 1 data (%d): %-.50s... \n", strlen(wave1a), wave1a);
  printf("  Channel 2 data (%d): %-.50s... \n", strlen(wave2a), wave2a);
  OscCom(":RUN");  /* Resume oscilloscope readings */

  fp = fopen(filename1, "append");  /* Save channel 1 as block of 500 */
  fprintf(fp, "%.500s", wave1a);    /*   bytes                        */
  fclose(fp);
  printf("  Channel 1 data stored in %s.\n", filename1);

  fp = fopen(filename2, "append");  /* And channel 2 also */
  fprintf(fp, "%.500s", wave2a);
  fclose(fp);
  printf("  Channel 2 data stored in %s.\n", filename2);

  Time = (Timer - Zero) / CLK_TCK;
  fp = fopen(filename3, "append");  /* Time channel */
  fprintf(fp, "%.4f\n", Time);  /* Save the elapsed time */
  fclose(fp);
  printf("  Time of pulse: %.3f.\n", Time);
}


main()
{
  FILE *fp;
  int pulseno = 1;
  int choice;
  char *preamble1 = "PREAMB1.M";  /* Preamble data file for channel 1 */
  char *preamble2 = "PREAMB2.M";  /* Preamble data file for channel 2 */
  char *waveform1 = "WAVE1.DAT";  /* Waveform data file for channel 1 */
  char *waveform2 = "WAVE2.DAT";  /* Waveform data file for channel 2 */
  char *timefile  = "TIME.DAT";   /* Time data for each pulse */
  clock_t Zero, Timer;
  double Time;

  printf("*** Program Initialization ***\n");
  printf("Initializing serial port 1....\n");
  InitCom1();

  printf("Setting up oscilloscope....\n");
  OscCom("*RST");  /* Reset oscilloscope */
  OscCom(":SYST:LOCK ON");  /* Prevents user from messing with settings */
  OscCom(":VIEW CHAN2");  /* Turn on channel 2 */
  OscCom(":DITH OFF");  /* Turn off errors (oscilloscope *adds* errors!) */
  OscCom(":WAV:POIN 500");  /* 500-byte data blocks.  Limit of what can */
    /*   be saved in under 5 s!                                        */
  OscCom(":WAV:FORM BYTE");  /* Data goes from 0 to 255 */
  OscCom(":ACQ:COMP 40");  /* Mininum threshold to trigger storage */
  OscCom(":ACQ:TYPE NORM");  /* Normal acquisition (no averaging) */

  /* Channel 1 = Uskin (high voltage probe, 1000x) */
  /* Channel 2 = I (10x probe)                     */
  OscCom(":TIM:RANG 5 MS");  /* Set x-axis to 5 ms across */
  OscCom(":TIM:REF LEFT");  /* Align pulse with left side */
  OscCom(":CHAN2:PROB X10");  /* 10x probe for current (channel 2) */
```

```
  OscCom(":CHAN2:BWL ON");  /* Clean up channel 2's signal */
  OscCom(":CHAN1:BWL ON");  /* Clean up channel 1's signal */
  OscCom(":TRIG:MODE NORM");  /* Set up oscilloscope to respond to pulses */
           /*   on channel 2 (Current)                    */
  OscCom(":TRIG:NREJ ON");  /* Turn on noise rejection */

  printf("Enter voltage settings:\n");  /* Select ranges to display/record */
  printf("  1. High voltage   (600 V/2.5 A)\n");
  printf("  2. Medium voltage (240 V/1 A)\n");
  printf("  3. Low voltage    (120 V/0.5 A)\n");
  printf("  4. Lower voltage  (60 V/0.25 A)\n");
  printf("Choice?");
  scanf("%d", &choice);
  if(choice == 1)
  {
    OscCom(":CHAN1:RANG 4V");
    OscCom(":CHAN1:OFFS 1.5V");
    OscCom(":CHAN2:RANG 4V");
    OscCom(":CHAN2:OFFS 1.5V");
    OscCom(":TRIG:SOUR CHAN1");
    OscCom(":TRIG:LEV 500MV");
  }
  else if(choice == 2)
  {
    OscCom(":CHAN1:RANG 1.6V");
    OscCom(":CHAN1:OFFS 600MV");
    OscCom(":CHAN2:RANG 1.6V");
    OscCom(":CHAN2:OFFS 600MV");
    OscCom(":TRIG:SOUR CHAN1");
    OscCom(":TRIG:LEV 250MV");
  }
  else if(choice == 3)
  {
    OscCom(":CHAN1:RANG 800MV");
    OscCom(":CHAN1:OFFS 300MV");
    OscCom(":CHAN2:RANG 800MV");
    OscCom(":CHAN2:OFFS 300MV");
    OscCom(":TRIG:SOUR CHAN1");
    OscCom(":TRIG:LEV 200MV");
  }
  else if(choice ==4)
  {
    OscCom(":CHAN1:RANG 400MV");
    OscCom(":CHAN1:OFFS 150MV");
    OscCom(":CHAN2:RANG 400MV");
    OscCom(":CHAN2:OFFS 150MV");
    OscCom(":TRIG:SOUR CHAN1");
    OscCom(":TRIG:LEV 50MV");
  }

  printf("Getting preambles...\n");
  Preamble(1, preamble1);  /* Get preamble data for channel 1 */
  Preamble(2, preamble2);  /* Get preamble data for channel 2 */

  fp = fopen(waveform1, "write");  /* Delete data files from disk   */
  fclose(fp);                      /*   so new files can be written */
  fp = fopen(waveform2, "write");
  fclose(fp);
  fp = fopen(timefile, "write");
  fclose(fp);
  printf("*** Initialization Completed ***\n\n");

  printf("*** Receiving Waveforms ***\n");
  printf("Press any key AFTER pulse to stop recording!\n");
  Zero = clock();  /* Reset timer */

  while(kbhit() == 0)  /* Stop reading waveforms when key is pressed */
  {
    printf("Pulse #%d...\n", pulseno);
    pulseno++;
    Waveform(waveform1, waveform2, timefile, Zero);  /* Get waves */
  }

  printf("*** All Waveforms Recorded ***\n");
  OscCom(":SYST:LOCK OFF");  /* Allow use of oscilloscope again */
  printf("\n*** End of Program ***\n");
  delay(1000);
}
```

V.5. Permeation Chamber Preparation.

The polyacrylamide gel around each pulsing electrode directs PBS in and out of the chamber, without contacting the donor or receptor solutions (the hollowed-out regions that run around each of the two pulsing electrodes in Figure V.2). The polyacrylamide also keeps the volumes of the donor and receptor compartments at a minimum. Embedded within the polyacrylamide gel are the tubes entering and leaving each compartment, and the measurement electrodes.

V.5.1. Preparation of the Mold.

Acrylamide in solution takes approximately 10 min to polymerize into polyacrylamide gel. In this time, the acrylamide solution has to poured into the chamber. To create the channels that run through the polyacrylamide gel, plastic tubes are inserted into the chamber, which are then removed once the acrylamide has polymerized. Preparing the mold within the permeation chambers can be done the day before the experiment.

1. Find two flexible plastic tubes, approximately 9 inches long, that will fit through the two small ports on each chamber half.
2. Slide the plastic tubes through these ports (use tweezers as needed), so that roughly 1 to 2 inches of the tube protrudes out on either side. These tubes are the mold for the electrode flow-protection channel.
3. Place Parafilm around each opening tightly. Use two layers of Parafilm. This should create a watertight seal around the openings, so the acrylamide solution can not leak out.
4. Insert the measuring electrodes into each compartment. Make sure the two tubes that lead into the compartment are at an angle toward the opening. Place Parafilm tightly around this electrode as well.
5. Due to the elasticity of the tubing, however, the two tubes of the electrode are probably stuck next to each other instead of on opposite sides of the chamber as shown in Figure V.2. Using a thin stainless steel wire, attach the outlet tubing to the top of the chamber. This wire will be removed after the polyacrylamide gel has been added.
6. Position each of the two chambers sideways, so that the large opening (where the skin is located) is on top. The chambers should be braced in some fashion (propping them up on pencils or test tubes) so that they can not tip or move when filled with liquid.

V.5.2. Adding the Polyacrylamide Gel.

Acrylamide monomer in solution (Solution 1) will polymerize into a gel in approximately 10 min upon addition of a catalyst (N,N,N',N'-tetramethylethylenediamine) (Bio-Rad) and a free radical initiator (Solution 4). Most of the gel is still liquid (PBS, in this case), surrounded by cross-linked polymer. Thus, the conductivity and the electrical properties of the polyacrylamide gel are essentially the same as PBS.

Synthesis of the polyacrylamide gel should be performed just before the experiment (the chambers should already be prepared), since polyacrylamide gel will begin dehydrating after a few hours.

1. Thoroughly mix together 10 ml of acrylamide solution (Solution 1), 87.5 µl of the initiator (Solution 4 from Section V.1), and 6 µl of N,N,N',N'-tetramethylethylenediamine in a 15 ml test tube.
2. Immediately pour in the acrylamide solution, completely filling each chamber. The top of the solution should be perfectly flush with the top of the chamber, and there should not be a meniscus above the chamber. The acrylamide solution will completely cover the plastic tubing of the flow-protection system, and the silver measurement electrode. Make sure that the liquid does not enter the two tubes that form each compartment. The solution will shrink slightly as it gels; this shrinkage is what forms the receptor compartment. Thus, to get a consistent, reproducible volume, the solution should always be poured so that it is flush with the.
3. Do not disturb the chambers while the gel is polymerizing, as disturbances will cause the gel to take longer to harden, and the gel will set poorly as a result. It will take approximately 10 min for the gel to harden. Any leftover acrylamide solution can be used to monitor the gelling process.
4. After the gel forms, carefully remove the Parafilm around the each of the plastic tubes of the electrode flow-protection system. Remove the plastic tubes through one of the small ports. Do not remove the measurement electrodes or the surrounding Parafilm.
5. Carefully remove the stainless steel wires holding the outlet tubes in place. The tubes should now be held in place by the polyacrylamide gel.
6. Using a syringe, force air through the inlet and outlet tubes of each compartment to ensure that they are not blocked by stray bits of polyacrylamide gel.
7. Connect a collection tube (see Section IV.3.1) to the outlet tube on the side of each measurement electrode, as shown in Figures V.2 and V.3). Hold it in place with Parafilm.
8. Before using, fill the permeation chambers with PBS to keep the polyacrylamide gel from drying out.

V.6. Preparing the Equipment.

On the day of the experiment, the following should have already been prepared and assembled: Solutions 1 through 4 (Section V.1), the permeation chamber and the electrodes (Sections V.2, IV.2, III.2.2, and V.5.1), the flow-protection system (Section III.3), the flow-through system in the spectrofluorimeter (Section IV.3), the electrical circuit (Section V.4), the high-voltage pulser (Section II.1), the donor recycle system (Section V.3), the impedance meter (Section V.4.1), and the skin (Section I.1). Immediately before the experiment, Solutions 5 and 6 from Section V.1, and the polyacrylamide gel in the chamber (Section V.5.2) need to be prepared. Once the gel in the chamber is ready, place the chamber on a magnetic stirring plate and connect it to a 37 °C water bath.

All of the tubes in the flow-through system, the electrode flow-protection system, and the donor recycling system should be flushed with PBS. Use a piece of Parafilm instead of human skin in the permeation chamber. There should be a steady stream of air bubbles entering the flow-through system at the collection tube and the spectrofluorimeter cuvette, and another stream of air bubbles entering the donor outflow system. The flushing should continue until the spectrofluorimeter gives stable readings for the fluorescence. This can take up to an hour in some cases, especially if the lines were not sufficiently cleaned and flushed the last time the equipment was used.

V.7. Loading Skin into the Chamber.

The condition of the skin is checked by measuring its electrical impedance and monitoring the passive flux of the donor solution. The impedance of "good skin" should be >25 $k\Omega\ cm^2$ at a frequency of 100 Hz (Prausnitz, *et al.*, 1993 [a]; Chen, *et al.*, 1998 [b]; M. R. Prausnitz, personal communication; Gowrishankar, personal communication). The passive flux of the donor solution across the skin after an hour should be negligible (below the detection limit of the spectrofluorimeter). Low impedances or large passive fluxes indicate that the skin's integrity has been compromised in some way.

The impedance is measured across the two measurement electrodes in the permeation chamber. However, besides the skin, this measurement also includes PBS and the polyacrylamide gel. The other impedances can be neglected, though, since the impedance of the skin is much larger than PBS (see Section 3.7).

1. Float a piece of skin (see Section I.1) in a dish of PBS for ~1 min.
2. Gently remove the wax paper backing. Do not use tweezers. The skin should float on the surface, with the stratum corneum side facing upwards.

3. Fill the receptor compartment completely with PBS. There should not be any air bubbles present.
4. Position the skin in the chamber so that the stratum corneum faces the donor compartment and the epidermis faces the receptor compartment. Clamp the chamber shut. Verify that the receptor compartment is still completely filled with PBS.
5. Turn on the donor recycle system and fill the donor with PBS. Some light "jiggling" of the donor compartment may be necessary to allow any air bubbles trapped within the donor compartment to escape.
6. Once the donor compartment has been completely filled with PBS (no more air bubbles), turn off the pumps.
7. Connect the impedance meter (see Section V.4.1) to the measurement electrodes. Good skin has an impedance >25 $k\Omega\ cm^2$ at 100 Hz. Poor skin should be discarded.
8. Set up the donor system so that fresh donor solution is pumped into the donor compartment, and the outflow from the donor compartment goes to a waste beaker.
9. Turn on the pumps. Once the donor solution has traveled through the entire donor compartment and out to the waste beaker, change the tubing so that the donor solution continuously gets recycled (see Figure V.3).
10. Connect the chamber to the pulsing circuit as shown in Figure V.4, verifying that all four electrodes are properly connected.
11. Turn on the water bath.
12.. Run the impedance monitoring program (Section V.4.1). Continue taking impedance measurements throughout the entire passive control period.

V.8. Passive Control.

After the skin has been loaded in the chamber, the flow-through system should be activated. The skin should be left for at least 1 h to fully hydrate the skin and check for leaks (holes or tears in the skin). Leaks can be detected by observing large or increasing readings in the background fluorescence observed on the spectrofluorimeter. If the skin begins to leak, it should be discarded. During this period, the impedance meter should continue to measure and record the impedance of the skin.

V.9. Pulsing Conditions.

High-voltage pulses should be applied to the skin at the rate of 1 pulse every ~5 s. Both the time constant and the applied voltage should be set on the pulser as needed before pulsing is started. The transdermal voltage is a nonlinear function of the applied voltage (see Figures 7.10 and 8.3) (Pliquett, *et al.*, 1995 [a]; Chen, *et al.*, 1998 [c]). Thus, given a desired transdermal voltage, a guess of the applied voltage should be made at this time.

1. Set the pulser to deliver the appropriate types of pulses.
2. Make sure the impedance meter and its computer are still running.
3. Gradually start the pumps for the electrode flow-protection system. Make sure that the polyacrylamide gel in the chamber does not crack or break when this is turned on. If the gel breaks, new gel will have to be made, and the experiment will have to be aborted.
4. Turn on the oscilloscope and the computer. They should be set to start recording once the first pulse is applied. Make sure that all screen savers, energy savers, and any other software drivers that can cause process interrupts in the computer have been completely turned off. The computer should not be doing anything during the experiment besides downloading data. Any timing glitches between the computer and the oscilloscope could cause either the computer or the oscilloscope to crash.
5. Start the spectrofluorimeter for a time-based scan. The spectrofluorimeter should record fluorescence for the time of pulsing (typically 1 h), plus some additional time at the beginning to measure the baseline, and some time at the end to measure recovery. The time interval between successive measurements should be as short as possible (e. g., 0.5 s). Record about a minute of passive flux (control) to establish the baseline.
6. Start the pulser. The oscilloscope and the computer should start recording pulses immediately with the first pulse. Note the exact time when pulsing starts, on the clock and on the spectrofluorimeter (t_{start}). These times will be needed later to synchronize the pulsing data and the fluorescence data.
7. Since the spectrofluorimeter, the pulser, the oscilloscope/computer, and the impedance meter/computer are all automated, during the experiment, the equipment should simply be monitored at all times in case something goes wrong.

V.10. Ending the Experiment.

After pulsing, the recovery of the skin can be measured by recording the fluorescence once the pulser has been turned off. Afterwards, the skin should be removed from the permeation chamber and mounted on a microscope side for analysis. Voltage, current, impedance, and time data from the two computers and data from the spectrofluorimeter should all be saved on disk for later analysis. The standard curve should also be measured (see Section IV.12).

1. After pulsing, turn off the pulser, but leave the rest of the equipment running. Wait until the fluorescence reaches steady state to stop recording on the spectrofluorimeter. Wait until the impedance measurements of the skin reaches steady state before stopping the impedance computer.
2. Turn off all of the pumps.
3. Open the permeation chamber and carefully remove the skin (some liquid within the donor and receptor compartments will come out when this is done). Place the skin gently on a microscope slide. Gently spread the skin out so it lies flat, and lightly blot it dry with a paper towel. Do not rub the skin.
4. Add a drop of mounting solution (Solution 3 from Section V.1).
5. Gently put a cover slip on top. This will cause the mounting solution to spread out and cover the skin. Seal in place with nail polish. Bring the slide to a fluorescence microscope for immediate analysis and photography (Section II.3).
6. Save the data from the two computers and from the spectrofluorimeter. These should be copied to a workstation for later analysis.

V.11. Analysis of the Flux, Voltage, and Impedance Data.

All of the fluorescence, voltage, current, impedance, time, and calibration data needs to be downloaded into a computer for analysis. Due to the amount of data one experiment can generate (up to 10 MB), a workstation, rather than a PC, is strongly recommended (e. g. Sun Sparc 10, Sun).

The first step in the analysis is to convert all of the flux and current data into the transdermal voltage data. The next step is to calibrate and deconvolute the fluorescence data into molecular flux data. The final step is to correlate in time the three sets of measurements: impedance, voltage, and flux.

Section IV.13.1 outlines the calculations to determine the transdermal voltage during each pulse. Section IV.13.2 outlines the method of deconvoluting the fluorescence data to determine the molecular

flux. Section V.11.1 describes how to combine the three sets of measurements in time. Section V.11.2 has a sample program that loads in all of the raw data, calibrates it, and records the time sequence of each measurement.

V.11.1. Time Correlations of the Data.

At this point in the analysis, there should be three arrays of data, representing the transdermal voltages appearing during each pulse, the molecular fluxes across the skin (at a time resolution of τ_{cuv}), and the impedance of the skin throughout the entire experiment. These data need to be correlated in time with each other.

1. Define the first pulse to occur at a time 0. If the pulsing times from the voltage data (t_{volt}) do not start at 0, subtract off the time of the first pulse (t_0), so the first pulse is at time 0:

$$t = t_{volt} - t_0. \tag{V.1}$$

2. To correlate the time on the spectrofluorimeter with the time of each pulse, the time on the spectrofluorimeter (t_{fluor}) needs to be corrected for the elapsed time before pulsing was started (t_{start}) and the plug flow time (t_{react}).

$$t = t_{fluor} - t_{start} - t_{react}. \tag{V.2}$$

3. To correlate the time of the impedance meter (t_{imp}) with the time of each pulse, the data set (which can be nearly 100 000 lines long at this point) has to be scanned through to find the time of the first "break" or "error" in the impedance measurements (this can and probably should be done graphically, rather than numerically; the first "glitch" in the impedance data can be spotted very quickly). This time (t_0) should correspond to the time when the first pulse was applied. The impedance meter should have been disconnected at this point; thus, the impedance measured at that point would be erroneous. Subtract off the time of the first pulse (t_0), so that the first pulse occurs at time 0:

$$t = t_{imp} - t_0. \tag{V.3}$$

V.11.2. JUZ.m.

The following is the script file for JUZ.m, a MatLab 5 program which loads in the flux, voltage, and impedance data, and calibrates and correlates the data in time. There are also several function calls to progress.m (see Section V.4.4).

```
% JUZ.m
% This program inputs data from the fluorimeter, the oscillscope, and the LRC meter,
%   synchronizes and calibrates the data, and outputs it as 2 final data files.
% Tani Chen 6/11/98

%234567890123456789012345678901234567890123456789012345678901234567890123456789012345678901234567890

% *** CLEAR OLD STUFF OUT ***
clc
disp 'Initializing...'
clear
close all
format

% *** INITIALIZING CONSTANTS ***
Cuts    = 500;                  % Number of data points in each pulse
Rcur    = 1.2;                  % Resistance of current-measuring resistor (Ohm)
Rpbs    = 240;                  % Resistance of PBS in chamber (Ohm)
Toffset = (19 + 18 + 19) / 3;   % Time lag to cuvette (s)
Area    = .64 / 100 / 100;      % Area of the skin (m2)
Flow    = (.0303030 + .03125 + .0318471) / 3 / 1000;   % Flowrate thru system
TauCuv  = (18.2856 + 22.0411 + 23.4928) / 3;           % Residence time of cuvette
Vcuv    = Flow * TauCuv;        % Volume of cuvette
MeasFrq = 0.170239344262;       % Time between measuremets on LRC meter in fast mode (s)
NA      = 6.0221367e23;         % Avogadro's number (1 / mol)
e       = 1.60217733e-19;       % Charge on the electron (C)
Condy   = 1 / (67 / 100);       % Conductivity of PBS (Ohm m)
Thickn  = 20 * 1e-6;            % Thickness of stratum corneum (m)

% *** INPUT PARAMETERS ***
Pulse  = input('  Enter number of pulses during delivery phase. ->');
Ext    = input('  Enter number of pulses during extraction phase. ->');
Total  = Pulse + Ext;
Tstart = input('  Enter starting time (don''t add offset). ->') + Toffset;
MW     = input('  Enter molecular weight of tracer. ->');
q      = input('  Enter molecular charge of tracer. ->');
q      = abs(q);  % Ignore negative sign

% *** LOAD VOLTAGE DATA ***
disp 'Loading preamble data from "preamb1.m"...'
preamb1
  % Format:  1(byte), 1(norm), 400(#points), 1(dummy), Xincr, Xorig, Xref, Yincr, Yorig, Yref
Xincr  = preamble1(5);   % Tick = (bucketnumber - Xref) * Xincr + Xorig
Xorig  = preamble1(6);
Xref   = preamble1(7);
Yincr1 = preamble1(8);   % Voltage = (data - Yref) * Yincr + Yorig
Yorig1 = preamble1(9);
Yref1  = preamble1(10);

disp 'Loading preamble data from "preamb2.m"...'
preamb2
Yincr2 = preamble2(8);  % Voltage = (data - Yref) * Yincr + Yorig
Yorig2 = preamble2(9);
Yref2  = preamble2(10);

disp 'Loading waveform data from "wave1.dat"...'   % Chamber voltage data
File = fopen('wave1.dat', 'r');
Uch  = fread(File, [Cuts, Total], 'uchar');
Uch  = ((Uch - Yref1) * Yincr1 + Yorig1) * 200;     % 200x high voltage probe
Uch  = Uch .* (Uch > 0);                            % Get rid of noise

disp 'Loading waveform data from "wave2.dat"...'   % Current voltage data
File = fopen('wave2.dat', 'r');
Ucur = fread(File, [Cuts, Total], 'uchar');
Ucur = (Ucur - Yref2) * Yincr2 + Yorig2;
Ucur = Ucur .* (Ucur > 0);                          % Get rid of negative current (noise)
Ucur = Ucur / Rcur;                                 % Convert volts to amps

% *** LOAD TIME DATA ***
disp 'Loading pulse time data from "time.dat"...'
```

```
load time.dat
PulseTime = time(1:Total);  % Delete extra time points
PulseTime = PulseTime + (30 + 24 * 3600) * (PulseTime < 0);
  % When time goes across midnight, computer clock resets causing the time to "jump" backwards
  %   by 86400 s
PulseTime = PulseTime - PulseTime(1);
clear time
PulseTime = PulseTime + 24 * 3600 * (PulseTime < 0);
  % When time goes across midnight, computer clock resets causing the time to "jump" backwards
  %   by 86400 s

% *** CONVERT VOLTAGE DATA TO Uskin, I, and Tau ***
% Calculates Uskin(time), Rskin(time), I(time), Tau(time)
disp 'Deleting prepulse data from chamber voltages...'
Handle = progress(0, 'Deleting prepulse data from chamber voltages...');
set(Handle, 'MenuBar', 'none');
set(Handle, 'NumberTitle', 'off');
for j = 1:Total
  Utemp = Uch(:, j);

  if max(Utemp) > 7
    Loc(j) = min(find(Utemp > 7));
  else
    Loc(j) = 50;
  end

  progress(j/Total)
end
close(Handle)

disp 'Deleting prepulse data from current measurements...'
Handle = progress(0, 'Deleting prepulse data from current measurements...');
set(Handle, 'MenuBar', 'none');
set(Handle, 'NumberTitle', 'off');
for j = 1:Total
  Utemp = Ucur(:, j);
  Loc1 = min(find(Utemp > .05));

  if Loc1 > Loc(j)
    Loc(j) = Loc1;
  end

  Ucur(1:(Cuts - Loc(j) + 1), j)     = Ucur(Loc(j):Cuts, j);
  Ucur((Cuts - Loc(j) + 2):Cuts, j) = NaN;
  Uch(1:(Cuts - Loc(j) + 1), j)      = Uch(Loc(j):Cuts, j);
    % Delete header and push data forward so 0 means start of pulse
  Uch((Cuts - Loc(j) + 2):Cuts, j)  = NaN;   % Fill holes with "NaN"

  progress(j/Total)
end
close(Handle)

disp 'Fitting chamber voltages (ignore log of zero errors)...'
Handle = progress(0, 'Fitting chamber voltages...');
set(Handle, 'MenuBar', 'none');
set(Handle, 'NumberTitle', 'off');
drawnow
Uch = log(Uch - Uch .* (Uch <= 0));
  % Take logs of only positive numbers.  Negative numbers are changed to 0's
  %   (since the log of a negative number is complex!), then -Inf.  NaN's
  %   reamain NaN's
Uch = isfinite(Uch) .* Uch;
  % Convert -Inf to NaN (former negative numbers)

for j = 1:Total
  Tick = ((1:500)' - Xref + Loc(j)) * Xincr + Xorig;
    %  Set up time vector for each pulse for curve fitting (s)
  Utemp = Uch(1:150, j);

  if sum(isnan(Utemp)) == size(Utemp, 1)  % If Utemp empty, then no line fit
    Chamber(j, :) = [NaN NaN];
  else
    Chamber(j, :) = polyfit(Tick(isfinite(Utemp)), Utemp(isfinite(Utemp)), 1);
      % Linear fit (ln y = m * PulseTime + b)
  end

  progress(j/Total)
end
close(Handle)

Chamber(:, 1) = -1 ./ Chamber(:, 1);   % Tau(s) = -1 / m
Tau           = Chamber(:, 1) * 1e3;   % Tau in (ms)
Chamber(:, 2) = exp(Chamber(:, 2));    % Uch(V) = exp(b)
  %  Chamber(:, 1) = Tau (s)
  %  Chamber(:, 2) = Peak voltage across differential electrodes (V)

disp 'Fitting current measurements (ignore log of zero errors)...'
Handle = progress(0, 'Fitting current measurements...');
set(Handle, 'MenuBar', 'none');
set(Handle, 'NumberTitle', 'off');
drawnow
Ucur = log(Ucur - Ucur .* (Ucur <= 0));   % Take logs of positives
```

```
Ucur = isfinite(Ucur) .* Ucur;            % Same routine as above

for j = 1:Total  % Same routine as above, except for current now
  Tick  = ((1:500)' - Xref + Loc(j)) * Xincr + Xorig;  % (s)
  Utemp = Ucur(1:150, j);
  Current(j, :) = polyfit(Tick(isfinite(Utemp)), Utemp(isfinite(Utemp)),1);
  progress(j/Total)
end
close(Handle)

Current(:, 2) = exp(Current(:, 2));   % Ucur(V) = exp(b)
  %  Current(:, 2) = Peak currents across measuring resistor, Rcur (A)
Icur          = Current(:,2);         % Icur(A) = Current

disp 'Finding transdermal voltages...'
Uskin = Chamber(:, 2) - Current(:, 2) * Rpbs;
  % Uskin = Uch - Upbs = Uch - I * Rpbs
Uskin = Uskin .* (Uskin<1e3) ./ (Uskin<1e3) .* (Uskin>0) ./ (Uskin>0);
  % Get rid of errors (negatives, too large)
Rskin = Chamber(:, 2) ./ Current(:, 2) - Rpbs;
  % Rskin = Uch / I - Rpbs  (Rskin = Uskin / I (Ohm)
Rskin = Rskin .* (Rskin<1e4) ./ (Rskin<1e4) .* (Rskin>0) ./ (Rskin>0);
  %  Get rid of errors (negatives, too large)


% *** LOAD IMPEDANCE DATA ***
disp 'Loading capacitance data from "intrskin.dat.cap" (ignore divide by zero'
disp '  errors)...'
load intrskin.dat.cap
Cap = intrskin;
Cap = Cap .* (Cap > 0) ./ (Cap > 0);
disp 'Loading impedance data from "intrskin.dat.imp" (ignore divide by zero errors)...'
load intrskin.dat.imp
Imp = intrskin;
Imp = Imp .* (Imp > 0) ./ (Imp > 0);
disp 'Loading impedance measurement time data from "intrskin.dat.ztime"...'
load intrskin.dat.ztime
ZTime = intrskin;
ZTime = ZTime + (30 + 24 * 3600) * (ZTime < 0);
  % Clock resets after midnight, need to add 86400 s to time
disp 'Loading passive impedance data from "passive.dat.imp" (ignore divide by zero'
disp '  errors)...'
load passive.dat.imp
Pass = passive;
Pass = Pass .* (Pass > 0) ./ (Pass > 0);
disp 'Loading passive impedance time data from "passive.dat.ztime"...'
load passive.dat.ztime
PassTime = passive;
clear passive
clear intrskin


% *** CALIBRATE ZTIME TO TIME ***
disp 'Calibrating impedance times...'
disp '  Click on figure to zoom to appropriate region.'
Handle = plot(ZTime(1:1200), zeros(1, 1200), 'y*');  % Plot calibration curve
set(figure(1), 'Position', [514 430 560 420])
xlabel('Time (s)')
title('Impedance Times')
axis tight
zoom on
Choice = input('  Type 0 when graph is zoomed over point. ->');
disp '  Click on starting point.'
ZCalb = ginput(1);                    % Find point
zoom off
close all

ZCalb = ZCalb(1);                     % X-axis is the time
ZCalb(1:size(ZTime, 2)) = ZCalb;      % Fill up matrix with that time
ZCalb = min(find(ZCalb < ZTime));     % And compare with ZTime to find element with that time
ZCalb = ZTime(ZCalb) + MeasFrq;       % ZCalb is that time, plus an offset (for next measurement)
ZTime = ZTime - ZCalb;                % Correct ZTime for ZCalb.  ZTime is now equivalent to Time.


% *** CALCULATING IMPEDANCES FOR EACH PULSE ***
disp 'Calculating impedances during each pulse (ignore divide by zero errors)...'
Handle = progress(0, 'Calculating impedances during each pulse...');
set(Handle, 'MenuBar', 'none');
set(Handle, 'NumberTitle', 'off');
ImRec     = zeros(Total, 20) ./ 0;    % Initialize matrixes
ImRecTime = zeros(Total, 20) ./ 0;

for j = 1:(Total - 1)
  PStart   = min(find(PulseTime(j) < ZTime)) - 1;
  PEnd     = min(find(PulseTime(j + 1) < ZTime)) - 1;
  TempImp  = Imp(PStart:PEnd);
  TempTime = ZTime(PStart:PEnd);

  TempImp(size(TempImp, 2)) = NaN;
  while isnan(TempImp(1)) == 1
    TempTime(1:size(TempImp, 2) - 1) = TempTime(2:size(TempImp, 2));
    TempImp(1:size(TempImp, 2) - 1)  = TempImp(2:size(TempImp, 2));
```

```
    TempTime(size(TempImp, 2)) = 0;
    TempImp(size(TempImp, 2))  = 0;
  end

  TempTime = TempTime(1:min(find(isnan(TempImp))) - 2);
  TempImp  = TempImp(1:min(find(isnan(TempImp))) - 2);

  if size(TempTime, 2) == 0
    TempTime = NaN;
    TempImp = NaN;
  end

  TempTime = TempTime - TempTime(1);
  MatSize  = size(TempImp, 2) * (size(TempImp, 2) < 20) + 20 * (size(TempImp, 2) > 20);
    % MatSize = 20 if TempImp> 20, otherwise MatSize = size of TempImp
  ImRec(j, 1:MatSize)     = TempImp(1:MatSize);
  ImRecTime(j, 1:MatSize) = TempTime(1:MatSize);

  TempImp    = sort(TempImp);
  TempImp    = mean(TempImp(1:(size(TempImp, 2) - sum(isnan(TempImp)))));
  ImPulse(j) = TempImp;
  progress(j / (Total - 1))
end

ImRec     = ImRec';                      % Flip matrixes to correct orientation
ImRecTime = ImRecTime';
ImRec     = ImRec(1:20, :);              % Delete excess points during recovery phases
ImRecTime = ImRecTime(1:20, :);
ImRec     = ImRec ./ (ImRec > 0);        % Fill 0's with NaN's
ImRecTime = ImRecTime ./ (ImRec > 0);
close(Handle)


% *** LOAD CALIBRATION DATA ***
disp 'Loading fluorescence calibration data from "calb.txt" (ignore file errors)...'
! rm temp.txt
% Delete header from calibration data (5 lines)
! tail +5 calb.txt > temp.txt
load temp.txt
Calb = temp(:, 2);  % Calibration curve (arbitrary x-axis)
! rm temp.txt


% *** CALCULATE CALIBRATION CURVE ***
disp 'Calibrating data...'  % Plot calibration data
Handle = semilogy(Calb);
set(figure(1), 'Position', [1160 6 1142 845])
set(Handle, 'Color', 'w')
xlabel('Point number')
ylabel('Fluorescence (counts/s)')
title('Raw Calibration Data from "calb.txt"')

disp '  Scaling graph (see page on right)...'
Choice = 1;
while Choice == 1
  disp '    Click on bottom left corner.'
  BotLeft = ginput(1);
  disp '    Click on top right corner.'
  TopRight = ginput(1);
  axis([BotLeft(1) TopRight(1) BotLeft(2) TopRight(2)])  % Scale graph
  Choice = input('    Enter 1 for re-scale, 2 to restart, 0 when done. ->');
  if Choice == 2
    axis auto
    Choice = 1;
  end
end

disp '  Entering calibration values...'
for j = 2:8
  Choice = 1;
  while Choice == 1
    String = num2str(j);
    eval(['disp ''    Click on left-most region of sample #', String, ' '' ']);
    MouseLeft  = ginput(1);
    Handle     = line([MouseLeft(1);MouseLeft(1)], [BotLeft(2);TopRight(2)]);
    set(Handle, 'Color', 'r')
    disp '    Click on right-most region.'
    MouseRight = ginput(1);
    Handle     = line([MouseRight(1);MouseRight(1)], [BotLeft(2);TopRight(2)]);
    set(Handle, 'Color', 'r')
    Choice     = input('    Enter 1 to re-do, 0 when done. ->');
  end
  Coord(j) = mean(Calb(round(MouseLeft(1)):round(MouseRight(1))));
end

disp '  Figuring calibration equation (ignore log of zero errors)...'
Conc  = log([NaN 1e-1 1e-2 1e-3 1e-4 1e-5 1e-6 1e-7 1e-8] * 1e-3);
  % Concentration values (M).  Sample #1 (= Donor = 1 mM) is ignored.
Coord = log(Coord);

close(1)
Handle = plot(Coord, 'co-');  % Plot calibration curve
```

```
set(figure(1), 'Position', [514 430 560 420])
set(Handle, 'MarkerSize', 4)
set(Handle, 'MarkerFaceColor', 'c')
ylabel('log(fluorescence intensity)')
xlabel('Sample #')
title('Standard Curve Data')
axis([2 8 floor(min(Coord(2:8))) ceil(max(Coord(2:8)))])

Low     = input('    Enter lowest sample number in linear region. ->');
High    = input('    Enter highest sample number in linear region. ->');
CalbEqn = polyfit(Coord(Low:High), Conc(Low:High), 1);  % Get curve fit


% *** LOAD FLUX DATA ***
% PTI format load (Bldg E25).
disp 'Loading fluorescence flux data from "fluor.txt" (ignore file errors)...'
! rm temp.txt
% Delete header from calibration data (5 lines)
! tail +5 fluor.txt > temp.txt
load temp.txt
Fluor    = temp(:, 2);
FlLength = size(Fluor, 1);   % Length of fluorescence measurements (1/2 s)


% *** DELETE JUNK (GLITCHES) ***
disp 'Glitch removal...'
Handle = plot(Fluor, 'g');
axis tight
ylabel('Fluorescence (counts/s)')
xlabel('Point Number')
title('Raw Fluorescence Data from "fluor.txt"')

Choice = input('  Enter 1 for glitch removal, 0 if OK. ->');
while Choice == 1
  Handle = plot(Fluor, 'g');
  set(figure(1), 'Position', [1160 6 1142 845])
  set(Handle, 'MarkerSize', 4)
  set(Handle, 'MarkerFaceColor', 'g')
  axis tight
  ylabel('Fluorescence (counts/s)')
  xlabel('Point Number')
  title('Raw Fluorescence Data from "fluor.txt"')

  disp '  Scaling graph (see page on right)...'
  Choice = 1;
  while Choice == 1
    disp '    Click on bottom left corner.'
    BotLeft  = ginput(1);
    disp '    Click on top right corner.'
    TopRight = ginput(1);
    axis([BotLeft(1) TopRight(1) BotLeft(2) TopRight(2)])  % Scale graph
    Choice   = input('    Enter 1 for re-scale, 2 to restart, 0 when done. ->');
    if Choice == 2
      axis auto
      axis tight
      Choice = 1;
    end
  end

  disp '  Click on left-most region.'
  MouseLeft  = ginput(1);
  Handle     = line([MouseLeft(1); MouseLeft(1)], [BotLeft(2) TopRight(2)]);
  set(Handle, 'Color', 'r')
  disp '  Click on right-most region.'
  MouseRight = ginput(1);
  Handle     = line([MouseRight(1); MouseRight(1)], [BotLeft(2) TopRight(2)]);
  set(Handle, 'Color', 'r')

  Choice = input('  Enter 1 to abort, 0 if correct. ->');
  if Choice == 0
    disp '  Deleting section...'
    Fluor(floor(MouseLeft):ceil(MouseRight)) = NaN;
  end
  Choice = input('  Enter 1 for more removals, 0 when done. ->');
end
close(1)


% *** CONVERT TO CONCENTRATIONS ***
disp 'Converting fluorescences into concentrations (ignore dividing by zero errors)...'
Fluor = Fluor(:) .^ (CalbEqn(1) * (1 - isnan(Fluor(:)))) * exp(CalbEqn(2)) .* ((1 - isnan(Fluor(:))) ./ (1 -
isnan((Fluor(:)))));
  % Fluorescence in (M) (from Conc)


% *** SIGNAL AVERAGING FLUORESCENCE MEASUREMENTS ***
disp 'Applying signal averaging over 28 points...'
  % This is now hard-wired into the program!!
FlSz = size(Fluor, 1) - 28;
Fluor(1:FlSz) = ( Fluor( 1:FlSz   ) + Fluor( 2:FlSz+ 1) + Fluor( 3:FlSz+ 2) + Fluor( 4:FlSz+ 3)                    +
Fluor( 5:FlSz+ 4) + Fluor( 6:FlSz+ 5) + Fluor( 7:FlSz+ 6) + Fluor( 8:FlSz+ 7)                    + Fluor( 9:FlSz+ 8)
+ Fluor(10:FlSz+ 9) + Fluor(11:FlSz+10) + Fluor(12:FlSz+11)                    + Fluor(13:FlSz+12) +
```

```
Fluor(14:FlSz+13) + Fluor(15:FlSz+14) + Fluor(16:FlSz+15)                    + Fluor(17:FlSz+16) + Fluor(18:FlSz+17)
+ Fluor(19:FlSz+18) + Fluor(20:FlSz+19)                  + Fluor(21:FlSz+20) + Fluor(22:FlSz+21) +
Fluor(23:FlSz+22) + Fluor(24:FlSz+23)                  + Fluor(25:FlSz+24) + Fluor(26:FlSz+25) + Fluor(27:FlSz+26)
+ Fluor(28:FlSz+27))/28;
Fluor((size(Fluor) - 28 + 1):size(Fluor)) = NaN;


% *** FIND LAG TIME ***
disp 'Finding lag times (see page on right)...'
Handle = plot(Fluor, 'g');
set(figure(1), 'Position', [1160 6 1142 845])
axis tight
ylabel('Fluorescence (counts/s)')
xlabel('Point Number')
title('Raw Fluorescence Data from "fluor.txt"')

disp '  Scaling graph...'
Choice = 1;
while Choice == 1
  disp '    Click on bottom left corner.'
  BotLeft  = ginput(1);
  disp '    Click on top right corner.'
  TopRight = ginput(1);
  axis([BotLeft(1) TopRight(1) BotLeft(2) TopRight(2)])  % Scale graph
  Choice   = input('    Enter 1 for re-scale, 2 to restart, 0 when done. ->');
  if Choice == 2
    axis auto
    axis tight
    Choice = 1;
  end
end

disp '  Click on start of rise.'
Tlag   = ginput(1);
Tlag   = Tlag(1);        % Need only x coordinate
Handle = line([Tlag; Tlag], [BotLeft(2) TopRight(2)]);
set(Handle, 'Color', 'r')
if Tlag > size(Fluor, 1)  % Didn't reach steady state
  Tlag = NaN;
end
if Tlag < 0  % Didn't reach steady state
  Tlag = NaN;
end
Tlag = Tlag/2 - Tstart; % Subtract off time until first pulse (includes Toffset)
close(1);


% *** REMOVE DATA BELOW DETECTION ***
disp 'Deleting data below detection limit (ignore divide by zero errors)...'
DetLmt = exp(Conc(High));
FlSize = size(Fluor, 1);
Fluor = Fluor .* (Fluor > DetLmt) ./ (Fluor > DetLmt);


% *** DECONVOLUTION ROUTINE ***
disp 'Deconvoluting fluxes...'
  % Routine taken from Pliquett, U., M. R. Prausnitz, Y. A. Chizmadzhev, and
  %   J. C. Weaver.  "Measurement of Rapid Release Kinetics for Drug Delivery,"
  %   _Pharm Res_, 12(4):549-55, 1995, Equations (7) and (8).  With some
  %   additional modifications and simplifications.
FlSize = size(Fluor, 1) - 1;
Flux(1:FlSize) = Vcuv * (Fluor(2:FlSize + 1) - Fluor(1:FlSize)) / Area / .5 + Flow / Area * (Fluor(2:FlSize + 1) +
Fluor(1:FlSize)) / 2;
  % Flux in (mol/m2 s)


% *** CORRELATE FLUXES AND PULSES ***
disp 'Correlating fluxes with pulses...'
FluxTime = (1:FlLength)' / 2  - Tstart;   % Time matrix for each flux measurement

Handle = progress(0, 'Correlating fluxes with pulses...');
set(Handle, 'MenuBar', 'none');
set(Handle, 'NumberTitle', 'off');
for j = 1:Total
  CorrFlux(j)  = Flux(min(find(PulseTime(j) < FluxTime)));   % (mol/m2 s)
  progress(j/Total)
end
close(Handle)


% *** INTEGRATE FLUORESCENCE CURVES ***
Transport = 0;
Extract   = 0;

for j = 1:(Pulse - 1)
  if (isnan(CorrFlux(j)) == 0 & isnan(CorrFlux(j + 1)) == 0)
    Transport = Transport + (CorrFlux(j) + CorrFlux(j + 1)) / 2 * (PulseTime(j + 1) - PulseTime(j)) * Area;
  end
end

for j = Pulse:(Total - 1)
  if (isnan(CorrFlux(j)) == 0 & isnan(CorrFlux(j + 1)) == 0)
```

```
    Extract = Extract + (CorrFlux(j) + CorrFlux(j + 1)) / 2 * (PulseTime(j + 1) - PulseTime(j)) * Area;
  end
end

TnptMass = Transport * MW * 1e6;
ExtMass = Extract * MW * 1e6;


% *** CALCULATIONS ***
AvgPass   = sort(Pass);
AvgPass   = mean(AvgPass(1:(size(AvgPass, 2) - sum(isnan(AvgPass)))));
AvgPass   = AvgPass / 1000;   % Convert to kOhms

AvgRskin  = sort(Rskin(1:Pulse));
AvgRskin  = mean(AvgRskin(1:(size(AvgRskin, 1) - sum(isnan(AvgRskin)))));
if (Pulse + 1) > Total
  AvgRskEx = NaN;
else
  AvgRskEx  = sort(Rskin(Pulse + 1:Total));
  AvgRskEx  = mean(AvgRskEx(1:(size(AvgRskEx, 1) - sum(isnan(AvgRskEx)))));
end

AvgUskin  = sort(Uskin(1:Pulse));
AvgUskin  = mean(AvgUskin(1:(size(AvgUskin, 1) - sum(isnan(AvgUskin)))));
if (Pulse + 1) > Total
  AvgUskEx = NaN;
else
  AvgUskEx  = sort(Uskin(Pulse + 1:Total));
  AvgUskEx  = mean(AvgUskEx(1:(size(AvgUskEx, 1) - sum(isnan(AvgUskEx)))));
end

AvgIcur   = sort(Icur(1:Pulse));
AvgIcur   = mean(AvgIcur(1:(size(AvgIcur, 1) - sum(isnan(AvgIcur)))));
if (Pulse + 1) > Total
  AvgIEx = NaN;
else
  AvgIEx    = sort(Icur(Pulse + 1:Total));
  AvgIEx    = mean(AvgIEx(1:(size(AvgIEx, 1) - sum(isnan(AvgIEx)))));
end

AvgTau    = sort(Tau(1:Pulse));
AvgTau    = mean(AvgTau(1:(size(AvgTau, 1) - sum(isnan(AvgTau)))));
if (Pulse + 1) > Total
  AvgTauEx = NaN;
else
  AvgTauEx  = sort(Tau(Pulse + 1:Total));
  AvgTauEx  = mean(AvgTauEx(1:(size(AvgTauEx, 1) - sum(isnan(AvgTauEx)))));
end

AvgFlux   = sort(CorrFlux(1:Pulse));
AvgFlux   = mean(AvgFlux(1:(size(AvgFlux, 2) - sum(isnan(AvgFlux)))));
AvgFluxM  = AvgFlux * MW * 1e6 * 3600 / 100 / 100;
if (Pulse + 1) > Total
  AvgFlEx = NaN;
else
  AvgFlEx   = sort(CorrFlux(Pulse + 1 :Total));
  AvgFlEx   = mean(AvgFlEx(1:(size(AvgFlEx, 2) - sum(isnan(AvgFlEx)))));
end
AvgFlExM  = AvgFlEx * MW * 1e6 * 3600 / 100 / 100;

if Total == Pulse
  ExtLen = NaN;
else
  ExtLen    = PulseTime(Total) - PulseTime(Pulse + 1);
end
NoImp     = size(Imp,2) - sum(isnan(Imp));
Anal      = Total - sum(isnan(CorrFlux));

if Total == 1
  Tr(1) = NaN;
else
  Tr(1:Total - 1) = CorrFlux(1:Total - 1)' * Area .* (PulseTime(2:Total) - PulseTime(1:Total - 1)) * NA * q * e ./
Icur(1:Total - 1) ./ Tau(1:Total - 1);
end
Tr(Pulse) = NaN;
Tr(Total) = NaN;

AvgTr     = sort(Tr(1:Pulse));
AvgTr     = mean(AvgTr(1:(size(AvgTr, 2) - sum(isnan(AvgTr)))));
if Total == Pulse
  AvgTrEx = NaN;
else
  AvgTrEx   = sort(Tr(Pulse + 1:Total));
  AvgTrEx   = mean(AvgTrEx(1:(size(AvgTrEx, 2) - sum(isnan(AvgTrEx)))));
end

Fw        = Thickn / Condy / Area ./ Rskin .* Tr' / (q / 150);
AvgFw     = sort(Fw(1:Pulse));
AvgFw     = mean(AvgFw(1:(size(AvgFw, 1) - sum(isnan(AvgFw)))));
if Total == Pulse
  AvgFwEx = NaN;
else
```

```
  AvgFwEx   = sort(Fw(Pulse + 1:Total));
  AvgFwEx   = mean(AvgFwEx(1:(size(AvgFwEx, 1) - sum(isnan(AvgFwEx)))));
end

if Total == Pulse
  AvgImpEx = NaN;
  AvgImp   = NaN;
  ImPulse  = NaN;
else
  AvgImp    = sort(ImPulse(1:Pulse));
  AvgImp    = mean(AvgImp(1:(size(AvgImp, 2) - sum(isnan(AvgImp)))));
  AvgImpEx  = sort(ImPulse(Pulse + 1:Total - 1));
  AvgImpEx  = mean(AvgImpEx(1:(size(AvgImpEx, 2) - sum(isnan(AvgImpEx)))));
end


% *** SAVE DATA ***
disp 'Saving data...'

disp '  Saving "final.txt"...'
disp '    Column 1:       Pulse number'
disp '    Column 2:       Pulse time (s)'
disp '    Column 3:       Peak transdermal voltage (V)'
disp '    Column 4:       Peak transdermal resistance during pulsing (Ohm)'
disp '    Column 5:       Peak current (A)'
disp '    Column 6:       Instantaneous molecular flux (mol/m2 s)'
disp '    Column 7:       Transport number'
disp '    Column 8:       Fractional aqueous area'
disp '    Column 9:       Average inter-pulse 100 Hz impedances (Ohm)'
disp '    Columns 10-29:  Inter-pulse 100 Hz impedances (Ohm)'
disp '    Columns 30-49:  Inter-pulse impedance measurement times (s)'

Final(:, 1) = (1:Total)';
Final(:, 2) = PulseTime;
Final(:, 3) = Uskin;
Final(:, 4) = Rskin;
Final(:, 5) = Icur;
Final(:, 6) = CorrFlux';
Final(:, 7) = Tr';
Final(:, 8) = Fw;
if Total == 1
  Final(:, 9) = NaN;
else
  Final(1:(Total - 1), 9) = ImPulse';
end
Final(Total, 9) = NaN;
Final(:, 10:29) = ImRec';
Final(:, 30:49) = ImRecTime';
save final.txt Final -ascii

disp '  Saving "finalimp.txt"...'
disp '    Column 1:  Impedance measurement time (s)'
disp '    Column 2:  100 Hz Impedance (Ohm)'
disp '    Column 3:  Capacitance (Farads)'

FinalImp(:, 1) = ZTime';
FinalImp(:, 2) = Imp';
FinalImp(:, 3) = Cap';
save finalimp.txt FinalImp -ascii


% *** PLOT RESULTS ***
disp 'Plotting results...'
figure
subplot(3,1,1)
Handle = plot(PulseTime, Uskin, 'wo');
set(figure(1), 'Position', [1160 6 1142 845])
axis tight
set(Handle, 'MarkerSize', 2)
set(Handle, 'MarkerFaceColor', 'w')
xlabel('Time (s)')
ylabel('Uskin, 0 (V)')
title('Peak Transdermal Voltage')

subplot(3,1,2)
Handle = plot(PulseTime, CorrFlux, 'go');
axis tight
set(Handle, 'MarkerSize', 2)
set(Handle, 'MarkerFaceColor', 'g')
xlabel('Time (s)')
ylabel('Flux (mol/m2 s)')
title('Instantaneous Molecular Flux')

if isnan(ImPulse) ~= 1
  subplot(3,1,3)
  Handle = plot(PulseTime(1:Total - 1), ImPulse, 'yo');
  axis tight
  set(Handle, 'MarkerSize', 2)
  set(Handle, 'MarkerFaceColor', 'g')
  xlabel('Time (s)')
  ylabel('Flux (mol/m2 s)')
  title('Inter-pulse 100 Hz Impedances')
```

```
end

figure
subplot(3,1,1)
Handle = plot(PulseTime(1:Pulse), Uskin(1:Pulse), 'wo');
set(figure(2), 'Position', [6 -895 1142 845])
axis tight
set(Handle, 'MarkerSize', 2)
set(Handle, 'MarkerFaceColor', 'w')
xlabel('Time (s)')
ylabel('Uskin, 0 (V)')
title('Peak Transdermal Voltage')

subplot(3,1,2)
Handle = plot(PulseTime(1:Pulse), CorrFlux(1:Pulse), 'go');
axis tight
set(Handle, 'MarkerSize', 2)
set(Handle, 'MarkerFaceColor', 'g')
xlabel('Time (s)')
ylabel('Flux (mol/m2 s)')
title('Instantaneous Molecular Flux')

subplot(3,1,3)
if Total ~= Pulse
  Handle = plot(PulseTime(1:Pulse), ImPulse(1:Pulse), 'yo');
  axis tight
  set(Handle, 'MarkerSize', 2)
  set(Handle, 'MarkerFaceColor', 'g')
  xlabel('Time (s)')
  ylabel('Flux (mol/m2 s)')
  title('Inter-pulse 100 Hz Impedances')
end

figure
subplot(3,1,1)
Handle = plot(PulseTime(Pulse + 1:Total), Uskin(Pulse + 1:Total), 'wo');
set(figure(3), 'Position', [1160 -895 1142 845])
axis tight
set(Handle, 'MarkerSize', 2)
set(Handle, 'MarkerFaceColor', 'w')
xlabel('Time (s)')
ylabel('Uskin, 0 (V)')
title('Peak Transdermal Voltage')

subplot(3,1,2)
Handle = plot(PulseTime(Pulse + 1:Total), CorrFlux(Pulse + 1:Total), 'go');
axis tight
set(Handle, 'MarkerSize', 2)
set(Handle, 'MarkerFaceColor', 'g')
xlabel('Time (s)')
ylabel('Flux (mol/m2 s)')
title('Instantaneous Molecular Flux')

if isnan(ImPulse) ~= 1
  subplot(3,1,3)
  Handle = plot(PulseTime(Pulse + 1:Total - 1), ImPulse(Pulse + 1:Total - 1), 'yo');
  axis tight
  set(Handle, 'MarkerSize', 2)
  set(Handle, 'MarkerFaceColor', 'g')
  xlabel('Time (s)')
  ylabel('Flux (mol/m2 s)')
  title('Inter-pulse 100 Hz Impedances')
end


% *** PRINT RESULTS ***
disp ' '
disp 'Summary:'
disp '--------'
disp 'Pre-pulse measurements:'
String = num2str(AvgPass);
eval(['disp ''  Average passive impedance:  ', String, ' kOhm'' ']);
String = num2str(max(PassTime));
eval(['disp ''  Length of passive phase:  ', String, ' s'' ']);
String = num2str(max(PassTime) / 3600);
eval(['disp ''                          = ', String, ' h'' ']);

disp ' '
disp 'Transport measurements:'
String = num2str(Pulse);
eval(['disp ''  Number of pulses:  ', String, ' '' ']);
String = num2str(PulseTime(Pulse));
eval(['disp ''  Length of transport phase:  ', String, ' s'' ']);
String = num2str(PulseTime(Pulse) / 3600);
eval(['disp ''                              = ', String, ' h'' ']);
String = num2str(AvgImp);
eval(['disp ''  Average skin impedance:  ', String, ' Ohm'' ']);
String = num2str(AvgUskin);
eval(['disp ''  Average peak transdermal voltage:  ', String, ' V'' ']);
String = num2str(AvgRskin);
eval(['disp ''  Average skin resistance:  ', String, ' Ohm'' ']);
String = num2str(AvgIcur);
```

```
eval(['disp ''  Average peak current:  ', String, ' A'' ']);
String = num2str(AvgTau);
eval(['disp ''  Average time constant:  ', String, ' ms'' ']);
String = num2str(Tlag);
eval(['disp ''  Time lag before detection of transport:  ', String, ' s'' ']);
String = num2str(AvgFlux);
eval(['disp ''  Average molecular flux:  ', String, ' mol/m2 s'' ']);
String = num2str(AvgFluxM);
eval(['disp ''                          = ', String, ' ug/cm2 h'' ']);
String = num2str(Transport);
eval(['disp ''  Total amount transported:  ', String, ' mol'' ']);
String = num2str(TnptMass);
eval(['disp ''                           = ', String, ' ug'' ']);
String = num2str(AvgTr);
eval(['disp ''  Average transport number:  ', String, ' '' ']);
String = num2str(AvgFw);
eval(['disp ''  Average fractional aqueous area:  ', String, ' '' ']);

disp ' '
disp 'Extraction measurements:'
String = num2str(Ext);
eval(['disp ''  Number of pulses:  ', String, ' '' ']);
String = num2str(ExtLen);
eval(['disp ''  Length of extraction phase:  ', String, ' s'' ']);
String = num2str(ExtLen / 3600);
eval(['disp ''                                 = ', String, ' h'' ']);
String = num2str(AvgImpEx);
eval(['disp ''  Average skin impedance:  ', String, ' Ohm'' ']);
String = num2str(AvgUskEx);
eval(['disp ''  Average peak transdermal voltage:  ', String, ' V'' ']);
String = num2str(AvgRskEx);
eval(['disp ''  Average skin resistance:  ', String, ' Ohm'' ']);
String = num2str(AvgIEx);
eval(['disp ''  Average peak current:  ', String, ' A'' ']);
String = num2str(AvgTauEx);
eval(['disp ''  Average time constant:  ', String, ' ms'' ']);
String = num2str(AvgFlEx);
eval(['disp ''  Average molecular flux:  ', String, ' mol/m2 s'' ']);
String = num2str(AvgFlExM);
eval(['disp ''                          = ', String, ' ug/cm2 h'' ']);
String = num2str(Extract);
eval(['disp ''  Amount extracted after pulsing:  ', String, ' mol'' ']);
String = num2str(ExtMass);
eval(['disp ''                                  = ', String, ' ug'' ']);
String = num2str(AvgTrEx);
eval(['disp ''  Average transport number:  ', String, ' '' ']);
String = num2str(AvgFwEx);
eval(['disp ''  Average fractional aqueous area:  ', String, ' '' ']);

disp ' '
disp 'Summary:'
String = num2str(Total);
eval(['disp ''  Total number of pulses:  ', String, ' '' ']);
tring = num2str(PulseTime(Total));
String = num2str(NoImp);
eval(['disp ''  Number of impedance measurements analyzed:  ', String, ' '' ']);
String = num2str(size(Fluor, 1));
eval(['disp ''  Number of fluorescence measurements analyzed:  ', String, ' '' ']);
String = num2str(PulseTime(Total));
eval(['disp ''  Total length of experiment:  ', String, ' s'' ']);
String = num2str(PulseTime(Total) / 3600);
eval(['disp ''                                 = ', String, ' h'' ']);
String = num2str(Anal);
eval(['disp ''  Total number of pulses analyzed:  ', String, ' '' ']);
String = num2str(DetLmt);
eval(['disp ''  Detection limit of spectrofluorimeter:  ', String, ' mol/m2 s'' ']);


% *** DONE! ***
disp ' '
disp 'End of program.'
disp '  Don''t forget to copy the results into "summary.txt"!!'
```